universität wien

DISSERTATION / DOCTORAL THESIS

Titel der Dissertation / Title of the Doctoral Thesis

"Design, Synthesis, and Pharmacological Optimisation of Potent Novel Small Molecule Inhibitors of Chikungunya Virus"

verfasst von / submitted by

Mag. pharm. Verena Battisti

angestrebter akademischer Grad / in partial fulfilment of the requirements for the degree of

Doktorin der Naturwissenschaften (Dr.rer.nat.)

Wien, 2022 / Vienna, 2022

Studienkennzahl lt. Studienblatt / degree programme code as it appears on the student record sheet:	UA 796 610 449
Studienrichtung lt. Studienblatt / degree programme as it appears on the student record sheet:	Pharmazie
Betreut von / Supervisor:	Univ.-Prof. Mag. Dr. Thierry Langer
Betreut von / Supervisor:	ao. Univ.-Prof. Mag. Dr. Ernst Urban

"Careful. We don't want to learn anything from this."

-Bill Watterson, "Calvin and Hobbes"

Acknowledgements

During the last four years, I was lucky to be supported by remarkable colleagues and family members. Without you, I would not be where I am today. Thank you!

I am especially grateful for the support of my two supervisors, Thierry Langer and Ernst Urban. Both are excellent and passionate supervisors who supported me patiently and quickly in all matters in which I needed help. I want to thank Thierry Langer for his inspirational academic and moral support, his guidance, the trust he placed in me, and most of all, for his encouragement to broaden my scientific horizon. I further want to thank Ernst Urban for always making time to answer academic and organisational questions, for offering his extraordinary and consistent care during this thesis, for helping me with much-needed moral support, and for his excellent academic expertise.

Additionally, I am very thankful to the fantastic team at KU Leuven for performing the antiviral biological assays. Especially for Leen Delang's support for the project - she was always there with her expertise and advice when scientific questions occurred.

I am thankful to Judith Wackerlig and Daniel Dobusch for the assistance with the chemical analysis of the compounds and to Christian Studenik and Mohammed Aufy for providing the cytotoxicity data. Further, I would like to thank all the master's students I helped to supervise for their support: M. Guèrin, E. V. Dalietou, C. Dworschak, and A. Hodzic.

Ebenso möchte ich mich bei meiner wundervollen Familie bedanken. Bei meinen beiden Schwestern und meinem großen Bruder Stefan, die mich in schwierigen Zeiten immer wieder zum Lachen bringen, und meinem einzigartigen Opa Hubert, der mich unaufhörlich bestärkt. Einen großen Dank möchte ich auch meiner wundervollen Mama Gerlinde aussprechen. Sie hat immer an mich geglaubt und mich ermutigt, meinen eigenen Weg zu gehen.

Ein besonderer Dank gilt Georg, der mir nicht nur die Kraft und Ausdauer gegeben hat, diese Arbeit abzuschließen, sondern mich auch in allen Lebensbereichen unterstütz und ermutigt.

Contents

List of Figures

List of Tables

Abbreviations

A549 adenocarcinomic human alveolar basal epithelial 549

ADME absorption, distribution, metabolism, and excretion

ADMET absorption, distribution, metabolism, excretion, and toxicity

AMS Aldrich Market Select

CADD computer-aided drug design

CC_{50} half maximal cytotoxic concentration

CHIKF Chikungunya fever

CHIKV Chikungunya virus

$CHVB^{res}$ CHVB-resistant variant

CPE cytopathic effect

EC_{50} half maximal effective concentration

GTase guanylyltransferase

GWAS genome wide association studies

HBA hydrogen bond acceptor

HBD hydrogen bond donor

HCl hydrochloric acid

HEK 293 human embryonic kidney 293

hERG human Ether-à-go-go-Related Gene

HLMs human liver microsomes

HTS high-throughput screening

KOL key opinion leader

LBDD ligand-based drug design

MW molecular weight

MTase methyltransferase

NROT number of rotatable bonds

nsP1 non-structural protein 1

nsP2 non-structural protein 2

nsP3 non-structural protein 3

PARP poly ADP ribose polymerase

PD pharmacodynamics

P-gp P glycoprotein

PK pharmacokinetics

POM proof of mechanism

PSA polar surface area

SAR structure-activity relationship

SBDD structure-based drug design

SMR structure-metabolism relationship

SI selectivity index

TEA triethylamine

UMN unmet medical need

To my father - you meant the world to me.

Chapter 1

Introduction

This chapter provides a brief overview of the drug discovery and development process's beginning phase - from identifying an unmet medical need to hit identification and lead optimisation strategies. Moreover, an introduction of the target virus (Chikungunya virus (CHIKV)), its impact on human lives, and current research strategies for identifying antiviral compounds against this alphavirus are given. This chapter aims to provide the reader with an understanding of the basic concept employed throughout this thesis, its motivation, and its scientific goal.

1.1 Drug Discovery and Development

Drug discovery is a process of identifying chemical compounds with the potential for future drug candidates. Despite the constantly rising costs of new drug development, as of November 2021, more than 20,000 FDA-approved drugs have been on the market [1–3]. Developing a new drug is highly time- and resource-consuming, which takes approximately twelve to fifteen years and, on average, $2.5 billion to launch a new drug on the market [4]. Nevertheless, the current SARS-CoV-2 pandemic has shown the far-reaching consequences of the lack of treatment options on human health, society, and the economic system [5–7]. This high unmet need for new therapeutics can be found especially for re-emerging or emerging viral diseases, making identifying novel antiviral drugs highly desirable.

Commonly, modern drug discovery initiates with the recognition of a disease or clinical condition without suitable treatment options, the selection and validation of a druggable target protein, and the screening of chemical libraries with relevant *in vitro* assays for identification of hits with biological activity. Next, various hit optimisation techniques

generate a new lead compound from the identified hits. After thoroughly lead optimisation in efficacy (in cell and animal models), pharmacokinetics and safety, the novel lead reaches the development phase with human clinical trials (see Figure 1.1.1). Realistically, there are no discrete stages in drug discovery and development, and it is commonly a continuous process with overlapping strategies [8, 9].

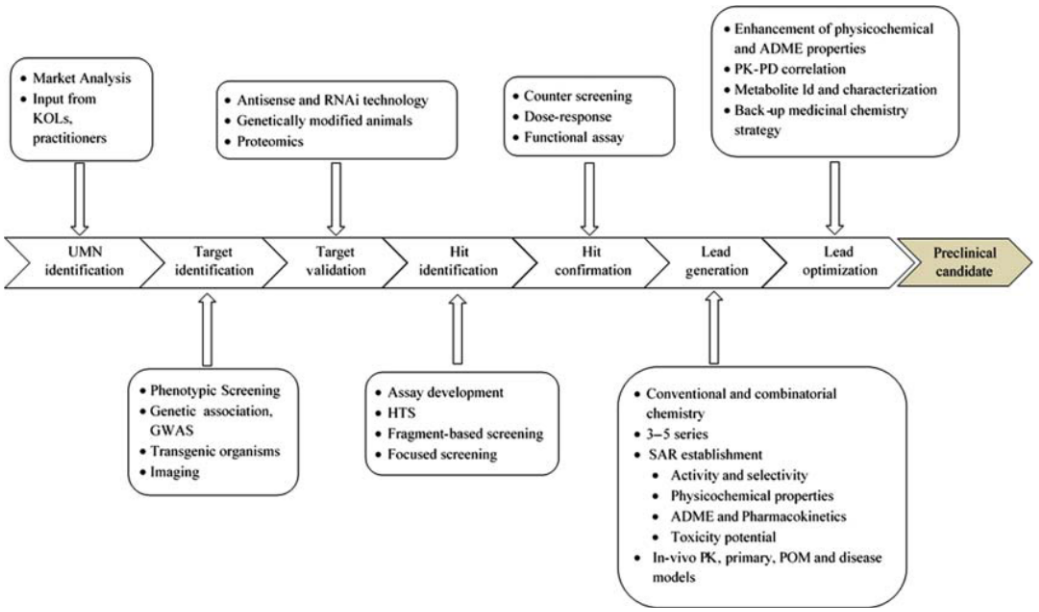

FIGURE 1.1.1: Overview of the drug-discovery process; unmet medical need (UMN); key opinion leader (KOL); structure-activity relationship (SAR); genome wide association studies (GWAS); high-throughput screening (HTS); proof of mechanism (POM); pharmacokinetics (PK); pharmacodynamics (PD) [9].

The following chapters elaborate on the phases of the drug discovery process that are relevant for this research project - from the hit discovery via screening and scaffold hopping to lead development and lead optimisation. Further, the Chikungunya fever (CHIKF), its causing agent CHIKV, and the lack of treatment options are discussed. The unmet medical need of the CHIKF makes the CHIKV a critical target for antiviral research.

1.1.1 Hit Discovery and Confirmation Process

A 'hit' is broadly defined as a chemical entity which shows the desired activity against the chosen target in a screening assay. Subsequently, the identified hits are counter-screened to eliminate false-positive results and to identify promiscuous or frequent hitters by follow-up assays [10]. Hits form the basis of the following lead generation and optimisation phases where the chemical compound is optimised for meeting drug-like criteria.

1.1.1.1 Screening Paradigms for Novel Hit Identification

For hit identification, various screening paradigms exist, some of which will be briefly discussed. Commonly, novel compounds are found by HTS if a suitable assay can be developed. The entire compound libraries are screened directly against the drug target or in cell-based assays within this screening method. No prior knowledge of structural requirements for activity is needed to perform an HTS - making it a powerful tool for identifying novel chemical entities for otherwise unmet targets [9, 11]. Nevertheless, drawbacks in the traditional HTS methods include the limitations in reaching new chemical space - as the compounds are determined by the library composition, which contains only a small amount of the estimated $\geq 10^{60}$ possible molecules [12, 13]. Further, a high rate of false-positives (e.g., promiscuous compounds or frequent hitters) and an unknown frequency of false-negative results are known concerns in HTS studies [14, 15].

Fragment- and focused-based screening are interesting alternatives to HTS for detecting novel chemical compounds if no suitable biochemical assay can be developed [16, 17]. Fragment-based screening uses libraries with fragment-like molecules for which the 'Rule of Three' is primarily applicable (molecular weight (MW): <300, number of hydrogen bond donor (HBD): $\leq$3, number of hydrogen bond acceptor (HBA) $\leq$3, ClogP: $\leq$3, number of rotatable bonds (NROT): $\leq$3, and polar surface area (PSA) $\leq$60) [18]. The fragments are evaluated at higher concentrations, and the retrieved hits are subsequently used as building blocks for synthesising potent novel leads [19].

Focused-based screening, on the other hand, evaluates a smaller set of compounds which are likely to possess activity against the desired target based on data-driven expectations (e.g., compounds that have already shown activity against a similar target, other compounds with comparable scaffold and already assessed activity against the target). Additionally, *in silico* methods are a powerful tool to prioritise compounds for focused screening [10, 16].

Computational approaches are integral in modern drug discovery and development processes as they are time and economically efficient and often outperform traditional methods [20–22]. The wide range of methods of the computer-aided drug design (CADD) can be divided into structure-based drug design (SBDD) and ligand-based drug design (LBDD). Depending on the availability of structural information of the target or the knowledge of the mode of action, different approaches are used to perform a computational-driven virtual screening [23]. One of the strategies in structure-based virtual screening is the prediction of the activity of a virtual library according to the docking ability in the three-dimensional target protein [9, 24]. Pharmacophore-based virtual screening, on the other hand, is also applicable for LBDD as the generated (ligand-based)

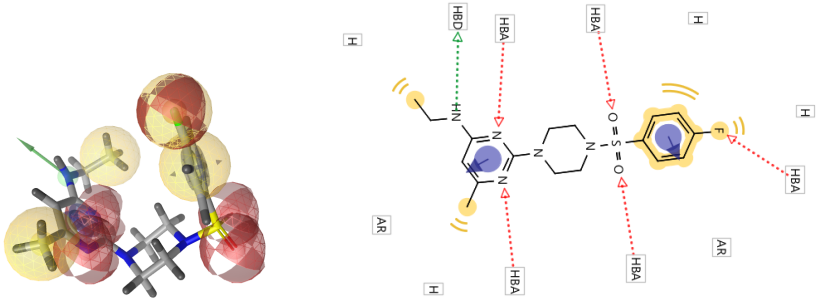

FIGURE 1.1.2: 3D and 2D pharmacophore model of hit **1** of the CHVB-compound series. Hydrogen bond donor (HBD): green; hydrogen bond acceptor (HBA): red; aromatic ring (AR): purple; hydrophobic interactions (H): yellow.

pharmacophore models are used as a query for the screening of an extensive compound library [25–27]. A pharmacophore can be considered an abstract description of steric and electronic molecular features that are (predicted as) necessary for the biological activity [28, 29]. Figure 1.1.2 gives an example of a pharmacophore model with its pharmacophore features.

1.1.1.2 Scaffold Hopping for Novel Hit Identification

Another possible approach to identify a new hit compound is a scaffold hop (or lead hop). Scaffold hopping is a computer-aided search for compounds with different central core structures of a bio-active molecule while retaining the desired activity. This is a common approach to access new territories of chemical space, reach free intellectual properties, and gain chemical structures with potentially improved characteristics for drug development (e.g., improved synthetic accessibility, toxicity or absorption, distribution, metabolism, and excretion (ADME) properties), while keeping the same activity profile [30–32].

A similar approach is the bioisosteric replacement. While the scaffold hop replaces the core framework of a molecule to identify similar novel potent compounds, the bioisosteric replacement approach involves "swapping" functional groups of the compound with their bioisosteres to improve the druggability of the compound [33]. Harris L. Friedman first described bioisosteres as molecules that: "*...fit the broadest definition of isosteres and have the same type of biological activity...*" [34]. Isosteric molecules or substructures possess the same number of atoms and valence electrons and can be defined more broadly as chemical entities with similar physiochemical properties [35, 36]. Alfred Burger extended this definition of bioisosteres to molecules with near similar molecular shapes and volumes, approximately the same distribution of electrons, similar physical properties, and the capability of similar biological activity [36, 37]. He further classified bioisosteres into classical and nonclassical bioisosteres, where the former includes groups with the

same valence electrons as well as ring equivalents. In contrast, the groups in the latter do not possess the same number of atoms or follow the same steric or electronic rules as the classical bioisosteres but yield similar biological activity (see Table 1.1) [36, 38].

Table 1.1: Example of classical and nonclassical bioisosteres [39].

Classical Bioisosteres					
$-O-$	$-S-$	$-Se-$	$-CH_2-$	$-NH-$	
Nonclassical Bioisosteres					
	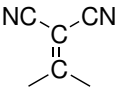		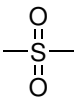	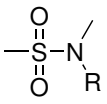	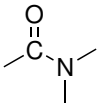

As bioisosteric replacement is generally used for lead optimisation and scaffold hopping, both methods can be seen as twin concepts. These two approaches replace a part of a bioactive molecule with a substructure to keep the bioactivity. Therefore, combining these methods can increase the structural diversity of a drug design project [33].

1.1.2 Lead Generation

Lead generation, also referred to as hit to lead optimisation, aims to refine the discovered hit to an optimised lead compound with improved potency, selectivity, and physicochemical characteristics. In this stage, suitable synthesis strategies are established to gain access to the desired compound, and appropriate *in silico*, *in vitro*, and *in vivo* assays are conducted to screen the compound for possible deficiencies in important drug-like properties [9, 40].

An overview of some key characteristics considered in the lead generation phase is shown in Table 1.2. This table should give an idea of the various parameters considered in lead generation. As drug development is a continuous process and every hit series faces different challenges, the investigated properties may vary from this list or are investigated in the next phase (lead optimisation).

A common strategy during the lead generation is an intensive and systematic SAR investigation around the chemical scaffold of the compound with the aim of identifying specific structural characteristics of a compound series that are associated with its biological activity (e.g., lipophilicity, hydrophilicity, flexibility, size). Multiple chemical modifications of the hit compounds are made and evaluated for their biological activity. The identified characteristics give an insight into the structural and chemical requirements of the compound series for high biological activity [8, 28, 49].

TABLE 1.2: Some Key Properties Evaluated During the Lead Generation Process.

Drug Properties	**Possible Parameters**	**Purpose**	
Potency	EC_{50}[a]	Lowest efficacious dose desirable	[41]
Selectivity	SI[b]	Minimisation side effects associated with other targets or toxicity	[41]
Patent status	–	Hit compound structures must be patentable	[41]
Physicochemistry	Aqueous solubility $LogD_{7.4}$[c]	Desired drug-like properties for performability of *in vitro* assays and sufficient *in vivo* delivery of drug	[42, 43]
Metabolism	Half-life time[d]	Prediction of relative clearance *in vivo* and dose frequency. High metabolic stability desired	[44]
Enzymology	CYP450 inhibition[e]	Prediction of potential toxicity drug-drug interactions	[45]
Permeability	Caco-2/MDR1-MDCK permeability[f]	Drug must be absorbed and reach the desired target	[8, 46]
Toxicity	Cytotoxicity in suitable cell line (e.g., HepG2)	Reduce the likelihood of cellular toxicity in vivo	[8, 47]
Pharmacological Safety	hERG interactions[g]	Reduce the likeliness of undesirable side effects	[48]

(a) The half maximal effective concentration (EC_{50}) is the compound concentration required to show 50% of bio-activity. (b) The selectivity index (SI) can be defined as the ratio of the toxic concentration of a sample against its effective bio-active concentration. (c) $LogD_{7.4}$ is a lipophilicity descriptor and refers to the water:octanol partition coefficient at pH 7.4. (d) The half-life time is the time it takes for a drug's active substance in the human body to reduce by half. (e) CYP450 are the main enzymes in the human body for drug metabolism. Their inhibition can cause toxicity. (f) Caco-2 colon carcinoma cells are used to examine the permeability across the intestinal epithelium. MDCK cells transfected with the MDR1 gene (encodes the efflux protein P glycoprotein (P-gp)) can be used to predict intestinal and brain permeability. (g) The inhibition of the human Ether-à-go-go-Related Gene (hERG) can cause severe cardiac adverse effects. [8]

1.1.3 Lead Optimisation

This final stage of the drug discovery phase aims to generate preclinical development candidates by maintaining the favourable properties of the lead compounds while enhancing their shortcomings. As already mentioned, the properties that determine the strategies and assays for lead optimisation can vary from compound series to compound

series. However, the lead compounds are generally further examined for their physicochemical and ADMET properties to identify a potentially safe compound with suitable pharmacokinetics [9, 28, 41].

Nevertheless, the synthetical exploration of the compound series is still ongoing to recover from a potential failure of the current lead in preclinical and clinical development [41].

1.2 The Chikungunya Virus

Chikungunya virus (CHIKV) is a mosquito-transmitted *alphavirus* that belongs to the *Togaviridae* family and was first described in 1952/53 in the Makonde plateau in Tanzania [50]. After sporadic and mainly local outbreaks in Africa and Asia, a new CHIKV mutation in 2004 led to a vector change from primarily *Aedes aegypti* to the more global *Ae. Albopictus* and thus enabling the virus to spread in new temperature areas colonised by *Aedes* mosquitoes [51, 52].

Consequently, CHIKV outbreaks are reported worldwide, causing millions of CHIKV infection cases every year [53–56]. Moreover, due to globalisation, climate change, and lack of immunity in the worldwide population, this rapid spread of CHIKV is not only ongoing, but it is also reaching new territories and higher numbers of infections every year [56–58].

Acute CHIKV infection leads to a febrile disease known as Chikungunya fever (CHIKF), characterised by high fever, arthralgia, maculopapular rash, nausea, severe joint pain, and myalgia [58, 59]. As approximately 50% of patients develop a painful chronic stage and complications in vulnerable groups (e.g., patients with comorbidities and the elderly) have been reported, CHIKV infections are now considered an imminent health threat [60, 61].

Despite the severity and worldwide spread, neither antiviral drugs nor vaccines are available - making the development of a potent CHIKV inhibiting drug crucial for CHIKF treatment [62, 63].

A comprehensive summary of current antiviral research and development of small-molecule inhibitors against CHIKV is presented in 1.2.1 [63]. This review gives a detailed description of the CHIKV spreading and replication cycle and highlights different approaches used to identify such compounds. Moreover, the identification and application of promising viral and host targeting small-molecule inhibitors are systematically discussed, and an overview of the current research development is given [63].

1.2.1 Current Research in Antivirals against Chikungunya Virus

viruses

MDPI

Review

Antivirals against the Chikungunya Virus

Verena Battisti, Ernst Urban and Thierry Langer *

Department of Pharmaceutical Sciences, Pharmaceutical Chemistry Division, University of Vienna, A-1090 Vienna, Austria; verena.battisti@univie.ac.at (V.B.); ernst.urban@univie.ac.at (E.U.)
* Correspondence: thierry.langer@univie.ac.at

Abstract: Chikungunya virus (CHIKV) is a mosquito-transmitted alphavirus that has re-emerged in recent decades, causing large-scale epidemics in many parts of the world. CHIKV infection leads to a febrile disease known as chikungunya fever (CHIKF), which is characterised by severe joint pain and myalgia. As many patients develop a painful chronic stage and neither antiviral drugs nor vaccines are available, the development of a potent CHIKV inhibiting drug is crucial for CHIKF treatment. A comprehensive summary of current antiviral research and development of small-molecule inhibitor against CHIKV is presented in this review. We highlight different approaches used for the identification of such compounds and further discuss the identification and application of promising viral and host targets.

Keywords: Chikungunya virus; alphavirus; antiviral therapy; direct-acting antivirals; host-directed antivirals; in silico screening; in vivo validation; antiviral drug development

Citation: Battisti, V.; Urban, E.; Langer, T. Antivirals against the Chikungunya Virus. *Viruses* **2021**, *13*, 1307. https://doi.org/10.3390/v13071307

Academic Editor: Leen Delang

Received: 9 June 2021
Accepted: 30 June 2021
Published: 5 July 2021

1. Introduction

Chikungunya virus (CHIKV) is a mosquito-borne alphavirus and belongs to the *Togaviridae* family. The virus was first isolated from a febrile patient in 1952/53 in the Makonde plateau (Tanzania) and has been named after the Makonde word for "that which bends you up", describing the characteristic posture of patients suffering severe joint pains due to the CHIKV infection [1]. In the following years, only local and periodic outbreaks have been documented. However, in 2004 the CHIKV re-emerged at the coast of Kenya, spreading to La Reunion Island and surrounding island in the Ocean and South Asia [2]. A new CHIKV mutation with the A226V amino acid variant in the envelope glycoprotein E1 (CHIKV 06.21) was reported during that outbreak. This mutation, along with specific mutations in the E2 protein, allowed the virus to expand its vector potential from primarily *Aedes aegypti* to the more global *Aedes albopictus* and thus permitting the virus to spread in different temperature zones [3].

Consequently, in 2013 a CHIKV outbreak was reported on the Caribbean island St. Martin, following Brazil in 2014 and afterwards the rest of the American continent –causing more than 1.2 million cases of CHIKV infection in one year [4,5]. Furthermore, the first autochthonous outbreaks started to occur also in Europe (Italy and France) [6–9]. Due to globalisation, climate change, and lack of immunity in the worldwide population, this global spreading of the CHIKV is still ongoing-reaching new territories and higher numbers of infections [10–12].

Infection with the Chikungunya virus causes a high onset of fever for 3 to 10 days, followed by rash, myalgia, nausea, and severe joint pain [12]. Although this Chikungunya Fever (CHIKF) is rarely fatal, in approximately 50% of infected patients, the severe arthralgia and myalgia can last for months to years even after clearance of the viral infection [13]. However, the precise mechanism of these chronic CHIKF symptoms is still unclear. Furthermore, complications in patients with comorbidities and the elderly have been reported [14]. Up today there are no licensed drugs or vaccines available, and the alleviation of symptoms by, e.g., NSAIDs, is the only possible treatment for CHIKF patients [15].

2. CHIKV Replication Cycle

Like other alphaviruses, the entry of the CHIKV in cells involves the initial interaction of viral proteins with attachment factors and specific receptors from the host cell [16]. The CHIKV virion's surface contains 80 trimeric spikes of E1 and E2 glycoproteins [17]. E2 facilitates the viral attachment to the host cell by interacting with surface host receptors followed by clathrin-mediated endocytosis (CME). The fusion of the viral membrane with the membrane of the host is triggered by a low pH environment leading to conformational changes of the viral envelop glycoprotein E1 [17]. Subsequently, the viral nucleocapsid is released into the cytoplasm, where it is disassembled to release the viral genome. The viral genome is then translated by the host cell translation machinery creating the non-structural-polyprotein P1234, which is cleaved into the precursor P123 and the viral non-structural-protein nsP4 [18]. P123 and nsP4 form the early replication complexes (RCs). They are responsible for synthesising the negative-strand RNA as a template to synthesise the desired positive-strand genomic RNA and sub-genomic RNA (26S RNA). Eventually, the formation of the P123 and nsP4 reaches a concentration threshold and the cleavage of the precursor P123 into fully processed nsPs is triggered. The 26S RNA, on the other hand, serves as the mRNA encoding the structural viral proteins C-pE2-6K-E1 [19–21].

Once formed, the capsid protein (C) is released by its autocleavage activity, while the remaining pE2-6K-E1 precursor is processed in the endoplasmic reticulum (ER) into pE2, 6K, and E1. While pE2 and E1 form heterodimer complexes, the cleaved capsid protein binds newly synthesised viral RNA, initiating to form the nucleocapsid core. This complex migrates towards the cell membrane through the Golgi secretory pathway, where pE2 is cleaved by the host enzyme furin or furin-like proteinases into the mature E2 and E3. E2 and E3 interact with the already formed nucleocapsid core and encapsidate the remaining viral RNA genome. Finally, the nucleocapsid core is recruited to the cell membrane where the particle buds from the cell where a new replication cycle begins [21–23].

3. Strategies for Identification of Antiviral Compounds

Various approaches have been utilised to identify antiviral compounds, such as cell-based high-throughput screening (HTS) and computational methods, including rational structure-based drug design on known crystal structures or homology models of viral and proviral host proteins. The most conventional method is the cell-based HTS with the virus-induced cytopathic effect (CPE) as readout. This method has the advantage of providing two simultaneous data points—the antiviral activity of the screened compounds and their cytotoxicity. Different compound libraries were used for the in silico and in vitro screening, ranging from libraries containing only FDA-approved drugs and libraries with compounds showing special chemical features to fragment-based libraries. The fast and economic computer-aided drug design has also been widely used for the identification of novel lead compounds by virtual screening. The identified hits were often further optimised by structure–activity relationship (SAR) assays. In addition, resistance selection in the presence of a compound was often performed in cell-based assays to identify the target protein of such compounds and give valuable insight into the viral pathways.

Theoretically, all involved factors of the viral replication cycle could be potential targets for antiviral compounds. Like other viruses, the CHIKV uses a variety of interactions of viral proteins and host factors for its replication. The known and utilised proviral host factors are discussed below. Targeting such a host factor could provide broad-spectrum antiviral compounds as many viruses use the same replication strategies. On the other hand, unwanted side effects are more often seen in compounds with such an approach. Therefore, a combination of antiviral compounds with a different mechanism of action could provide a synergistic effect, leading to the reduction of antiviral drug concentration and thus may help decrease serious side effects. Moreover, such a combination could prevent the formation of drug resistance.

4. Virus Targeting Inhibitors

A comprehensive overview of small molecules targeting viral proteins is given in Table 1. Furthermore, compounds with suggested viral target but without confirmation of the mode of action are summarized in Table 2. Studies without any in vivo or in vitro data were excluded. It is worth mentioning that the values given in Tables 1 and 2 are not directly comparable to each other as they performed experiments, and setups differed between the discussed studies. Different virus strains, readouts (e.g., CPE and virus titer reduction) and cell lines were, for example, used and influence the assay results.

Table 1. Virus targeting compounds [a].

		In Vitro				In Vivo		
Compound [b]	**Viral Target [c]**	**EC_{50} (μM) [d]**	**CC_{50} (μM)**	**SI**	**Cell Line**	**Efficacy**	**Mouse Model**	**Ref.**
Arbidol *	E2	12.2 ± 2.2	376	36	MRC5	—	—	[24]
Suramin *	E2	8.8 ± 0.5	>700	>39.1	BHK-21	Reduced viral burden and decreased foot swelling	C57BL/6	[25–27]
Picolinic acid	C	60.63% inhibition with 2 mM	n.s.	n.s.	Vero	—	—	[28]
Amantadine *	6K	29.51	n.s.	n.s.	Vero	—	—	[29]
MADTP (9b)	nsP1	1.2 ± 0.009	84 ± 19	70	Vero	—	—	[30–33]
CHVB-032	nsP1	2.7	>75	n.s.	Vero	—	—	[34,35]
Lobaric acid	nsP1	5.3 ± 0.4	50 ± 1.3	7	Huh-7	—	—	[36]
FHA	nsP1	0.12 ± 0.04	>250	>1000	Vero	—	—	[37,38]
FHNA	nsP1	0.18 ± 0.11	>250	>1000	Vero	—	—	[37,38]
5-IT	nsP1	0.409	>50	n.s.	Vero	—	—	[39]
Compound 25	nsP2	3.2 ± 1.8	101 ± 50	32	Vero	—	—	[40–42]
Compound 8	nsP2	1.5	>200	>133.3	BHK-21	—	—	[43]
ID1452-2	nsP2	31	>31	n.s.	HEK293T	—	—	[44]
Novobiocin *	nsP2	20	n.s.	n.s.	Vero	—	—	[45]
Telmisartan *	nsP2	45	n.s.	n.s.	Vero	—	—	[45]
SRI-43750	nsP3	23	>40	n.s.	NHDF	—	—	[46]
Favipiravir *	nsP4	25 ± 3	>636	n.s.	Vero	decreased mortality by >50% and improved disease outcome	AG129	[47]
						Reduced viral replication in joints	C57BL/6J	[48]
NHC	nsP4	0.2 ± 0.1	7.7	n.s.	Vero	—	—	[49,50]
Sofosbuvir *	nsP4	2.7 ± 0.5	402 ± 3 2	149	Huh-7	Reduced viremia and joint pain	SwissWebster	[51]
Compound-A	nsP4	0.54 ± 0.08	3.70 ± 0.32	n.s.	Vero	—	—	[52]

[a] EC_{50}, 50% effective concentration (if no EC_{50} value was reported another readout is presented); CC_{50}, 50% cytotoxic concentration; SI, selectivity index; n.s., not specified; —, not determined; *, repurposed drug. [b] If the study reported a compound series/class with anti-CHIKV activity, the antiviral data of the most potent or most representative compound is reported. Only compounds with in vitro or in vivo data are included. [c] Compounds are only included in Table 1 if there is enough data about the mode of action. [d] If a compound was reported in multiple studies, cell lines, and CHIKV strains, the best activity value with the corresponding cell line is listed.

Table 2. Compounds with suggested viral target but without a clear mode of action [a].

Compound [b]	Suggested Viral Target	In Vitro				In Vivo		Ref.
		EC_{50} (μM) [c]	CC_{50} (μM)	SI	Cell Line	Efficacy	Mouse Model	
IIc	E2	6.5 ± 1	156	22	Vero	—	—	[53]
Bis(benzofuran-thiazolidone)s (3g)		1.5	>200	<133	Vero	—	—	[54]
LQM334	E2	81.1 ± 6.4% viral inhibition	n.s.	n.s.	Vero	—	—	[55]
Micafungin *	E1/E2	17.2 ± 1.08	>100	>5.81	U2OS	—	—	[56]
Doxycycline *	E2/nsP2	15.51 ± 1.62	n.s.	n.s.	Vero	+ ribavirin: Reduction of pathological signs and virus titre	Adult ICR	[57]
AP4	C	10.66 ± 2.25	2172 ± 104	n.s.	Vero	—	—	[58]
EAC	C	4.01 ± 1.96	1657 ± 1109	n.s.	Vero	—	—	[58]
PSU	C	22.91 ± 3.83	2505 ± 0683	n.s.	Vero	—	—	[58]
MBZM-N-IBT	nsP2	38.68	>800	>21	Vero	—	—	[59]
1,3-thiazolidin-4-one (compound 7)	nsP2	0.42	>100	n.s.	Vero	—	—	[60]
peptidomimetic 3a	nsP2	8.76	n.s.	n.s.	Vero	—	—	[61]
PEP-I	nsP2	34	Maximum nontoxic dose is 50 μM	n.s.	BHK-21	—	—	[62]
Nelfinavir *	nsP2	14 ± 1	22 ± 6	1.6	Vero	—	—	[63]

[a] EC_{50}, 50% effective concentration (if no EC_{50} value was reported another readout is presented); CC_{50}, 50% cytotoxic concentration; SI, selectivity index; n.s., not specified; —, not determined; *, repurposed drug. [b] If the study reported a compound series/class with anti-CHIKV activity, the antiviral data of the most potent or most representative compound is reported. Only compounds with in vitro or in vivo data are included. [c] If a compound was reported in multiple studies, cell lines, and CHIKV strains, the best activity value with the corresponding cell line is listed.

4.1. Viral Entry and Membrane Fusion

Many different factors and, therefore, potential targets are involved in the viral entry and fusion of the CHIKV, making it a widely used target for many antiviral compounds. The broad-spectrum antiviral drug arbidol (Figure 1), also known as umifenovir, and its metabolites, have shown to be early-stage inhibitors of CHIKV replication in different cell lines. The mode of action was confirmed by selecting an arbidol-resistant variant carrying an arginine (G407R) mutation localised in the viral E2 glycoprotein–a type I transmembrane protein involved in the virus binding to the host membrane [24]. Indole-based arbidol analogues with sulfoxides and tert-butyl esters have demonstrated an increased potency and selectivity index. Although docking studies with the most promising analogue IIc (Figure 1) identified two potential binding sites in E2, a post entry inhibition of CHIKV was observed in a time of addition assay. Furthermore, IIc was ~6-fold less potent than arbidol in an entry assay with CHIKV pseudoparticles—suggesting that IIc may have a different mode of action [53,64].

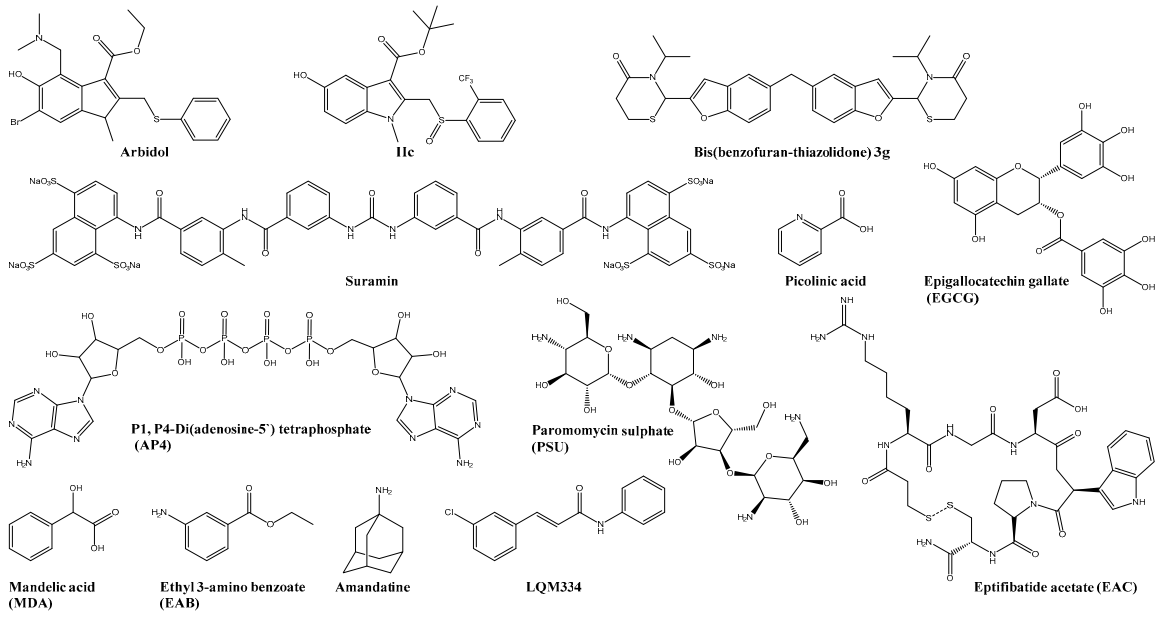

Figure 1. Chemical structure of virus-targeting compounds. Inhibitors of viral entry and membrane fusion: arbidol, IIc, suramin, epigallocatechin gallate, bis(benzofuran-thiazolidone) 3g, and LQM334. Inhibitor of the viral capsid protease: picolinic acid, mandelic acid, ethyl 3-aminobenzoate, P1, P4-di(adenosine-5′) tetraphosphate, eptifibatide acetate, and paromomycin sulphate. Inhibitor of 6K Protein: amantadine.

Suramin (Figure 1), a symmetrical sulfonated naphthylurea compound and an FDA approved drug against trypanosomiasis, has also demonstrated to inhibit the early-stage of the CHIKV replication cycle in different independent studies–using not only time of addition assays but also in silico methods [25,27,65]. A more detailed investigation of the mechanism of action was performed by Albulescu et al., where suramin was found to interact directly with the viral particles of CHIKV by inhibiting the viral attachment to the host membrane and interfering with the fusion step by suppressing the conformational changes of viral envelope glycoproteins [66]. Moreover, suramin showed a synergistic effect with the green tea catechin epigallocatechin gallate (EGCG, Figure 1)—a known in vitro early-stage inhibitor of CHIKV infection [67,68]. Although an in vivo study with CHIKV-infected C57BL/6 mice demonstrated amelioration of CHIKV-induced foot swelling, inflammation, and cartilage damage, clinical trials have shown severe side effects during long term treatment of suramin [26,69,70]. Additionally, the suramin-based analogues with the chemical structures of bis(benzofuran-thiazolidinone)s (Figure 1) and bis(benzofuran-thiazinanone)s demonstrated a 29–42 fold more potent anti-CHIKV activity than suramin, but their high toxicity remains an unsolved issue [54].

An in silico screening experiment based on a molecular docking approach utilising a variety of biological targets of CHIKV and the following in vitro evaluation by an MTT assay of the obtained hits identified LQM334 (Figure 1) as a promising inhibitor of CHIKV. The mode of action of the newly found lead compound remains unclear, but a molecular docking study indicates a possible interaction between LQM334 and the E2 domain A from the mature E3-E2-E1 glycoprotein complex [55]. In addition, Agarwal et al. performed an in silico docking study using the structure of the envelope glycoprotein of CHIKV to identify promising new lead compounds, but the in vitro confirmation of their antiviral activity has still to be shown [71].

Micafungin, an FDA approved drug to treat candidiasis, showed a broad spectrum of inhibitory effects against different alphaviruses—including SINV, SFV and CHIKV. Although a molecular docking study indicated a possible interaction with the CHIKV envelope glycoprotein, a time of addition assay also pointed to a late-stage inhibition of the CHIKV infection, indicating an inhibitory effect against viral replication, extracellular and cell-to-cell transmission of CHIKV [56].

4.2. Capsid Protease

The pyridine containing compound Picolinic acid (PCA, Figure 1) is a known antiviral against various viruses, including the alphavirus SINV. Furthermore, PCA was demonstrated to bind the hydrophobic region of CHIKV capsid protein, interfering with the interaction of the cytoplasmic domain of E2 glycoprotein (cdE2) and the capsid, which is needed to facilitate the budding of the virus from the plasma membrane of the host cells [28,72]. A significant reduction in vRNA levels and infectious virus was observed when treated with PCA [28]. The same research group used these findings in combination with other studies about proposed capsid protease inhibitors such as dioxane and piperazine to perform an in silico screening for potential new lead compounds targeting the capsid protease [28,73–76]. Their most promising hits (S)-(+)-mandelic acid (MDA, Figure 1) and ethyl 3-aminobenzoate (EAB, Figure 1) showed better binding tendencies than dioxane and PCA in silico, but the in vitro evaluation of their antiviral activity is still pending [76]. More recently, a structure-assisted drug-repositioning study based on in silico screening and ranking of the hits by their docking score identified three compounds targeting the auto-proteolytic activity of the capsid protease: P1, P4-Di(adenosine-5′) tetraphosphate (AP4, Figure 1), eptifibatide acetate (EAC, Figure 1) and paromomycin sulphate (PSU, Figure 1) [58].

4.3. 6K Protein

The potential of the 6K protein as a possible target for antiviral drug development demonstrates the potent antiviral drug amantadine. This FDA approved anti-influenza drug targets the ion channel-forming M2 viroporin of the influenza virus [77]. Furthermore, electrophysiology experiments indicated that amantadine hinders the ion channel activity of CHIKV 6K and alters the morphology of CHIKV virus-like particles. The anti-CHIKV potential of amantadine was shown in infected Vero cells [29].

4.4. Non-Structural Proteins

4.4.1. Non-Structural Protein 1 (nsP1)

The first class of small molecules reporting the nsP1 of CHIKV as the potential target is the MADTP series (Figure 2), with a triazolopyrimidinone scaffold and MADTP-314 as the initial lead compound [30–33]. Overall, three consecutive structure–activity-relationship studies were performed-aggregating detailed information about the influence of various structural changes and demonstrating potent inhibitory effects on various CHIKV strains and VEEV nsP1 in an enzymatic assay [30,32,33]. The selection of a MADTP-resistant CHIKV strain in cell culture and the following reverse genetics identified the single-amino-acid substitution P34S in the GTase functional domain of nsP1 as responsible for the MADTP-resistance [31]. Recently, 2-(4-(Phenylsulfonyl)piperazine-1-yl)pyrimidine analogues, i.e., the CHVB series (Figure 2), were identified as potent and selective anti-CHIKV compounds and analysed based on their structure–activity relationship [34]. In addition, CHVB compounds showed potent inhibitory effects of the MTase and GTase activities of nsP1 of Semiliki Forest virus (SFV) and VEEV [35]. Interestingly, a CHVB-resistant virus demonstrated cross-resistant to the MADTP series, suggesting that both compound families utilise a similar mode of action. However, the CHVB series required the presence of at least two mutations in nsP1, namely, S454G and W456R, indicating that the barrier of resistance is higher for the CHVB series and the occurrence of resistance in clinical settings is less likely [35].

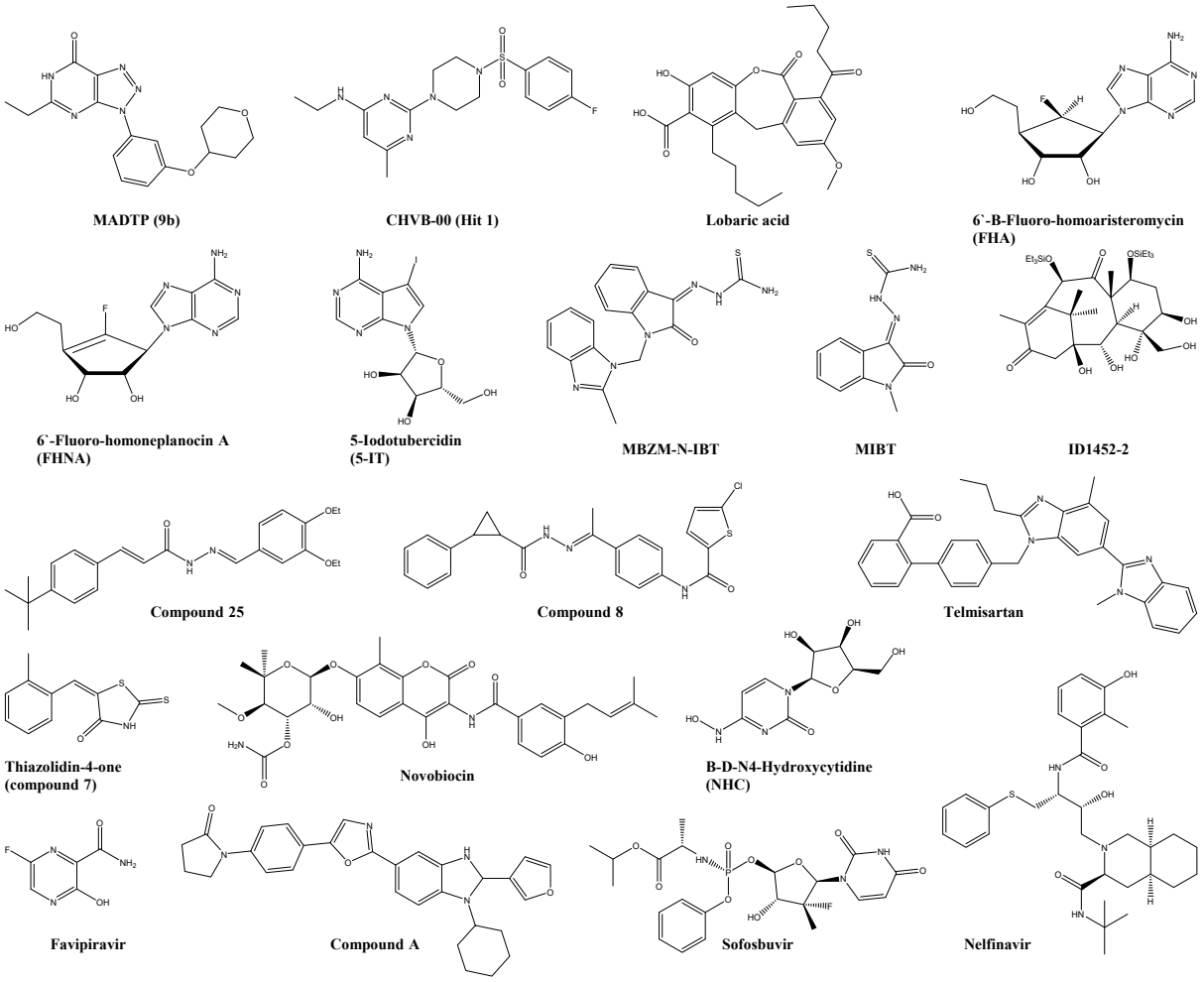

Figure 2. Chemical structure of virus-targeting compounds. Inhibitors of nsP1: MADTP, CHVB, lobaric acid, 6′-β-fluoro-homoaristeromycin, 6′-fluoro-homoneplanocin A, and 5-iodotubercidin. Inhibitor of nsP2: compound 25, compound 8, MBZM-N-IBT, MIBT, thiazolidin-4-one, ID1452-2, telmisartan, novobiocin, and nelfinavir. Inhibitor of nsP4: favipiravir, β-D-N4-Hydroxycytidine, sofosbuvir, and compound-A.

A fluorescence polarisation-based assay measuring the GTP binding site was used to perform an HTS and led to the identification of a series of hits [36]. The cherrypicked hits were subsequently not only evaluated with an orthogonal assay to measured their ability to interfere with the guanylation step of the capping reaction of nsP1 but also tested for their antiviral activity [36]. These findings led to the identification of the naturally-derived compound, lobaric acid (Figure 2), as a potent CHIKV nsP1 inhibitor [36].

More recently, two carbocyclic adenosine analogues, namely, 6′-β-fluoro-homoaristero mycin (FHA, Figure 2) and 6′-fluoro-homoneplanocin A (FHNA, Figure 2), have been identified as inhibitors of the MTase activity of nsP1 by screening a library designed to inhibit the host target SAH hydrolase (see 5.5.1.1. Hydrolases) [37,38]. Resistance selection unveiled two mutations G230R and K299E in nsP1 to develop resistance against both compounds [38]. Additionally, 5-iodotubercidin (5-IT, Figure 2) showed also an inhibitor of the MTase activity of nsP1 in a capillary electrophoresis-based assay [39]. This derivate of tubercidine and a known adenosine kinase inhibitor demonstrated potent anti-CHIKV activity in a plaque-reduction assay [39].

4.4.2. Non-Structural Protein 2 (nsP2)

The nsP2 has become a significant target of interest in the development of anti-CHIKV drugs primarily because of its essential role in the CHIKV replication but also because of

its relatively early publication of its 3D structure (PDB: 3RTK) [78]. This led to a significant number of publications focussing on the in silico approach to identify potential new nsP2 inhibitors [79–87]. However, for all of those hits predicted in these studies, no in vitro evaluation was made. This vital evaluation step was made by Bassetto et al. by the combination of virtual screening with an optimised homology model of nsP2 and the following evaluation by virus-cell-based CPE reduction assay [40]. This approach led to discovering the first lead compound, compound 25 (Figure 2), with potential nsP2 protease inhibition activity. Two following structure–activity-relationship studies with altogether 100 analogues were additionally performed by this research group to determine the compound series's critical components and investigate the impact of some chemical-structure changes on antiviral activity and water solubility [41,42]. Interestingly, molecular docking on nsP2 showed no significant differences in binding mode between the most active compound (compound 25 with EC_{50} = 3.2 μM) and some of its poorly active analogues. In their virtual screening study based on pharmacophoric features of the initial hit of Bassetto et al., Das et al. describe a set of 12 compounds with anti-CHIKV activity with the most potent inhibitor compound 8 (EC_{50} = 1.5 μM, Figure 2) [40,43]. A cell-free protease assay was performed to verify their effects on nsP2, in which the majority of the compounds demonstrated inhibitory effects against nsP2 [43]. Surprisingly, the initial hit of Bassetto et al. did not show any inhibition [40,43]. However, three analogues showed significant inhibitory effects, pointing to two different sites of actions in the compound series [41,43]. This example highlights the significance of biological evaluations of in silico predictions as they may sometimes not correlate with the in vitro results. On the other hand, molecular docking and molecular dynamic simulations may be an economical and fast starting point to investigate a possible mode of action of potential new antiviral drugs. Mishra et al. used such a computational approach to examine the target of their antiviral compounds MBZM-N-IBT and MIBT (Figure 2) [59]. Although their docking result points to an nsP2 inhibition, a time-of-addition assay revealed an early stage and a late-stage inhibition of the CHIKV–indicating multiple modes of actions. Another study described five arylalkylidene derivates of 1,3-thiazolidin-4-one (Figure 2) with low micromolar antiviral concentrations and interactions with the nsP2 protease domain in MD-simulations [60].

Small peptidomimetics were discovered using quantum mechanics-based ligand descriptors and biologically evaluated in virus-cell-based assay [61]. Docking of the most potent analogues, peptidomimetic 3a/4b, with the crystal structure of nsP2 exposed the advantage of lower molecular weight in this compound series, likely due to their more accessibility to the target pocket [61]. Other peptidomimetics, PEP-I and PEP-II, were identified by screening based on pharmacophoric features derived from nsP2-nsP3/4 (protein-peptide) interaction and evaluated by their anti-CHIKV activity using plaque reduction assay [62,88]. Their inhibitory effect on chikungunya nsP2 protease and the proteolytic activity of nsP2 was investigated by a FRET-based protease assay [62]. Both compounds inhibited their target protein in the micromolar range [62].

The natural compound, ID1452-2 (Figure 2), was discovered by high-throughput screening to identify small molecules targeting the chikungunya nsP2 protease [44]. ID1452-2 showed moderate anti-CHIKIV activity (IC_{50} = 31 μM) and inhibited nsP2 effects in dose-dependent manner [44]. More recently, a target-based drug screening with 30,000 FDA approved molecules and SPR experiments identified telmisartan (Figure 2), an antihypertensive drug, and the antibiotic novobiocin (Figure 2) as a strong inhibitor of the chikungunya nsP2 protease [45]. Both drugs inhibited the nsP2 protease activity in low micromolar concentrations [45]. This strategy of repurposing of FDA approved drugs were also used by Bhakat et al. to accelerate the identification and development of future anti-CHIKV drugs [63]. MM/GBSA-based binding free energy results and molecular docking on nsP2 determined nelfinavir (Figure 2), an HIV/HCV inhibitor, as a potential new anti-CHIKV drug [63]. This compound showed a moderate antiviral effect in the CPE-reduction assay [63].

4.4.3. Non-Structural Protein 3 (nsP3)

No small molecules targeting CHIKV nsP3 are reported up to date. Recently, a fragment library and x-ray crystallography screening led to the discovery of 40 fragments binding to the distal ribose binding site of ADP-ribose in the nsP3 macrodomain crystal structure (PDB-code: 6VUQ) [46]. As most of the fragments share a similar pyrimidine-based scaffold, it could be an interesting starting point for further development of a CHIKV nsP3 inhibitor [46]. A similar approach to identify small molecules with anti-nsP3 activity was conducted by Nguyen et al. [89]. With virtual screening and molecular docking, various hits were detected, but the ability of the compounds to inhibit the CHIKV in vitro has not yet been published [89].

4.4.4. Non-Structural Protein 4 (nsP4)

The nsP4 protease functions as an RNA-dependent polymerase (RdRp) and is the most highly conserved protein in the alphavirus family [90]. Consequently, many compounds targeting this protease have been reported to inhibit the CHIKV and other alphavirus replication cycles. Favipiravir (T-705, Figure 2) and its defluorinated analogue T-1105, for example, were reported to inhibit in vitro replication of different CHIKV strains as well as other (arthritogenic) alphaviruses [47]. All favipiravir resistant CHIKV strains carried a unique K291R mutation in a highly conserved F1 motif of the RNA-dependent RNA polymerase of +ssRNA viruses in nsP4 [47]. This highly conserved lysine is crucial for the anti-CHIKV activity and responsible for the broad-spectrum antiviral activity of T-705 [91]. In addition, a CHIKV-mouse model of lethal infection in AG129 mice, favipiravir treatment (300 mg/kg/day for seven days) prevented the development of severe neurological disease and increased the survival rate [47]. Further, favipiravir treatment (300 mg/kg/day for four days) in C57BL/6J mice reduced the viral replication in the joints when administered in the acute phase and prevented systemic viral spread [48]. Recent findings highlight the influence of different cell lines on the antiviral outcome in biological assays of T-705 and the impact of various CHIKV strains on the disease severity in mouse strains, and the efficacy of favipiravir treatment [92,93].

Another nucleoside analogue, β-D-N^4-hydroxycytidine (NHC, Figure 2), showed more potent anti-CHIKV effects in Vero Cells than the control nucleoside analogues favipiravir and ribavirin [49]. The alphavirus VEEV needs for the development of even low-level resistance against NHC multiple cooperative mutations within the RdRp of nsP4 [50]. Additionally, NHC has shown in a time-of-addition assay to have no effect on viral entry but in the early stage of the CHIKV replication circle [49]. Both findings indicate the RdRp domain of nsP4 as the potential target of NHC, but the precise mode of action remains unclear.

Sofosbuvir (Figure 2), the FDA approved drug against hepatitis C virus, and uridine analogue also showed interesting activity against CHIKV in different cell lines [51]. Additionally, treatment with sofosbuvir in the CHIKV-mouse model of adult Swiss mice (20 mg/kg/day) protected against CHIKV-induced disease and increased the survival rate of neonate mice (40 and 80 mg/kg/day) [51].

Although the nsP4-targeting compounds have shown to be primarily nucleoside analogues, a high throughput screening of chemical compound libraries identified compound-A (Figure 2) as a CHIKV infection inhibitor [52]. This benzimidazole-related compound inhibited several different CHIKV strains and SINV strains in Vero cells [52]. A key mutation for development compound-A resistance was identified in a mechanism of action study–the M2295I residue located in the functional domain of RdRp of nsP4 [52]. Kumar et al. conducted an in silico study on a CHIKV nsP4 homology model to identify potential new hits. However, the biological evaluation of their collected data has yet to be done [94].

5. Targeting Host Factors

As discussed above, a variety of proviral host factors have been shown to influence the viral replication cycle. Therefore, many small molecules modulating such factors have been reported to possess antiviral activity. A comprehensive overview of anti-CHIKV

compounds with proviral host targets is given in Table 3. The same criteria for inclusion and issues with data comparison as in Tables 1 and 2 (see Section 4, Virus Targeting Inhibitors) are also applied here.

5.1. Viral Entry and Membrane Fusion

Alphaviruses use a receptor-mediated endocytotic entry and pH-dependent fusion to release their viral RNA genome into the host cell cytoplasm. Recent findings in biochemistry and structural identification of involved proteins have given a valuable insight into this process, where many different host factors could be used as potential antiviral targets [16].

One of such antiviral compounds is chloroquine (Figure 3), a 9-aminoquinoline known since 1934 as an antimalarial drug [141]. It has been used in clinical trials against CHIKV even long before its anti-CHIKV effect was reported in vitro assays. The reasoning behind this unique approach lies in the lack of other treatment options and promising research results published before. Chloroquine and other NSAIDs such as mefenamic acid (see Section 5.3, Pyrimidine and Purine Synthesis Inhibitors) have been reported to inhibit the multiplication of various viruses (e.g., Sindbis, influenza A2, herpes simplex, etc.) in chick and mouse embryo cells [142,143]. Additionally, it has been shown to influence the pH-dependent fusion of the Sindbis virus and Semiliki Forest virus with the endosomal membrane by raising the endosomal pH in BHK-21 cells [144,145]. Other weak bases such as NH_4Cl, amantadine, methylamine and tributylamine showed similar lysosomotropic effects [144,145]. Moreover, chloroquine has been reported to lessen the joint inflammation of patient with rheumatoid arthritis in several trials in the 1950s [146]. The first clinical trial 1984 with chloroquine phosphate on 10 CHIKF patients was conducted after empirical observations that one of the patients joint pains improved while taking antimalarial drugs prophylactically [147]. Treatment with chloroquine led to alleviating patients' symptoms and opened the door for further clinical trials [147]. However, a randomised, double-blind, placebo-controlled, prospective trial (CuraChik trail) with 54 adult patients diagnosed with CHIKV showed no significant difference between the placebo and the chloroquine groups in terms of fever clearance time or viremia clearance time [148,149]. Moreover, patients treated with chloroquine were more likely to complain about persistent arthralgia ($p < 0.01$) and suffered moderate adverse effects of the treatment [148,149]. Another clinical trial showed no advantage of chloroquine treatment over the NSAID meloxicam in patients with early musculoskeletal pain and arthritis following acute chikungunya virus infection [150]. While the in vivo performance of chloroquine in humans and non-human primate models is limited, the in vitro effects of chloroquine are remarkable better [95,151–153]. These contradictory findings may be due to the immunomodulatory effects of chloroquine in vivo: it inhibits, i.e., IFN-I responses, which may influence the immune response to the viral replication negatively and may have been missed in the used Vero-E6 cells, which do not produce IFN-I [152].

Table 3. Host factor targeting compounds [a].

Compound [b]	Host Target [c]	In Vitro				In Vivo		Ref.
		EC_{50} (μM) [d]	CC_{50} (μM)	SI	Cell Line	Efficacy	Mouse Model	
Viral Entry and Membrane Fusion								
Chloroquine *	pH	7.0 ± 1.15	>260	37.14	Vero	—	—	[95]
Obatoclax *	Bcl-2/E1	0.03 ± 0.01	20.1 ± 4.8	670	BHK-21	—	—	[96]
Niclosamide *	pH	0.36 ± 0.08	>20	>55.55	U2OS	—	—	[97]
Nitazoxanide *	pH	2.96 ± 0.18	25	8.45	BHK-21	—	—	[97]
EIPA	pH **	Detectable inhibition observed at 0.03 μM	n.s.	n.s.	HSMM	—	—	[98]
Lipid Pathway Inhibitors								
Orlistat *	FASN	0.82	8.67	10.57	HEK293T	—	—	[99–101]
Cerulenin *	FASN	3	7.57	2.53	HEK293T	—	—	[99,100]
CAY10566	SCD1				HEK293T	—	—	[100]
TOFA	FASN	0.15	>60	n.s.	HEK293T	Reduction of the viral replication and joint swelling	C57BL/6	[99]
Tivozanib *	FLT4	0.8	8.34	n.s.	HEK293T	—	—	[99]
Pimozide *	calmodulin	0.28	19.18	69.75	HEK293T	Reduction of the viral replication and joint swelling	C57BL/6	[99]
Imipramine *	NPC **	Detectable inhibition observed at 10 μM	n.s.	n.s.	HFF1	—	—	[102]
U18666A	NPC **	Detectable inhibition observed at 0.63 μM	n.s.	n.s.	HFF1	—	—	[102]
LXR-623	LXRβ	2.50	63.30	25.3	HFF	—	—	[103]
Pyrimidine and Purine Synthesis Inhibitors								
Ribavirin *	IMPDH/ (viral) RdRp **	341.1	>30,000	24	Vero	+ doxycycline: Reduction of pathological signs and virus titre	Adult ICR	[57,104]
Merimepodib *	IMPDH	1.8 ± 1.0	27 ± 3	n.s.	Vero	—	—	[105]
6-Azauridine	OMP	0.816	208	204	Vero	—	—	[104]
DD363	DHODH	3.6 ± 0.6	87 ± 7	n.s.	HEK293T	—	—	[106,107]
RYL-634	DHODH	0.26	>2.5	>10	Vero	—	—	[108]
Atovaquone *	DHODH **	<0.75	>11.25	n.s.	Vero	—	—	[109]

Table 3. *Cont.*

Compound [b]	Host Target [c]	In Vitro				In Vivo		Ref.
		EC_{50} (μM) [d]	CC_{50} (μM)	SI	Cell Line	Efficacy	Mouse Model	
Protein Synthesis Inhibitors								
Halofuginone	EPRS	3 log_{10} viral titer reduction at 100 nM	n.s.	n.s.	HFF	—	—	[110]
Harringtonine		0.24	n.s	n.s.	BHK21	—	—	[111]
Sorafenib *	FLT4	0.16	n.s.	n.s.	Vero	—	—	[99,112]
Bortezomib *	UPS **	0.023	0.47	20.6	HeLA	—	—	[113]
SR9009 *	Rev-erb α/β **	100-fold reduction in viral titer at 10 μM	n.s.	n.s.	Huh7	—	—	[114]
Cellular Protein Inhibitors								
Sirtinol	SIRT	>2 log_{10} viral titer reduction at 200 μM	n.s.	n.s.	U2OS	—	—	[115]
Geldanamycin *	HSP90	2.5 log_{10} viral titer reduction at 1.4 μM	>100	n.s.	HEK293T	—	—	[116]
HS-10	HSP90	>2 log_{10} viral reduction in titre with 6.25 μM	>100	n.s.	HEK293T	Reduced viral titer, inflammation, and swelling	SVA129	[116]
SNX-2112	HSP90	>2 log_{10} viral reduction in titre with 6.25 μM	>100	n.s.	HEK293T	Reduced viral titer, inflammation, and swelling	SVA129	[116]
HA15	GRP78	reduction in titre with 25 μM	n.s.	n.s.	Vero	—	—	[117]
16F16	PDI	6.6 ± 0.45	8.9 ± 9.2	1.35	HEK293T	—	—	[118]
PACMA31	PDI	12.1 ± 0.3	12.2 ± 9.7	1.00	HEK293T	Less reduction in footbed swelling and viremia than in auranofin group	C57BL/6	[118]
Auranofin *	TRX	1.0 ± 0.13	1.6 ± 8.6	1.6	HEK293T	reduced footbed swelling and viremia	C57BL/6	[118]

Table 3. *Cont.*

Compound [b]	Host Target [c]	In Vitro				In Vivo		Ref.
		EC_{50} (μM) [d]	CC_{50} (μM)	SI	Cell Line	Efficacy	Mouse Model	
Cellular Enzyme Inhibitors-Hydrolases								
Amodiaquine *	Cathepsin B	18.3	>50	>2	HFF	—	—	[119]
DEAQ	Cathepsin B	17.3	>50	>2.9	HFF	—	—	[119]
Aristeromycin	SAH	0.8	6.3	7.9	Vero	—	—	[120]
6,6′-Difluoroaristeromycin (2c)	SAH	0.13	1.25	>9.6	Vero	—	—	[120]
Cellular Enzyme Inhibitors-Kinases								
Dasatinib *	SFK	>10-fold reduction in viral titer at 20 μM	>50	n.s.	NHDF	—	—	[121]
Torin 1	mTORC1/2	>10-fold reduction in viral titer at 1 μM	>1	n.s.	NHDF	—	—	[121]
CND3514	PKR **	2.2	>50	>22.7	HuH-7	—	—	[122]
Berberine	MAPK	1.8 ± 0.5	>100	>55.6	BHK21	Reduced viremia and disease symptoms	C57BL6/J	[123,124]
Miltefosine *	Pi3-Akt	antiviral activity was observed at 20–40 μM	n.s.	n.s.	hPDF	—	—	[125]
Prostatin	PCK	0.2 ± 0.05	50	n.s.	CRL-2522	—	—	[126]
Bryostatin analogue (4)	PCK	0.8 ± 0.1	>50	n.s.	BGM			[127,128]
Isothiazolo[4,3-b]pyridine (12r)	GAK	antiviral activity was observed <10 μM	n.s.	n.s.	Vero	—	—	[129]
Cellular Enzyme Inhibitors–Lyases/Transferases								
DFMO *	ODC1	200-fold reduction in viral titer at 500 μM	n.s.	n.s.	BHK-21	Low reduction in viral titer	C57BL6/J	[130]
Cellular Receptor Inhibitors–Channel-linked Receptors								
Digoxin *	Na^+/K^+ ATPase	0.049	>10	n.s.	U2OS	—	—	[20]
Lanatoside C *	Na^+/K^+ ATPase	38.99% reduction of viral titer with 1 μM	>1	n.s.	BHK-21	—	—	[131]
DIDS	CLIC1/4	8-fold reduction in viral titer	n.s.	n.s.	HuH-7	—	—	[132]
9-ACA	CLIC1/4	8-fold reduction in viral titer	n.s.	n.s.	HuH-7	—	—	[132]
NPPB	CLIC1/4	18-fold reduction in viral titer	n.s.	n.s.	HuH-7	—	—	[132]

Table 3. *Cont.*

Compound [b]	Host Target [c]	In Vitro				In Vivo		Ref.
		EC_{50} (μM) [d]	CC_{50} (μM)	SI	Cell Line	Efficacy	Mouse Model	
Cellular Receptor Inhibitors–Enzyme-linked Receptors								
5-NT	5-HT	2.8	>5	n.s.	U2OS	—	—	[133,134]
MM	5-HT	97 ± 1.0% viral reduction 10 μM	>10	n.s.	U2OS	—	—	[133]
Immunomodulatory Agents								
Tilorone *	IFN-inducer	4.2	32	7.6	Vero76	—	—	[135]
C11	STING	EC_{90}: 16.44 μM	>50	n.s.	THF	—	—	[136]
G10	STING	IC_{90}: 8.01 μM	n.s.	n.s.	THF	—	—	[137]
AV-10	TRIF	IC_{90}: 3.54 μM	n.s.	n.s.	THF	—	—	[138]
Pentosan polysulfate *	IL-10 inducer; decreased proinflammatory cytokines levels	—	—	—	—	Reduced disease symptoms	C57BL/6	[139]
Pixatimod *	HPSE **	0.51 ± 0.50	n.s.	n.s.	Vero	Reduced disease symptoms	C57BL/6	[140]

[a] EC_{50}, 50% effective concentration (if no EC_{50} value was reported another readout is presented); CC_{50}, 50% cytotoxic concentration; SI, selectivity index; n.s., not specified; —, not determined; *, repurposed drug; **, suggested target. [b] If the study reported a compound series/class with anti-CHIKV activity, the antiviral data of the most potent or most representative compound is reported. Only compounds with in vitro or in vivo data are included. [c] The host target is only reported if there is enough data about the mode of action. [d] If a compound was reported in multiple studies, cell lines, and CHIKV strains, the best activity value with the corresponding cell line is reported.

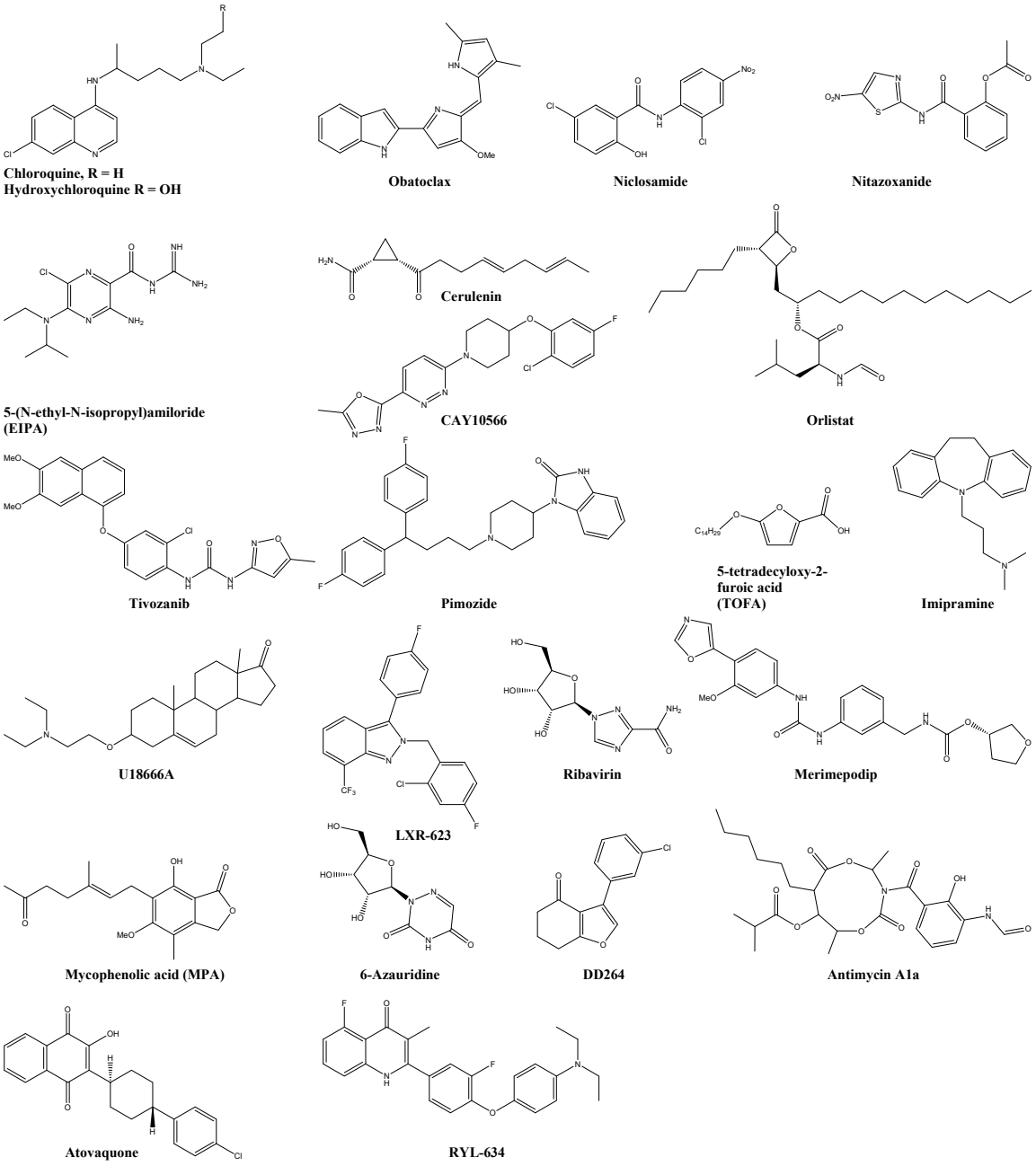

Figure 3. Chemical structure of selected host-targeting compounds. Inhibitor of the viral entry and membrane fusion: chloroquine, hydroxychloroquine, obatoclax, niclosamide, nitazoxanide, and 5-(N-ethyl-N-isopropyl)amiloride. Inhibitor of the lipid pathway: orlistat, cerulenin, CAY10566, tivozanib, pimozide, 5-tetradecyloxy-2-furoic acid, imipramine, U18999A, and LXR-623. Inhibitor of the pyrimidine and purine synthesis: ribavirin, merimepodip, mycophenolic acid, 6-azauridine, DD264, antimycin A1a, RYL-634, and atovaquone.

Several clinical trials were conducted to investigate hydroxychloroquine (HCQ, Figure 3) on Chikungunya virus infection [154]. HCG seems to have no beneficial impact in the early stage of CHIKV infection or reduction of joint pain when administered alone or in combination with aceclofenac [155]. However, the combination of HCQ with methotrexate improved the disease activity and reduced disability and pain in patients [156,157]. In contrast, HCQ treatment in the RHUMATOCHIK study had to be interrupted in 4 out of 39 patients because of adverse effects such as nausea, rash, stomatitis, and headache [158].

A 50% reduction of synovitis and 19.2% complete remission was reported in the remaining sample [158].

The pH-dependent endocytosis and the high sensitivity of CHIKV to the antiviral activity of type I and type II interferons was also shown by Sourisseau et al. [159]. Their study demonstrated the anti-CHIKV effect of chloroquine and the vacuolar proton ATPase inhibitor bafilomycin-A. Furthermore, the high sensitivity of CHIKV to the antiviral effect of IFNs (see Section 5.7, Immunomodulatory) has been reported [159]. Concamycin A, another vacuolar proton ATPase inhibitor, and the Bcl-2 inhibitor obatoclax (Figure 3) inhibited the viral fusion of Semiliki forest virus and, in the case of obatoclax, also of CHIKV due to their lysosomotropic characteristics [96,160].

A broad range of antiviral effect on pH-dependent viruses demonstrated the anithelmic drugs niclosamide and nitazoxanide (Figure 3) [161]. Radiometric imaging allowed the precise measurement of endosomal pH and revealed their neutralising effect of acidic endosomes [161]. An additional structure–activity relationship study exposed the importance of the hydroxy and chloride group in position R1 and R4 for the antiviral effect of this compound series [161]. An HTS for CHIKV fusion inhibitors with FDA approved drugs found not only niclosamide and nitazoxanide as potential anti-CHIKV candidates but also suramin (see Section 4.1., Viral Membrane Fusion and Entry) [97]. All of them showed an additional inhibitory effect on the cell-to-cell transmission of CHIKV. Additionally, the antiviral effect of the hits was evaluated, measuring the CHIKV-induced CPE in BHK-21 cells, and no toxicity in the used micromolar range was observed in zebrafish embryos [97].

Pre-infection treatment with the macropinocytosis inhibitor 5-(N-ethyl-N-isopropyl)amiloride (EIPA, Figure 3) results in a dose-dependent inhibition of CHIKV infection [98]. Amiloride and an amiloride analogue HOE-694 have been reported to block the activity of Na(+)/H(+) exchanger, lowering the submembranous pH and consequently preventing the necessary macropinocytosis [162]. Macropinocytosis has been identified as a significant pathway of CHIKV into muscle cells and is, therefore, an attractive target for new anti-CHIKV compounds [98].

5.2. Lipid Pathway Inhibitors

Alphavirus fusion is dependent on the cholesterol and sphingolipid in the host cell membrane [16]. Consequently, inhibition of the fatty acid synthase by the anti-obesity drug orlistat, the antibiotic FASN inhibitor cerulenin, and the SCD1 inhibitor CAY10566 resulted in decreased CHIKV and MAYV genome replication (see Figure 3) [99,100]. Both enzymes play a central role in the de novo synthesis of long-chain fatty acids and are crucial in the replication of various viruses [100]. Furthermore, orlistat was reported as a potential broad-spectrum agent against mosquito-transmitted viruses such as DENV, JEV, ZIKV and CHIKV [101].

Additionally, the fatty acid synthase was identified by Bakhache et al. as an important proviral host factor [100]. Further, a genome-wide CHIKV/HEK-293 loss-of-function siRNA screen led to identifying 156 proviral and 41 host targets influencing the CHIKV replication cycle [99]. The validated host proviral factors were used to screen a drug repurposing database [99]. This approach led to the identification of 20 compounds interacting with six unique host targets, including enzymes of fatty acid synthesis (fatty acid synthase, ATP citrate lyase, and acetyl CoA carboxylase), calmodulin signaling, the vacuolar-type H^+ ATPase (vATPase), CLK1, fms-related tyrosine kinase 4 (FLT4 or VEGFR3), and K (lysine) acetyltransferase 5 (KAT5 or TIP60). All 20 compounds showed strong antiviral activity when tested in HEK293-T cells, but, as expected, some of them exhibited a narrow therapeutic index. The in vitro outcome was further validated in a CHIKV-C57BL/6 mouse model, in which tivozanib (targeting FLT4), pimozide (calmodulin inhibitor) and 5-tetradecyloxy-2-furoic acid (TOFA, fatty acid synthesis inhibitor) reduced the viral replication in the footbed significantly (see Figure 3). The combination of TOFA and pimozide had a synergistic effect in reducing the viral replication and joint swelling [99].

The host membrane cholesterol is a key component in the unmasking of the fusion peptide in class II envelope glycoproteins [102]. Compounds interfering with the cholesterol transport such as the tricyclic antidepressant imipramine (Figure 3) and the class II cationic amphiphilic compound U18666A (Figure 3) have shown to affect the fusion and replication step from not only the CHIKV but also several Flaviviridae such as ZIKV, West Nile virus, and DENV [102].

The ubiquitously expressed liver X receptors (LXRs) are essential in the regulation of cholesterol homeostasis and a potential proviral host target for antiviral compounds [103]. The selective, synthetic agonist of LXRβ LXR-623 (Figure 3) inhibited the CHIKV replication in human foreskin fibroblasts in a dose-dependent manner. This effect was partially reversed when the cells were incubated with cholesterol [103].

5.3. Pyrimidine and Purine Synthesis Inhibitors

The inosine monophosphate dehydrogenase (IMPDH) is a key enzyme in the de novo guanine nucleotide biosynthesis by converting inosine-5′-monophosphate to xanthine 5′-monophosphate and is, therefore, an interesting target for antibacterial, anticancer and antiviral drugs [163]. Ribavirin (Figure 3), an FDA-approved drug against respiratory syncytial virus infection in infants and chronic hepatitis C infection, is a guanosine analogue with multiple postulated biomechanisms [164,165]. The inhibition of IMPDH leading to depletion of GTP pools as well as the inhibition of the RNA-dependent RNA polymerase (RdRp) is considered the major causes of the broad-spectrum antiviral activity of ribavirin [165]. The scientific research about the precise mode of action is still ongoing, but a time-of-addition study unveiled that ribavirin is primarily active at the early stage of the CHIKV replication cycle [59]. Ribavirin showed antiviral activity against CHIKV in vitro and in vivo studies and exhibited a synergistic effect with the tetracycline doxycycline, IFN α2a, and the NSAID mefenamic acid (MEFE) [57,104,166,167]. Moreover, a 7-day treatment with 200 mg ribavirin twice daily significantly improved joint pains in human patients [168].

Another potent and selective IMPDH inhibitor, merimepodib (Figure 3), inhibited the CHIKV and the ZIKV in a dose-dependent manner [105]. On the other hand, the immunosuppressive agent and non-competitive inhibitor of IMPDH, mycophenolic acid (MPA, Figure 3), has been reassessed regarding its anti-CHIKV inhibitory effect [169]. Although it has demonstrated high antiviral effects in a virus-induced cytopathic effect assay, 19 synthesised analogues of MPA did not show any CHIKV inhibition [169,170]. The following retest of MPA revealed the unexpected characteristic of MPA: after reduction of GTP and downregulation of CHIKV replication, the antiviral effect of MPA diminishes, and the virus regains its full replication potential [169].

6-Azauridine (Figure 3), on the other hand, inhibits the orotidylic acid decarboxylase (OMP)–resulting in depletion of UTP pools in cells [171]. It is used in the treatment of psoriasis and showed broad-spectrum antiviral activity [171–173]. Additionally, 6-azauridine has been reported to reduce the viral titer of CHIKV and SFV [104].

Another proviral host target is the dihydroorotate dehydrogenase (DHODH)–the fourth enzyme in the pyrimidine biosynthetic pathway bound to the inner mitochondria membrane [107]. DHODH is the suggested target of the DD264 series (Figure 3)—a small compound series found through an HTS with broad-spectrum antiviral activity (DNA and RNA viruses, including CHIKV) [106,107]. Interestingly, the antiviral effect of DD264 was suppressed when added exogenous uridine but not with added guanosine, which supports the theory that the pyrimidine level is essential for the CHIKV replication [106]. Antimycin A1a (Figure 3) also inhibits the cellular mitochondrial electron transport, suppressing the de novo pyrimidine synthesis and resulting in a broad spectrum of antiviral activity [174].

Phenotypic screening of around 200 biaryl-substituted quinolones and the following in vitro validation and SAR study led to the identification of the broad-spectrum antiviral compound RYL-634 (Figure 3) [108]. Via activity-based protein profiling (ABPP), 78 potential human proteins were identified as possible targets of RYL-634. Further in

silico investigations and enzymatic activity assays validated the DHODH as the target enzyme [108]. Although it has been already shown that the antimalaria drug atovaquone (Figure 3) has an inhibitory effect on DHODH, its biomechanism regarding the antiviral effect on CHIKV remains unclear [109,175]. A mechanism of action study showed an early stage inhibition of ZIKV infection and a possible inhibitory effect on the pyrimidine biosynthesis pathway [109].

5.4. Protein Synthesis Inhibitors

Halofuginone (Figure 4) is an antagonist of the host prolyl-tRNA synthetase enzyme (EPRS), causing the accumulation of uncharged $tRNA^{pro}$ and forcing the cell to suppress the translation even when proline levels are sufficient [176]. This orally available synthetic derivative of the plant compound febrifugine has been reported to inhibit the viral progeny production of CHIKV, ONNV, ZIKV and DENV [110]. Harringtonine (Figure 4), another naturally derived compound, has been identified to inhibit CHIKV RNA production and viral protein expression in a dose-dependent manner [111]. This cephalotaxine alkaloid is known to inhibit eukaryotic translation [177].

The anticancer drug sorafenib tosylate (Figure 4) inhibited CHIKV replication at 8 and 16 h post-infection through dephosphorylation of several key enzymes for the viral translation-including the cap-binding protein eIF4E (eukaryotic translation factor 4E) and p70S6K [99,112]. As the research from McKendrick et al. suggest that the phosphorylation of eIF4E is not essential for the global cellular protein synthesis, this enzyme could be an attractive target for further antiviral drug development [112,178]. Moreover, sylvestrol (Figure 4), a specific inhibitor of the RNA helicase eIF4A (eukaryotic translation factor 4A), inhibited the CHIKV replication cycle at an early stage [179]. The DEAD-box helicase eIF4A unwinds the RNA secondary structure in the 5′-untranslated regions (5′-UTRs) of mRNA and allows translation. Silvestrol holds the eIF4A helicase to its mRNA substrate and inhibits thereby the following translation [179]. More recently, Blum et al. reported the influence of sylvestrol on the inflammatory status of immune cells [180].

The ubiquitin-proteasome system (UPS) is central for ensuring protein quality control and maintaining a critical level of important regulatory proteins [181]. As many viruses have evolved to manipulate this cellular machinery in their favour, it is not surprising that the FDA-approved proteasome inhibitor bortezomib (Figure 4) was reported to inhibit different CHIKV strains in various cell lines [113,181]. Investigation of the CHIKV protein level by Western plot analysis revealed a 50% to 80% reduction of E2, E1 and capsid protein [113]. The synthetic agonist of the nuclear receptors Rev-erb α/β SR9009 (Figure 4) showed inhibitory effects against the CHIKV and O′nyong′nyong virus [114]. Although the precise mechanism of action is still unclear, a subgenomic RNA translation inhibition was observed [114].

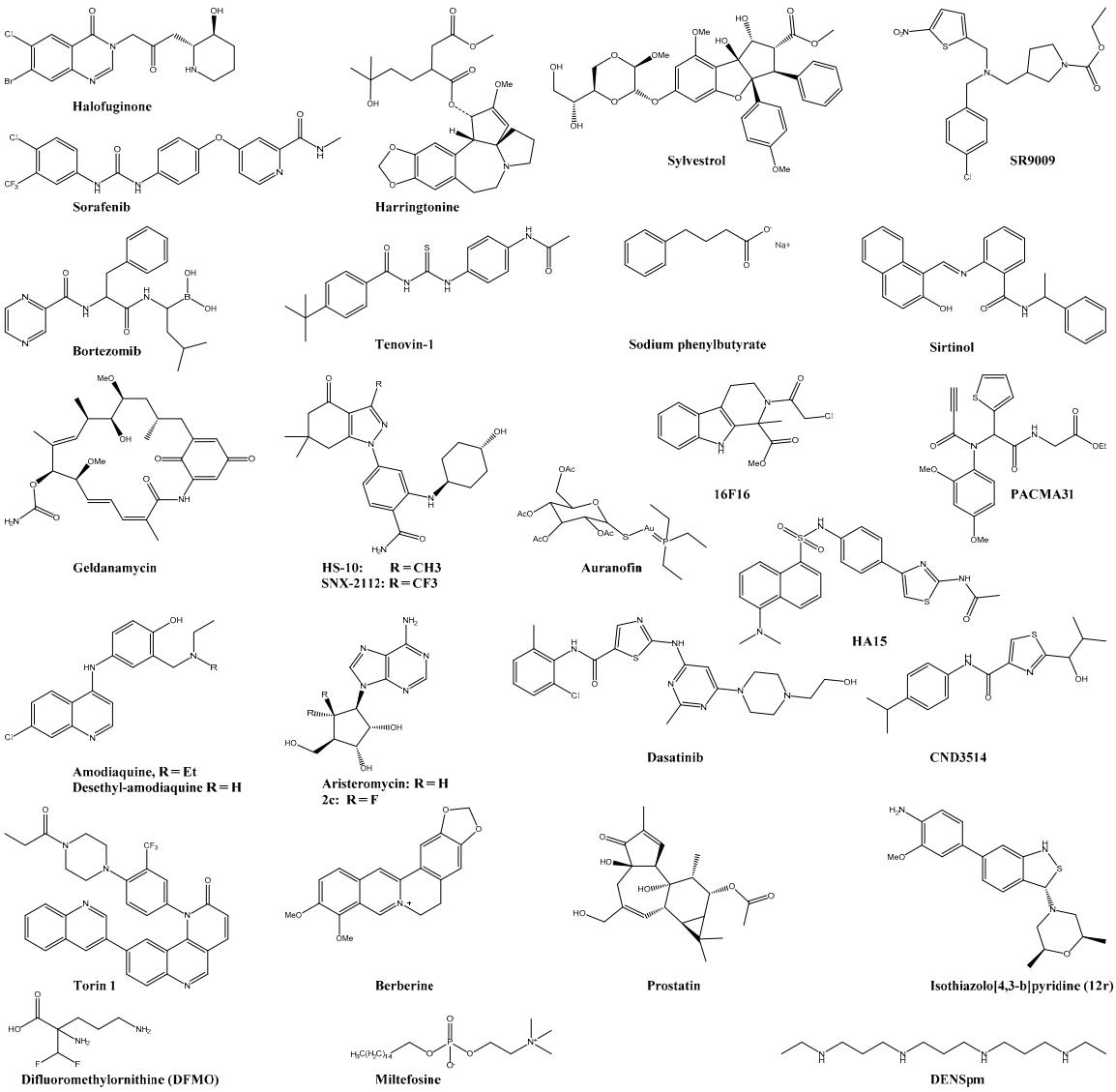

Figure 4. Chemical structure of selected host-targeting compounds. Inhibitor of the protein synthesis: halofuginone, harringtonine, sorafenib, sylvestrol, bortezomib, and SR9009. Inhibitor of cellular proteins: tenovin-1, sodium phenylbutyrate, sirtinol, geldanamycin, HS-10, SNX-2112, HA15, 16F16, PACMA31, and auranofin. Inhibitor of cellular enzymes: amodiaquine, desethyl-amodiaquine, aristeromycin, dasatinib, Torin 1, CND3514, berberine, miltefosine, prostatin, isothiazolo[4,3-b]pyridine, difluoromethylornithine, and DENSpm.

5.5. Cellular Protein Inhibitors

Sirtuins (SIRTs) are an evolutionarily conserved family of seven lysine deacetylases (KDACs) and are present in nuclear and cytoplasmic compartments [115]. Their precise functions in human cells are not fully elucidated, and their impact on viral replications varies not only on the viral pathogen but also on the subgroup of SIRTs itself [115]. Different sirtuin inhibitors, such as tenovin-1 (Figure 4), sodium phenylbutyrate (a pan-KDAC inhibitor, Figure 4), and sirtinol (a specific SIRT1 and SIRT2 inhibitor, Figure 4) have been reported to inhibit a set of flaviviruses, bunyaviruses, and alphaviruses–including the CHIKV. Interestingly, the inhibition of only SIRT1/2 was not enough to block the viral infection [115].

Like cellular proteins, viral proteins need chaperones for proper folding and assembling for precise and stable function. Three different chaperon families, namely the heat shock protein 90 (HSP90), the protein disulfide isomerase (PDI), and the ER chaperon

GRP78, were reported as proviral host factors in the case of CHIKV infection [116–118]. HSP90 has a critical role in the proper folding, maturation, localisation, and turn-over of cellular and viral proteins. Its essential function for RNA and DNA viruses makes it a desirable host target for broad-spectrum antivirals [182]. Interestingly, the known HSP90 inhibitor geldanamycin (Figure 4) showed antiviral effects in CHIKV infected HEK-293T cells. Further, the antiviral effects of two specific HSP90 inhibitors, HS-10 and SNX-2112 (Figure 4), ruled out any off-target effects of geldanamycin during the CHIKV replication cycle. They even prevented joint swelling and inflammation in a CHIKV-SVA129 mouse model [116]. Further, geldanamycin treatment led to reducing the nsP2 concentration and the for viral replication essential interaction between HSP90 and nsP2 [183]. Another chaperon inhibitor, namely the compound HA15 (Figure 4), was recently found to inhibit various viruses—including VEEV, EEEV, SINV, and CHIKV. The ER chaperon GRP78 showed interactions with the viral E2 glycoprotein and was confirmed as a possible proviral host target [117].

Alphaviruses require specific disulfide bonding in their envelope proteins E1 and E2 for proper folding and assembling and, therefore, likely depend on the host protein disulfide isomerase (PDI) [118]. Consistent with these findings, the in vitro assays with the PDI inhibitor 16F16 (Figure 4) led to a significant reduction of cell-cell fusion events. Although 16F16 and PACMA31 (another PDI inhibitor, Figure 4) showed interesting antiviral effects, their toxicity profile was remarkably poor. However, the FDA approved TRX-inhibitor auranofin (Figure 4) had a much better therapeutic index of 104.5 at 12 h post-infection and even reduced food swelling in a CHIKV mouse model [118].

5.5.1. Cellular Enzyme Inhibitors

Hydrolases

So far, three different hydrolase families have been reported as proviral host targets for the inhibition of the CHIKV infection, namely furin, cathepsin B, and the SAH-hydrolase [120,153,184]. The membranous furin hydrolase is vital for the cleavage of the alphavirus envelope glycoproteins E1 and E2 precursor P62 [153,185]. As this process is a crucial moment in replicating the CHIKV and many other alphaviruses, furin is a desirable target for antiviral compounds [185–187]. Accordingly, the inhibition of the P62 cleavage by the irreversible furin inhibitor decanoyl-RVKR-chloromethyl ketone (dec-RVKR-chmk) leads to a significant viral reduction envelope glycoproteins E1 and E2 in infected myoblast cultures. Furthermore, given chloroquine, almost total viral spread and yield were observed [153]. The furin inhibitor phenylacetyl-Arg-Val-Arg-4-amidinobenzylamide and a set of its analogues significantly reduced the viral titer in BHK-21 cells [188].

The endosomal cathepsin B protease was recently confirmed as a proviral host target not only for MLV, Ebola virus, and SARS-CoV infections but also for CHIKV. Cathepsin B mediates the lysosomes-endosomes-fusion and is used by pathogens to enter the cell [119,184]. The antimalaria drug amodiaquine and its primary active metabolite desethyl-amodiaquine (DEAQ) have shown to act as an anti-pathogen against various bacteria toxins and as an inhibitor of multiple viruses (e.g., the CHIKV) by inhibiting the host cathepsin B protease (see Figure 4) [119].

The naturally occurring carboxylic nucleotide aristeromycin (Figure 4) showed potent anti-CHIKV effects, but further usage was limited by its high cytotoxicity [120,189]. This type I S-adenosyl-L-homocysteine hydrolase (SAH) inhibitor was the starting point of a series of 6′-fluorinated aristeromycin analogues (Figure 4). Since both the viral RdRp and the host SAH hydrolase are crucial for the viral RNA capping and replication, the design of dual-target antiviral compounds was performed by Yoon et al. [120]. Surprisingly, the inhibition of the viral RdRp was found to be less important in this new compound series than the SAH inhibition [120]. As already discussed in 4.4.1. nsP1, based on these results, 6′-fluorinated-5′-homoaristeromycin (FHA) and 6′-fluoro-homoneplanocin (FHNA) were synthesised and showed potent anti-CHIKV activity [37]. Interestingly, they seem to target the viral nonstructural protein nsP1 rather than the proviral host factor SAH [38].

Kinases

Targeting the proviral host kinases has led to the identification of multiple compounds with interesting antiviral activity. Many viruses modify the host kinases signaling pathways to regulate the cellular environment and to stimulate their replication [190]. The Src family kinases (SFKs), for example, have been identified through kinome profiling as essential proteins for the replication of several viruses, including the CHIKV. Accordingly, the chemical inhibitors of these membrane-associated kinases, dasatinib and the mTORC1/2 inhibitor Torin 1, were able to reduce the viral yields in human fibroblasts (see Figure 4) [121]. Other kinase inhibitor compounds, the CND series (Figure 4), were found through HTS utilising a kinase inhibitory chemical library (BioFocus). A mechanism of action study with this compound series suggested that the inhibition of virus-induced CPE was likely performed by targeting kinases involved in apoptosis [122]. However, their precise target kinase requires further investigation [122].

Another potential proviral host kinase target is the mitogen-activated protein kinase (MAPK) signaling pathway. Berberine (Figure 4), a plant-derived alkaloid, was found with ivermectin and abamectin through a high throughput screening. All three compounds showed good activity against different alphaviruses [123]. Furthermore, the activation of the MAPK during a CHIKV infection and the resulting changes in phosphorylation levels were detected by a human phosphokinase array detected [124]. Berberine treatment decreased the viral titer in HEK-293T cells by reducing this CHIKV induced MAPK activity. Additionally, berberine treatment in CHIKV-infected C57BL6/J led to reduced inflammation in the joint footbed [124]. Recently, berberine was reported to interfere with the virus ability to form a stable cytoplasmic nucleocapsid core (NC)–inhibiting the formation of infectious virus particles [191].

Depending on the host cell, the CHIKV entry occurs via endocytosis or macropinocytosis [98,184]. Macropinocytosis activation occurs when the virus activates signal transduction in the host cell via different cellular proteins such as the phosphatidylinositol-3kinase (PI3K) and the protein kinase C [98]. The inhibition of the AKT-phosphorylation through the interaction with the Pi3-Akt signaling pathway by the anti-leishmaniosis drug miltefosine (Figure 4) led to a reduction of the CHIKV replication in human dermal fibroblasts [125].

The serin/threonine-protein kinase C (PKC) regulates several cellular processes, including cell proliferation and apoptosis [126]. PCK modulators have been reported to inhibit CHIKV replication in vitro. The phorbol ester prostatin (Figure 4) is a potent activator of PCK and showed antiviral activity on different CHIKV strains [126,192]]. The antiviral activity of prostatin, however, was strongly dependent on the used cell type. Potent antiviral activity were reported in BGM and Vero A cells, but the PCK inhibitor showed no antiviral activity in HEL cells [126]. Furthermore, prostatin has been reported to have tumour promoting effects [126]. Analogues of the pan-PCK modulator bryostatin, also potently inhibited the CHIKV replication. Interestingly, when the hydroxyl group on C26, which is vital for the PCK interaction, was capped, the antiviral activity was still found. This suggests an additional PCK-independent mode of action [127,128,193].

Additionally, the cyclin G-associated kinase (GAK) inhibitors with an isothiazolo [4,3-b]pyridine (Figure 4) scaffold showed moderate antiviral activity against the Dengue virus, Ebola virus, and the Chikungunya virus [129].

Lyases/transferases

Reducing the polyamine concentration in host cells has negative effects on the viral replication of various RNA viruses as they need it for viral translation and transcription [194]. Intracellular polyamine synthesis relies on a set of different proteins such as ornithine decarboxylase 1 (ODC1) and spermidine/spermine N1-acetyltransferase 1 (SAT1). Depletion of spermidine and spermine by induction of SAT1 led to decreased CHIKV replication [194]. Interestingly, the resistance of this polyamine dependency was found in a CHIKV variant with mutations in the viral nsP1 and nsP4 [195]. The irreversible inhibitor of ODC1, difluoromethylornithine (DFMO, Figure 4), and the SAT1 upregulator, diethyl-

norspermine (DENSpm, Figure 4), reduced the viral titer in different cell lines. Despite these good in vitro results, DFMO showed a low reduction in viral titer in CHIKV-infected C57BL/6 mice [130].

5.6. Cellular Receptor Inhibitors

5.6.1. Inhibitors of Channel-Linked Receptors

Critical steps of the viral replication cycle have been reported to depend on the virus's ability to manipulate the host cell ionic environment. Consistent with these findings, several viral proteins have been shown to influence cellular ion channel activity [196]. So far, two different ion channel families have been exploited as anti-CHIKV targets–the sodium-potassium ATPase and the chloride channel 1 and 4 (CLIC1, CLIC4) [20,131,132]

A high throughput screening has identified the known sodium-potassium ATPase inhibitor digoxin and its related cardiac glycoside ouabain as a potent CHIKV inhibitor in human cell lines (see Figure 5) [20]. Furthermore, mechanistic studies revealed that digoxin is acting in a post-entry step of the viral replication. Its antiviral effect was reversed when exogenous potassium was added during digoxin treatment, which led to the hypothesis that the CHIKV may require a specific ion balance for its replication. Digoxin-resistant CHIKV mutations carried the V209I mutation in the viral nonstructural protein nsP4, indicating that digoxin may also interact with the viral replication [20]. In addition, another FDA approved cardiac glycoside, lanatoside C (Figure 5), was reported to inhibit a broad spectrum of viruses, including the dengue virus, the Sindbis virus, and the CHIKV [131].

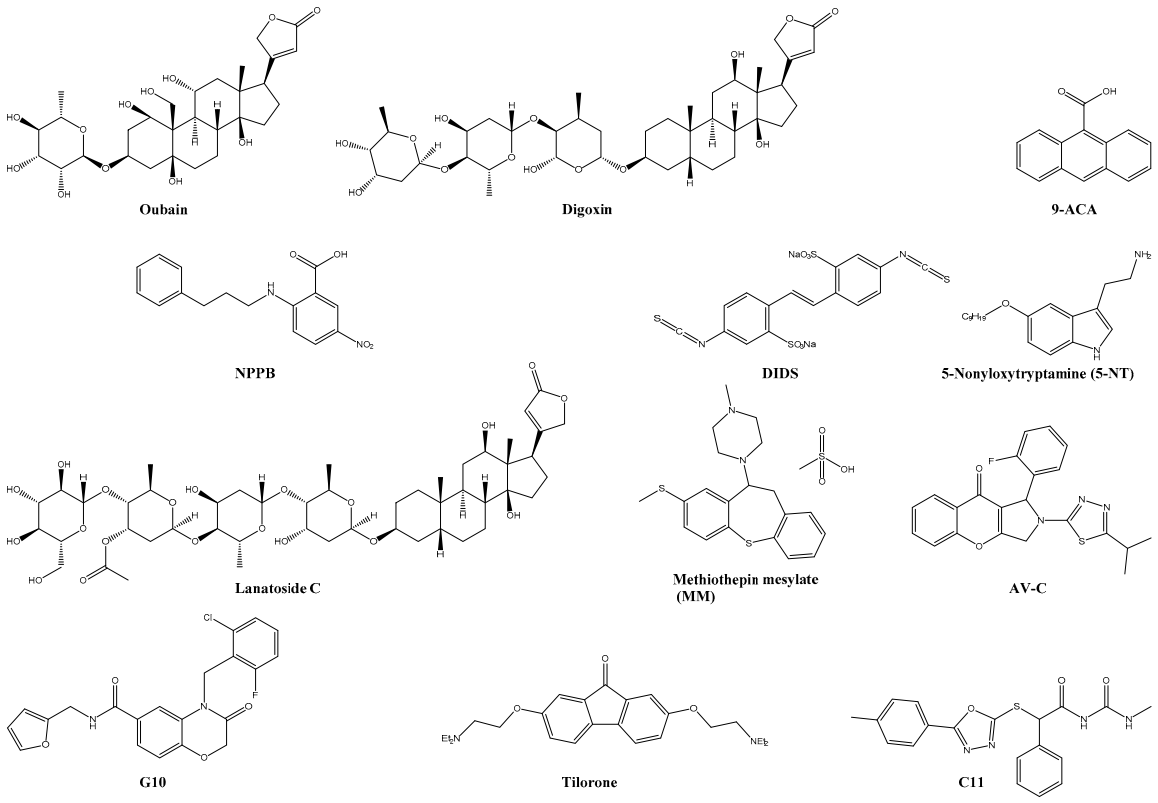

Figure 5. Chemical structure of selected host-targeting compounds. Inhibitors of cellular receptors: oubain, digoxin, lanatoside C, DIDS, 9-ACA, NPPB, 5-nonyloxytryptamine, and methiothepin mesylate. Immunomodulatory agents: tilorone, C11, G10, and AV-C.

The discovery of CLIC1 and CLIC4 as proviral factors in human cells was performed using the siRNA silencing technique. This resulted in the identification of three chloride channel inhibitors, 4,4′-Diisothiocyanostilbene-2,2′-disulfonic acid (DIDS), 9-Anthracenecarboxylic acid (9-ACA), and 5-Nitro-2-(3-phenylpropylamino)benzoic acid

(NPPB, Figure 5). All three compounds showed a significant reduction in CHIKV replication not only in human cell lines (Huh-7) but also in mosquito cells (C6/C3) [132].

5.6.2. Inhibitors of Enzyme-linked Receptors

The serotonin or 5-hydroxytryptamine (5-HT) receptors are primarily G-protein coupled and regulate essential physiological functions and various signaling pathways [134]. The serotonin receptor agonist 5-nonyloxytryptamine (5-NT, Figure 5) has been shown to inhibit CHIKV replication in U2OS cells [134]. Interestingly, also the 5-HT antagonist methiothepin mesylate (MM, Figure 5) was able to inhibit 97 ± 1.0% of the CHIKV replication at 10 µM. A time-of-addition study suggested two different modes of actions: for 5-NT, the inhibition of the uncoating and for MM, the internalisation and membrane hemifusion step [133].

5.7. Immunomodulatory Agents

The host immune system and responses, primarily the type I interferon (IFN) signaling, are crucial for controlling and preventing CHIKV infections [197]. Accordingly, many antiviral compounds have shown synergistic effects when given with IFNs [92,104,106,130,166]. Furthermore, the orally available IFN-inducer tilorone dihydrochloride (Figure 5) is known since 1970 for its antiviral activity against SFV in mice [198]. More recently, tilorone was reported to inhibit CHIKV infections in Vero cells [135].

Polyinosinic acid: polycytidylic acid (poly(I:C)), a double-stranded RNA, is another potent IFN inducer and interacts with the toll-like receptor 3 (TLR3) which are expressed in the membrane of B-cells, macrophages, and dendritic cells. The TLR3 receptors are part of the innate immune response and recognize proteins, lipids, carbohydrates and others from invading microorganism. When activated by poly(I:C), they suppress the CHIKV infection by inducing IFNs and other antiviral genes [199]. Pre-treatment of mice with poly(I:C) reduced viral titer in the brain and achieved 100% survivability of the mice [200]. The double-stranded RNA 5′pppRNA is, like poly(I:C), a well-studied adjuvant for enhancing the efficacy of influenza virus vaccines [201,202]. In addition, 5′pppRNA and its analogue M8 inhibited the in vitro and in vivo replication of different viruses (including the CHIKV) by interacting with the retinoic acid-inducible gene I (RIG-I) [203–205].

The IFN-inducible protein viperin was also reported to play an essential role in the in vivo infection of the CHIKV and could be an interesting target for antiviral drugs. Mice lacking viperin were reported to develop higher viremia and more severe joint inflammation than infected wild-type mice [206,207]. A novel small molecule (C11, Figure 5) was recently shown to induce IFN secretion from human cells and transcription/translation of interferon-dependent antiviral genes such as viperin. Reverse genetics and a loss-of-function assay suggested the adaptor protein STING for its IFN activation ability. C11 had antiviral effects against the Ross River virus, VEEV, Mayaro virus, O'nyong-nyong virus, and CHIKV [136]. G10 (Figure 5) is another small molecule preventing the replication of various alphaviruses (e.g., VEEV, Sindbis virus, and CHIKV) by indirectly activating the STING protein, which supports the hypothesis of STING as a possible antiviral target [137]. The same research group reported AV-C (Figure 5) as a novel interferon-activating small molecule. AV-C showed inhibitory effects against ZIKV, Dengue virus, and CHIKV infection in THF cells [138].

Further, heparan sulfate mimetics such as pentosan polysulfate and PG545 (pixatimod) have been reported as interesting compounds for alleviating alphavirus-induced disease in vivo. Pentosan polysulfate is an FDA-approved drug against cystitis, whereas pixatimod is currently in a clinical trial to treat advanced cancer and pancreatic adenocarcinoma [139,208,209]. Although pentosan polysulfate treatment did not influence the kinetics of virus infection, it alleviated virus-induced arthritis in C57BL/6 mice [139]. Furthermore, it was recently successfully evaluated in phase II clinical trials for the treatment of RRV-induced arthritic disease (PARA_004, Paradigm BioPharmaceuticals) [210]. Pixatimod treatment also reduced the severity of alphavirus-induced arthritis and showed good antiviral effects against different CHIKV strains [140].

6. Undefined Targets

Quinolones, like ciprofloxacin and N-acyl hydrazones, were reported as compounds with antibacterial and antiviral properties. Therefore, a series of quinolone-N-acylhydrazone hybrids (Figure 6) were synthesized in a four step synthesis route. Accordingly, they demonstrated antiviral effects against the ZIKV and CHIKV in Vero cells. A mechanism of action study suggests that the compounds act in the early stages and in some post-infection stages of the CHIKV replication cycle. Nevertheless, the precise mode of action remains unknown [211].

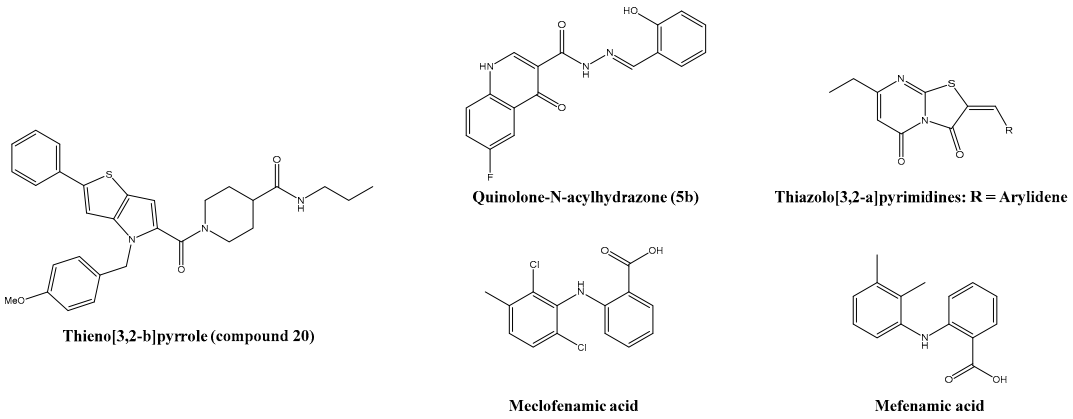

Figure 6. Chemical structure of anti-CHIKV compounds without known target.

The thieno[3,2-b]pyrrole (Figure 6) scaffold was initially found by screening and has been shown to be a potential lead compound. Two structure–activity-relationship studies were made to improve its antiviral activity and its metabolic stability and yielded in the design of the most promising analogue: compound 20. This compound series has been reported to inhibit the expression of viral nsP1, nsP3, capsid, and E2 proteins and to affect the CHIKV life cycle. Additionally, they have been shown to inhibit other alphaviruses such as the O′nyong-nyong and Sindbis virus [212,213].

Recently, Fares et al. reported a new scaffold of a CHIKV inhibitor based on the fusion of uracil and rhodanine pharmacophoric features, which were previously identified as antiviral active (Figure 6) [30,60,214,215]. The best performing analogue, compound 15, had a p-methyl biphenyl tail functionality and may be an interesting lead compound for further drug development [214]]. An overview of compounds without a known target is given in Table 4.

Table 4. Antiviral compounds without a known target [a].

Compound [b]	In Vitro				In Vivo		Ref.
	EC_{50} (μM) [c]	CC_{50} (μM)	SI	Cell Line	Efficacy	Mouse Model	
Quinolone-N-acylhydrazone (5b)	1.06 ± 0.08	669 ± 4.33	631.7	Vero	—	—	[211]
Thieno[3,2-b]pyrrole (compound 20)	3-4	>100	n.s.	HEK293T	Good in vivo pharmacokinetics	C57BL/6	[212,213]
Compound 15	42	n.s.	n.s.	MCF-7	—	—	[214]
Mefenamic acid *	13	>100	n.s.	Vero	+ ribavirin: Reduction of viral titre and hypertrophic effects in liver and spleen	Adult ICR	[167]
Meclofenamic acid	18	>100	n.s.	Vero	—	—	[167]
Ivermectin *	0.6 ± 0.1	37.9 ± 7.6	62.4	BHK-21	—	—	[123]
Abamectin *	1.5 ± 0.6	28.2 ± 1.1	19.2	BHK-21	—	—	[123]

[a] EC_{50}, 50% effective concentration; CC_{50}, 50% cytotoxic concentration; n.s., not specified; —, not determined; *, repurposed drug. [b] If the study reported a compound series/class with anti-CHIKV activity, the antiviral data of the most potent or most representative compound is reported. Only compounds with in vitro or in vivo data are shown. [c] If a compound was reported in multiple studies, cell lines, or if different CHIKV strains have been used, the best activity value with the corresponding cell line is reported.

7. Conclusions

Due to the severity and chronicity of the Chikungunya fever and the rapid worldwide spread, the CHIKV remains a clinically relevant pathogen. Moreover, the lack of approved antiviral compounds and vaccines against this alphavirus further lightens the crucial development of inhibitors against the Chikungunya virus. A comprehensive overview of several antiviral compounds is given in this review, but most of them are still in the early stage of drug development as their activity against the CHIKV is only tested in in vitro assays. This issue could be overcome by repurposing already approved drugs for the anti-CHIKV treatment. As they already have been intensively investigated for their safety in humans, the clinical evaluation of such drugs could be a fast and safe option for emergency treatment in CHIKV infection outbreaks. The advantage of this approach is illustrated by the fact that out of all compounds discussed in this review only 15 were tested against CHIKV in an animal model, and only one of them (thieno[3,2-b]pyrrole, compound 20) was purposely designed to inhibit the alphavirus. Repurposed drugs such as suramin, favipiravir, sofosbuvir, pimozide, auranofin, PPS, pixatimob, and ribavirin (alone and in combination) showed a reduction of pathological signs in vivo. Furthermore, known inhibitors of proviral host targets (such as TOFA, HS-10, SNX-2112, PACMA31, berberine, and DFMO) reduced the viral titer in the performed in vivo assays. By demonstrating their effects in animal assays, they further confirmed their mode of action to be a valid and potential host target for the development of anti-CHIKV drugs not only in vitro but also in vivo. A broad spectrum of various proviral host targets such as the fatty acid synthase (FASN), calmodulin, IMPDH, TRX, and MAP kinase and more can be therefore considered as interesting targets for future antiviral drug development.

On the other hand, a much more effective and stronger antiviral activity can be expected from compounds directly designed to inhibit the alphavirus. These compounds, such as bis(benzofuran-thiazolidone) (3g), MADTP (9b), CHVB-032, compound 25, compound 8, and compound-A (see Section 4, Virus Targeting Inhibitors) demonstrated already promising antiviral activity in vitro and could be therefore considered for further development and testing.

Another challenge in the development of CHIKV antiviral drugs is its already shown ability to mutate and to develop resistance to antiviral therapy. A combinatory approach of compounds with synergistic effect or the design of an antiviral with multiple targets could

diminish this escape mechanism of the virus. Furthermore, recent studies have identified new promising host factors as possible targets for CHIKV inhibitors. Such inhibitors could demonstrate pan-viral inhibitory effects as many viruses use the same replication strategies. However, targeting a crucial host cell factor could also lead to more (serious) side effects due to the manipulation of important biomechanism of the host. More research is required to identify new and safe targets by collecting more detailed information about the CHIKV life cycle. Furthermore, the current absence of a vaccine makes the development of a potent and safe CHIKV inhibitor crucial for the treatment of this severe disease.

Author Contributions: V.B. wrote the manuscript, E.U. and T.L. contributed with feedback and corrections. All authors have read and agreed to the published version of the manuscript.

Funding: This research received no external funding.

Acknowledgments: We thank Georg Unterholzner for carefully reading the manuscript and providing valuable feedback. The authors thank the University of Vienna for financial support. Open Access Funding by the University of Vienna.

Conflicts of Interest: The authors declare no conflict of interest.

References

1. Robinson, M.C. An epidemic of virus disease in Southern Province, Tanganyika Territory, in 1952-53. I. Clinical features. *Trans. R. Soc. Trop. Med. Hyg.* **1955**, *49*, 28–32. [CrossRef]
2. Chretien, J.P.; Anyamba, A.; Bedno, S.A.; Breiman, R.F.; Sang, R.; Sergon, K.; Powers, A.M.; Onyango, C.O.; Small, J.; Tucker, C.J.; et al. Drought-associated chikungunya emergence along coastal East Africa. *Am. J. Trop. Med. Hyg.* **2007**, *76*, 405–407. [CrossRef]
3. Vazeille, M.; Moutailler, S.; Coudrier, D.; Rousseaux, C.; Khun, H.; Huerre, M.; Thiria, J.; Bastien Dehecq, J.-S.; Fontenille, D.; Schuffenecker, I.; et al. Two Chikungunya Isolates from Two Chikungunya Isolates from the Outbreak of La Reunion (Indian Ocean) Exhibit Different Patterns of Infection in the Mosquito, Aedes albopictus. *PLoS ONE* **2007**, *2*, e1168. [CrossRef]
4. Cassadou, S.; Boucau, S.; Petit-Sinturel, M.; Huc, P.; Leparc-Goffart, I.; Ledrans, M. Emergence of chikungunya fever on the French side of Saint Martin island, October to December 2013. *Eurosurveillance* **2014**, *19*, 20752. [CrossRef]
5. Zeller, H.; Van Bortel, W.; Sudre, B. Chikungunya: Its History in Africa and Asia and Its Spread to New Regions in 2013–2014. *J. Infect. Dis.* **2015**, *214*, 436–440. [CrossRef] [PubMed]
6. Rezza, G.; Nicoletti, L.; Angelini, R.; Romi, R.; Finarelli, A.C.; Panning, M.; Cordioli, P.; Fortuna, C.; Boros, S.; Magurano, F.; et al. CHIKV study group. Infection with chikungunya virus in Italy: An outbreak in a temperate region. *Lancet* **2007**, *370*, 1840–1846. [CrossRef]
7. Venturi, G.; Di Luca, M.; Fortuna, C.; Remoli, M.E.; Riccardo, F.; Severini, F.; Toma, L.; Del Manso, M.; Benedetti, E.; Caporali, M.G.; et al. Detection of a chikungunya outbreak in central Italy, August to September 2017. *Eurosurveillance* **2017**, *22*, 11–14. [CrossRef]
8. Delisle, E.; Rousseau, C.; Broche, B.; Leparc-Goffart, I.; L'ambert, G.; Cochet, A.; Prat, C.; Foulongne, V.; Ferré, J.B.; Catelinois, O.; et al. Chikungunya outbreak in Montpellier, France, September to October 2014. *Eurosurveillance* **2015**, *20*. [CrossRef]
9. Calba, C.; Guerbois-Galla, M.; Franke, F.; Jeannin, C.; Auzet-Caillaud, M.; Grard, G.; Pigaglio, L.; Decoppet, A.; Weicherding, J.; Savaill, M.C.; et al. Preliminary report of an autochthonous chikungunya outbreak in France, July to September 2017. *Eurosurveillance* **2017**, *22*, 5–10. [CrossRef]
10. Campbell, L.P.; Luther, C.; Moo-Llanes, D.; Ramsey, J.M.; Danis-Lozano, R.; Peterson, A.T. Climate change influences on global distributions of dengue and chikungunya virus vectors. *Philos. Trans. R. Soc. B Biol. Sci.* **2015**, *370*, 1–9. [CrossRef]
11. WHO Media Centre. Chikungunya—Key Facts. Available online: https://www.who.int/news-room/fact-sheets/detail/chikungunya (accessed on 31 May 2021).
12. Thiberville, S.-D.; Moyen, N.; Dupuis-Maguiraga, L.; Nougairede, A.; Gould, E.A.; Roques, P.; De Lamballerie, X. Chikungunya fever: Epidemiology, clinical syndrome, pathogenesis and therapy. *Antivir. Res.* **2013**, *99*, 345–370. [CrossRef]
13. Borgherini, G.; Poubeau, P.; Jossaume, A.; Gouix, A.; Cotte, L.; Michault, A.; Arvin-Berod, C.; Paganin, F. Persistent arthralgia associated with chikungunya virus: A study of 88 adult patients on reunion island. *Clin. Infect. Dis.* **2008**, *47*, 469–475. [CrossRef]
14. Lebrun, G.; Chadda, K.; Reboux, A.H.; Martinet, O.; Gaüzère, B.A. Guillain-Barré Syndrome after Chikungunya Infection. *Emerg. Infect. Dis.* **2009**, *15*, 495–496. [CrossRef]
15. Kennedy Amaral Pereira, J.; Schoen, R.T. Management of chikungunya arthritis. *Clin. Rheumatol.* **2017**, *36*, 2179–2186. [CrossRef] [PubMed]
16. Kielian, M.; Chanel-Vos, C.; Liao, M. Alphavirus Entry and Membrane Fusion. *Viruses* **2010**, *2*, 796–825. [CrossRef]
17. Voss, J.E.; Vaney, M.-C.; Duquerroy, S.; Vonrhein, C.; Girard-Blanc, C.; Crublet, E.; Thompson, A.; Bricogne, G.; Rey, F.A. Glycoprotein organization of Chikungunya virus particles revealed by X-ray crystallography. *Nature* **2010**, *468*, 709–712. [CrossRef] [PubMed]

18. Solignat, M.; Gay, B.; Higgs, S.; Briant, L.; Devaux, C. Replication cycle of chikungunya: A re-emerging arbovirus. *Virology* **2009**, *393*, 183–197. [CrossRef]
19. Van Der Heijden, M.W.; Bol, J.F. Composition of alphavirus-like replication complexes: Involvement of virus and host encoded proteins. *Arch Virol* **2002**, *147*, 875–898. [CrossRef] [PubMed]
20. Ashbrook, A.W.; Lentscher, A.J.; Zamora, P.F.; Silva, L.A.; May, N.A.; Bauer, J.A.; Morrison, T.E.; Dermody, T.S. Antagonism of the Sodium-Potassium ATPase Impairs Chikungunya Virus Infection. *MBio* **2016**, *7*, e00693-16. [CrossRef]
21. Abdelnabi, R.; Neyts, J.; Delang, L. Towards antivirals against chikungunya virus. *Antivir. Res.* **2015**, *121*, 59–68. [CrossRef]
22. Jose, J.; Snyder, J.E.; Kuhn, R.J.; Snyder, E.J.; Kuhn, R.J. A structural and functional perspective of alphavirus replication and assembly. *Futur. Med.* **2009**, *4*, 837–856. [CrossRef]
23. Strauss, J.H.; Strauss, E.G. The alphaviruses: Gene expression, replication, and evolution. *Microbiol. Rev* **1994**, *58*, 491–562. [CrossRef] [PubMed]
24. Delogu, I.; Pastorino, B.; Baronti, C.; Nougairède, A.; Bonnet, E.; de Lamballerie, X. In vitro antiviral activity of arbidol against Chikungunya virus and characteristics of a selected resistant mutant. *Antivir. Res.* **2011**, *90*, 99–107. [CrossRef] [PubMed]
25. Ho, Y.-J.; Wang, Y.-M.; Lu, J.; Wu, T.-Y.; Lin, L.-I.; Kuo, S.-C.; Lin, C.-C. Suramin Inhibits Chikungunya Virus Entry and Transmission. *PLoS ONE* **2015**, *10*, e0133511. [CrossRef] [PubMed]
26. Kuo, S.-C.; Wang, Y.-M.; Ho, Y.-J.; Chang, T.-Y.; Lai, Z.-Z.; Tsui, P.-Y.; Wu, T.-Y.; Lin, C.-C. Suramin treatment reduces chikungunya pathogenesis in mice. *Antivir. Res.* **2016**, *134*, 89–96. [CrossRef] [PubMed]
27. Albulescu, I.C.; Van Hoolwerff, M.; Wolters, L.A.; Bottaro, E.; Nastruzzi, C.; Yang, S.C.; Tsay, S.-C.; Hwu, J.R.; Snijder, E.J.; Van Hemert, M.J. Suramin inhibits chikungunya virus replication through multiple mechanisms. *Antivir. Res.* **2015**, *121*, 39–46. [CrossRef] [PubMed]
28. Sharma, R.; Fatma, B.; Saha, A.; Bajpai, S.; Sistla, S.; Dash, P.K.; Parida, M.; Kumar, P.; Tomar, S. Inhibition of chikungunya virus by picolinate that targets viral capsid protein. *Virology* **2016**, *498*, 265–276. [CrossRef] [PubMed]
29. Dey, D.; Siddiqui, S.I.; Mamidi, P.; Ghosh, S.; Kumar, C.S.; Chattopadhyay, S.; Ghosh, S.; Banerjee, M. The effect of amantadine on an ion channel protein from Chikungunya virus. *PLoS Negl. Trop. Dis.* **2019**, *13*, e0007548. [CrossRef]
30. Gigante, A.; Canela, M.-D.D.; Delang, L.; Priego, E.-M.M.; Camarasa, M.-J.J.; Querat, G.; Neyts, J.; Leyssen, P.; Pérez-Pérez, M.-J.J. Identification of [1,2,3]triazolo[4,5-d]pyrimidin-7(6H)-ones as novel inhibitors of Chikungunya virus replication. *J. Med. Chem.* **2014**, *57*, 4000–4008. [CrossRef]
31. Delang, L.; Li, C.; Tas, A.; Quérat, G.; Albulescu, I.C.; De Burghgraeve, T.; Guerrero, N.A.S.; Gigante, A.; Piorkowski, G.; Decroly, E.; et al. The viral capping enzyme nsP1: A novel target for the inhibition of chikungunya virus infection. *Sci. Rep.* **2016**, *6*, 31819. [CrossRef]
32. Gigante, A.; Gómez-SanJuan, A.; Delang, L.; Li, C.; Bueno, O.; Gamo, A.-M.; Priego, E.-M. Antiviral activity of [1,2,3]triazolo[4,5-d]pyrimidin-7(6H)-ones against chikungunya virus targeting the viral capping nsP1. *Antivir. Res.* **2017**, *144*, 216–222. [CrossRef] [PubMed]
33. Gómez-SanJuan, A.; Gamo, A.-M.; Delang, L.; Pérez-Sánchez, A.; Amrun, S.N.; Abdelnabi, R.; Jacobs, S.; Priego, E.-M.; Camarasa, M.-J.; Jochmans, D.; et al. Inhibition of the Replication of Different Strains of Chikungunya Virus by 3-Aryl-[1,2,3]triazolo[4,5-d]pyrimidin-7(6 H)-ones. *ACS Infect. Dis.* **2018**, *4*, 605–619. [CrossRef]
34. Moesslacher, J.; Battisti, V.; Delang, L.; Neyts, J.; Abdelnabi, R.; Pürstinger, G.; Urban, E.; Langer, T. Identification of 2-(4-(Phenylsulfonyl)piperazine-1-yl)pyrimidine Analogues as Novel Inhibitors of Chikungunya Virus. *ACS Med. Chem. Lett.* **2020**, *11*, 906–912. [CrossRef] [PubMed]
35. Abdelnabi, R.; Kovacikova, K.; Moesslacher, J.; Donckers, K.; Battisti, V.; Leyssen, P.; Langer, T.; Puerstinger, G.; Quérat, G.; Li, C.; et al. Novel Class of Chikungunya Virus Small Molecule Inhibitors That Targets the Viral Capping Machinery. *Antimicrob. Agents Chemother.* **2020**, *64*, e00649-20. [CrossRef]
36. Feibelman, K.M.; Fuller, B.P.; Li, L.; LaBarbera, D.V.; Geiss, B.J. Identification of small molecule inhibitors of the Chikungunya virus nsP1 RNA capping enzyme. *Antivir. Res.* **2018**, *154*, 124–131. [CrossRef] [PubMed]
37. Shin, Y.S.; Jarhad, D.B.; Jang, M.H.; Kovacikova, K.; Kim, G.; Yoon, J.; Kim, H.R.; Hyun, Y.E.; Tipnis, A.S.; Chang, T.S.; et al. Identification of 6′-β-fluoro-homoaristeromycin as a potent inhibitor of chikungunya virus replication. *Eur. J. Med. Chem.* **2020**, *187*, 111956. [CrossRef] [PubMed]
38. Kovacikova, K.; Morren, B.M.; Tas, A.; Albulescu, I.C.; Van Rijswijk, R.; Jarhad, D.B.; Shin, Y.S.; Jang, M.H.; Kim, G.; Lee, H.W.; et al. 6′-β-Fluoro-Homoaristeromycin and 6′-Fluoro-Homoneplanocin A Are Potent Inhibitors of Chikungunya Virus Replication through Their Direct Effect on Viral Nonstructural Protein 1. *Antimicrob. Agents Chemother.* **2020**, *64*, e02532-19. [CrossRef] [PubMed]
39. Mudgal, R.; Mahajan, S.; Tomar, S. Inhibition of Chikungunya virus by an adenosine analog targeting the SAM-dependent nsP1 methyltransferase. *FEBS Lett.* **2020**, *594*, 678–694. [CrossRef] [PubMed]
40. Bassetto, M.; De Burghgraeve, T.; Delang, L.; Massarotti, A.; Coluccia, A.; Zonta, N.; Gatti, V.; Colombano, G.; Sorba, G.; Silvestri, R.; et al. Computer-aided identification, design and synthesis of a novel series of compounds with selective antiviral activity against chikungunya virus. *Antivir. Res.* **2013**, *98*, 12–18. [CrossRef] [PubMed]
41. Tardugno, R.; Giancotti, G.; De Burghgraeve, T.; Delang, L.; Neyts, J.; Leyssen, P.; Brancale, A.; Bassetto, M. Design, synthesis and evaluation against Chikungunya virus of novel small-molecule antiviral agents. *Bioorg. Med. Chem.* **2018**, *26*, 869–874. [CrossRef]

42. Giancotti, G.; Cancellieri, M.; Balboni, A.; Giustiniano, M.; Novellino, E.; Delang, L.; Neyts, J.; Leyssen, P.; Brancale, A.; Bassetto, M. Rational modifications on a benzylidene-acrylohydrazide antiviral scaffold, synthesis and evaluation of bioactivity against Chikungunya virus. *Eur. J. Med. Chem.* **2018**, *149*, 56–68. [CrossRef]
43. Das, P.K.; Puusepp, L.; Varghese, F.S.; Utt, A.; Ahola, T.; Kananovich, D.G.; Lopp, M.; Merits, A.; Karelson, M. Design and Validation of Novel Chikungunya Virus Protease Inhibitors. *Antimicrob. Agents Chemother.* **2016**, *60*, 7382–7395. [CrossRef]
44. Lucas-Hourani, M.; Lupan, A.; Desprès, P.; Thoret, S.; Pamlard, O.; Dubois, J.; Guillou, C.; Tangy, F.; Vidalain, P.-O.; Munier-Lehmann, H. A phenotypic assay to identify Chikungunya virus inhibitors targeting the nonstructural protein nsP2. *J. Biomol. Screen.* **2013**, *18*, 172–179. [CrossRef]
45. Tripathi, P.K.; Soni, A.; Singh Yadav, S.P.; Kumar, A.; Gaurav, N.; Raghavendhar, S.; Sharma, P.; Sunil, S.; Ashish; Jayaram, B.; et al. Evaluation of novobiocin and telmisartan for anti-CHIKV activity. *Virology* **2020**, *548*, 250–260. [CrossRef] [PubMed]
46. Zhang, S.; Garzan, A.; Haese Id, N.; Bostwick, R.; Martinez-Gzegozewska, Y.; Rasmussen, L.; Streblow, D.N.; Haise, M.T.; Pathak, A.K.; Augelli-Szafran, C.E.; et al. Pyrimidone inhibitors targeting Chikungunya Virus nsP3 macrodomain by fragment-based drug design. *PLoS ONE* **2021**, *16*, e0245013.
47. Delang, L.; Segura Guerrero, N.; Tas, A.; Quérat, G.; Pastorino, B.; Froeyen, M.; Dallmeier, K.; Jochmans, D.; Herdewijn, P.; Bello, F.; et al. Mutations in the chikungunya virus non-structural proteins cause resistance to favipiravir (T-705), a broad-spectrum antiviral. *J. Antimicrob. Chemother.* **2014**, *69*, 2770–2784. [CrossRef]
48. Abdelnabi, R.; Jochmans, D.; Verbeken, E.; Neyts, J.; Delang, L. Antiviral treatment efficiently inhibits chikungunya virus infection in the joints of mice during the acute but not during the chronic phase of the infection. *Antivir. Res.* **2017**, *149*, 113–117. [CrossRef] [PubMed]
49. Ehteshami, M.; Tao, S.; Zandi, K.; Hsiao, H.-M.; Jiang, Y.; Hammond, E.; Amblard, F.; Russell, O.O.; Merits, A.; Schinazi, R.F. Characterization of β-d-N4-Hydroxycytidine as a Novel Inhibitor of Chikungunya Virus. *Antimicrob. Agents Chemother.* **2017**, *61*, e02395-16. [CrossRef] [PubMed]
50. Urakova, N.; Kuznetsova, V.; Crossman, D.K.; Sokratian, A.; Guthrie, D.B.; Kolykhalov, A.A.; Lockwood, M.A.; Natchus, M.G.; Crowley, M.R.; Painter, G.R.; et al. β-D-N4- Hydroxycytidine is a potent anti-alphavirus compound that induces a high level of mutations in the viral genome. *J. Virol.* **2017**, *92*, e01965-17. [CrossRef] [PubMed]
51. Ferreira, A.C.; Reis, P.A.; de Freitas, C.S.; Sacramento, C.Q.; Hoelz, L.V.B.; Bastos, M.M.; Mattos, M.; Rocha, N.; de Azevedo Quintanilha, I.G.; da Silva Gouveia Pedrosa, C.; et al. Beyond members of the Flaviviridae family, sofosbuvir also inhibits chikungunya virus replication. *Antimicrob. Agents Chemother.* **2019**, *63*, e01389-18. [CrossRef]
52. Wada, Y.; Orba, Y.; Sasaki, M.; Kobayashi, S.; Carr, M.J.; Nobori, H.; Sato, A.; Hall, W.W.; Sawa, H. Discovery of a novel antiviral agent targeting the nonstructural protein 4 (nsP4) of chikungunya virus. Virology. *Virology* **2017**, *505*, 102–112. [CrossRef]
53. Scuotto, M.; Abdelnabi, R.; Collarile, S.; Schiraldi, C.; Delang, L.; Massa, A.; Ferla, S.; Brancale, A.; Leyssen, P.; Neyts, J.; et al. Discovery of novel multi-target indole-based derivatives as potent and selective inhibitors of chikungunya virus replication. *Bioorg. Med. Chem.* **2017**, *25*, 327–337. [CrossRef] [PubMed]
54. Hwu, J.R.; Gupta, N.K.; Tsay, S.C.; Huang, W.C.; Albulescu, I.C.; Kovacikova, K.; van Hemert, M.J. Bis(benzofuran-thiazolidinone)s and bis(benzofuran-thiazinanone)s as inhibiting agents for chikungunya virus. *Antivir. Res.* **2017**, *146*, 96–101. [CrossRef]
55. Passos, G.F.S.; Gomes, M.G.M.; de Aquino, T.M.; de Araújo-Júnior, J.X.; de Souza, S.J.M.; Cavalcante, J.P.M.; Dos Santos, E.C.; Bassi, Ê.J.; da Silva-Júnior, E.F. Computer-Aided Design, Synthesis, and Antiviral Evaluation of Novel Acrylamides as Potential Inhibitors of E3-E2-E1 Glycoproteins Complex from Chikungunya Virus. *Pharmaceuticals* **2020**, *13*, 141. [CrossRef] [PubMed]
56. Ho, Y.J.; Liu, F.C.; Yeh, C.T.; Yang, C.M.; Lin, C.C.; Lin, T.Y.; Hsieh, P.S.; Hu, M.K.; Gong, Z.; Lu, J.W. Micafungin is a novel anti-viral agent of chikungunya virus through multiple mechanisms. *Antivir. Res.* **2018**, *159*, 134–142. [CrossRef]
57. Rothan, H.A.; Bahrani, H.; Mohamed, Z.; Teoh, T.C.; Shankar, E.M.; Rahman, N.A.; Yusof, R. A Combination of Doxycycline and Ribavirin Alleviated Chikungunya Infection. *PLoS ONE* **2015**, *10*, e0126360. [CrossRef] [PubMed]
58. Fatma, B.; Kumar, R.; Singh, V.A.; Nehul, S.; Sharma, R.; Kesari, P.; Kuhn, R.J.; Tomar, S. Alphavirus capsid protease inhibitors as potential antiviral agents for Chikungunya infection. *Antivir. Res.* **2020**, *179*, 104808. [CrossRef]
59. Mishra, P.; Kumar, A.; Mamidi, P.; Kumar, S.; Basantray, I.; Saswat, T.; Das, I.; Nayak, T.K.; Chattopadhyay, S.; Subudhi, B.B.; et al. Inhibition of Chikungunya Virus Replication by 1-[(2-Methylbenzimidazol-1-yl) Methyl]-2-Oxo-Indolin-3-ylidene] Amino] Thiourea (MBZM-N-IBT). *Sci. Rep.* **2016**, *6*, 20122. [CrossRef]
60. Singh Jadav, S.; Sinha, B.N.; Hilgenfeld, R.; Pastorino, B.; De Lamballerie, X.; Jayaprakash, V. Thiazolidone derivatives as inhibitors of chikungunya virus. *Eur. J. Med. Chem.* **2015**, *89*, 172–178. [CrossRef]
61. El-labbad, E.M.; Ismail, M.A.H.; Abou Ei Ella, D.A.; Ahmed, M.; Wang, F.; Barakat, K.H.; Abouzid, K.A.M. Discovery of Novel Peptidomimetics as Irreversible CHIKV NsP2 Protease Inhibitors Using Quantum Mechanical-Based Ligand Descriptors. *Chem. Biol. Drug Des.* **2015**, *86*, 1518–1527. [CrossRef]
62. Singh, H.; Mudgal, R.; Narwal, M.; Kaur, R.; Singh, V.A.; Malik, A.; Chaudhary, M.; Tomar, S. Chikungunya virus inhibition by peptidomimetic inhibitors targeting virus-specific cysteine protease. *Biochimie* **2018**, *149*, 51–61. [CrossRef] [PubMed]
63. Bhakat, S.; Delang, L.; Kaptein, S.; Neyts, J.; Leyssen, P.; Jayaprakash, V. Reaching beyond HIV/HCV: Nelfinavir as a potential starting point for broad-spectrum protease inhibitors against dengue and chikungunya virus. *RSC Adv.* **2015**, *5*, 85938–85949. [CrossRef]

64. Di Mola, A.; Peduto, A.; La Gatta, A.; Delang, L.; Pastorino, B.; Neyts, J.; Leyssen, P.; de Rosa, M.; Filosa, R. Structure–activity relationship study of arbidol derivatives as inhibitors of chikungunya virus replication. *Bioorg. Med. Chem.* **2014**, *22*, 6014–6025. [CrossRef] [PubMed]
65. Henß, L.; Beck, S.; Weidner, T.; Biedenkopf, N.; Sliva, K.; Weber, C.; Becker, S.; Schnierle, B.S. Suramin is a potent inhibitor of Chikungunya and Ebola virus cell entry. *Virol. J.* **2016**, *13*, 149. [CrossRef] [PubMed]
66. Albulescu, I.C.; White-Scholten, L.; Tas, A.; Hoornweg, T.E.; Ferla, S.; Kovacikova, K.; Smit, J.M.; Brancale, A.; Snijder, E.J.; van Hemert, M.J. Suramin Inhibits Chikungunya Virus Replication by Interacting with Virions and Blocking the Early Steps of Infection. *Viruses* **2020**, *12*, 314. [CrossRef]
67. Lu, J.W.; Hsieh, P.S.; Lin, C.C.; Hu, M.K.; Huang, S.M.; Wang, Y.M.; Liang, C.Y.; Gong, Z.; Ho, Y.J. Synergistic effects of combination treatment using EGCG and suramin against the chikungunya virus. *Biochem. Biophys. Res. Commun.* **2017**, *491*, 595–602. [CrossRef]
68. Weber, C.; Sliva, K.; von Rhein, C.; Kümmerer, B.M.; Schnierle, B.S. The green tea catechin, epigallocatechin gallate inhibits chikungunya virus infection. *Antivir. Res.* **2015**, *113*, 1–3. [CrossRef]
69. Loke, R.H.T.; Anderson, M.G.; Coleman, J.C.; Murray-Lyon, I.M.; Tsiquaye, K.N.; Zuckerman, A.J. Suramin treatment for chronic active hepatitis B—toxic and ineffective. *J. Med. Virol.* **1987**, *21*, 97–99. [CrossRef]
70. Kaplan, L.D.; Wolfe, P.R.; Volberding, P.A.; Feorino, P.; Abrams, D.I.; Levy, J.A.; Wong, R.; Kaufman, L.; Gottlieb, M.S. Lack of response to suramin in patients with AIDS and AIDS-related complex. *Am. J. Med.* **1987**, *82*, 615–620. [CrossRef]
71. Agarwal, G.; Gupta, S.; Gabrani, R.; Gupta, A.; Chaudhary, V.K.; Gupta, V. Virtual screening of inhibitors against Envelope glycoprotein of Chikungunya Virus: A drug repositioning approach. *Bioinformation* **2019**, *15*, 439–447. [CrossRef]
72. Fernandez-Pol, J.A.; Fernandez-Pol, S. Method to Control Dengue Viruses in Humans by Picolinic Acid and Derivates Thereof 2010. U.S. Patent 12/175,277, 21 January 2010.
73. Kim, H.Y.; Kuhn, R.J.; Patkar, C.; Warrier, R.; Cushman, M. Synthesis of dioxane-based antiviral agents and evaluation of their biological activities as inhibitors of Sindbis virus replication. *Bioorganic Med. Chem.* **2007**, *15*, 2667–2679. [CrossRef]
74. Aggarwal, M.; Tapas, S.; Preeti; Siwach, A.; Kumar, P.; Kuhn, R.J.; Tomar, S. Crystal Structure of Aura Virus Capsid Protease and Its Complex with Dioxane: New Insights into Capsid-Glycoprotein Molecular Contacts. *PLoS ONE* **2012**, *7*, e51288. [CrossRef] [PubMed]
75. Aggarwal, M.; Kaur, R.; Saha, A.; Mudgal, R.; Yadav, R.; Dash, P.K.; Parida, M.; Kumar, P.; Tomar, S. Evaluation of antiviral activity of piperazine against Chikungunya virus targeting hydrophobic pocket of alphavirus capsid protein. *Antivir. Res.* **2017**, *146*, 102–111. [CrossRef]
76. Sharma, R.; Kesari, P.; Kumar, P.; Tomar, S. Structure-function insights into chikungunya virus capsid protein: Small molecules targeting capsid hydrophobic pocket. *Virology* **2018**, *515*, 223–234. [CrossRef]
77. Jing, X.; Ma, C.; Ohigashi, Y.; Oliveira, A.F.; Jardetzky, S.T.; Pinto, H.L.; Lamb, A.R. Functional studies indicate amantadine binds to the pore of the influenza A virus M2 proton-selective ion channel. *Proc. Natl. Acad. Sci. USA* **2008**, *105*, 10967–10972. [CrossRef]
78. Cheung, J.; Frankling, M.; Mancia, F.; Rudolph, M.; Cassidy, M.; Gary, E.; Burshteyn, F.; Love, J. RCSB PDB—3TRK: Structure of the Chikungunya Virus nsP2 Protease; 2011. Available online: https://www.rcsb.org/structure/3TRK (accessed on 2 June 2021).
79. Meena, M.K.; Kumar, D.; Kumari, K.; Kaushik, N.K.; Kumar, R.V.; Bahadur, I.; Vodwal, L.; Singh, P. Promising inhibitors of nsp2 of CHIKV using molecular docking and temperature-dependent molecular dynamics simulations. *J. Biomol. Struct. Dyn.* **2021**, *21*, 1–9. [CrossRef]
80. Montes-Grajales, D.; Puerta-Guardo, H.; Espinosa, D.A.; Harris, E.; Caicedo-Torres, W.; Olivero-Verbel, J.; Martínez-Romero, E. In silico drug repurposing for the identification of potential candidate molecules against arboviruses infection. *Antivir. Res.* **2020**, *173*, 104668. [CrossRef] [PubMed]
81. Khan, N.; Bhat, R.; Patel, A.K.; Ray, P. Discovery of small molecule inhibitors of chikungunya virus proteins (nsP2 and E1) using in silico approaches. *J. Biomol. Struct. Dyn.* **2021**, *39*, 1373–1385. [CrossRef]
82. Kumar, P.; Kumar, D.; Giri, R. Targeting the nsp2 cysteine protease of Chikungunya virus using FDA approved library and selected Cysteine protease inhibitors. *Pathogens* **2019**, *8*, 128. [CrossRef] [PubMed]
83. Jain, J.; Kumari, A.; Somvanshi, P.; Grover, A.; Pai, S.; Sunil, S. In silico analysis of natural compounds targeting structural and nonstructural proteins of chikungunya virus. *F1000Research* **2017**, *6*, 1601. [CrossRef] [PubMed]
84. Agarwal, T.; Asthana, S.; Bissoyi, A. Molecular modeling and docking study to elucidate novel chikungunya virus nsP2 protease inhibitors. *Indian J. Pharm. Sci.* **2015**, *77*, 453–460.
85. Nguyen, P.T.V.; Yu, H.; Keller, P.A. Identification of chikungunya virus nsP2 protease inhibitors using structure-base approaches. *J. Mol. Graph. Model.* **2015**, *57*, 1–8. [CrossRef] [PubMed]
86. Bora, L. Homology Modeling and Docking to Potential Novel Inhibitor for Chikungunya (37997) Protein nsP2 Protease. *J Proteomics Bioinform* **2012**, *5*, 54–59. [CrossRef]
87. Singh, K.D.; Kirubakaran, P.; Nagarajan, S.; Sakkiah, S.; Muthusamy, K.; Velmurgan, D.; Jeyakanthan, J. Homology modeling, molecular dynamics, e-pharmacophore mapping and docking study of Chikungunya virus nsP2 protease. *J. Mol. Model.* **2012**, *18*, 39–51. [CrossRef] [PubMed]
88. Dhindwal, S.; Kesari, P.; Singh, H.; Kumar, P.; Tomar, S.; Sarma, R.H. Conformer and pharmacophore based identification of peptidomimetic inhibitors of chikungunya virus nsP2 protease. *J. Biomol. Struct. Dyn.* **2017**, *35*, 3522–3539. [CrossRef] [PubMed]
89. Nguyen, P.T.V.; Yu, H.; Keller, P.A. Discovery of in silico hits targeting the nsP3 macro domain of chikungunya virus. *J. Mol. Model.* **2014**, *20*, 2216. [CrossRef]

90. Abu Bakar, F.; Ng, L. Nonstructural Proteins of Alphavirus—Potential Targets for Drug Development. *Viruses* **2018**, *10*, 71. [CrossRef] [PubMed]
91. Abdelnabi, R.; de Morais, A.T.S.; Leyssen, P.; Imbert, I.; Beaucourt, S.; Blanc, H.; Froeyen, M.; Vignuzzi, M.; Canard, B.; Neyts, J.; et al. Understanding the Mechanism of the Broad-Spectrum Antiviral Activity of Favipiravir (T-705): Key Role of the F1 Motif of the Viral Polymerase. *J. Virol.* **2017**, *91*, e00487-17. [CrossRef] [PubMed]
92. Franco, E.J.; Rodriquez, J.L.; Pomeroy, J.J.; Hanrahan, K.C.; Brown, A.N. The effectiveness of antiviral agents with broad-spectrum activity against chikungunya virus varies between host cell lines. *Antivir. Chem. Chemother.* **2018**, *26*, 204020661880758. [CrossRef]
93. Julander, J.G.; Dagley, A.; Gebre, M.; Komeno, T.; Nakajima, N.; Smee, D.F.; Furuta, Y. Strain-dependent disease and response to favipiravir treatment in mice infected with Chikungunya virus. *Antivir. Res.* **2020**, *182*, 104904. [CrossRef]
94. Kumar, S.P.; Kapopara, R.G.; Patni, M.I.; Pandya, H.A.; Jasrai, Y.T.; Patel, S.K. Exploring the polymerase activity of chikungunya viral non structural protein 4 (nsP4) using molecular modeling, e-pharmacophore and docking studies. *Int. J. Pharm. Life Sci.* **2012**, *3*, 1752–1765.
95. Khan, M.; Santhosh, S.R.; Tiwari, M.; Lakshmana Roa, P.V.; Parida, M. Assessment of in vitro prophylactic and therapeutic efficacy of chloroquine against chikungunya virus in Vero cells. *J. Med. Virol.* **2010**, *88*, 817–824. [CrossRef] [PubMed]
96. Varghese, F.S.; Rausalu, K.; Hakanen, M.; Saul, S.; Kümmerer, B.M.; Susi, P.; Merits, A.; Ahola, T. Obatoclax Inhibits Alphavirus Membrane Fusion by Neutralizing the Acidic Environment of Endocytic Compartments. *Antimicrob. Agents Chemother.* **2017**, *61*, e02227-16. [CrossRef] [PubMed]
97. Wang, Y.-M.; Lu, J.-W.; Lin, C.-C.; Chin, Y.-F.; Wu, T.-Y.; Lin, L.-I.; Lai, Z.-Z.; Kuo, S.-C.; Ho, Y.-J. Antiviral activities of niclosamide and nitazoxanide against chikungunya virus entry and transmission. *Antivir. Res.* **2016**, *135*, 81–90. [CrossRef]
98. Hua, C.; Lee, R.; Hussain, K.M.; Jang, J.; Chuid, H. Macropinocytosis dependent entry of Chikungunya virus into human muscle cells. *PLoS Negl. Trop. Dis.* **2019**, *13*, e0007610.
99. Karlas, A.; Berre, S.; Couderc, T.; Varjak, M.; Braun, P.; Meyer, M.; Gangneux, N.; Karo-Astover, L.; Weege, F.; Raftery, M.; et al. A human genome-wide loss-of-function screen identifies effective chikungunya antiviral drugs. *Nat. Commun.* **2016**, *7*, 11320. [CrossRef]
100. Bakhache, W.; Neyret, A.; McKellar, J.; Clop, C.; Bernard, E.; Weger-Lucarelli, J.; Briant, L. Fatty acid synthase and stearoyl-CoA desaturase-1 are conserved druggable cofactors of Old World Alphavirus genome replication. *Antivir. Res.* **2019**, *172*, 104642. [CrossRef]
101. Hitakarun, A.; Khongwichit, S.; Wikan, N.; Roytrakul, S.; Yoksan, S.; Rajakam, S.; Davidson, A.D.; Smith, D.R. Evaluation of the antiviral activity of orlistat (tetrahydrolipstatin) against dengue virus, Japanese encephalitis virus, Zika virus and chikungunya virus. *Sci. Rep.* **2020**, *10*, 1499. [CrossRef]
102. Wichit, S.; Hamel, R.; Bernard, E.; Talignani, L.; Diop, F.; Ferraris, P.; Liegeois, F.; Ekchariyawat, P.; Luplertlop, N.; Surasombatpattana, P.; et al. Imipramine Inhibits Chikungunya Virus Replication in Human Skin Fibroblasts through Interference with Intracellular Cholesterol Trafficking. *Sci. Rep.* **2017**, *7*, 3145. [CrossRef]
103. Hwang, J.; Wang, Y.; Fikrig, E. Inhibition of chikungunya virus replication in primary human fibroblasts by liver X receptor agonist. *Antimicrob. Agents Chemother.* **2019**, *63*, e01220-19. [CrossRef]
104. Briolant, S.; Garin, D.; Scaramozzino, N.; Jouan, A.; Crance, J.M. In vitro inhibition of Chikungunya and Semliki Forest viruses replication by antiviral compounds: Synergistic effect of interferon-alpha and ribavirin combination. *Antivir. Res.* **2004**, *61*, 111–117. [CrossRef]
105. Tong, X.; Smith, J.; Bukreyeva, N.; Koma, T.; Manning, J.T.; Kalkeri, R.; Kwong, A.D.; Paessler, S. Merimepodib, an IMPDH inhibitor, suppresses replication of Zika virus and other emerging viral pathogens. *Antivir. Res.* **2018**, *149*, 34–40. [CrossRef] [PubMed]
106. Lucas-Hourani, M.; Dauzonne, D.; Jorda, P.; Lle Cousin, G.; Lupan, A.; Helynck, O.; Gory Caignard, G.; Ve Janvier, G.; Naë Lle André -Leroux, G.; Khiar, S.; et al. Inhibition of Pyrimidine Biosynthesis Pathway Suppresses Viral Growth through Innate Immunity. *PLoS Pathog.* **2013**, *9*, e1003678. [CrossRef] [PubMed]
107. Lucas-Hourani, M.; Dauzonne, D.; Munier-Lehmann, H.; Khiar, S.; Nisole, S.; Dairou, J.; Helynck, O.; Afonso, P.V.; Tangy, F.; Vidalain, P.O. Original chemical series of pyrimidine biosynthesis inhibitors that boost the antiviral interferon response. *Antimicrob. Agents Chemother.* **2017**, *61*, e00383-17. [CrossRef] [PubMed]
108. Yang, Y.; Cao, L.; Gao, H.; Wu, Y.; Wang, Y.; Fang, F.; Lan, T.; Lou, Z.; Rao, Y. Discovery, Optimization, and Target Identification of Novel Potent Broad-Spectrum Antiviral Inhibitors. *J. Med. Chem.* **2019**, *62*, 4056–4073. [CrossRef] [PubMed]
109. Cifuentes Kottkamp, A.; De Jesus, E.; Grande, R.; Brown, J.A.; Jacobs, A.R.; Lim, J.K.; Stapleford, K.A. Atovaquone Inhibits Arbovirus Replication through the Depletion of Intracellular Nucleotides. *J. Virol.* **2019**, *93*, e00389-19. [CrossRef]
110. Hwang, J.; Jiang, A.; Fikrig, E. A potent prolyl tRNA synthetase inhibitor antagonizes Chikungunya and Dengue viruses. *Antivir. Res.* **2019**, *161*, 163–168. [CrossRef]
111. Kaur, P.; Thiruchelvan, M.; Lee, R.C.H.; Chen, H.; Chen, K.C.; Ng, M.L.; Chu, J.J.H. Inhibition of chikungunya virus replication by harringtonine, a novel antiviral that suppresses viral protein expression. *Antimicrob. Agents Chemother.* **2013**, *57*, 155–167. [CrossRef]
112. Lundberg, L.; Brahms, A.; Hooper, I.; Carey, B.; Lin, S.C.; Dahal, B.; Narayanan, A.; Kehn-Hall, K. Repurposed FDA-Approved drug sorafenib reduces replication of Venezuelan equine encephalitis virus and other alphaviruses. *Antivir. Res.* **2018**, *157*, 57–67. [CrossRef]

113. Kaur, P.; Lello, L.S.; Utt, A.; Dutta, S.K.; Merits, A.; Chu, J.J.H. Bortezomib inhibits chikungunya virus replication by interfering with viral protein synthesis. *PLoS Negl. Trop. Dis.* **2020**, *14*, e0008336. [CrossRef]
114. Hwang, J.; Jiang, A.; Fikrig, E. Rev-erb Agonist Inhibits Chikungunya and O'nyong'nyong Virus Replication. *Open Forum Infect. Dis.* **2018**, *5*, ofy315. [CrossRef]
115. Hackett, B.A.; Dittmar, M.; Segrist, E.; Pittenger, N.; To, J.; Griesman, T.; Gordesky-Gold, B.; Schultz, D.C.; Cherry, S. Sirtuin inhibitors are broadly antiviral against arboviruses. *MBio* **2019**, *10*, e01446-19. [CrossRef] [PubMed]
116. Rathore, A.P.S.; Haystead, T.; Das, P.K.; Merits, A.; Ng, M.L.; Vasudevan, S.G. Chikungunya virus nsP3 & nsP4 interacts with HSP-90 to promote virus replication: HSP-90 inhibitors reduce CHIKV infection and inflammation in vivo. *Antivir. Res.* **2014**, *103*, 7–16.
117. Barrera, M.D.; Callahan, V.; Akhrymuk, I.; Bhalla, N.; Zhou, W.; Campbell, C.; Narayanan, A.; Kehn-hall, K. Proteomic discovery of veev e2-host partner interactions identifies grp78 inhibitor ha15 as a potential therapeutic for alphavirus infections. *Pathogens* **2021**, *10*, 283. [CrossRef]
118. Langsjoen, R.M.; Auguste, A.J.; Rossi, S.L.; Roundy, C.M.; Penate, H.N.; Kastis, M.; Schnizlein, M.K.; Le, K.C.; Haller, S.L.; Chen, R.; et al. Host oxidative folding pathways offer novel anti-chikungunya virus drug targets with broad spectrum potential. *Antivir. Res.* **2017**, *143*, 246–251. [CrossRef] [PubMed]
119. Zilbermintz, L.; Leonardi, W.; Jeong, S.Y.; Sjodt, M.; McComb, R.; Ho, C.L.C.; Retterer, C.; Gharaibeh, D.; Zamani, R.; Soloveva, V.; et al. Identification of agents effective against multiple toxins and viruses by host-oriented cell targeting. *Sci. Rep.* **2015**, *5*, 13476. [CrossRef]
120. Yoon, J.S.; Kim, G.; Jarhad, D.B.; Kim, H.R.; Shin, Y.S.; Qu, S.; Sahu, P.K.; Kim, H.O.; Lee, H.W.; Wang, S.B.; et al. Design, Synthesis, and Anti-RNA Virus Activity of 6′-Fluorinated-Aristeromycin Analogues. *J. Med. Chem.* **2019**, *62*, 6346–6362. [CrossRef] [PubMed]
121. Broeckel, R.; Sarkar, S.; May, N.A.; Totonchy, J.; Kreklywich, C.N.; Smith, P.; Graves, L.; DeFilippis, V.R.; Heise, M.T.; Morrison, T.E.; et al. Src family kinase inhibitors block translation of alphavirus subgenomic mRNAs. *Antimicrob. Agents Chemother.* **2019**, *63*, e02325-18. [CrossRef]
122. Cruz, D.J.M.; Bonotto, R.M.; Gomes, R.G.B.; da Silva, C.T.; Taniguchi, J.B.; No, J.H.; Lombardot, B.; Schwartz, O.; Hansen, M.A.E.; Freitas-Junior, L.H. Identification of Novel Compounds Inhibiting Chikungunya Virus-Induced Cell Death by High Throughput Screening of a Kinase Inhibitor Library. *PLoS Negl. Trop. Dis.* **2013**, *7*, e2471. [CrossRef]
123. Varghese, F.S.; Kaukinen, P.; Gläsker, S.; Bespalov, M.; Hanski, L.; Wennerberg, K.; Kümmerer, B.M.; Ahola, T. Discovery of berberine, abamectin and ivermectin as antivirals against chikungunya and other alphaviruses. *Antivir. Res.* **2016**, *126*, 117–124. [CrossRef]
124. Varghese, F.S.; Thaa, B.; Amrun, S.N.; Simarmata, D.; Rausalu, K.; Nyman, T.A.; Merits, A.; McInerney, G.M.; Ng, L.F.P.; Ahola, T. The Antiviral Alkaloid Berberine Reduces Chikungunya Virus-Induced Mitogen-Activated Protein Kinase Signaling. *J. Virol.* **2016**, *90*, 9743–9757. [CrossRef]
125. Sharma, A.; Bhomia, M.; Yeh, T.-J.J.; Singh, J.; Maheshwari, R.K. Miltefosine inhibits Chikungunya virus replication in human primary dermal fibroblasts. *F1000Research* **2018**, *7*, 9. [CrossRef]
126. Abdelnabi, R.; Amrun, S.N.; Ng, L.F.P.; Leyssen, P.; Neyts, J.; Delang, L. Protein kinases C as potential host targets for the inhibition of chikungunya virus replication. *Antivir. Res.* **2017**, *139*, 79–87. [CrossRef] [PubMed]
127. Staveness, D.; Abdelnabi, R.; Schrier, A.J.; Loy, B.A.; Verma, V.A.; DeChristopher, B.A.; Near, K.E.; Neyts, J.; Delang, L.; Leyssen, P.; et al. Simplified Bryostatin Analogues Protect Cells from Chikungunya Virus-Induced Cell Death. *J. Nat. Prod.* **2016**, *79*, 675–679. [CrossRef] [PubMed]
128. Staveness, D.; Abdelnabi, R.; Near, K.E.; Nakagawa, Y.; Neyts, J.; Delang, L.; Leyssen, P.; Wender, P.A. Inhibition of Chikungunya Virus-Induced Cell Death by Salicylate-Derived Bryostatin Analogues Provides Additional Evidence for a PKC-Independent Pathway. *J. Nat. Prod.* **2016**, *79*, 680–684. [CrossRef]
129. Pu, S.-Y.; Wouters, R.; Schor, S.; Rozenski, J.; Barouch-Bentov, R.; Prugar, L.I.; O'brien, C.M.; Brannan, J.M.; Dye, J.M.; Herdewijn, P.; et al. Optimization of Isothiazolo[4,3-b]pyridine-Based Inhibitors of Cyclin G Associated Kinase (GAK) with Broad-Spectrum Antiviral Activity. *J. Med. Chem.* **2018**, *61*, 6178–6192. [CrossRef] [PubMed]
130. Mounce, B.C.; Cesaro, T.; Moratorio, G.; Hooikaas, P.J.; Yakovleva, A.; Werneke, S.W.; Smith, E.C.; Poirier, E.Z.; Simon-Loriere, E.; Prot, M.; et al. Inhibition of Polyamine Biosynthesis Is a Broad-Spectrum Strategy against RNA Viruses. *J. Virol.* **2016**, *90*, 9683–9692. [CrossRef] [PubMed]
131. Cheung, Y.Y.; Chen, K.C.; Chen, H.; Seng, E.K.; Chu, J.J.H. Antiviral activity of lanatoside C against dengue virus infection. *Antivir. Res.* **2014**, *111*, 93–99. [CrossRef] [PubMed]
132. Müller, M.; Slivinski, N.; Todd, E.J.A.A.; Khalid, H.; Li, R.; Karwatka, M.; Merits, A.; Mankouri, J.; Tuplin, A. Chikungunya virus requires cellular chloride channels for efficient genome replication. *PLoS Negl. Trop. Dis.* **2019**, *13*, e0007703. [CrossRef]
133. Bouma, E.M.; van de Pol, D.P.I.; Sanders, I.D.; Rodenhuis-Zybert, I.A.; Smit, J.M. Serotonergic Drugs Inhibit Chikungunya Virus Infection at Different Stages of the Cell Entry Pathway. *J. Virol.* **2020**, *94*, e00274-20. [CrossRef]
134. Mainou, B.A.; Ashbrook, A.W.; Smith, E.C.; Dorset, D.C.; Denison, M.R.; Dermody, T.S. Serotonin Receptor Agonist 5-Nonyloxytryptamine Alters the Kinetics of Reovirus Cell Entry. *J. Virol.* **2015**, *89*, 8701–8712. [CrossRef] [PubMed]
135. Ekins, S.; Madrid, P.B. Tilorone, a broad-spectrum antiviral for emerging viruses. *Antimicrob. Agents Chemother.* **2020**, *64*, e00440-20. [CrossRef] [PubMed]

136. Gall, B.; Pryke, K.; Abraham, J.; Mizuno, N.; Botto, S.; Sali, T.M.; Broeckel, R.; Haese, N.; Nilsen, A.; Placzek, A.; et al. Emerging Alphaviruses Are Sensitive to Cellular States Induced by a Novel Small-Molecule Agonist of the STING Pathway. *J. Virol.* **2017**, *92*, e01913-17. [CrossRef] [PubMed]
137. Sali, T.M.; Pryke, K.M.; Abraham, J.; Liu, A.; Archer, I.; Broeckel, R.; Staverosky, J.A.; Smith, J.L.; Al-Shammari, A.; Amsler, L.; et al. Characterization of a Novel Human-Specific STING Agonist that Elicits Antiviral Activity Against Emerging Alphaviruses. *PLoS Pathog.* **2015**, *11*, e1005324. [CrossRef]
138. Pryke, K.M.; Abraham, J.; Sali, T.M.; Gall, B.J.; Archer, I.; Liu, A.; Bambina, S.; Baird, J.; Gough, M.; Chakhtoura, M.; et al. A novel agonist of the trif pathway induces a cellular state refractory to replication of Zika, Chikungunya, and dengue viruses. *MBio* **2017**, *8*, e00452-17. [CrossRef] [PubMed]
139. Herrero, L.J.; Foo, S.-S.; Sheng, K.-C.; Chen, W.; Forwood, M.R.; Bucala, R.; Mahalingam, S. Pentosan Polysulfate: A Novel Glycosaminoglycan-Like Molecule for Effective Treatment of Alphavirus-Induced Cartilage Destruction and Inflammatory Disease. *J. Virol.* **2015**, *89*, 8063–8076. [CrossRef]
140. Supramaniam, A.; Liu, X.; Ferro, V.; Herrero, L.J. Prophylactic antiheparanase activity by PG545 is antiviral in vitro and protects against Ross River virus disease in mice. *Antimicrob. Agents Chemother.* **2018**, *62*, e01959-17. [CrossRef]
141. Pou, S.; Winter, R.W.; Nilsen, A.; Kelly, J.X.; Li, Y.; Doggett, J.S.; Riscoe, E.W.; Wegmann, K.W.; Hinrichs, D.J.; Riscoe, M.K. Sontochin as a guide to the development of drugs against chloroquine-resistant malaria. *Antimicrob. Agents Chemother.* **2012**, *56*, 3475–3480. [CrossRef]
142. Inglot, A.D. Comparison of the Antiviral Activity in vitro of some Non-steroidal Anti-inflammatory Drugs. *J. Gen. Virol* **1969**, *4*, 203–214. [CrossRef]
143. Shimizu, Y.; Yamamoto, S.; Homma, M.; Ishida, N. Effect of chloroquine on the growth of animal viruses. *Arch. Gesamte Virusforsch.* **1972**, *36*, 93–104. [CrossRef]
144. Helenius, A.; Marsht, M.; Whiter, J. Inhibition of Semliki Forest Virus Penetration by Lysosomotropic Weak Bases. *J. Gen. Virol* **1982**, *58*, 47–61. [CrossRef] [PubMed]
145. Cassell, S.; Edwards, J.; Brown, D.T. Effects of lysosomotropic weak bases on infection of BHK-21 cells by Sindbis virus. *J. Virol.* **1984**, *52*, 857–864. [CrossRef] [PubMed]
146. Freedman, A.; Steinberg, V.L. Chloroquine in rheumatoid arthritis; a double blindfold trial of treatment for one year. *Ann. Rheum. Dis* **1960**, *19*, 243–250. [CrossRef] [PubMed]
147. Brighton, S.W. Chloroquine phosphate treatment of chronic Chikungunya arthritis An open pilot study. *S. Afr. Med. J.* **1984**, *66*, 217–218.
148. De Lamballerie, X.; Boisson, V.; Reynier, J.-C.; Enault, S.; Charrel, R.N.; Flahault, A.; Roques, P.; Le Grand, R. On Chikungunya Acute Infection and Chloroquine Treatment. *Vector-Borne Zoonotic Dis.* **2008**, *8*, 837–839. [CrossRef] [PubMed]
149. Thiberville, S.D.; Boisson, V.; Gaudart, J.; Simon, F.; Flahault, A.; de Lamballerie, X. Chikungunya Fever: A Clinical and Virological Investigation of Outpatients on Reunion Island, South-West Indian Ocean. *PLoS Negl. Trop. Dis.* **2013**, *7*, e2004. [CrossRef]
150. Chopra, A.; Saluja, M.; Venugopalan, A. Effectiveness of chloroquine and inflammatory cytokine response in patients with early persistent musculoskeletal pain and arthritis following chikungunya virus infection. *Arthritis Rheumatol.* **2014**, *66*, 319–326. [CrossRef]
151. Rodrigo, C.; Fernando, S.D.; Rajapakse, S.; Paul, M. Systematic review Clinical evidence for repurposing chloroquine and hydroxychloroquine as antiviral agents: A systematic review. *Clin. Microbiol. Infect.* **2020**, *26*, 979–987. [CrossRef]
152. Roques, P.; Thiberville, S.D.; Dupuis-Maguiraga, L.; Lum, F.M.; Labadie, K.; Martinon, F.; Gras, G.; Lebon, P.; Ng, L.F.P.; de Lamballerie, X.; et al. Paradoxical effect of chloroquine treatment in enhancing chikungunya virus infection. *Viruses* **2018**, *10*, 268. [CrossRef]
153. Ozden, S.; Lucas-Hourani, M.; Ceccaldi, P.-E.; Basak, A.; Valentine, M.; Benjannet, S.; Hamelin, J.; Jacob, Y.; Mamchaoui, K.; Mouly, V.; et al. Inhibition of Chikungunya virus infection in cultured human muscle cells by furin inhibitors: Impairment of the maturation of the E2 surface glycoprotein. *J. Biol. Chem.* **2008**, *283*, 21899–21908. [CrossRef] [PubMed]
154. Faraone, I.; Labanca, F.; Ponticelli, M.; De Tommasi, N.; Milella, L. Recent Clinical and Preclinical Studies of Hydroxychloroquine on RNA Viruses and Chronic Diseases: A Systematic Review. *Molecules* **2020**, *25*, 5318. [CrossRef] [PubMed]
155. Padmakumar, B.; Jayan, J.B.; Menon, R.M.R.; Krishnankutty, B.; Payippallil, R.; Nisha, R.S. Comparative evaluation of four therapeutic regimes in Chikungunya arthritis: A prospective randomized parallel-group study. *Indian J. Rheumatol.* **2009**, *4*, 94–101. [CrossRef]
156. Ravindran, V.; Alias, G. Efficacy of combination DMARD therapy vs. hydroxychloroquine monotherapy in chronic persistent chikungunya arthritis: A 24-week randomized controlled open label study. *Clin. Rheumatol.* **2017**, *36*, 1335–1340. [CrossRef] [PubMed]
157. Pandya, S. Methotrexate and hydroxychloroquine combination therapy in chronic chikungunya arthritis: A 16 week study. *Indian J. Rheumatol.* **2008**, *3*, 93–97. [CrossRef]
158. Bouquillard, E.; Fianu, A.; Bangil, M.; Charlette, N.; Ribéra, A.; Michault, A.; Favier, F.; Simon, F.; Flipo, R.M. Rheumatic manifestations associated with Chikungunya virus infection: A study of 307 patients with 32-month follow-up (RHUMATOCHIK study). *Jt. Bone Spine* **2018**, *85*, 207–210. [CrossRef]
159. Sourisseau, M.; Schilte, C.; Casartelli, N.; Trouillet, C.; Guivel-Benhassine, F.; Rudnicka, D.; Sol-Foulon, N.; Le Roux, K.; Prevost, M.-C.; Fsihi, H.; et al. Characterization of Reemerging Chikungunya Virus. *PLoS Pathog.* **2007**, *3*, e89. [CrossRef]

160. Irurzun, A.; Nieva, J.L.; Carrasco, L. Entry of Semliki forest virus into cells: Effects of concanamycin A and nigericin on viral membrane fusion and infection. *Virology* **1997**, *227*, 488–492. [CrossRef]
161. Jurgeit, A.; Mcdowell, R.; Moese, S.; Meldrum, E.; Schwendener, R. Niclosamide Is a Proton Carrier and Targets Acidic Endosomes with Broad Antiviral Effects. *PLoS Pathog.* **2012**, *8*, e1002976. [CrossRef]
162. Koivusalo, M.; Welch, C.; Hayashi, H.; Scott, C.C.; Kim, M.; Alexander, T.; Touret, N.; Hahn, K.M.; Grinstein, S. Amiloride inhibits macropinocytosis by lowering submembranous pH and preventing Rac1 and Cdc42 signaling. *J. Cell Biol.* **2010**, *188*, 547–563. [CrossRef]
163. Shu, Q.; Nair, V. Inosine monophosphate dehydrogenase (IMPDH) as a target in drug discovery. *Med. Res. Rev.* **2008**, *28*, 219–232. [CrossRef] [PubMed]
164. Turner, T.L.; Kopp, B.T.; Paul, G.; Landgrave, L.C.; Hayes, D.; Thompson, R. Respiratory syncytial virus: Current and emerging treatment options. *Clin. Outcomes Res.* **2014**, *6*, 217–225. [CrossRef]
165. Paeshuyse, J.; Dallmeier, K.; Neyts, J. Ribavirin for the treatment of chronic hepatitis C virus infection: A review of the proposed mechanisms of action. *Curr. Opin. Virol.* **2011**, *1*, 590–598. [CrossRef] [PubMed]
166. Gallegos, K.M.; Drusano, G.L.; D'Argenio, D.Z.; Brown, A.N. Chikungunya Virus: In Vitro Response to Combination Therapy With Ribavirin and Interferon Alfa 2a. *J. Infect. Dis.* **2016**, *214*, 1192–1197. [CrossRef] [PubMed]
167. Rothan, H.A.; Bahrani, H.; Abdulrahman, A.Y.; Mohamed, Z.; Teoh, T.C.; Othman, S.; Rashid, N.N.; Rahman, N.A.; Yusof, R. Mefenamic acid in combination with ribavirin shows significant effects in reducing chikungunya virus infection in vitro and in vivo. *Antivir. Res.* **2016**, *127*, 50–56. [CrossRef] [PubMed]
168. Ravichandran, R.; Manian, M. Ribavirin therapy for Chikungunya arthritis. *J. Infect. Dev. Ctries.* **2008**, *2*, 140–142. [CrossRef] [PubMed]
169. Rashad, A.A.; Neyts, J.; Leyssen, P.; Keller, P.A. A reassessment of mycophenolic acid as a lead compound for the development of inhibitors of chikungunya virus replication. *Tetrahedron* **2018**, *74*, 1294–1306. [CrossRef]
170. Khan, M.; Dhanwani, R.; Patro, I.K.; Rao, P.V.L.; Parida, M.M. Cellular IMPDH enzyme activity is a potential target for the inhibition of Chikungunya virus replication and virus induced apoptosis in cultured mammalian cells. *Antivir. Res.* **2010**, *89*, 1–8. [CrossRef]
171. Rada, B.; Dragúň, M. Antiviral Action and Selectivity of 6-Azauridine. *Ann. N. Y. Acad. Sci.* **1977**, *284*, 410–417. [CrossRef]
172. Deneau, D.G.; Farber, E.M. The treatment of psoriasis with azaribine. *Dermatologica* **1975**, *151*, 158–163. [CrossRef]
173. Cruthcher, W.A.; Moschella, S.L. Double-blind controlled crossover high-dose study of Azaribine in psoriasis. *Br. J. Dermatol.* **1975**, *92*, 199–205. [CrossRef]
174. Raveh, A.; Delekta, P.C.; Dobry, C.J.; Peng, W.; Schultz, P.J.; Blakely, P.K.; Tai, A.W.; Matainaho, T.; Irani, D.N.; Sherman, D.H.; et al. Discovery of Potent Broad Spectrum Antivirals Derived from Marine Actinobacteria. *PLoS ONE* **2013**, *8*, e82318. [CrossRef] [PubMed]
175. Ashton, T.M.; Fokas, E.; Kunz-Schughart, L.A.; Folkes, L.K.; Anbalagan, S.; Huether, M.; Kelly, C.J.; Pirovano, G.; Buffa, F.M.; Hammond, E.M.; et al. The anti-malarial atovaquone increases radiosensitivity by alleviating tumour hypoxia. *Nat. Commun.* **2016**, *7*, 12308. [CrossRef] [PubMed]
176. Keller, T.L.; Zocco, D.; Sundrud, M.S.; Hendrick, M.; Edenius, M.; Yum, J.; Kim, Y.-J.; Lee, H.-K.; Cortese, J.F.; Wirth, D.F.; et al. Halofuginone and other febrifugine derivatives inhibit prolyl-tRNA synthetase. *Nat. Chem. Biol.* **2012**, *8*, 311–317. [CrossRef] [PubMed]
177. Fresno, M.; Jiménez, A.; Vázquez, D. Inhibition of Translation in Eukaryotic Systems by Harringtonine. *Eur. J. Biochem.* **1977**, *72*, 323–330. [CrossRef] [PubMed]
178. McKendrick, L.; Morley, S.J.; Pain, V.M.; Jagus, R.; Joshi, B. Phosphorylation of eukaryotic initiation factor 4E (eIF4E) at Ser209 is not required for protein synthesis in vitro and in vivo. *Eur. J. Biochem.* **2001**, *268*, 5375–5385. [CrossRef]
179. Henss, L.; Scholz, T.; Grünweller, A.; Schnierle, B.; Henss, L.; Scholz, T.; Grünweller, A.; Schnierle, B.S. Silvestrol Inhibits Chikungunya Virus Replication. *Viruses* **2018**, *10*, 592. [CrossRef]
180. Blum, L.; Geisslinger, G.; Parnham, M.J.; Grünweller, A.; Schiffmann, S. Natural antiviral compound silvestrol modulates human monocyte-derived macrophages and dendritic cells. *J. Cell. Mol. Med.* **2020**, *24*, 6988–6999. [CrossRef] [PubMed]
181. Luo, H. Interplay between the virus and the ubiquitin-proteasome system: Molecular mechanism of viral pathogenesis. *Curr. Opin. Virol.* **2016**, *17*, 1–10. [CrossRef]
182. Geller, R.; Taguwa, S.; Frydman, J. Broad action of Hsp90 as a host chaperone required for viral replication. *Biochim. Biophys. Acta Mol. Cell Res.* **2012**, *1823*, 698–706. [CrossRef]
183. Das, I.; Basantray, I.; Mamidi, P.; Nayak, T.K.; Pratheek, B.M.; Chattopadhyay, S.; Chattopadhyay, S. Heat Shock Protein 90 Positively Regulates Chikungunya Virus Replication by Stabilizing Viral Non-Structural Protein nsP2 during Infection. *PLoS ONE* **2014**, *9*, e100531. [CrossRef]
184. Izumida, M.; Hayashi, H.; Tanaka, A.; Kubo, Y. Cathepsin B Protease Facilitates Chikungunya Virus Envelope Protein-Mediated Infection Via Endocytosis or Macropinocytosis. *Viruses* **2020**, *12*, 722. [CrossRef]
185. Klimstra, W.B.; Heidner, H.W.; Johnston, R.E.; Klimstra, B.; Ryman, K.D.; Johnston, R.E.; Virol, J. The Furin Protease Cleavage Recognition Sequence of Sindbis Virus PE2 Can Mediate Virion Attachment to Cell Surface Heparan Sulfate. *J. Virol.* **1999**, *73*, 6299–6306. [CrossRef]

186. Heidner, H.W.; Knott, T.A.; Johnston, R.E.; Heidner, H.W.; McKnight, K.L.; Davis, N.L.; Johnston, R.E.; Virol, J. Differential Processing of Sindbis Virus Glycoprotein PE2 in Cultured Vertebrate and Arthropod Cells. *J. Virol.* **1996**, *70*, 2069–2073. [CrossRef]
187. Zhang, X.; Fugère, M.; Day, R.; Kielian, M. Furin Processing and Proteolytic Activation of Semliki Forest Virus. *J. Virol.* **2003**, *77*, 2981–2989. [CrossRef]
188. Hardes, K.; Ivanova, T.; Thaa, B.; McInerney, G.M.; Klokk, T.I.; Sandvig, K.; Künzel, S.; Lindberg, I.; Steinmetzer, T. Elongated and Shortened Peptidomimetic Inhibitors of the Proprotein Convertase Furin. *ChemMedChem* **2017**, *12*, 613–620. [CrossRef]
189. Wolfe, M.S.; Borchardt, R.T. S-Adenosyl-L-homocysteine Hydrolase as a Target for Antiviral Chemotherapy. *J. Med. Chem.* **1991**, *34*, 1521–1530. [CrossRef]
190. Keating, J.A.; Striker, R. Phosphorylation events during viral infections provide potential therapeutic targets. *Rev. Med. Virol.* **2012**, *22*, 166–181. [CrossRef]
191. Wan, J.J.; Brown, R.S.; Kielian, M. Berberine chloride is an alphavirus inhibitor that targets nucleocapsid assembly. *MBio* **2020**, *11*, e01382-20. [CrossRef]
192. Bourjot, M.; Delang, L.; Nguyen, V.H.; Neyts, J.; Oise Gueitte, F.; Leyssen, P.; Litaudon, M. Prostratin and 12-O-Tetradecanoylphorbol 13-Acetate Are Potent and Selective Inhibitors of Chikungunya Virus Replication. *J. Nat. Prod.* **2012**, *75*, 2183–2187. [CrossRef]
193. Abdelnabi, R.; Staveness, D.; Near, K.E.; Wender, P.A.; Delang, L.; Neyts, J.; Leyssen, P. Comparative analysis of the anti-chikungunya virus activity of novel bryostatin analogs confirms the existence of a PKC-independent mechanism. *Biochem. Pharmacol.* **2016**, *120*, 15–21. [CrossRef]
194. Mounce, B.C.; Poirier, E.Z.; Passoni, G.; Simon-Loriere, E.; Cesaro, T.; Prot, M.; Stapleford, K.A.; Moratorio, G.; Sakuntabhai, A.; Levraud, J.-P.; et al. Interferon-Induced Spermidine-Spermine Acetyltransferase and Polyamine Depletion Restrict Zika and Chikungunya Viruses. *Cell Host Microbe* **2016**, *20*, 167–177. [CrossRef] [PubMed]
195. Mounce, B.C.; Cesaro, T.; Vlajnić, L.; Vidina, A.; Vallet, T.; Weger-Lucarelli, J.; Passoni, G.; Stapleford, K.A.; Levraud, J.-P.; Vignuzzi, M. Chikungunya Virus Overcomes Polyamine Depletion by Mutation of nsP1 and the Opal Stop Codon To Confer Enhanced Replication and Fitness. *J. Virol.* **2017**, *91*, e00344-17. [CrossRef]
196. Hover, S.; Foster, B.; Barr, J.N.; Mankouri, J. Viral dependence on cellular ion channels—An emerging antiviral target? *J. Gen. Virol.* **2017**, *98*, 345–351. [CrossRef] [PubMed]
197. Cook, L.E.; Locke, M.C.; Young, A.R.; Monte, K.; Hedberg, M.L.; Shimak, R.M.; Sheehan, K.C.F.; Veis, D.J.; Diamond, M.S.; Lenschow, D.J. Distinct Roles of Interferon Alpha and Beta in Controlling Chikungunya Virus Replication and Modulating Neutrophil-Mediated Inflammation. *J. Virol.* **2019**, *94*, e00841-19. [CrossRef] [PubMed]
198. Krueger, R.F.; Mayer, G.D. Tilorone hydrochloride: An orally active antiviral agent. *Science* **1970**, *169*, 1213–1214. [CrossRef] [PubMed]
199. Li, Y.G.; Siripanyaphinyo, U.; Tumkosit, U.; Noranate, N.; A-Nuegoonpipat, A.; Pan, Y.; Kameoka, M.; Kurosu, T.; Ikuta, K.; Takeda, N.; et al. Poly (I:C), an agonist of toll-like receptor-3, inhibits replication of the Chikungunya virus in BEAS-2B cells. *Virol. J.* **2012**, *9*, 114. [CrossRef]
200. Priya, R.; Patro, I.K.; Parida, M.M. TLR3 mediated innate immune response in mice brain following infection with Chikungunya virus. *Virus Res.* **2014**, *189*, 194–205. [CrossRef]
201. Ichinohe, T.; Watanabe, I.; Ito, S.; Fujii, H.; Moriyama, M.; Tamura, S.; Takahashi, H.; Sawa, H.; Chiba, J.; Kurata, T.; et al. Synthetic Double-Stranded RNA Poly(I:C) Combined with Mucosal Vaccine Protects against Influenza Virus Infection. *J. Virol.* **2005**, *79*, 2910–2919. [CrossRef]
202. Beljanski, V.; Chiang, C.; Kirchenbaum, G.A.; Olagnier, D.; Bloom, C.E.; Wong, T.; Haddad, E.K.; Trautmann, L.; Ross, T.M.; Hiscott, J. Enhanced Influenza Virus-Like Particle Vaccination with a Structurally Optimized RIG-I Agonist as Adjuvant. *J. Virol.* **2015**, *89*, 10612–10624. [CrossRef]
203. Goulet, M.-L.; Olagnier, D.; Xu, Z.; Paz, S.; Belgnaoui, S.M.; Lafferty, E.I.; Janelle, V.; Arguello, M.; Paquet, M.; Ghneim, K.; et al. Systems Analysis of a RIG-I Agonist Inducing Broad Spectrum Inhibition of Virus Infectivity. *PLoS Pathog.* **2013**, *9*, e1003298. [CrossRef]
204. Olagnier, D.; Scholte, F.E.M.; Chiang, C.; Albulescu, I.C.; Nichols, C.; He, Z.; Lin, R.; Snijder, E.J.; van Hemert, M.J.; Hiscott, J. Inhibition of Dengue and Chikungunya Virus Infections by RIG-I-Mediated Type I Interferon-Independent Stimulation of the Innate Antiviral Response. *J. Virol.* **2014**, *88*, 4180–4194. [CrossRef]
205. Chiang, C.; Beljanski, V.; Yin, K.; Olagnier, D.; Ben Yebdri, F.; Steel, C.; Goulet, M.-L.; DeFilippis, V.R.; Streblow, D.N.; Haddad, E.K.; et al. Sequence-Specific Modifications Enhance the Broad-Spectrum Antiviral Response Activated by RIG-I Agonists. *J. Virol.* **2015**, *89*, 8011–8025. [CrossRef] [PubMed]
206. Teng, T.S.; Foo, S.S.; Simamarta, D.; Lum, F.M.; Teo, T.H.; Lulla, A.; Yeo, N.K.W.; Koh, E.G.L.; Chow, A.; Leo, Y.S.; et al. Viperin restricts chikungunya virus replication and pathology. *J. Clin. Investig.* **2012**, *122*, 4447–4460. [CrossRef] [PubMed]
207. Carissimo, G.; Teo, T.H.; Chan, Y.H.; Lee, C.Y.P.; Lee, B.; Torres-Ruesta, A.; Tan, J.J.L.; Chua, T.K.; Fong, S.W.; Lum, F.M.; et al. Viperin controls chikungunya virus-specific pathogenic T cell IFNγ Th1 stimulation in mice. *Life Sci. Alliance* **2019**, *2*, e201900298. [CrossRef]
208. Hammond, E.; Haynes, N.M.; Cullinane, C.; Brennan, T.V.; Bampton, D.; Handley, P.; Karoli, T.; Lanksheer, F.; Lin, L.; Yang, Y.; et al. Immunomodulatory activities of pixatimod: Emerging nonclinical and clinical data, and its potential utility in combination with PD-1 inhibitors. *J. Immunother. Cancer* **2018**, *6*, 54. [CrossRef]

209. Dredge, K.; Brennan, T.V.; Hammond, E.; Lickliter, J.D.; Lin, L.; Bampton, D.; Handley, P.; Lankesheer, F.; Morrish, G.; Yang, Y.; et al. A Phase i study of the novel immunomodulatory agent PG545 (pixatimod) in subjects with advanced solid tumours. *Br. J. Cancer* **2018**, *118*, 1035–1041. [CrossRef]
210. Krishnan, R.; Duiker, M.; Rudd, P.A.; Skerrett, D.; D Pollard, J.G.; Siddel, C.; Rifat, R.; K Ng, J.H.; Georgius, P.; Hererro, L.J.; et al. Pentosan polysulfate sodium for Ross River virus-induced arthralgia: A phase 2a, randomized, double-blind, placebo-controlled study. *BMC Musculoskelet. Disord.* **2021**, *1*, 271.
211. Marra, R.K.F.; Kümmerle, A.E.; Guedes, G.P.; de Barros, S.C.; Gomes, R.S.P.; Cirne-Santos, C.C.; Paixão, I.C.N.P.; Neves, A.P. Quinolone-N-acylhydrazone hybrids as potent Zika and Chikungunya virus inhibitors. *Bioorganic Med. Chem. Lett.* **2020**, *30*, 126881. [CrossRef]
212. Ching, K.-C.; Kam, Y.-W.; Merits, A.; Ng, L.F.P.; Chai, C.L.L. Trisubstituted Thieno[3,2-b]pyrrole 5-Carboxamides as Potent Inhibitors of Alphaviruses. *J. Med. Chem.* **2015**, *58*, 9196–9213. [CrossRef] [PubMed]
213. Ching, K.-C.; Ngoc Quy Tran, T.; Naqiah Amrun, S.; Kam, Y.-W.; P Ng, L.F.; L Chai, C.L. Structural Optimizations of Thieno[3,2-b]pyrrole Derivatives for the Development of Metabolically Stable Inhibitors of Chikungunya Virus. *J. Med. Chem.* **2017**, *60*, 3165–3186. [CrossRef]
214. Fares, M.; McCosker, P.M.; Alsherbiny, M.A.; Willis, A.C.; Clark, T.; Neyts, J.; Jochmans, D.; Keller, P.A. Regioselective convergent synthesis of 2-arylidene thiazolo[3,2- a] pyrimidines as potential anti-chikungunya agents. *RSC Adv.* **2020**, *10*, 5191–5195. [CrossRef]
215. Hwu, J.R.; Kapoor, M.; Tsay, S.-C.; Lin, C.-C.; Hwang, K.C.; Horng, J.-C.; Chen, I.-C.; Shieh, F.-K.; Leyssen, P.; Neyts, J. Benzouracil–coumarin–arene conjugates as inhibiting agents for chikungunya virus. *Antivir. Res.* **2015**, *118*, 103–109. [CrossRef] [PubMed]

1.3 Scientific Goal and Motivation

This doctoral thesis's main goal was to identify a novel potent small-molecule inhibitor against the CHIKV and investigate and improve its physiochemical and pharmacological characteristics to enhance its potential for reaching the next step in the drug development process (*in vivo* studies). As elaborated in detail in section 1.2 and 1.2.1 ([63]), the severity and chronicity of the CHIKF, the rising morbidity associated with the CHIKV, the worldwide re-emergence of this alphavirus, and the lack of vaccines or pharmacotherapy available makes the development of potent and safe inhibitors against the Chikungunya virus crucial and highly desirable.

The following chapter 2 describes the identification of a novel compound series (published as the CHVB series) with good antiviral activity against this alphavirus by high-throughput screening (HTS). Further, a SAR study was performed, which led to identifying a new lead compound [64]. Additional twenty-eight compounds were analysed for their anti-CHIKV activity under the lead of Dr Moesslacher and later incorporated in the [65] discussed in chapter 4 [66].

Based on these findings, a new lead optimisation process was performed with the following goals:

1. improving or maintaining *in vitro* antiviral activity (accessed via the EC_{50}),
2. enhancing the safety and toxicological profile:
    - half maximal cytotoxic concentration (CC_{50}) values and cell viability accessed in relevant cell lines,
    - possible hERG channel interactions,
3. investigating their antiviral profile (different CHIKV strains, other (alpha)viruses),
4. reaching drug-like physicochemical and pharmacological characteristics (ADME profiling),
5. increasing the information about relevant functional groups for a high activity through an additional SAR study,
6. investigating the potential target and possible compound-target interactions.

Further, a pharmacophore, SAR-driven scaffold hop is planned to find a new starting point for future CHIKV research projects (for detailed information about scaffold hopping see section 1.1.1.2).

Chapter 2

Identification of a Novel Hit Series against Chikungunya Virus - the *CHVB Series*

2.1 Introduction

The following publication (further referred to [64]) describes the identification of the small molecule hit CIM016321 (referred to as compound **1**) in a large scale cytopathic effect (CPE)-based anti-CHIKV screening (33,000 molecules), and thus the beginning of the CHVB series project. Further, a four-step synthesis and a SAR study of the novel small molecule inhibitors against CHIKV were carried out to optimise the hit compound considering the antiviral activity and cytotoxicity profile [64].

Therefore the compound's scaffold was divided into five groups suitable for systematic variations to unveil the molecular requirements for a highly active and safe anti-CHIKV compound. As guidance for systematic structural variations of the molecule, ligand-based approaches like the concept of bioisosterism and the Topliss decision tree were applied - as the molecular target was still unknown [36, 39, 67, 68].

2.2 Identification of 2-(4-(phenylsulfonyl)piperazine-1-yl)pyrimidine Analogues as Novel Inhibitors of Chikungunya Virus

ACS Medicinal Chemistry Letters

pubs.acs.org/acsmedchemlett

Letter

Identification of 2-(4-(Phenylsulfonyl)piperazine-1-yl)pyrimidine Analogues as Novel Inhibitors of Chikungunya Virus

Julia Moesslacher,[⊥] Verena Battisti,[⊥] Leen Delang, Johan Neyts, Rana Abdelnabi, Gerhard Pürstinger, Ernst Urban, and Thierry Langer*

Cite This: *ACS Med. Chem. Lett.* 2020, 11, 906−912

Read Online

ACCESS | Metrics & More | Article Recommendations | Supporting Information

ABSTRACT: The chikungunya virus (CHIKV) is a mosquito-transmitted alphavirus, and it is the causative agent of chikungunya fever (CHIKF). Although it has re-emerged as an epidemic threat, so far there are neither vaccines nor pharmacotherapy available to prevent or treat an infection. Herein, we describe the synthesis and structure−activity relationship studies of a class of novel small molecule inhibitors against CHIKV and the discovery of a new potent inhibitor (compound **6a**). The starting point of the optimization process was *N*-ethyl-6-methyl-2-(4-(4-fluorophenylsulfonyl)piperazine-1-yl)pyrimidine-4-amine (**1**) with an EC_{50} of 8.68 μM, a CC_{50} of 122 μM, and therefore a resulting selectivity index (SI) of 14.2. The optimized compound **6a**, however, displays a much lower micromolar antiviral activity (EC_{50} value of 3.95 μM), considerably better cytotoxic liability (CC_{50} value of 260 μM) and consequently an improved SI of greater than 61. Therefore, we report the identification of a promising novel compound class that has the potential for further development of antiviral drugs against the CHIKV.

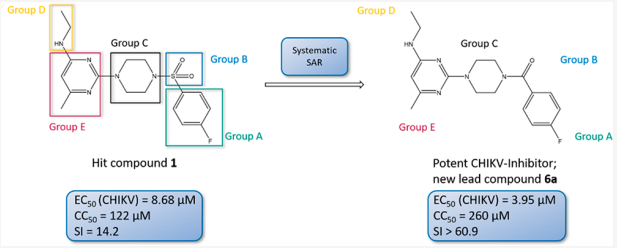

KEYWORDS: *Novel small-molecule antivirals, Chikungunya virus, Structure−activity relationship studies, Medicinal chemistry*

INTRODUCTION

The chikungunya virus (CHIKV) is a member of the *Togaviridae*, genus alphavirus and was first described in East Africa (southern province of Tanzania) in 1952−1953.[1,2] This mosquito-transmitted alphavirus (mainly by *Aedes spp.*) is the causative agent of chikungunya fever (CHIKF), a disease characterized by myalgia, polyarthralgia, fever, nausea, headaches, maculopapular rash, and complications including lymphopenia, lethal hepatitis, dermatologic lesions, and encephalitis.[3−5] Although chikungunya fever is rarely fatal, symptoms such as myalgia and arthralgia have been reported to last for years after clearance of the infection, resulting in an impaired quality of life.[6−8] Since the re-emergence of the virus in 2005, outbreaks have occurred in more than 40 countries throughout the world, not only in Southeast Asia and Africa but also in Europe (Italy and France) as well as America.[9−11] Currently, neither vaccines nor pharmacotherapy are available to prevent or treat an infection.[12−14] To date, the only available treatment is the alleviation of symptoms by using NSARs like ibuprofen, naproxen, or acetaminophen. Occasionally, corticosteroids are administered to patients to relieve symptoms like fever and pain.[15−17] Up to now, the antiviral activity of small molecules, compounds from natural sources, and immune modulators on the replication of chikungunya virus have been investigated. Several compounds, ranging from antivirals with a broad spectrum like ribavirin to harringtonine (a cephalotaxine alkaloid) and IFN-α, were found to be active, targeting different stages in the alphavirus life cycle. Despite the demonstrated effectiveness and, in some cases, potent antiviral activity *in vitro*, none of these drugs passed the clinical trial phase.[18−25] Also, the utilization of the already known antimalaria drug chloroquine as possible antiviral treatment is highly discussed regarding the potential risks and benefits for the patients.[26−30] Therefore, the development of safe and effective new antivirals against CHIKV is highly desirable.[31] This problem was addressed within the EU FP7 collaborative project SILVER. In this project, the small molecular hit CIM016321 (later referred as **1**, Figure 1), which was identified previously by high-throughput screening by the Center for Innovation and Stimulation of Drug Discovery (CISTIM) and the University of Leuven (KU Leuven), was further investigated and a hit to lead program was initiated.

To optimize **1**, we divided the structure of this compound into five parts suitable for systematic variation (shown in Figure 1). The aim of the optimization was to achieve (i) an increase in antiviral activity and (ii) a decrease in cytotoxicity, therefore resulting in a compound exhibiting an improved

Special Issue: In Memory of Maurizio Botta: His Vision of Medicinal Chemistry

Received: December 30, 2019
Accepted: March 5, 2020
Published: March 5, 2020

https://dx.doi.org/10.1021/acsmedchemlett.9b00662
ACS Med. Chem. Lett. 2020, 11, 906−912

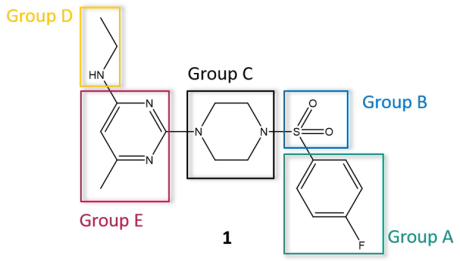

Figure 1. For optimization, we divided the initial hit **1** into five parts. Compounds with modifications at the same part of the molecule are summarized to "Groups".

selectivity index (SI). As guidance for systematic structural variations of the molecule, approaches like the concept of bioisosterism and the Topliss decision tree were applied.[32−35]

In this study, we have identified that analogues of **1** are potent and safe inhibitors of chikungunya virus *in vitro*. Moreover, structure−activity relationship studies unveiled the molecular requirements for highly active and safe antiviral compounds.

RESULTS AND DISCUSSION

The initial hit 1 was prepared using a four-step-synthesis and was also established to give access to the entire compound series. The synthesis of these compounds is summarized in Scheme 1, starting from 2-chloro-*N*-ethyl-6-methylpyrimidin-4-amine (2a), which was synthesized following the procedures reported by Martyn et al.[36] The reaction with *tert*-butyl piperazine-1-carboxylate, obtained according to the protocol from Moussa et al.,[37] under microwave conditions gave a high yield of 85% of the desired Boc-protected piperazine−pyrimidine intermediate. The following deprotection and the N-sulfonamidation of piperazine were performed according to Martyn et al.,[36] but with additional THF. The fourth step of the synthesis with *p*-fluorobenzenesulfonyl chloride afforded the desired target in a moderate yield of 32%.

The first alteration was performed using modifications on, or replacement of, the 4-fluorophenyl ring (Group A). All compounds from this group (**5a**−**5s**), except **5s**, were synthesized following Scheme 2. Synthesis of **5s** was achieved by reducing the nitro group using tin(II) chloride **5f** to the corresponding amine. The first three steps of the synthesis remained the same as for **1**, as well as the reaction conditions as described before. For the preparation of analogues, in the fourth step, instead of the 4-fluorobenzenesulfonyl chloride, a suitable sulfonyl chloride was used. The conditions for the reaction remained unchanged and provided analogues in 13−92% yield.

The synthesis of the analogues **6a** and **6b** from Group B, replacing the sulfonamide linker with an amide or a methyl group was carried out with the established synthesis route. The conditions and reagents remained the same as for **1** and Group A, however, with 4-fluorobenzoyl chloride or 4-fluorobenzyl chloride instead of the benzenesulfonyl chlorides (Scheme 2).

Substituents of the piperazine linker (Group C) where introduced to investigate the function of this group. The reaction for Group C (**7a** and **7b**) followed the established synthesis route, with a small alteration for **7b**: 2-chloro-*N*-ethyl-6-methylpyrimidin-4-amine (**2a**) was reacted directly with the tetrahydroquinoxaline (as modified linker) under microwave irradiation to access **4c**. This reaction was performed without protecting one of the two amino groups before and gave still a high yield of 75%. The third step of the synthesis was identical to the fourth step of the previously used standard procedure−performed with 4-fluorobenzenesulfonyl chloride and triethylamine as a base in dichloromethane at room temperature for 24 h (**7a**: 55% yield, **7b**: 28% yield; Scheme 3).

For Group D, the target compounds were accessed via the alteration of the first synthesis step. Instead of ethylamine as reactant, propane-2-amine, 2-methylpropan-2-amine, sodium ethoxide, or pyrrolidine were used to prepare the analogue compounds **8a**−**8d**. The successive reaction between the substituted pyrimidine and the piperazine, following the sulfonamidation as the last step, was adopted according the established synthesis route (Scheme 4).

Compounds of Group E (**9a**−**9d**) were synthesized following Scheme 4. The synthesis remained the same as for **1**, as well as the reaction conditions. To prepare the analogues of this group, a differently substituted pyrimidine building block was used as starting reactant in the first step of the synthesis. The pyrimidine ring **2f** (4-chloro-*N*-ethyl-6-methyl-pyrimidin-2-amine), used to prepare **9a**, was obtained as a product out in the first step of the synthesis of **1** in a moderate yield of 17%.

Finally, the modifications with the most promising antiviral activities were combined, utilizing the established synthesis route described above (Scheme 4 and Scheme 5).

All compounds were evaluated for their potential antiviral activity against CHIKV by determining the inhibition of CHIKV-induced cytopathogenic effect (CPE) in Vero cells (Table 1).

The purpose of Group A was to investigate if a fluorine atom as substituent is essential, which turned out not to be the case: the analogue with the nonsubstituted phenyl ring (**5a**) also showed antiviral activity, although **5a** was less active than **1** (EC_{50} = 14 ± 3 μM). In a next step, para fluorine was replaced by other halogens such as chlorine (**5b**), bromine (**5c**), and iodine (**5d**). All these compounds were more active than the initial hit: the chlorine-substituted **5b** gave the best result with an EC_{50} of 5.3 μM, the iodine-substituted **5d** showed similar antiviral activity with an EC_{50} of 5.9 μM, while the bromine-

Scheme 1. Synthesis of the Initial Hit 1[a]

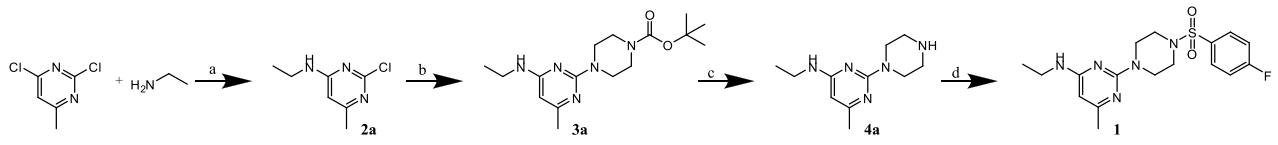

[a]Reagents and conditions: (a) EtOH, 24−48 h, rt; (b) EtOH, microwave, 3 min, 155 °C, 250 W, 12 bar, *tert*-butyl piperazine-1-carboxylate; (c) 4.5 M HCl, dioxane/THF, 24 h rt; (d) DCM, $N(CH_2CH_3)_3$, 24 h rt, 4-fluorobenzenesulfonyl chloride.

https://dx.doi.org/10.1021/acsmedchemlett.9b00662
ACS Med. Chem. Lett. 2020, 11, 906−912

Scheme 2. Synthesis of the Compounds from Group A (5a−5r) and Group B (6a, 6b)[a]

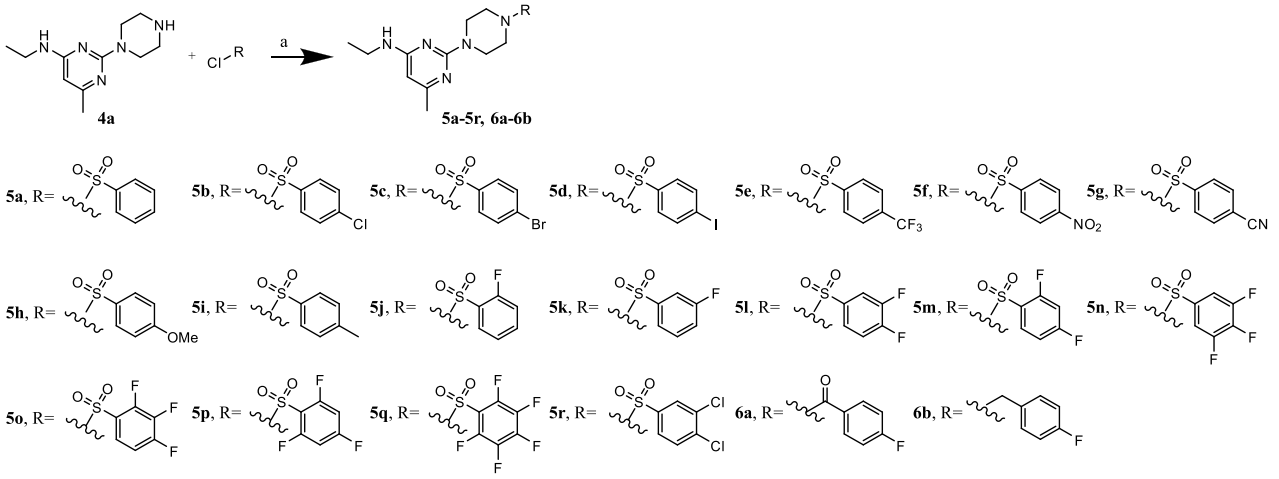

[a]Reagents and condition: (a) DCM, $N(CH_2CH_3)_3$, 24 h rt.

Scheme 3. Synthesis of the Compounds from Group C (7a, 7b)[a]

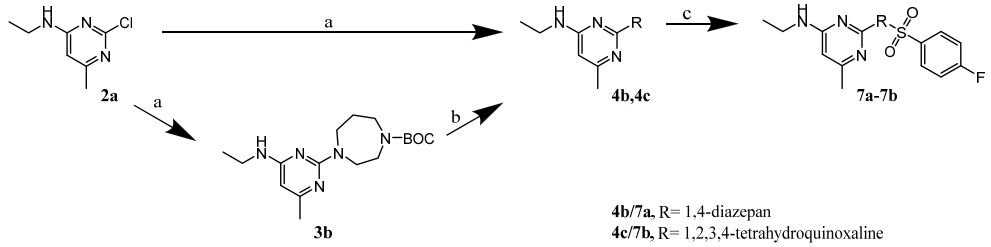

[a]Reagents and conditions: (a) EtOH, microwave, 3 min, 155 °C, 250 W, 12 bar; **3b**, *tert*-butyl 1,4-diazepane-1-carboxylate; **4c**, 1,2,3,4-tetrahydroquinoxaline; (b) **4b**, 4.5 M HCl, dioxane/THF, 24 h rt; (c) DCM, $N(CH_2CH_3)_3$, 24 h rt, 4-fluorobenzenesulfonyl chloride.

Scheme 4. Synthesis of the Compounds from Group D (8a−8d), from Group E (9a−9d), and 10a, 10b[a]

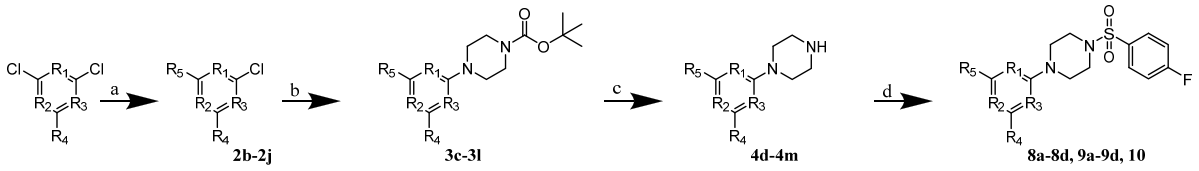

	2b/3c/4d/8a	2c/3d/4e/8b	2d/3e/4f/8c	2e/3f/4g/8d	2f/3g/4h/9a	2g/3h/4i/9b	2h/3i/4j/9c	2i/3j/4k/9d	3k/4l/10	2j/3l/4m
R_1	N	N	N	N	N	C	N	N	N	N
R_2	C	C	C	C	N	N	C	N	C	N
R_3	N	N	N	N	C	N	N	C	N	C
R_4	$-CH_3$	$-CH_3$	$-CH_3$	$-CH_3$	$-CH_3$	$-CH_3$	-H	-H	-H	$-CH_3$
R_5		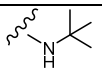	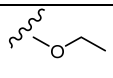		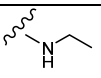	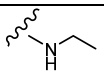	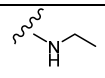	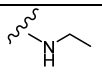	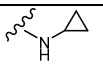	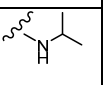

[a]Reagents and conditions: (a) EtOH, 24−48 h rt; **2b**/**2j**, propan-2-amine; **2c**, 2-methylpropan-2-amin; **2d**, sodium ethoxide; **2e**, pyrrolidine; **2f−i**, ethylamine; (b) EtOH, microwave, 3 min, 155 °C, 250 W, 12 bar, *tert*-butyl piperazine-1-carboxylate; (c) 4.5 M HCl, dioxane/THF, 24 h rt; (d) DCM, $N(CH_2CH_3)_3$, 24 h rt, 4-fluorobenzenesulfonyl chloride.

substituted **5c** was less active (EC_{50} = 7.1 μM). The nitro-substituted **5f** (EC_{50} = 14 ± 3 μM) and the methyl-substituted **5i** (EC_{50} = 15 ± 2 μM) were also less active than **1**. On the contrary, the trifluoromethyl substituted **5e** was inactive, as well as **5g** with CN substitution. The other para-substituted compounds (**5h** and **5s**) showed less antiviral activity than the initial hit **1**.

Shifting the para fluorine atom to other positions on the benzene ring resulted in less active compounds than the initial hit **1** (**5j** and **5k**). Also, combining the ortho or meta to the

https://dx.doi.org/10.1021/acsmedchemlett.9b00662
ACS Med. Chem. Lett. 2020, 11, 906−912

Scheme 5. Synthesis of 11a−11c[a]

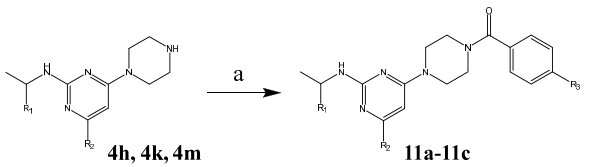

	4h	11a	4k	11b	4m	11c
R_1	H		H		$-CH_3$	
R_2	$-CH_3$		H		$-CH_3$	
R_3		Cl		Cl		F

[a]Reagents and conditions: (a) DCM, $N(CH_2CH_3)_3$, 24 h rt; **11a**/**11b**, 4-chlorobenzoyl chloride; **11c**, 4-fluorobenzoyl chloride.

para substitution did not result in an additive antiviral effect compared to **1**: **5l** with two fluorine atoms on the meta and para position and **5m** with an ortho/para disubstitution pattern were less active than **1**. Additionally, neither of the triple substituted compounds showed an improved additive antiviral effect (**5n**, **5o**, and **5p**). **5q**, in which all hydrogen atoms on the phenyl ring were replaced by fluorine, was found to be poorly active. Conclusively, concerning the antiviral activity of the monosubstituted analogues, the 4-F substituted analogue is more active than the 3-F-substituted one, which is more active than the 2-F-substituted compound. Concerning the double- and triple-substituted compounds, the 3,4-F substituted **5l** and the 2,3,4-F-substituted **5o** are active; while the compounds with 2,4-F (**5m**) and 3,4,5-F substitution patterns (**5n**) are both only moderately active compared to **1**.

To investigate if the double substitution on the aromatic ring with different halogens would also decrease the antiviral activity, **5r** was prepared. It showed moderate activity against the virus, confirming our previous observation, that the chloride substitution enhances the antiviral activity. Nevertheless, the doubly substituted ring also showed a weaker antiviral effect using chlorides (**5r**) than the matching single substituted ring (**5b**).

Summarizing the results from Group A, 17 out of the 19 compounds were active against CHIKV, with three compounds being more potent than **1** (**5b**, **5c**, and **5d**). In those three compounds, other halogens replaced the fluorine at the para position. Therefore, replacing fluorine on the benzene ring by another halogen leads to an improvement in antiviral activity (chlorine > iodine > bromine > fluorine). **5b** with the chlorine atom as substituent on the para position of the benzene ring showed the best test results; therefore, the fluorine/chlorine replacement should be considered for further optimization.

In Group B, both compounds showed impressive test results: **6a** has an EC_{50} of 4.0 ± 1 μM, and **6b** has an EC_{50} of 2.5 μM. Conclusively, both compounds are more than twice as active as **1**. Although **6b** is even more active than **6a**, compound **6a** should be considered for further optimization due to cytotoxicity reasons (**1**, CC_{50} = 122 μM, SI = 14.2; **6a**, CC_{50} = 260 μM, SI = 60.9; **6b**, CC_{50} = 69.3 μM, SI = 19.7). Therefore, compared to **1**, the modification in **6a** led to an improvement in activity, cytotoxicity, and selectivity, while the modification in **6b** led to a higher cytotoxicity.

In Group C, the prepared analogues were less active than **1**. Conclusively, 1,4-piperazine as a linker has proven to be the better choice to reach a potent antiviral activity.

Table 1. Antiviral Evaluation of 1 and Analogues against CHIKV in Vero Cells[a]

compound	EC_{50} (μM)[b]	EC_{90} (μM)[c]	CC_{50} (μM)[d]
1	8.7 ± 1	14 ± 1	122 ± 24
5a	14 ± 3	28 ± 6	156 ± 35
5b	5 ± 0.4	7 ± 1	51 ± 19
5c	7.1 ± 0.01	13 ± 2	44 ± 19
5d	5.9 ± 0.2	8.7 ± 1	19 ± 2
5e	>233	>233	45 ± 1
5f	14 ± 3	24 ± 7	62 ± 1
5g	>259	>250	ND
5h	82 ± 11	125 ± 3	178 ± 31
5i	15 ± 2	22 ± 2	95 ± 74
5j	27 ± 9	52 ± 17	91 ± 7
5k	20 ± 3	31 ± 2	131 ± 43
5l	12 ± 5	19 ± 10	53 ± 7
5m	16 ± 6	16 ± 4	67 ± 13
5n	19 ± 5	ND	29 ± 3
5o	10 ± 0.2	17 ± 5	181 ± 0.4
5p	28 ± 5	36 ± 14	55 ± 3
5q	75 ± 19	>166	122 ± 23
5r	10 ± 1	13 ± 3	15 ± 3
5s	22 ± 3	51 ± 16	183 ± 17
6a	4.0 ± 1	20 ± 8	>260
6b	2.5 ± 1	5 ± 1	69 ± 7
7a	77 ± 5	123 ± 0.2	202 ± 18
7b	16 ± 1	29 ± 8	106 ± 69
8a	9.5 ± 2	17 ± 4	66 ± 6
8b	12 ± 2	ND	19 ± 3
8c	>197	>197	ND
8d	33 ± 7	34 ± 1	50 ± 8
9a	3.2 ± 0.2	14 ± 4	59 ± 18
9b	48 ± 9	98 ± 34	>329
9c	14 ± 3	29 ± 2	91 ± 10
9d	70 ± 0.2	124 ± 1	217 ± 3
10	37 ± 4	55 ± 8	76 ± 16
11a	32 ± 2	108 ± 3	202 ± 27
11b	51 ± 7	88 ± 17	204 ± 1
11c	92 ± 9	102 ± 17	159 ± 31

[a]EC_{50}, EC_{90}, and CC_{50} data represent median values ± standard deviation from at least three independent experiments. ND = not detectable. [b]The 50% effective concentration (EC_{50}) is the concentration of compound that is required to inhibit virus-induced cell death by 50%. [c]The 90% effective concentration (EC_{90}) is the concentration of compound that is required to inhibit virus-induced cell death by 90%. [d]The 50% cytostatic/cytotoxic concentration (CC_{50}) is the concentration of compound that reduces the overall metabolic activity of the uninfected, compound-treated cells by 50% as compared to the untreated, uninfected cell.

The replacement of the ethylamine side chain with isopropylamine (**8a**) or *tert*-butylamine (**8b**) demonstrated good activity against the CHIKV, which unfortunately was accompanied by increased cytotoxicity (**8a**, CC_{50} = 66.4 μM, SI = 9.83; **8b**, CC_{50} = 18.6 μM, SI = 1.17). In addition, it was investigated whether the nitrogen or the hydrogen atom of the ethylamine side chain is essential for activity and whether the antiviral activity of the compound would increase with higher molecular lipophilicity. Therefore, **8c** was prepared in which an ethoxy side chain replaced the ethylamine side chain. However, **8c** did not show any antiviral activity. To understand whether this loss of activity depends on the missing nitrogen atom or the absence of the hydrogen bond donor function, **8d** was

https://dx.doi.org/10.1021/acsmedchemlett.9b00662
ACS Med. Chem. Lett. 2020, 11, 906−912

synthesized, in which a pyrrolidine ring replaced the ethylamine side chain. The result from **8d** (EC_{50} of 33 ± 7 μM) indicated that the hydrogen bond donor is not essential for actively enhancing the antiviral activity, although its pure absence seemed to decrease the activity. Taken together with the results from Group D, the nitrogen atom of the ethylamine side chain seems to be essential for antiviral activity, while the hydrogen bond donor is not. Also, a bifurcation at the ethylamine side chain may be taken into consideration with caution.

In Group E, in a first step the optimal positions for the nitrogen atoms in the pyrimidine ring were investigated. In a second step, it was investigated whether the methyl group as a substituent on the pyrimidine ring is essential or not. The nitrogen at position R_1 seemed to be necessary for good antiviral activity. Shifting the nitrogen from position $R_{1/3}$ (as in the initial hit **1**) to position $R_{1/2}$ (**9a**) resulted in an improved antiviral activity.

Finally, the most interesting modifications were combined to either reach a higher antiviral activity (**11a** and **11c**) or to deepen the knowledge of the chosen variation (**10**, **11b**). The result of **10** and **11b** underline the importance of the methyl group on the pyrimidine ring and the shifting of the nitrogen to position $R_{1/2}$. Moreover, the decrease of activity with the cyclopropylamine side chain (**10**) , although its size is comparable to the original ethylamine, can possibly be explained by his impaired flexibility and different three-dimensional geometry.

Surprisingly, the combination of the most promising alterations (Group B:, amide; Group E, shifted N to position $R_{1/2}$) in combination with either the best alteration of Group A (para chloride, **11a**) or with the introduction of an isopropyl side chain (Group D, **11c**) did not give the desired gain of antiviral activity.

CONCLUSION

In this study, we present several 2-(4-(phenylsulfonyl)-piperazine-1-yl)pyrimidine and analogues as selective and potent inhibitors of CHIKV. All compounds described are easily accessible in a four-step synthesis route: starting from the required substituted pyrimidine reacting with the Boc-protected piperazine or other suitable nitrogen-containing functional groups under microwave irradiation, followed by deprotection and finally reaction with a benzenesulfonyl chloride. Additionally, the structural requirements for a significant anti-CHIKV activity have been determined on all five structural molecular subgroups. During this optimization process, **6a** was identified as a potent and selective inhibitor of CHIKV, demonstrating a much better profile than the starting point, hit **1**, and a selectivity index greater than 61. Furthermore, the optimized compound showed a wide-spectrum antiviral activity against all tested strains of CHIKV (data will be published elsewhere). Further structure−activity studies and optimization of the antiviral activity are ongoing and mechanism of action studies are being performed to determine the molecular target of this novel class of anti-CHIKV compounds. These studies point toward the viral capping machinery and more specifically to the viral protein nsP1 as the antiviral target of these compounds. Cross-resistance with another class of capping inhibitors, the MADTP series, was confirmed in antiviral assays (data not shown). As other classes of inhibitors that target the viral capping have been reported, the capping machinery of alphaviruses might be a hot spot for antiviral molecules.

ASSOCIATED CONTENT

Supporting Information

The Supporting Information is available free of charge at https://pubs.acs.org/doi/10.1021/acsmedchemlett.9b00662.

Cell lines and virus strain, instrumentation and experimental procedures, characterization and spectral data, HPLC-determined purity data, and NMR spectra for all the compounds (PDF)

AUTHOR INFORMATION

Corresponding Author

Thierry Langer − *University of Vienna, Department of Pharmaceutical Chemistry, A-1090 Vienna, Austria;* orcid.org/0000-0002-5242-1240; Email: thierry.langer@univie.ac.at

Authors

Julia Moesslacher − *University of Innsbruck, Department of Pharmacy, 6020 Innsbruck, Austria*

Verena Battisti − *University of Vienna, Department of Pharmaceutical Chemistry, A-1090 Vienna, Austria;* orcid.org/0000-0001-9794-366X

Leen Delang − *KU Leuven Department of Microbiology and Immunology, Rega Institute for Medical Research, Laboratory of Virology and Chemotherapy, B-3000 Leuven, Belgium*

Johan Neyts − *KU Leuven Department of Microbiology and Immunology, Rega Institute for Medical Research, Laboratory of Virology and Chemotherapy, B-3000 Leuven, Belgium*

Rana Abdelnabi − *KU Leuven Department of Microbiology and Immunology, Rega Institute for Medical Research, Laboratory of Virology and Chemotherapy, B-3000 Leuven, Belgium*

Gerhard Pürstinger − *University of Innsbruck, Department of Pharmacy, 6020 Innsbruck, Austria*

Ernst Urban − *University of Vienna, Department of Pharmaceutical Chemistry, A-1090 Vienna, Austria*

Complete contact information is available at: https://pubs.acs.org/10.1021/acsmedchemlett.9b00662

Author Contributions

[⊥]Moesslacher Julia and Battisti Verena have contributed equally to this manuscript. All authors have given approval to the final version of the manuscript.

Funding

This work was funded in parts (University of Innsbruck, KU Leuven) by the European Union Seventh Framework Program (FP7/2007-2013) under a SILVER grant (No. HEALTH-F3-2010-260644).

Notes

The authors declare no competing financial interest.

ACKNOWLEDGMENTS

We thank S. Delmotte, T. Bellon, and K. Donckers for their excellent technical assistance in the acquisition of the antiviral data. Furthermore, we are grateful to J. Wackerlig and D. Dobusch for the support with the chemical analysis of the compounds.

DEDICATION

This paper is dedicated to the memory of Prof. Maurizio Botta, who passed away much too early in August 2019.

ABBREVIATIONS

THF, tetrahydrofuran; EtOAc, ethyl acetate; TEA, triethylamine; DIPE, diisopropyl ether; DMSO-d_6, deuterated dimethyl sulfoxide; dia, diazepane; Ph, phenyl; pyr, pyrimidine; pip, piperazine; ipr, isopropyl; qu, quinoxaline; TLC, thin layer chromatography; ND, not detectable.

REFERENCES

(1) Robinson, M. C. An Epidemic of Virus Disease in Southern Province, Tanganyika Territory, in 1952−1953. I. Clinical Features. *Trans. R. Soc. Trop. Med. Hyg.* **1955**, *49* (1), 28−32.

(2) Thiberville, S.-D.; Moyen, N.; Dupuis-Maguiraga, L.; Nougairede, A.; Gould, E. A.; Roques, P.; De Lamballerie, X. Chikungunya Fever: Epidemiology, Clinical Syndrome, Pathogenesis and Therapy. *Antiviral Res.* **2013**, *99*, 345−370.

(3) Schwartz, O.; Albert, M. L. Biology and Pathogenesis of Chikungunya Virus. *Nat. Rev. Microbiol.* **2010**, *8* (7), 491−500.

(4) Burt, F. J.; Chen, W.; Miner, J. J.; Lenschow, D. J.; Merits, A.; Schnettler, E.; Kohl, A.; Rudd, P. A.; Taylor, A.; Herrero, L. J.; et al. Chikungunya Virus: An Update on the Biology and Pathogenesis of This Emerging Pathogen. *Lancet Infect. Dis.* **2017**, *17* (4), e107−e117.

(5) Couderc, T.; Lecuit, M. Chikungunya Virus Pathogenesis: From Bedside to Bench. *Antiviral Res.* **2015**, *121*, 120−131.

(6) Moro, M. L.; Grilli, E.; Corvetta, A.; Silvi, G.; Angelini, R.; Mascella, F.; Miserocchi, F.; Sambo, P.; Finarelli, A. C.; Sambri, V.; et al. Long-Term Chikungunya Infection Clinical Manifestations after an Outbreak in Italy: A Prognostic Cohort Study. *J. Infect.* **2012**, *65* (2), 165−172.

(7) Couturier, E.; Guillemin, F.; Mura, M.; Leon, L.; Virion, J.-M.; Letort, M.-J.; De Valk, H.; Simon, F.; Vaillant, V. Impaired Quality of Life after Chikungunya Virus Infection: A 2-Year Follow-up Study. *Rheumatology* **2012**, *51* (7), 1315−1322.

(8) Rodriguez-Morales, A. J.; Restrepo-Posada, V. M.; Acevedo-Escalante, N.; Rodríguez-Muñoz, E. D.; Valencia-Marín, M.; Castrillón-Spitia, J. D.; Londoño, J. J.; Bedoya-Rendón, H. D.; de Jesús Cárdenas-Pérez, J.; Cardona-Ospina, J. A.; et al. Impaired Quality of Life after Chikungunya Virus Infection: A 12-Month Follow-up Study of Its Chronic Inflammatory Rheumatism in La Virginia, Risaralda. *Rheumatol. Int.* **2017**, *37* (10), 1757−1758.

(9) Rezza, G.; Nicoletti, L.; Angelini, R.; Romi, R.; Finarelli, A. C.; Panning, M.; Cordioli, P.; Fortuna, C.; Boros, S.; Magurano, F.; et al. Infection with Chikungunya Virus in Italy: An Outbreak in a Temperate Region. *Lancet* **2007**, *370* (9602), 1840−1846.

(10) Delisle, E.; Rousseau, C.; Broche, B.; Leparc-Goffart, I.; L'ambert, G.; Cochet, A.; Prat, C.; Foulongne, V.; Ferré, J. B.; Catelinois, O. Chikungunya Outbreak in Montpellier, France, September to October 2014. *European Centre for Disease Prevention and Control* **2015**, *20*, 21108.

(11) Rashad, A. A.; Mahalingam, S.; Keller, P. A. Chikungunya Virus: Emerging Targets and New Opportunities for Medicinal Chemistry. *J. Med. Chem.* **2014**, *57* (4), 1147−1166.

(12) Subudhi, B.; Chattopadhyay, S.; Mishra, P.; Kumar, A. Current Strategies for Inhibition of Chikungunya Infection. *Viruses* **2018**, *10* (5), 235.

(13) Reyes-Sandoval, A. 51 Years in of Chikungunya Clinical Vaccine Development: A Historical Perspective. *Hum. Vaccines Immunother.* **2019**, *15* (10), 2351−2358.

(14) Silva, J. V. J.; Lopes, T. R. R.; De Oliveira-Filho, E. F.; Oliveira, R. A. S.; Durães-Carvalho, R.; Gil, L. H. V. G. Current Status, Challenges and Perspectives in the Development of Vaccines against Yellow Fever, Dengue. *Acta Trop.* **2018**, *182*, 257−263.

(15) Caglioti, C.; Lalle, E.; Castilletti, C.; Carletti, F.; Capobianchi, M. R.; Bordi, L. Chikungunya Virus Infection: An Overview. *New Microbiol.* **2013**, *36*, 211−227.

(16) Kennedy Amaral Pereira, J.; Schoen, R. T. Management of Chikungunya Arthritis. *Clin. Rheumatol.* **2017**, *36* (10), 2179−2186.

(17) World Health Organization. Guidelines on clinical management of Chikungunya Fever http://www.wpro.who.int/mvp/topics/ntd/Clinical_Mgnt_Chikungunya_WHO_SEARO.pdf (accessed Aug 2, 2019).

(18) da Silva-Júnior, E. F.; Leoncini, G. O.; Rodrigues, É. E. S.; Aquino, T. M.; Araújo-Júnior, J. X. The Medicinal Chemistry of Chikungunya Virus. *Bioorg. Med. Chem.* **2017**, *25* (16), 4219−4244.

(19) Ching, K.-C.; Ng, L. F. P.; Chai, C. L. L. A Compendium of Small Molecule Direct-Acting and Host-Targeting Inhibitors as Therapies against Alphaviruses. *J. Antimicrob. Chemother.* **2017**, *72* (11), 2973−2989.

(20) Lani, R.; Hassandarvish, P.; Shu, M.-H.; Hong Phoon, W.; Jang Hann Chu, J.; Higgs, S.; Vanlandingham, D.; Abu Bakar, S.; Zandi, K. Antiviral Activity of Selected Flavonoids against Chikungunya Virus. *Antiviral Res.* **2016**, *133*, 50−61.

(21) Briolant, S.; Garin, D.; Scaramozzino, N.; Jouan, A.; Crance, J. M. In Vitro Inhibition of Chikungunya and Semliki Forest Viruses Replication by Antiviral Compounds: Synergistic Effect of Interferon-Alpha and Ribavirin Combination. *Antiviral Res.* **2004**, *61*, 111−117.

(22) Kaur, P.; Thiruchelvan, M.; Lee, R. C. H.; Chen, H.; Chen, K. C.; Ng, M. L.; Chu, J. J. H. Inhibition of Chikungunya Virus Replication by Harringtonine, a Novel Antiviral That Suppresses Viral Protein Expression. *Antimicrob. Agents Chemother.* **2013**, *57* (1), 155−167.

(23) Mounce, B. C.; Poirier, E. Z.; Passoni, G.; Simon-Loriere, E.; Cesaro, T.; Prot, M.; Stapleford, K. A.; Moratorio, G.; Sakuntabhai, A.; Levraud, J.-P.; et al. Interferon-Induced Spermidine-Spermine Acetyltransferase and Polyamine Depletion Restrict Zika and Chikungunya Viruses. *Cell Host Microbe* **2016**, *20* (2), 167−177.

(24) Kaur, P.; Chu, J. J. H. Chikungunya Virus: An Update on Antiviral Development and Challenges. *Drug Discovery Today* **2013**, *18* (19−20), 969−983.

(25) Abdelnabi, R.; Neyts, J.; Delang, L. Antiviral Strategies Against Chikungunya Virus. In *Chikungunya Virus: Methods and Protocols*; Chu, J. J. H., Ang, S. K., Eds.; Springer Science+Business Media: New York, 2016; Vol. *1426*, pp 243−253. DOI: 10.1007/978-1-4939-3618-2_22.

(26) Lamballerie, X. D.; Boisson, V.; Reynier, J.-C.; Enault, S.; Charrel, R. N.; Flahault, A.; Roques, P.; Grand, R. L. On Chikungunya Acute Infection and Chloroquine Treatment. *Vector-Borne Zoonotic Dis.* **2008**, *8* (6), 837−840.

(27) Roques, P.; Thiberville, S. D.; Dupuis-Maguiraga, L.; Lum, F. M.; Labadie, K.; Martinon, F.; Gras, G.; Lebon, P.; Ng, L. F. P.; de Lamballerie, X.; et al. Paradoxical Effect of Chloroquine Treatment in Enhancing Chikungunya Virus Infection. *Viruses* **2018**, *10* (5), 268.

(28) Khan, M.; Santhosh, S. R.; Tiwari, M.; Lakshmana Rao, P. V.; Parida, M. Assessment of in Vitro Prophylactic and Therapeutic Efficacy of Chloroquine against Chikungunya Virus in Vero Cells. *J. Med. Virol.* **2010**, *82* (5), 817−824.

(29) Vincent, M. J.; Bergeron, E.; Benjannet, S.; Erickson, B. R.; Rollin, P. E.; Ksiazek, T. G.; Seidah, N. G.; Nichol, S. T. Chloroquine Is a Potent Inhibitor of SARS Coronavirus Infection and Spread. *Virol. J.* **2005**, *2* (1), 69.

(30) Savarino, A.; Di Trani, L.; Donatelli, I.; Cauda, R.; Cassone, A.; Damme, V. New Insights into the Antiviral Effects of Chloroquine. *Lancet Infect. Dis.* **2006**, *6* (2), 67−69.

(31) Abdelnabi, R.; Neyts, J.; Delang, L. Chikungunya Virus Infections: Time to Act, Time to Treat Transmission and Prevalence. *Curr. Opin. Virol.* **2017**, *24*, 25−30.

(32) Patani, G. A.; LaVoie, E. J. Bioisosterism: A Rational Approach in Drug Design. *Chem. Rev.* **1996**, *96* (8), 3147−3176.

(33) Brown, N. Bioisosterism in Medicinal Chemistry. In *Bioisosteres in Medicinal Chemistry*; Brown, N., Ed.; Wiley-VCH Verlag GmbH & Co. KGaA: Weinheim, Germany, 2012; pp 1−14.

https://dx.doi.org/10.1021/acsmedchemlett.9b00662
ACS Med. Chem. Lett. 2020, 11, 906−912

(34) Topliss, J. G. Utilization of Operational Schemes for Analog Synthesis in Drug Design. *J. Med. Chem.* **1972**, *15* (10), 1006−1011.
(35) Topliss, J. G. A Manual Method for Applying the Hansch Approach to Drug Design. *J. Med. Chem.* **1977**, *20* (4), 463−469.
(36) Martyn, D. C.; Nijjar, A.; Celatka, C. A.; Mazitschek, R.; Cortese, J. F.; Tyndall, E.; Liu, H.; Fitzgerald, M. M.; O'Shea, T. J.; Danthi, S.; et al. Synthesis and Antiplasmodial Activity of Novel 2,4-Diaminopyrimidines. *Bioorg. Med. Chem. Lett.* **2010**, *20* (1), 228−231.
(37) Moussa, I. A.; Banister, S. D.; Beinat, C.; Giboureau, N.; Reynolds, A. J.; Kassiou, M. Design, Synthesis, and Structure-Affinity Relationships of Regioisomeric N-Benzyl Alkyl Ether Piperazine Derivatives as σ-1 Receptor Ligands. *J. Med. Chem.* **2010**, *53* (16), 6228−6239.

https://dx.doi.org/10.1021/acsmedchemlett.9b00662
ACS Med. Chem. Lett. 2020, 11, 906−912

2.3 Conclusion

In this publication, the described 37 first-generation CHVB analogues were identified as safe and potent inhibitors of CHIKV.

Further, all (phenylsulfonyl)piperazine-1-yl)pyrimidine analogues were easily accessible in a four-step synthesis route: starting from a substitution reaction between 2,4-dichloro-6-methylpyrimidine and the corresponding primary or secondary alkyl amines. The obtained pyrimidine halides were further reacted with the sec. amine of tert-butyl-piperazine-1-carboxylate or other suitable nitrogen-containing functional groups under microwave conditions and the following acidic catalysed deprotection with hydrochloric acid (HCl) achieved excellent yields. Subsequent amidation with different benzoyl and sulfonyl chlorides with triethylamine (TEA) as a base formed the desired CHVB compounds.

Additionally, the structural requirements for a significant anti-CHIKV activity have been determined in all five structural molecular subgroups:

- Group A (phenyl): halogen substitution in the para position most active,
- Group B (sulfonyl): amide and methylene alteration more active, albeit in combination with other variations loss of activity (amide) or toxic (methylene),
- Group C (piperazine): no other substitution performed better,
- Group D (ethylamine side-chain): HBD improves activity; bifurcated side-chains are active but also more toxic,
- Group E (pyrimidine): nitrogen on position three and methyl side-chain essential for activity.

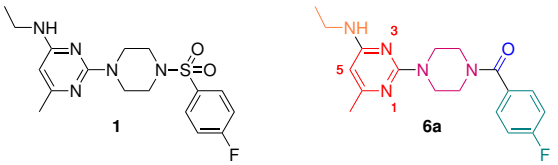

FIGURE 2.3.1: Structures of lead compounds **1** and **6a** and their biological properties. The different colour of **6a** indicate the various groups of the CHVB series in which variations were performed and analysed in the SAR studies. The compounds are referred in the following chapters as **1a** and **1b** and their analogues categorized according their nitrogen positions on the pyrimidine ring.

During this optimisation process, **6a** was identified as a potent and selective inhibitor of CHIKV, demonstrating a much better profile than the starting point, hit **1**, and a selectivity index greater than 61 (see figure 2.3.1). **6a** was therefore selected as a new lead compound for further studies. In the following publications the original hit is referred as **CHVB-00** or **1a** and the new lead **6a** as **1b**.

Chapter 3

Antiviral Profiling and Target Identification of the *CHVB Series*

3.1 Introduction

This chapter provides an insight into the particular characteristics of the anti-CHIKV activity of this class of compounds and the molecular mechanism underlying the antiviral activity [69].

The antiviral efficacy of the CHVB series was determined against various CHIKV isolates (CHIKV-899, Venturini [Italy 2008], St Martin 20235 P2, St Martin 20236 P3, EFS-1 P3 Martinique, and Congo 95 [2011]) by a CPE reduction assay in Vero cells. Further, additional antiviral assays with other alphaviruses, i.e. O'Nyong Nyong virus, Mayaro virus strain TC625, Barmah Forest virus strain BH2193, and Ross River virus 5281v were performed to assess the antiviral profile of the compounds.

A delay-of-treatment assay was first carried out to investigate the molecular mechanism and the viral target, which gave an estimation of the stage of the CHIKV replication cycle inhibited by the CHVB series. Further, a resistance selection procedure generated compound-resistant virus variants, and cross-resistant studies identified the viral target. Finally, the enzymatic activities of CHVB compounds on the identified target protein (non-structural protein 1 (nsP1)) were assessed with purified recombinant nsP1 of VEEV and Semiliki Forest virus [69–72].

3.2 Novel Class of Chikungunya Virus Small Molecule Inhibitors That Targets the Viral Capping Machinery

AMERICAN SOCIETY FOR MICROBIOLOGY | Antimicrobial Agents and Chemotherapy®

ANTIVIRAL AGENTS

Novel Class of Chikungunya Virus Small Molecule Inhibitors That Targets the Viral Capping Machinery

Rana Abdelnabi,[a] Kristina Kovacikova,[b] Julia Moesslacher,[c] Kim Donckers,[a] Verena Battisti,[d] Pieter Leyssen,[a] Thierry Langer,[d] Gerhard Puerstinger,[c] Gilles Quérat,[e] Changqing Li,[f] Etienne Decroly,[f] Ali Tas,[b] Arnaud Marchand,[g] Patrick Chaltin,[g] Bruno Coutard,[e] Martijn van Hemert,[b] Johan Neyts,[a] Leen Delang[a]

[a]KU Leuven, Department of Microbiology, Immunology and Transplantation, Rega Institute for Medical Research, Laboratory of Virology and Chemotherapy, Leuven, Belgium
[b]Molecular Virology Laboratory, Department of Medical Microbiology, Leiden University Medical Center, Leiden, the Netherlands
[c]Department of Pharmaceutical Chemistry, University of Innsbruck, Innsbruck, Austria
[d]University of Vienna, Department of Pharmaceutical Chemistry, Vienna, Austria
[e]Unité des Virus Emergents (UVE: Aix-Marseille University–IRD 190 –Inserm 1207–IHU Méditerranée Infection), Marseille, France
[f]Aix Marseille University, CNRS, AFMB UMR7257, Marseille, France
[g]Centre for Drug Design and Discovery, KU Leuven, Leuven, Belgium

Rana Abdelnabi and Kristina Kovacikova contributed equally to this work. Author order was determined alphabetically. Johan Neyts and Leen Delang contributed equally to this work.

ABSTRACT Despite the worldwide reemergence of the chikungunya virus (CHIKV) and the high morbidity associated with CHIKV infections, there is no approved vaccine or antiviral treatment available. Here, we aimed to identify the target of a novel class of CHIKV inhibitors, i.e., the CHVB series. CHVB compounds inhibit the *in vitro* replication of CHIKV isolates with 50% effective concentrations in the low-micromolar range. A CHVB-resistant variant ($CHVB^{res}$) was selected that carried two mutations in the gene encoding nsP1 (responsible for viral RNA capping), one mutation in nsP2, and one mutation in nsP3. Reverse genetics studies demonstrated that both nsP1 mutations were necessary and sufficient to achieve ~18-fold resistance, suggesting that CHVB targets viral mRNA capping. Interestingly, $CHVB^{res}$ was cross-resistant to the previously described CHIKV capping inhibitors from the MADTP series, suggesting they share a similar mechanism of action. In enzymatic assays, CHVB inhibited the methyltransferase and guanylyltransferase activities of alphavirus nsP1 proteins. To conclude, we identified a class of CHIKV inhibitors that targets the viral capping machinery. The potent anti-CHIKV activity makes this chemical scaffold a potential candidate for CHIKV drug development.

KEYWORDS chikungunya virus, antivirals, nonstructural protein 1, capping, MADTP, CHIKV, nsP1

Chikungunya virus (CHIKV) is an arthropod-borne virus that belongs to the genus *Alphavirus* of the *Togaviridae* family (1, 2). After 2 decades of sporadic outbreaks in Africa and Asia, CHIKV reemerged in Kenya in 2004, after which large epidemics of CHIKV infections were reported in several Indian Ocean islands and Southeast Asian countries (3). At the end of 2013, the first local transmission of CHIKV occurred in the Americas. Since then, millions of CHIKV cases have been reported in the Caribbean region as well as in several countries of Central and South America (4). Most recently, in 2018, CHIKV caused outbreaks in Brazil, India, Sudan, and Thailand (5). Due to the high socioeconomic impact of CHIKV infections, the virus is now considered an imminent health threat to tropical and temperate areas colonized by *Aedes* mosquitoes.

Acute CHIKV infections are characterized by fever, arthralgia, and, in many cases,

Citation Abdelnabi R, Kovacikova K, Moesslacher J, Donckers K, Battisti V, Leyssen P, Langer T, Puerstinger G, Quérat G, Li C, Decroly E, Tas A, Marchand A, Chaltin P, Coutard B, van Hemert M, Neyts J, Delang L. 2020. Novel class of chikungunya virus small molecule inhibitors that targets the viral capping machinery. Antimicrob Agents Chemother 64:e00649-20. https://doi.org/10.1128/AAC.00649-20.

Address correspondence to Leen Delang, Leen.Delang@kuleuven.be.

Received 3 April 2020
Returned for modification 18 April 2020
Accepted 23 April 2020
Accepted manuscript posted online 27 April 2020
Published 23 June 2020

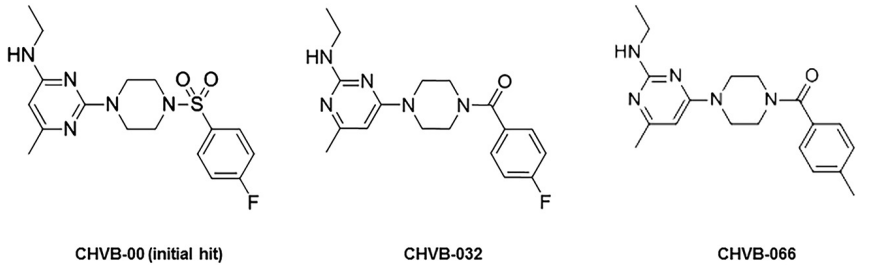

FIG 1 Chemical structures of the initial hit and selected analogs of the CHVB series.

maculopapular rash (6). Although a CHIKV infection is rarely fatal, 15 to 60% of patients suffer from chronic debilitating polyarthritis that can last for weeks up to years after the acute infection (1, 6). Recently, severe neurological complications, such as Guillain-Barré syndrome and meningoencephalitis, have also been reported during CHIKV infections (1, 7). Other complications associated with CHIKV infections include myocarditis, pancreatitis, and kidney failure (8).

Despite the worldwide spread and the high morbidity rate of CHIKV infections, there is no licensed vaccine or antiviral treatment available. The current treatment is only symptomatic (2). A number of classes of antiviral compounds targeting either a viral or a host factor have been reported to inhibit CHIKV replication in cell-based assays (9, 10), but none have progressed to clinical trials.

We previously reported on the first class of inhibitors ([1,2,3]triazolo[4,5-d]pyrimidin-7(6×H)-ones, the MADTP series) that block the capping of CHIKV RNA genomes. The MADTP compounds mainly target the guanylyltransferase activity of Venezuelan equine encephalitis virus (VEEV) nsP1 (11). This class of compounds has a low barrier to resistance, since only a single mutation in CHIKV nsP1 (proline-34-serine) resulted in high resistance to the compounds (11). Ideally, antiviral drugs should have a high barrier to resistance to avoid the rapid emergence of drug-resistant variants.

In a large-scale cytopathic effect (CPE)-based anti-CHIKV screening campaign (33,000 molecules), we identified CHVB-00 [*N*-ethyl-2-(4-((4-fluorophenyl) sulfonyl) piperazin-1-yl)-6-methylpyrimidin-4-amine] as a molecule that was able to completely inhibit CHIKV replication at nontoxic concentrations (50% effective concentration [EC_{50}] value of 8.7 ± 0.5 μM, 50% cytotoxic concentration [CC_{50}] of 122 ± 24 μM) (Fig. 1). Initial hit optimization resulted in the synthesis and biological evaluation of 67 analogs. Of these analogs, 24 molecules were more potent than the original hit compound. The synthesis of this class of molecules and the structure-activity relationship will be published elsewhere (29). Here, we report on the particular characteristics of the anti-CHIKV activity of this class of compounds and the molecular mechanism underlying the antiviral activity.

RESULTS

Molecules of the CHVB series inhibit the replication of various CHIKV isolates in cell culture. The antiviral efficacy of CHVB-032 and CHVB-066 against the CHIKV-899 strain was assessed in a CPE reduction assay on Vero cells. Both molecules exerted potent inhibition of virus-induced CPE, with EC_{50} values of 2.7 μM and 0.45 μM, respectively (Fig. 2A). When assessing the potential adverse effects of the compounds on Vero cells (by colorimetric readout using MTS/PMS), CHVB-032 was less cytotoxic than CHVB-066 (CC_{50} values of >75 μM and 15 μM, respectively) (Fig. 2A). The anti-CHIKV activity was further confirmed in a virus yield assay in which treatment with both CHVB compounds resulted in a marked dose-dependent reduction of viral RNA replication and production of infectious virus progeny, with a pronounced >4-$\log_{10}$ reduction at the highest tested concentrations (Fig. 2B and C).

The antiviral activity of CHVB-032 was further evaluated against various CHIKV isolates (Venturini [Italy 2008], St Martin 20235 P2, St Martin 20236 P3, EFS-1 P3 Martinique, and Congo 95 [2011]). CHVB-032 reduced the viral RNA yield of all the

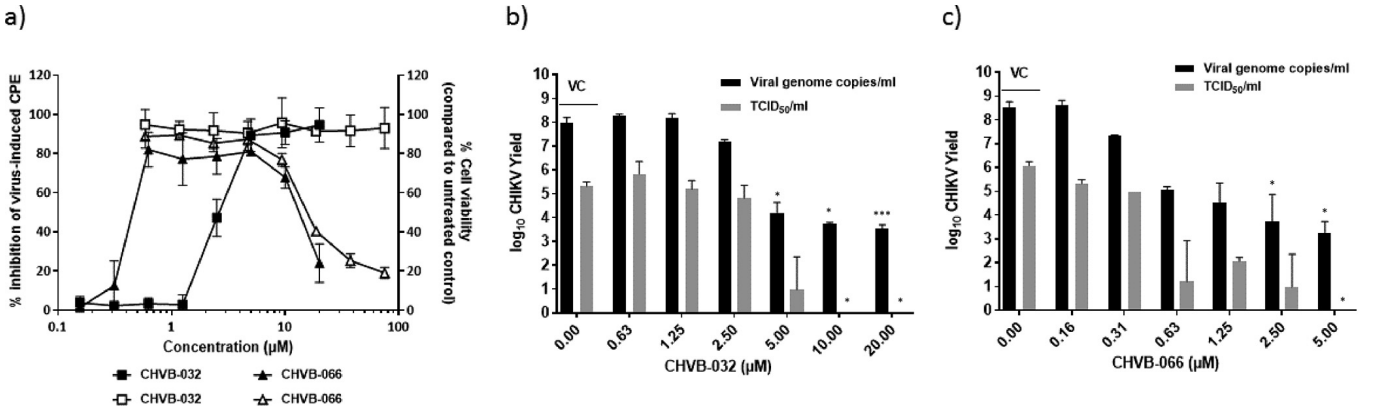

FIG 2 CHVB compounds are selective inhibitors of CHIKV replication. (a) Dose-response effect of CHVB-032 and CHVB-066 on CHIKV899-induced cytopathic effect (CPE) (filled squares and filled triangles, respectively) (MOI 0.01) and cell viability (open squares and open triangles, respectively), as quantified in Vero cells by the MTS/PMS method. Data are mean values ± standard deviations (SD) from at least three independent experiments. The effect of different concentrations of CHVB-032 (b) and CHVB-066 (c) on the release of CHIKV particles by CHIV899-infected Vero cells (MOI, 0.01) was quantified by real-time qRT-PCR (for viral RNA; black columns) and endpoint titration assay (for infectious progeny virus particles; gray columns) at 48 h p.i. Data shown are mean values ± SD from at least two independent experiments. Significant differences from untreated virus control were analyzed by two-tailed Student's *t* test (*, $P < 0.05$; ***, $P < 0.005$). TCID, tissue culture infectious dose; VC, virus control (untreated).

tested CHIKV isolates, with EC_{50} values in the range of 1.2 to 7.3 μM (Table 1). However, the compound was devoid of antiviral activity against other alphaviruses, i.e., O'Nyong Nyong virus, Mayaro virus strain TC625, Barmah Forest virus strain BH2193, and Ross River virus 5281v (data not shown).

CHVB compounds inhibit a postentry step in the CHIKV replication cycle. A delay-of-treatment assay was performed to estimate the stage of CHIKV replication cycle inhibited by the CHVB series. Chloroquine was used in this assay as a reference compound for early-stage inhibition, as this molecule is known to interfere with virus entry (12). MADTP-0372 (inhibits viral RNA capping) and T-705 (inhibits viral RNA synthesis) were used as reference molecules for replication stage inhibition (11, 13). Similar to the inhibition profile of the MADTP-0372 compound, CHVB-032 and CHVB-066 reduced viral RNA (Fig. 3A) and infectious virus loads (Fig. 3B) when added to the infected cells up to 4 h postinfection (p.i.), suggesting that compounds in the CHVB series target a postentry step in the CHIKV replication cycle.

To confirm the absence of an effect on virus entry, a CHIKV entry assay was performed using CHIKV pseudoparticles (CHIKVpp) as described before (14). In contrast to chloroquine, the CHVB compounds did not inhibit the entry of CHIKVpp in BGM cells (Fig. 3C), demonstrating that CHVB compounds act at a postentry stage of the CHIKV replication cycle.

CHVB-resistant variants carry mutations in CHIKV nsP1, nsP2, and nsP3 proteins. To identify the viral target of the CHVB series, a resistance selection procedure (11) was performed using CHVB-032 to generate compound-resistant virus variants. In

TABLE 1 Antiviral activity of CHVB-032 compound against different chikungunya virus isolates

	CHVB-032	
CHIKV strain	EC_{50} (μM)	EC_{90} (μM)
899 (laboratory)	2.7 ± 0.4[a]	5.5 ± 0.2[a]
OPY1 (La Reunion)	1.24 ± 0.3[b]	6.7 ± 0.5[b]
Venturini (Italy)	2.1 ± 0.4[b]	2.6 ± 0.4[b]
Congo (Congo)	1 ± 0.15[b]	1.2 ± 0.1[b]
St Martin 20235 P2	1.7 ± 0.4[b]	5 ± 0.3[b]
St Martin 20236 P3	4.1 ± 0.6[b]	17 ± 8[b]
EFS-1 P3 Martinique	7.3 ± 2.3[b]	13 ± 3[b]

[a]CPE reduction.
[b]Viral RNA reduction.

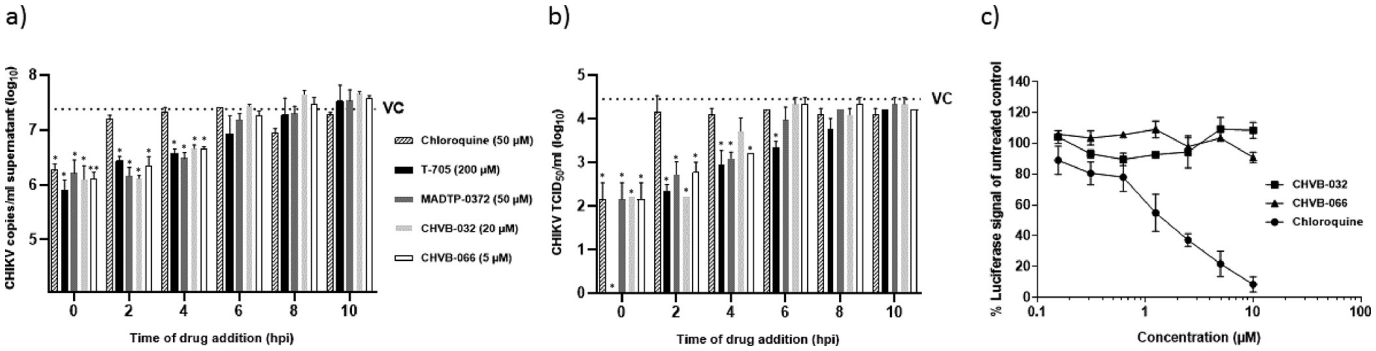

FIG 3 CHVB compounds inhibit a postentry step in CHIKV replication cycle. The delay of treatment effect of CHVB-032 (20 μM; light gray columns) and CHVB-066 (5 μM; white columns) on viral replication in CHIKV899-infected Vero cells (MOI of 1) was determined at 12 h p.i. by real-time qRT-PCR (a) and endpoint titration assay (b). Chloroquine (50 μM, dashed columns) served as a reference compound for early-stage inhibition, whereas MADTP-0372 (50 μM, dark gray columns) and T-705 (200 μM, black columns) served as references for postentry-stage inhibition. Data are mean values ± SD from at least two independent experiments. Significant differences from untreated virus control were analyzed by two-tailed Student's *t* test (*, $P < 0.05$; **, $P < 0.01$). (c) The effect of CHVB-032 (filled squares) and CHVB-066 (filled triangles) on CHIKV entry using CHIKV pseudoparticles (CHIKVpp). Chloroquine (filled circles) served as a reference compound for early-stage inhibition. BGM cells were treated with serial dilutions of each compound and then were infected with CHIKVpp. On day 3 p.i., cells were washed and then lysed to determine the luciferase activity. Data are presented as percent relative light units (RLU) of the untreated control, and the values plotted are mean values ± SD from at least three independent experiments. TCID, tissue culture infectious dose; VC, virus control (untreated).

total, four independent, putative CHVB-resistant virus variants were obtained. CPE reduction assays showed that only resistant virus strain 4 was markedly less susceptible to CHVB compounds, displaying a 19-fold resistance to CHVB-066 (Table 2). Resistant variant 4 was also resistant to other CHVB analogs (Table 3). Whole-genome sequencing of the resistant viruses revealed that all the variants carried an S454G mutation in nsP1 and an M703T mutation in the methyltransferase-like domain of nsP2 (Table 4). Resistant virus 4 acquired two additional mutations, W456R in nsP1 and L494P in the highly variable domain of nsP3, whereas resistant virus 3 had an additional mutation, H280Q, in the alphavirus unique domain (AUD) of nsP3 (Table 4). Deep sequencing of the original virus stock used for resistance selection revealed that only the nsP3-L494P mutation was preexisting in the virus population with a frequency of 23.5%.

To determine which of the identified mutations contributed to phenotypic resistance against the compound, these mutations were introduced into the CHIKV LS3 cDNA clone using site-directed mutagenesis as described before (11). The susceptibility of the recombinant CHIKV variants to the antiviral activity of the CHVB compounds was determined in a CPE reduction assay (Fig. 4). Despite the presence of S454G and M703T mutations in all resistant clones, the single mutants rCHIKV+S454G and rCHIKV+M703T were not resistant to CHVB-032 or CHVB-066 (Fig. 4). With EC_{50} values of 0.38 μM and 0.31 μM, respectively, these variants were even more sensitive to the antiviral effect of CHVB-066 than wt virus (Table 5). A more sensitive phenotype was also found for CHVB-032. The combination of the S454G and M703T mutations in rCHIKV+S454G+M703T also did not yield a compound-resistant phenotype but rather one with increased susceptibility, as an EC_{50} value of 0.32 μM was determined (Table 5). The other mutations present in resistant virus 4 then were introduced into the CHIKV infectious clone in various combinations. Recombinant rCHIKV+W456R was as susceptible to CHVB-066 (EC_{50} of 0.76 μM) as wt virus, and it was even more susceptible to

TABLE 2 Phenotype of putative CHVB-resistant clones

	CHVB-066	
CHIKV strain	EC_{50} (μM)	Fold resistance[a]
wt	0.55 ± 0.01	1
Resistant virus 1	1.6 ± 0.3	2.9
Resistant virus 2	0.94 ± 0.05	1.7
Resistant virus 3	0.63 ± 0.4	1.1
Resistant virus 4	13 ± 0.4	19

[a]Fold resistance is EC_{50} variant/EC_{50} wt.

TABLE 3 Phenotype of resistant virus 4 against different CHVB analogues

Compound	EC_{50} (μM)		Fold resistance[a]
	wt	Resistant virus 4	
CHVB-023	1.2	7.5	6.5
CHVB-057	0.86	17.3	20
CHVB-032	2.7	>100	>37

[a]Fold resistance is EC_{50} variant/EC_{50} wt.

CHVB-032 (EC_{50} of 1.76 μM) than wt virus. Interestingly, it was specifically the combination of the two nsP1 mutations S454G and W456R that increased the resistance to CHVB-066 8-fold (EC_{50} of 5.4 μM) and to CHVB-032 more than 18-fold (EC_{50} of >100 μM) (Table 5). The S454G and W456R mutations in nsP1 provided the virus the same level of resistance against CHVB-032 as the originally isolated resistant variant 4 and, thus, were sufficient to result in the CHVB-032-resistant phenotype. Introduction of the nsP2-M703T mutation in the variant with the nsP1-S454G and -W456R mutations (rCHIKV+S454G+W456R+M703T) did not further increase the resistance to both compounds (EC_{50} of 2.6 μM for CHVB-066 and EC_{50} of 81 μM for CHVB-032) (Table 5). This amino acid at position 703 is located in the MTase-like domain of nsP2, suggesting an interaction of this domain with nsP1 during the viral RNA capping. Importantly, the presence of all four mutations that were identified in resistant virus 4 in the reverse-engineered virus resulted in a CHVB-066-resistant phenotype comparable to that of the originally isolated virus 4 (EC_{50} of 12 μM) (Fig. 4). This reverse-engineered virus, rCHIKV+S454G+W456+M703T+L494P, was also fully resistant to CHVB-032 (EC_{50} of >100 μM). In summary, the S454G and W456R mutations in CHIKV nsP1 are sufficient and required for CHVB-032 resistance and a high level of resistance to CHVB-066. Maximum resistance to CHVB-066 required two additional mutations in nsP2 and nsP3, suggesting CHVB-066 has a higher barrier to resistance than CHVB-032.

To exclude that the observed resistance is due to increased replication, the growth kinetics of the three variants with the highest fold resistance values were investigated. All the recombinant variants replicated with kinetics very similar to those of rCHIKV wt. At 6 h postinfection, the reverse-engineered viruses with the M703T substitution in nsP2 produced noticeably higher titers than the other viruses, but at later time points there were no differences (Fig. 5).

The CHVB-resistant variants are cross-resistant to other CHIKV nsP1 inhibitors. Cross-resistance studies were performed with favipiravir and MADTP-0372. Favipiravir was able to protect cells against CHIKV-induced CPE for all the recombinant viruses tested, with EC_{50} values in the range of 90 to 142 μM, comparable to the wt (Table 6). Interestingly, the CHVB-resistant mutant with two mutations in nsP1 and the CHVB-resistant mutant with four mutations proved fully cross-resistant to MADTP-0372 (EC_{50} of >25 μM). Likewise, the MADTP-resistant mutant (carrying the nsP1-P34S mutation) was fully cross-resistant to CHVB-066 (EC_{50} of >12.5 μM), suggesting that the modes of action of the CHVB and MADTP series are similar (Table 6).

CHVB compounds inhibit the enzymatic functions of VEEV and SFV nsP1. The alphavirus nsP1 possesses both MTase and GTase activities, which are required for the capping of viral RNA (15). Because CHVB-resistant mutants displayed clear cross-

TABLE 4 CHVB-resistant variants carry mutations in CHIKV nsP1 to nsP3 genes

Protein	wt	Resistant virus 1	Resistant virus 2	Resistant virus 3	Resistant virus 4	% conserved in CHIKV
nsP1	S454	S454G	S454G	S454G	S454G	82
	W456				W456R	97.9
nsP2	M703	M703T	M703T	M703T	M703T	99.3
nsP3	H280			H280Q		99.8
	L494				L494P	99.3

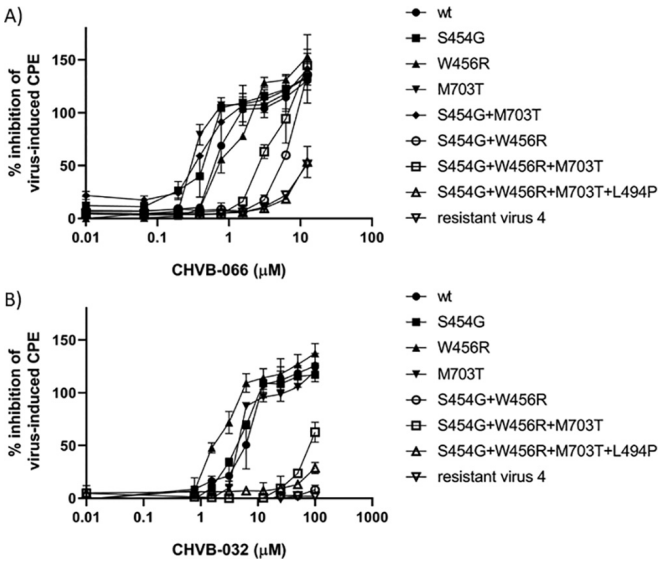

FIG 4 Phenotypic resistance of reverse-engineered CHVB-resistant mutants compared to resistant virus 4 and rCHIKV wt. Wild-type (filled circles) and recombinant CHIKV strains with individual or combined mutations that were identified in the CHVB-resistant isolate 4 (open down triangles) were assessed in a CPE reduction assay with increasing doses of CHVB-066 (A) and CHVB-032 (B). Vero E6 cells were treated with 0 to 12.5 μM CHVB-066 or 0 to 100 μM CHVB-032 and infected with rCHIKV LS3 wt or the recombinant CHIKV mutants at an MOI of 0.05. Four days postinfection, the cell viability was determined by the MTS/PMS method. Data represent the means ± SD from at least two independent experiments performed in quadruplicate ($n = 8$). CPE, cytopathic effect; wt, wild type.

resistance to the MADTP series, we assessed the effect of CHVB-032 and CHVB-066 on the enzymatic activities of purified recombinant nsP1. Since attempts to purify recombinant CHIKV nsP1 from *Escherichia coli* failed to obtain enzymatically active protein, *in vitro* assays with purified nsP1 of VEEV (15) and Semliki Forest virus (SFV) (16) were used. The *in vitro* GTase activity of VEEV nsP1 was quantified by measuring the formation of the m^{7}GMP-nsP1 complex by Western blotting, using m^{7}GTP as a substrate and an anti-m^{3}G/m^{7}Gp antibody for detection. The MTase activity of VEEV nsP1 was quantified by a filter-based assay using ^{3}H-*S*-adenosylmethionine (SAM). CHVB-066 inhibited the GTase activity of VEEV nsP1 in a concentration-dependent manner with a 50% inhibitory concentration (IC_{50}) of <0.5 μM, more potently than the known inhibitor sinefungin (Fig. 6A). The MTase activity of VEEV nsP1 was also inhibited, but the effect was less pronounced (IC_{50} of 1.9 μM) (Fig. 6B). Since VEEV belongs to a different serocomplex than CHIKV, we wanted to confirm the inhibition of m^{7}GMP-nsP1 complex formation using the nsP1 protein of SFV, which is genetically more closely related to CHIKV (17). The readout of the SFV nsP1 assay is the formation of the covalent

TABLE 5 Phenotypic resistance of CHVB-resistant mutants compared to those of original resistant virus 4 and rCHIKV wt

	CHVB-066		CHVB-032	
CHIKV strain	EC_{50} (μM)	Fold resistance[a]	EC_{50} (μM)	Fold resistance
wt	0.65 ± 0.002	1	5.45 ± 1.64	1
S454G	0.38 ± 0.09	<1	4.10 ± 0.16	<1
W456R	0.76 ± 0.1	1.2	1.76 ± 0.27	<1
M703T	0.31 ± 0.01	<1	4.53 ± 0.02	<1
S454G+M703T	0.32 ± 0.01	<1	ND[b]	ND
S454G+W456R	5.4 ± 0.2	8.3	>100	>18
S454G+W456R+M703T	2.6 ± 0.3	4.1	81 ± 10	15
S454G+W456R+M703T+L494P	12 ± 3.7	18.5	>100	>18
Resistant virus 4	13 ± 0.4	20	>100	>18

[a]Fold resistance is EC_{50} variant/EC_{50} wt.
[b]ND, not determined.

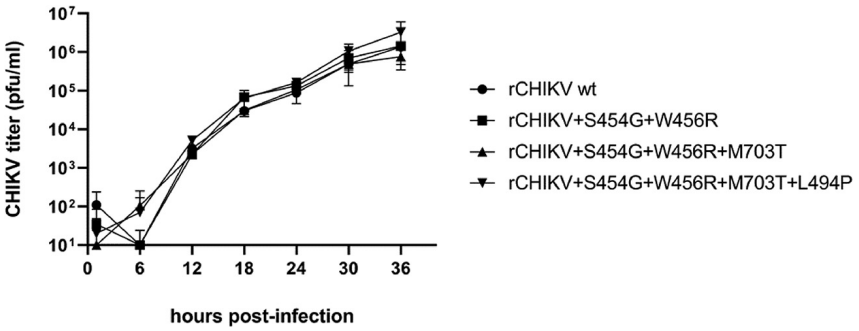

FIG 5 Growth kinetics of CHVB-066-resistant mutants versus rCHIKV wt. Vero E6 cells were infected with CHIKV LS3 wt (filled circles) and the reverse-engineered double (filled squares), triple (filled up triangles), and quadruple (filled down triangles) mutants at an MOI of 0.1 for 1 h at 37°C. Following infection, the cells were washed twice with warm phosphate-buffered saline, and the medium was replaced with Eagle's minimal essential medium–2% fetal calf serum. At 6-h intervals, samples from the medium were harvested and stored at −80°C. At 1 h postinfection, a sample was taken to determine how much virus of the inoculum remained after washing. The virus titers in the samples were determined by plaque assay. The experiment represents means ± SD from two independent infections titrated in duplicate ($n = 4$). PFU, plaque-forming units; wt, wild type; rCHIKV, recombinant CHIKV.

^{32}P-labeled m^{7}GMP-nsP1 complex by using [α^{32}-P]GTP and SAM as reaction substrates, thereby measuring the combined activities of the MTase and GTase. An active-site mutant with the D64A substitution was included as a negative control, since this mutant lacks MTase and GTase activity (18). CHVB-066 and CHVB-032 completely inhibited the activity of the wt SFV nsP1 protein at all tested doses (50 μM to 1 mM) (Fig. 7). These data demonstrate that the CHVB compounds directly inhibit the enzymatic activity of nsP1, particularly the MTase activity.

DISCUSSION

Capping of viral mRNA is an essential posttranscriptional modification that influences subsequent downstream processing, translation, nuclear export, and stability of mRNA. Viruses have developed different strategies to cap their genomes and thereby mimic the cap structure of the host cell. Viral RNA caps can be acquired by a cap-snatching mechanism (orthomyxoviruses), or viruses can covalently attach a peptide (picornaviruses) or a cap moiety to their 5′ ends (such as alphaviruses) (19, 20). The alphavirus nsP1 and nsP2 proteins contain the RNA methyltransferase, guanylyltransferase, and triphosphatase functions that are needed for the viral RNA capping pathway. This alphavirus capping mechanism is unique and proceeds in a sequence that differs from the capping mechanism in the host cell. First, a GTP molecule is methylated using SAM as a methyl donor and producing SAH as a by-product of the reaction. In the second step, the methylated GTP (m^{7}GTP) is transferred onto nsP1, releasing pyrophosphate and forming the m^{7}GMP-nsP1 covalent intermediate (21). In the third step, the m^{7}GMP is attached to the first nucleotide of the viral RNA, which had been modified by the RNA triphosphatase activity of nsP2 to remove the γ-phosphate (22). Inhibitors targeting this unique capping pathway may have a limited effect on cellular capping and host MTases (23).

We previously demonstrated, for the first time, that small molecule inhibitors of the

TABLE 6 Cross-resistance of CHVB-resistant mutants against favipiravir and MADTP-372

	Favipiravir		MADTP-372	
CHIKV strain	EC_{50} (μM)	Fold resistance[a]	EC_{50} (μM)	Fold resistance
wt	115 ± 5.4	1	1.2 ± 0.06	1
S454G+W456R	136 ± 7.5	1.2	>25	20
S454G+W456R+M703T	90 ± 8.6	<1	ND	ND
S454G+W456R+M703T+L494P	142 ± 25	1.2	>25	20

[a]Fold resistance is EC_{50} variant/EC_{50} wt.

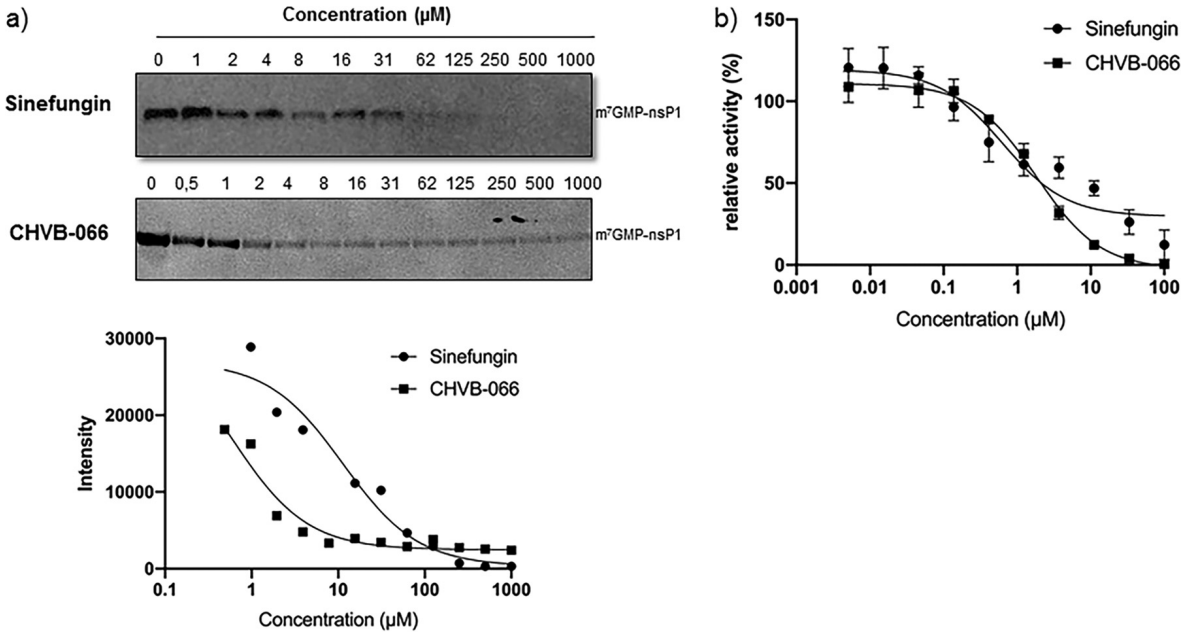

FIG 6 Effect of CHVB-066 on the enzymatic activities of VEEV nsP1. (a) Dose-response effect of CHVB-066 (filled squares) on the *in vitro* guanylylation of VEEV nsP1. Sinefungin (filled circles) was included in the assay as a reference compound. The formation of m7GMP-nsP1 complex was detected by Western blotting using an anti-methyl3/7Gp antibody. (b) Dose-response effect of CHVB-066 (filled squares) on the methyltransferase activity of VEEV nsP1. The nsP1-MTase product (3H-methyl)GIDP was measured by a scintillation counter. Data presented are the average values ± SD from two independent experiments.

alphavirus capping machinery could efficiently and completely inhibit CHIKV replication in cell culture (11). This compound series with a triazolopyrimidinone scaffold, known as the MADTP series, inhibits the GTase activity of VEEV nsP1 in an *in vitro* assay. Recently, 6′-β-fluoro-homoaristeromycin and 6′-fluoro-homoneplanocin A also have been shown to potently inhibit CHIKV replication by targeting nsP1 (16). These compounds affected the MTase activity of SFV nsP1 in enzymatic assays. Other reports on CHIKV nsP1 as an antiviral target have followed, using target-based screening methods. An nsP1-GTP competition screen resulted in the identification of several small molecules able to compete with GTP for the CHIKV nsP1-GTP binding site (24). In contrast, an enzyme-linked immunosorbent assay to identify inhibitors of CHIKV nsP1 by mea-

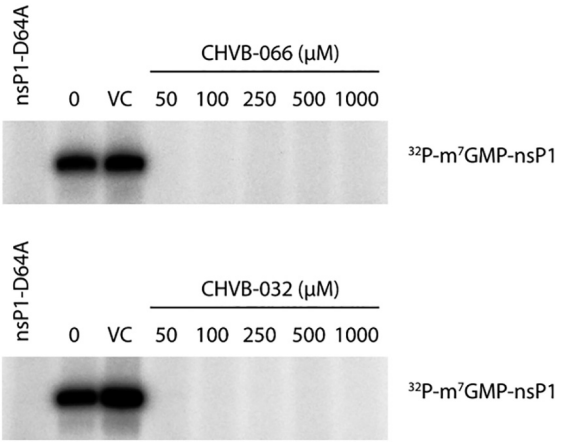

FIG 7 Effect of CHVB-032 and CHVB-066 on the enzymatic activities of SFV nsP1. Purified wt SFV nsP1 was incubated for 30 min at 30°C with increasing doses (50 μM to 1 mM) of CHVB-032 or CHVB-066, the concentration of solvent present at the highest dose of compound, i.e., 5% of dimethyl sulfoxide (VC), or left untreated (0). The D64A mutant was used as a negative control (left lane). The samples were resolved on a 10% SDS-PAGE gel, and the covalent [^{32}P]m^{7}GMP-nsP1 reaction product was detected by autoradiography after overnight exposure. VC, virus control (untreated).

suring the formation of the m^7GMP-nsP1 complex did not result in the identification of new inhibitors (25). A similar assay using VEEV nsP1, on the other hand, resulted in the identification of a number of molecules that inhibited the GTase activity (by >80%), and cross-resistance studies indicated that their mechanism differed from that of the MADTP series (23). We now describe a third series of CHIKV nsP1-targeting compounds with yet another chemical scaffold but the same target as the MADTP series, since CHVB-resistant viruses were cross-resistant to MADTP-0372 and vice versa. The described MADTP-resistant virus carried the P34S mutation in nsP1, whereas the CHVB-resistant viruses described here require at least two mutations, S454G and W456R, in nsP1 to confer resistance. Interestingly, during our initial attempts to produce virus stocks of recombinant CHIKV mutants, we noticed the emergence of the P34S mutation in viruses with the W456R mutation. Because several mutants, in particular the ones containing the W456R mutation, exhibited the tendency to revert to wild type (wt), we started culturing our virus stocks in the presence of compound to retain mutations. Under this selection pressure, the P34S mutation was no longer identified by Sanger sequencing. This might explain why the mutation did not appear during the resistance selection procedure for the CHVB compounds, as these conditions might have favored the presence of the W456R mutation over the P34S mutation. Although a crystal structure of CHIKV nsP1 is currently not available to support our hypothesis, we suggest that the P34 residue in the N-terminal region of the protein is in close proximity to W456 in the C-terminal region of the protein.

Similar to the MADTP series, the CHVB series is also CHIKV specific, with no or modest antiviral activity against other alphaviruses in cell-based assays. Because the enzymatically active region of the alphavirus nsP1 is well conserved, it is puzzling that neither series is inactive against other alphaviruses. It was recently shown that the Sindbis virus generates a large amount of noncapped viral genomes, more specifically during the early stage of the replication cycle (26). It is not known whether the same holds true for CHIKV. A possible explanation for the differential susceptibility of alphaviruses to the 2 series of compounds is that CHIKV is very susceptible to capping inhibitors because it generates more capped viral genomes than other alphaviruses. The crystal structures of nsP1 proteins of CHIKV and other alphaviruses could provide answers, but such structures have not yet been resolved.

In contrast to the MADTP series, which required only one amino acid substitution at position 34 (P34S) in nsP1 to develop full resistance, resistance to CHVB-032 required the presence of two mutations in nsP1, and full resistance to CHVB-066 even required two additional mutations in nsP2 and nsP3. Moreover, in the second step of the resistance selection protocol, 17% of culture wells showed full CHIKV-induced CPE for the MADTP series (24 wells out of 144) versus only 2.5% (4 wells out of 162) in the case of the CHVB series. These data suggest that the barrier to resistance is higher for the CHVB series and that the development of resistance in the clinical settings is less likely to occur, as two mutations are needed. Furthermore, in the reverse-engineered variants, mutations causing resistance to CHVB compounds tended to revert to wt in the absence of selective pressure.

In conclusion, we report on a novel class of small molecule inhibitors of the CHIKV capping machinery. Several other CHIKV inhibitors that target the capping have been reported, indicating that the capping machinery of the virus is an interesting target for antiviral drug development.

MATERIALS AND METHODS

Cells, viruses, and compounds. African green monkey kidney cells (Vero cells [ATCC CCL-81], Vero E6 cells [ATCC CRL-1586], and baby hamster kidney [BHK-21]) cells were maintained as described before (11).

CHIKV and other alphavirus strains are as mentioned before (11). CHIKV LS3 (GenBank accession no. KC149888), which was used for reverse genetics studies, is derived from a full-length cDNA clone belonging to the collection of the Leiden University Medical Center, The Netherlands (27).

CHVB-032 and CHVB-066 (Fig. 1) were synthesized in the laboratory of G. Pürstinger (University of Innsbruck, Austria) and T. Langer (University of Vienna, Austria). MADTP-0372 was synthesized by M. J.

Pérez-Pérez (Spanish National Research Council [CSIC]) (11). T-705 (favipiravir) was purchased as a custom synthesis product from BOC Sciences. Chloroquine was purchased from Sigma.

CPE reduction assay. Vero cells were seeded at a density of 2.5×10^4 in 96-well plates (BD Falcon) and were allowed to adhere overnight. The next day, cells were treated with a dilution series of the compounds, after which the cultures were infected with CHIKV-899 (multiplicity of infection [MOI] of 0.01). On day 5 postinfection, the inhibition of CPE was quantified using MTS/PMS as described by the manufacturer (Promega). The cells were checked by microscope for minor signs of virus-induced CPE or compound-induced adverse effects on the cell monolayer morphology. The 50% effective concentration (EC_{50}), which is defined as the concentration of compound that is required to inhibit virus-induced cell death by 50%, was determined using logarithmic interpolation.

Virus yield assay. Vero cells were seeded in 96-well plates at a density of 5×10^4 cells/well. The next day, cells were treated with serial dilutions of the compound and then infected with CHIKV-899 (MOI of 0.01). Two hours postinfection, the cells were washed to remove nonadsorbed virus, followed by incubation with the same serial dilutions of compounds. After 48 h of incubation, supernatants were collected and viral RNA was quantified by real-time quantitative RT-PCR (qRT-PCR), while the amount of infectious progeny virus was determined by titration assay (50% cell culture infectious dose [$CCID_{50}$]/ml) as described before (28).

Delay of treatment assay. Vero cells were seeded in 96-well plates at a density of 5×10^4 cells/well. The following day, cells were infected with CHIKV 899 (MOI of 1) for 1 h at 37°C, after which the viral inoculum was removed, and cells were washed 3 times with the assay medium. The selected compounds (20 μM CHVB-032, 5 μM CHVB-066, 50 μM MADTP-0372, 200 μM T-705, and 50 μM chloroquine) were added to cells at 0, 2, 4, 6, 8, and 10 h after infection. At 12 h postincubation (i.e., one viral replication cycle), culture supernatants were collected for quantification of extracellular viral RNA load (by qRT-PCR) and infectious virus progeny (by endpoint titration).

Selection of compound-resistant virus isolates. A 5-step clonal resistance selection protocol was used to isolate CHVB-resistant virus variants as previously described (13). In the first step, Vero cells were seeded in 96-well plates at a density of 2.5×10^4 cells/well and were allowed to adhere overnight. Subsequently, antiviral assays were performed in a checkerboard format using serial dilutions of CHVB-032 and different amounts of CHIKV-899 (ranging from 10 to 1,000 $CCID_{50}$). After 5 days of incubation, all assay wells were checked microscopically. Based on these data, the lowest concentration of compound and the highest virus input at which complete and reproducible inhibition of virus-induced CPE was observed were selected. In the second step, three 96-well plates containing adherent Vero cells were treated with the selected CHVB-032 concentration of 29 μM and then were infected with the optimal amount of virus (50 $CCID_{50}$). After 5 days, 7 assay wells (out of 162) showed signs of virus-induced CPE, with only 4 of them showing full CPE. The supernatants of these 4 wells were collected and semipurified 6-fold by titration (1:5 dilution series) in the presence of 29 μM CHVB-032. Four virus isolates (one from each original sample) were selected that produced the most pronounced signs of CPE in the presence of CHVB-032 at the lowest virus input possible. Subsequently, the resistant phenotype of the selected virus isolates was determined in comparison with the wild-type virus in CPE reduction assays. In parallel, the genotype was determined by full-genome sequencing.

Assays for alphavirus nsP1 enzymatic activity. The DNA sequence encoding SFV nsP1 (amino acids 1 to 537) with a C-terminal hexahistidine (6×His) tag was cloned into the pET34 vector. Recombinant wild-type and active-site mutant D64A were expressed in *E. coli* Rosetta cells (Novagen) following overnight induction with 0.5 mM isopropyl-β-D-thiogalactopyranoside (IPTG) at 19°C. The recombinant proteins were batch purified by immobilized metal affinity chromatography (IMAC) using Talon (Cobalt) beads (TaKaRa), and the eluted protein was concentrated and used in the covalent m^7GMP-nsP1 complex formation assay (16). This assay was performed in a 30-μl mixture containing 25 mM HEPES, pH 7.5, 5 mM dithiothreitol, 10 mM KCl, 2 mM $MgCl_2$, 10 μM *S*-adenosylmethionine (SAM), 0.75 mCi of [α^{32}-P]GTP (3,000 Ci/mmol), and 0.5 μM SFV nsP1 wt or D64A mutant. The reaction mixture was incubated at 30°C for 30 min and stopped by adding 3 μl of 10% SDS. The inactivated reaction mixture was mixed with 4× LSB (Laemmli sample buffer), and 10-μl samples were resolved on a 10% SDS-PAGE gel. The gel was dried, and a PhosphorImager screen was placed on top. After overnight exposure, the ^{32}P-labeled covalent m^7GMP-nsP1 intermediate products were visualized with a Typhoon Imager (Amersham).

The protocols for VEEV nsP1 enzymatic activity assays were previously described (11).

Statistical analysis. Graphing and statistical analysis were performed using Prism8 software (GraphPad).

ACKNOWLEDGMENTS

We thank Caroline Collard, Tom Bellon, and Nick Verstraeten for their excellent technical assistance in the acquisition of the antiviral data.

This work was supported by the European Union FP7 Program under SILVER grant agreement no. 260644 and the Marie Curie ITN "EUVIRNA" grant agreement no. 264286, as well as the Horizon 2020 research and innovation program under the Marie Sklodowska-Curie grant agreement no. 642434, Marie Curie ITN "Antivirals." R.A. was funded by a PDM postdoctorate scholarship of KU Leuven (PDM 17/178). The funding source had no role in the design, implementation, analysis, interpretation, or decision to publish this study.

We have no conflicts of interest to declare.

L.D., J.N., M.V.H., and G.P. supervised the project; R.A., K.K., J.M., G.Q., B.C., L.D., and M.V.H. designed research; R.A., K.K., J.M., K.D., A.T., C.L., and E.D. performed experiments; R.A., K.K., K.D., C.L., E.D., B.C., and G.Q. collected and analyzed data; A.M., P.C., J.M., V.B., T.L., and G.P. provided compounds; R.A., K.K., J.N., M.V.H., and L.D. wrote the manuscript; and A.M., P.C., T.L., and P.L. gave conceptual advice.

REFERENCES

1. Morrison CR, Plante KS, Heise MT. 2016. Chikungunya virus: current perspectives on a reemerging virus. Microbiol Spectr 4:10.1128/microbiolspec.EI10-0017-2016. https://doi.org/10.1128/microbiolspec.EI10-0017-2016.
2. Lahariya C, Pradhan SK. 2006. Emergence of chikungunya virus in Indian subcontinent after 32 years: a review. J Vector Borne Dis 43:151–160.
3. Burt FJ, Rolph MS, Rulli NE, Mahalingam S, Heise MT. 2012. Chikungunya: a re-emerging virus. Lancet 379:662–671. https://doi.org/10.1016/S0140-6736(11)60281-X.
4. Weaver SC, Forrester NL. 2015. Chikungunya: evolutionary history and recent epidemic spread. Antiviral Res 120:32–39. https://doi.org/10.1016/j.antiviral.2015.04.016.
5. European Centre for Disease Prevention and Control. 2019. Communicable disease threats report week 4, 20–26 January 2019. European Centre for Disease Prevention and Control, Solna, Sweden. https://ecdc.europa.eu/sites/portal/files/documents/communicable-disease-threats-report-26-january-2019.pdf.
6. Gasque P, Couderc T, Lecuit M, Roques P, Ng LF. 2015. Chikungunya virus pathogenesis and immunity. Vector Borne Zoonotic Dis 15:241–249. https://doi.org/10.1089/vbz.2014.1710.
7. Gerardin P, Encephalchik Study Group, Couderc T, Bintner M, Tournebize P, Renouil M, Lemant J, Boisson V, Borgherini G, Staikowsky F, Schramm F, Lecuit M, Michault A. 2016. Chikungunya virus-associated encephalitis: a cohort study on La Reunion Island, 2005–2009. Neurology 86:94–102. https://doi.org/10.1212/WNL.0000000000002234.
8. Thiberville SD, Moyen N, Dupuis-Maguiraga L, Nougairede A, Gould EA, Roques P, de Lamballerie X. 2013. Chikungunya fever: epidemiology, clinical syndrome, pathogenesis and therapy. Antiviral Res 99:345–370. https://doi.org/10.1016/j.antiviral.2013.06.009.
9. Abdelnabi R, Neyts J, Delang L. 2015. Towards antivirals against chikungunya virus. Antiviral Res 121:59–68. https://doi.org/10.1016/j.antiviral.2015.06.017.
10. Abdelnabi R, Neyts J, Delang L. 2017. Chikungunya virus infections: time to act, time to treat. Curr Opin Virol 24:25–30. https://doi.org/10.1016/j.coviro.2017.03.016.
11. Delang L, Li C, Tas A, Querat G, Albulescu IC, De Burghgraeve T, Guerrero NA, Gigante A, Piorkowski G, Decroly E, Jochmans D, Canard B, Snijder EJ, Perez-Perez MJ, van Hemert MJ, Coutard B, Leyssen P, Neyts J. 2016. The viral capping enzyme nsP1: a novel target for the inhibition of chikungunya virus infection. Sci Rep 6:31819. https://doi.org/10.1038/srep31819.
12. Khan M, Santhosh SR, Tiwari M, Lakshmana Rao PV, Parida M. 2010. Assessment of in vitro prophylactic and therapeutic efficacy of chloroquine against Chikungunya virus in vero cells. J Med Virol 82:817–824. https://doi.org/10.1002/jmv.21663.
13. Delang L, Segura Guerrero N, Tas A, Querat G, Pastorino B, Froeyen M, Dallmeier K, Jochmans D, Herdewijn P, Bello F, Snijder EJ, de Lamballerie X, Martina B, Neyts J, van Hemert MJ, Leyssen P. 2014. Mutations in the chikungunya virus non-structural proteins cause resistance to favipiravir (T-705), a broad-spectrum antiviral. J Antimicrob Chemother 69:2770–2784. https://doi.org/10.1093/jac/dku209.
14. Salvador B, Zhou Y, Michault A, Muench MO, Simmons G. 2009. Characterization of Chikungunya pseudotyped viruses: identification of refractory cell lines and demonstration of cellular tropism differences mediated by mutations in E1 glycoprotein. Virology 393:33–41. https://doi.org/10.1016/j.virol.2009.07.013.
15. Li C, Guillen J, Rabah N, Blanjoie A, Debart F, Vasseur JJ, Canard B, Decroly E, Coutard B. 2015. mRNA capping by Venezuelan equine encephalitis virus nsP1: functional characterization and implications for antiviral research. J Virol 89:8292–8303. https://doi.org/10.1128/JVI.00599-15.
16. Kovacikova K, Morren BM, Tas A, Albulescu IC, van Rijswijk R, Jarhad DB, Shin YS, Jang MH, Kim G, Lee HW, Jeong LS, Snijder EJ, van Hemert MJ. 2020. 6′-Beta-fluoro-homoaristeromycin and 6′-fluoro-homoneplanocin a are potent inhibitors of chikungunya virus replication through their direct effect on viral nonstructural protein 1. Antimicrob Agents Chemother 64:e02532-19. https://doi.org/10.1128/AAC.02532-19.
17. Powers AM, Brault AC, Shirako Y, Strauss EG, Kang W, Strauss JH, Weaver SC. 2001. Evolutionary relationships and systematics of the alphaviruses. J Virol 75:10118–10131. https://doi.org/10.1128/JVI.75.21.10118-10131.2001.
18. Ahola T, Laakkonen P, Vihinen H, Kaariainen L. 1997. Critical residues of Semliki Forest virus RNA capping enzyme involved in methyltransferase and guanylyltransferase-like activities. J Virol 71:392–397.
19. Decroly E, Ferron F, Lescar J, Canard B. 2011. Conventional and unconventional mechanisms for capping viral mRNA. Nat Rev Microbiol 10:51–65. https://doi.org/10.1038/nrmicro2675.
20. Strauss JH, Strauss EG. 1994. The alphaviruses: gene expression, replication, and evolution. Microbiol Rev 58:491–562.
21. Ahola T, Kaariainen L. 1995. Reaction in alphavirus mRNA capping: formation of a covalent complex of nonstructural protein nsP1 with 7-methyl-GMP. Proc Natl Acad Sci U S A 92:507–511. https://doi.org/10.1073/pnas.92.2.507.
22. Vasiljeva L, Merits A, Auvinen P, Kaariainen L. 2000. Identification of a novel function of the alphavirus capping apparatus. RNA 5′-triphosphatase activity of Nsp2. J Biol Chem 275:17281–17287. https://doi.org/10.1074/jbc.M910340199.
23. Ferreira-Ramos AS, Li C, Eydoux C, Contreras JM, Morice C, Querat G, Gigante A, Perez Perez MJ, Jung ML, Canard B, Guillemot JC, Decroly E, Coutard B. 2019. Approved drugs screening against the nsP1 capping enzyme of Venezuelan equine encephalitis virus using an immunobased assay. Antiviral Res 163:59–69. https://doi.org/10.1016/j.antiviral.2019.01.003.
24. Feibelman KM, Fuller BP, Li L, LaBarbera DV, Geiss BJ. 2018. Identification of small molecule inhibitors of the Chikungunya virus nsP1 RNA capping enzyme. Antiviral Res 154:124–131. https://doi.org/10.1016/j.antiviral.2018.03.013.
25. Kaur R, Mudgal R, Narwal M, Tomar S. 2018. Development of an ELISA assay for screening inhibitors against divalent metal ion dependent alphavirus capping enzyme. Virus Res 256:209–218. https://doi.org/10.1016/j.virusres.2018.06.013.
26. LaPointe AT, Moreno-Contreras J, Sokoloski KJ. 2018. Increasing the capping efficiency of the Sindbis virus nsP1 protein negatively affects viral infection. mBio 9:e02342-18. https://doi.org/10.1128/mBio.02342-18.
27. Scholte FE, Tas A, Martina BE, Cordioli P, Narayanan K, Makino S, Snijder EJ, van Hemert MJ. 2013. Characterization of synthetic Chikungunya viruses based on the consensus sequence of recent E1-226V isolates. PLoS One 8:e71047. https://doi.org/10.1371/journal.pone.0071047.
28. Abdelnabi R, Amrun SN, Ng LF, Leyssen P, Neyts J, Delang L. 2017. Protein kinases C as potential host targets for the inhibition of chikungunya virus replication. Antiviral Res 139:79–87. https://doi.org/10.1016/j.antiviral.2016.12.020.
29. Moesslacher J, Battisti V, Delang L, Neyts J, Abdelnabi R, Pürstinger G, Urban E, Langer T. 5 May 2020. Identification of 2-(4-(phenylsulfonyl)piperazine-1-yl)pyrimidine analogues as novel inhibitors of chikungunya virus. ACS Med Chem Lett https://doi.org/10.1021/acsmedchemlett.9b00662.

3.3 Conclusion

In this publication, the antiviral profile of the CHVB series and their mechanism of action as inhibitors of the CHIKV capping machinery were reported [69].

The selected CHVB-resistant variant ($CHVB^{res}$) carried four mutations: two in the gene encoding nsP1 (responsible for viral RNA capping), one mutation in non-structural protein 2 (nsP2), and one in non-structural protein 3 (nsP3). Reverse genetics studies identified both nsP1 mutations (S454G and W456R) necessary to achieve approximately 18-fold resistance. Further, the S454G and W456R mutations in nsP1 resulted in the same level of resistance as the $CHVB^{res}$ variant with the two additional mutations on nsP2 and nsP3, suggesting that CHVB targets the viral mRNA capping.

Moreover, $CHVB^{res}$ was cross-resistant to the previously reported CHIKV capping inhibitors known as the MADTP series, indicating a similar mechanism of action [70, 73, 74]. The MADTP-resistant virus carried the P34S mutation in nsP1, whereas the CHVB-resistant viruses require at least two mutations. These data suggest a higher barrier of resistance for the CHVB series and, therefore, a less likely occurrence of development of clinical resistance, as two mutations are needed. Furthermore, the two mutations responsible for the CHVB-resistance tended to revert to wild type (wt) in conditions lacking the selective pressure.

Interestingly, similar to the MADTP series, the CHVB series is also CHIKV specific, with potent anti-CHIKV activities in all tested CHIKV isolates but with no or modest antiviral activity against other alphaviruses. This selectivity toward the CHIKV may result from the CHIKV characteristic of generating more capped viral genomes than other alphaviruses making the viral mRNA capping machinery an even more desirable target in developing a highly active CHIKV inhibitor.

In enzymatic assays, CHVB inhibited the methyltransferase (MTase) and guanylyltransferase (GTase) activities of alphavirus nsP1 proteins, demonstrating that the CHVB compounds directly inhibit the enzymatic activities of nsP1.

Chapter 4

Lead Optimisation and DMPK Profiling of the *CHVB Series*

4.1 Introduction

The following publication (further referred to as [65]) elaborates on the lead optimisation process performed with the CHVB series. As discussed in chapert 1, the final stage of the drug discovery phase aims to generate a possible drug candidate for clinical trials by maintaining the favourable properties of the generated lead compound while improving its shortcomings. Therefore, this publication focuses on preserving/enhancing the anti-CHIKV activity while reducing toxicological characteristics and improving metabolic stability and drug-like properties (e.g., aqueous solubility and lipophilicity).

In addition, an optimised and more versatile synthesis route (named Synthesis Route B) is described, which improved the accessibility of the designed analogues and the overall yield in remarkable shorter synthesis and work-up time. Overall, 100 analogues were synthesized, tested, and categorized according to their positioning of the nitrogens in the pyrimidine ring (P1/3, P3/5, and P1/5) and whether their scaffold has a sulfonamide or an amide. Further, additional assays to expand the knowledge about the antiviral profile of the CHVB series were conducted, and a successful scaffold hop for future antiviral research studies was carried out.

4.2 Design, Synthesis, and Lead Optimization of CHVB Series Analogues as Potent Small Molecule Inhibitors of Chikungunya Virus

Design, Synthesis, and Lead Optimisation of CHVB Series Analogues as Potent Small Molecule Inhibitors of Chikungunya Virus

Verena Battisti,[*,†] Julia Moesslacher,[‡,⊥] Rana Abdelnabi,[¶] Pieter Leyssen,[¶] Ana Lucia Rosales Rosas,[¶] Lana Langendries,[¶] Mohammed Aufy,[§] Christian Studenik,[§] Jadel Kratz,[∥,#] Judith M. Rollinger,[∥] Gerhard Puerstinger,[‡] Johan Neyts,[¶] Leen Delang,[¶] Ernst Urban,[†] and Thierry Langer[*,†]

†*Department of Pharmaceutical Sciences, Pharmaceutical Chemistry Division, University of Vienna, Josef-Holaubek-Platz 2, A-1090 Vienna, Austria*

‡*Department of Pharmacy, University of Innsbruck, Innrain 80/82, A-6020 Innsbruck, Austria*

¶*Department of Microbiology, Immunology and Transplantation, Rega Institute for Medical Research, Laboratory of Virology and Chemotherapy, Herestraat 49, B-3000 Leuven, Belgium*

§*Department of Pharmaceutical Sciences, Division of Pharmacology and Toxicology, University of Vienna, Josef-Holaubek-Platz 2, A-1090 Vienna, Austria*

∥*Department of Pharmaceutical Sciences, Division of Pharmacognosy, University of Vienna, Josef-Holaubek-Platz 2, A-1090 Vienna, Austria*

⊥*Current address: CURA Marketing GmbH, Dr. Franz-Werner-Straße 19, A-6020 Innsbruck, Austria*

#*Drugs for Neglected Diseases initiative (DNDi), 1202 Geneva, Switzerland*

E-mail: verena.battisti@univie.ac.at; thierry.langer@unive.ac.at

Abstract

The worldwide re-emerge of the Chikungunya virus (CHIKV), the high morbidity associated with it, and the lack of an available vaccine or antiviral treatment make the development of a potent CHIKV-inhibitor highly desirable. Therefore, an extensive lead optimisation was performed based on the previously reported CHVB compound **1b** and the reported synthesis route was optimised - improving the overall yield in remarkable shorter synthesis and work-up time. 100 CHVB analogues were designed, synthesised, and investigated for their antiviral activity, physiochemistry, and toxicological profile. An extensive structure-activity relationship study (SAR) was performed, which focused mainly on the combination of scaffold changes and revealed the key chemical features for a high anti-CHIKV inhibition. Further, to investigate the druggability of the compound series, a thorough ADMET investigation was carried out: the compounds were screened for their aqueous solubility, lipophilicity, their toxicity in CaCo-2 cells, and possible hERG channel interactions. Additionally, 55 analogues were assessed for their metabolic stability in human liver microsomes (HLMs) which led to a structure-metabolism relationship study (SMR). The compounds showed an excellent safety profile, favourable physicochemical characteristics, and the required metabolic stability. A cross-resistance study confirmed the viral capping machinery (nsP1) to be the viral target of these second-generation CHVB compounds. This study identified five compounds (**31b**, **31d**, **32d**, **34**, and **35d**) as potent, safe, and stable lead compounds for further development as selective CHIKV inhibitors - with **32d** as the most promising candidate. Finally, the collected insight led to a successful scaffold hop (**64b**) for future antiviral research studies.

Introduction

Chikungunya virus (CHIKV) is a mosquito-borne alphavirus (*Togaviridae* family), first isolated from a febrile patient in 1952/53 in the Makonde plateau in Tanzania.[1] After only local and periodic outbreaks, a variant of CHIKV containing the A226V mutation in the E1

glycoprotein gene led to its re-emerging in 2004 on the coast of Kenya - marking the beginning of the successful CHIKV spreading worldwide.[2] This new CHIKV mutation changed the vector potential from primarily *Aedes aegypti* to the more global *Ae. albopictus* and thus enabling the virus to spread in new temperature zones.[3]

Consequently, since then, CHIKV outbreaks have been reported frequently in countries worldwide, causing millions of CHIKV infections every year.[4–7] Moreover, due to globalization, climate change, and lack of immunity in the worldwide population, this rapid spread of CHIKV is not only ongoing, but it is also reaching new territories and higher numbers of infections every year.[7–9]

Patients suffering from Chikungunya Fever (CHIKF) develop a high onset of fever for three to ten days, followed by a rash, myalgia, and nausea.[9] In addition, severe joint pain leads to the characteristic posture, which is also described in the Makonde word *Chikungunya* for "that which bends you up".[10] Moreover, approximately 50 % of CHIKF-patients develop chronic symptoms like severe arthralgia and myalgia persisting for months to years even after clearance of the acute viral infection.[11] Further, complications in vulnerable groups (e.g., patients with comorbidities, the elderly) have been reported.[12] Despite the severity and rapid spreading of CHIKV, there are no licensed drugs or vaccines available, and the alleviation of symptoms by, e.g. NSAIDs, remains the only possible treatment for CHIKF patients.[13,14] Therefore, developing safe and potent anti-CHIKV small molecules is highly desirable.

We previously reported a novel series N-ethyl-6-methyl-2-(4-(4-fluorophenylsulfonyl)piperazine-1-yl)pyrimidine-4-amine **1a** analogues with good biological activity against the CHIKV: the CHVB series. A structure-activity relationship (SAR) study was performed by dividing the compound into five groups. This led to the identification of the new lead compound **1b** (see **Figure 1**).[15,16]

However, although **1b** showed an improved *in vitro* anti-CHIKV activity and enhanced toxicological profile, these properties could still be improved, and additional assays of cru-

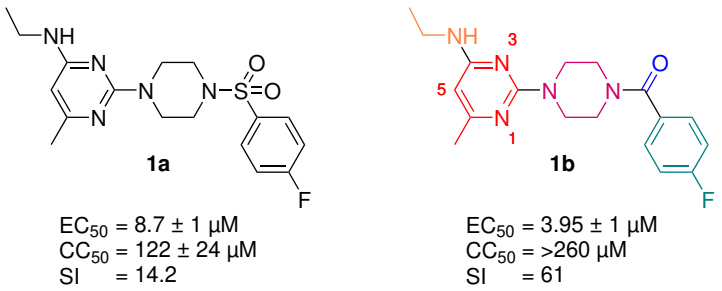

Figure 1. Structures of the first hit **1a** and the generated lead compound **1b** with their biological properties. The different colors of **1b** indicate the various groups of the CHVB series in which variations were performed and analyzed in the SAR studies. The described analogues were categorized according to their positioning of the nitrogens in the pyrimidine ring (P1/3, P3/5, and P1/5).

cial parameters in early drug design were missing. Therefore, a focused lead optimization based on the 2-(4-(phenylsulfonyl)piperazine-1-yl)pyrimidine scaffold was made to identify a CHVB analogue with enhanced antiviral activity, reduced toxicity, higher stability, and improved drug-like properties. For better accessibility of the designed analogues, an additional optimized synthesis route (Synthesis Route B) was established, and the overall 100 investigated analogues were categorized according to their positioning of the nitrogens in the pyrimidine ring (P1/3, P3/5, and P1/5).

Results and Discussion

Chemistry. **Scheme 1** depicts the established synthesis route (Synthesis Route A) for the synthesis of the 2-(4-phenylsulfonyl)piperazine-1-yl)pyrimidine analogues – also known as the CHVB series. The key intermediate **3a** was prepared via substitution reaction between 2,4-dichloro-6-methylpyrimidine **8a** and ethylamine and further reacted with tert-butyl-piperazine-1-carboxylate **2** under microwave conditions (**Scheme 2**). After deprotection of the piperazine, the desired compound **1b** was obtained via amidation.[15]

An easy and fast synthesis route was searched for the detailed investigation of the pyrimidine and ethylamine side chain. Therefore, Synthesis Route B was established, starting with the nucleophilic acyl substitution between the unprotected amino group of the Boc-protected

Scheme 1. Overview of possible synthesis routes for the lead compound 1b.[a]

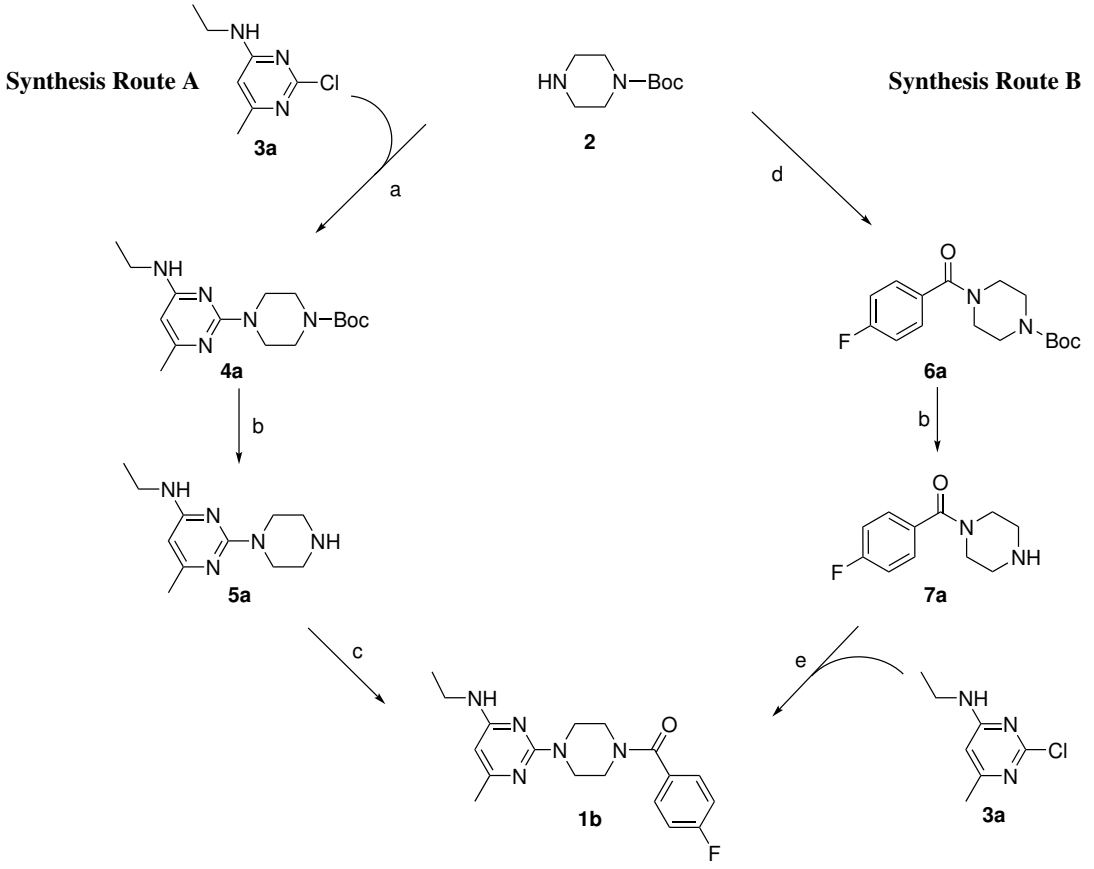

[a]Reagents and conditions: (a) EtOH, µwave, 30 min, 155 °C, 250 W, 12 bar (b) HCl/TFA, THF, 1 to 24 h, rt; (c) DCM, $N(CH_2CH_3)_3$, 24 h, rt, 4-fluorobenzenesulfonyl chloride; (d) pyridine, DMAP, 0 °C-rt, 15 h, 4-fluorobenzoyl chloride; (e) EtOH, DIPEA, µwave, 30 min, 155 °C, 250 W, 12 bar.

piperazine **2** and benzoyl chlorides. This reaction route enables synthesising significant variations on the desired pyrimidine and side-chain group of the compound series – as the modifications are introduced in the last and not the first step of the synthesis route. Furthermore, shortened reaction times, more accessible and sometimes unnecessary purification steps, and higher-yielding reactions lead to remarkable time- and yield-wise advantages to the published Synthesis Route A. Therefore, Synthesis Route B was subsequently used to synthesise all following analogues.

Synthesis Route B starts with a nucleophilic acyl substitution between Boc-protected piperazine and benzoyl chloride in pyridine with catalytic quantities of additional 4-dimethylaminopyridine (DMAP). The intermediate tert-butyl 4-(4-fluorobenzoyl)piperazine-

Scheme 2. Synthesis of the key intermediates 3a-h and 9a-h.[a]

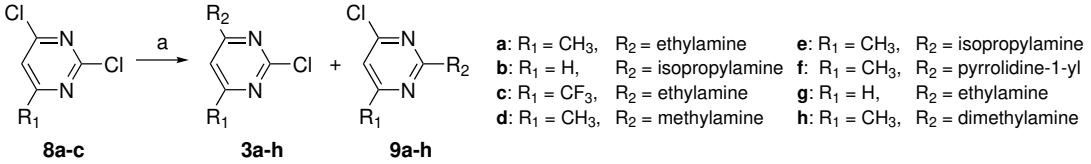

[a]Reagents and conditions: (a) Synthesis Route A: EtOH, 24 to 48 h, rt; Synthesis Route B: THF, 14 h, 0 °C-rt.

1-carboxylate **6a** precipitates in excellent yield while pouring the crude mixture on ice – facilitating the purification as the formed side products are water-soluble. Moreover, the following Boc-deprotection with trifluoroacetic acid (TFA) or hydrochloric acid (HCl) can also be performed without any purification step, which shortens the synthesis time by avoiding the time-consuming and challenging purification steps and increases the overall yield. This synthesis route's fourth and last step is the substitution reaction of the prepared arylamine **3a** and the de-protected piperazine intermediate **7a** under microwave irradiation in dry EtOH. The Hünig's base N,N-diisopropylethylamine (DIPEA), was introduced to this reaction as a proton scavenger. In addition, the solvent of the arylamine synthesis by amination of the commercially available 2,4-dichloropyrimidines shown in **Scheme 2** was changed from dry ethanol (EtOH) to dry Tetrahydrofuran (THF) – shifting the yield of 2-chloro-pyrimidin-4-amine **3a-h** to the much more desired 4-chloro-pyrimidin-2-amine **9a-h**.

Scheme 3 and **Scheme 4** outline the synthesis of 2-(piperazin-1-yl)pyrimidine **5a-d** and 4-(piperazin-1-yl)pyrimidine **21a-e** intermediates via Synthesis Route A. The reaction of these intermediates is essential for the synthesis of **1b** analogues - designed to carefully investigate the effects of various substitutions on both aromatic groups of an amide or sulfonamide bridge and their numerous combinations. The preparation of **2** was carried out similar to the published procedure of Moussa et al..[17]

13 was synthesized directly from the purchased 2-(piperazin-1-yl)pyrimidine **5e** and 4-fluorobenzenesulfonyl chloride in one step. To investigate the importance of a carbonyl- or sulfonyl-linker, analogue **23** with a methyl-4-fluorobenzene group was synthesized via Synthesis Route A using 1-(chloromethyl)-4-fluorobenzene. Similarly, to explore the precise

Scheme 3. Synthesis Route A for synthesis of compounds with a P1/3 pyrimidine nitrogen position (10a-19).[a]

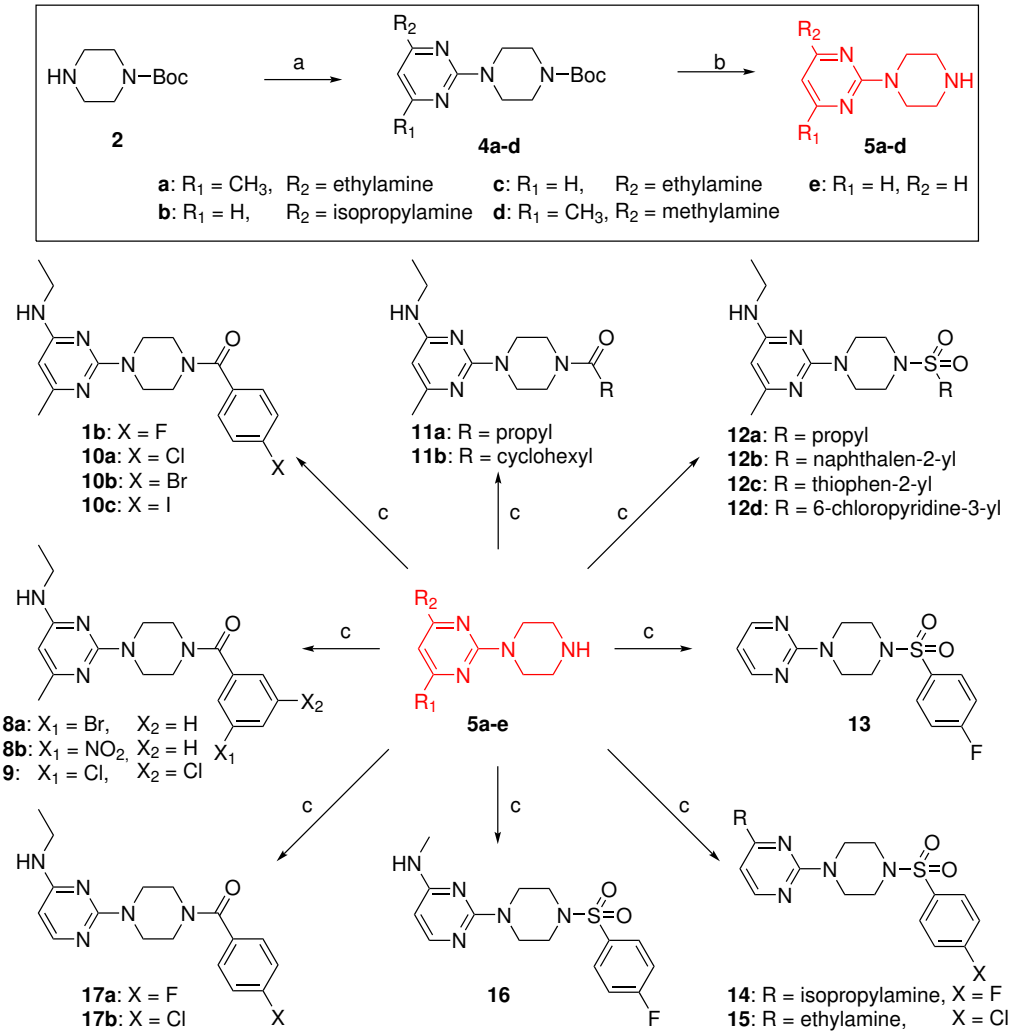

[a]Reagents and conditions: (a) EtOH, µwave, 30 min, 155 °C, 250 W, 12 bar, **8a**; (b) HCl, THF, 24 h, rt; (c) DCM, $N(CH_2CH_3)_3$, 24 h, rt, benzenesulfonyl chloride/benzoyl chloride. Key intermediates **4a-d** are highlighted in red.

role of the nitrogens and their position in the pyrimidine ring analogue N-ethyl-6-(4-((4-fluorophenyl)sulfonyl)piperazin-1-yl)pyrimidin-4-amine **39** was prepared to deploy the same reaction conditions from Synthesis Route A with 6-chloro-N-ethylpyrimidin-4-amine **36** (see Supporting Information, **Scheme S1**).

Scheme 5 depicts the synthesis of pyrimidine and side-chain analogues of our compound series using the versatile Synthesis Route B. The acylation of the Boc-protected piperazine with neat benzoyl chlorides to form monosubstituted amide products **6a-f** was carried out

Scheme 4. Synthesis Route A for synthesis of compounds with a P3/5 pyrimidine nitrogen position (22-35d).[a]

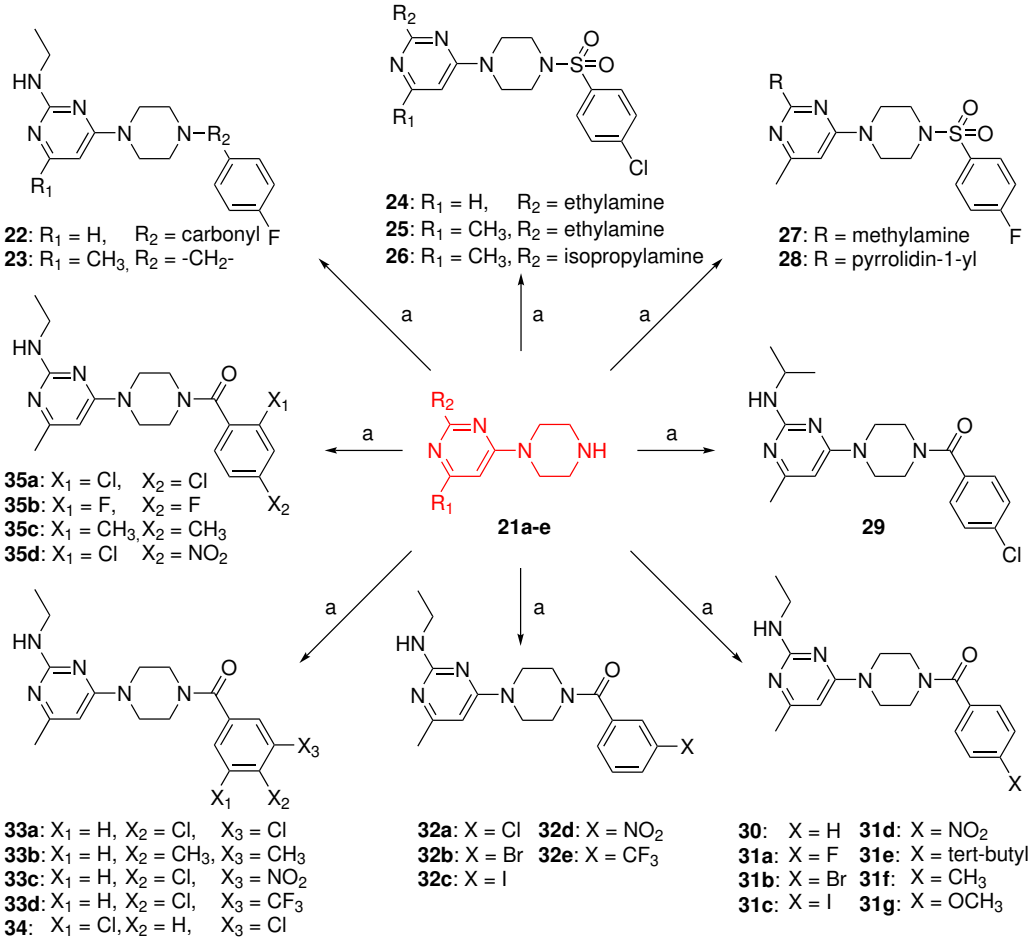

[a]Reagents and conditions: (a) DCM, $N(CH_2CH_3)_3$, 24 h, rt, benzenesulfonyl chloride/benzoyl chloride/1-(chloromethyl)-4-fluorobenzene. Key intermediates **21a-e** are shown in red.

in pyridine under basic conditions. DMAP was employed as a strong nucleophilic catalyst. After deprotection of the piperazine-nitrogen, the coupling of the aryl halide (**3a-h**, **9a-h**) with the secondary amine of **7a-f** was performed under microwave irradiation (250 W) and pressure (12 bar) for 30 min while heated to 100 °C.

The synthesis of the intermediate **51**, which is used to form the analogues **52a** and **52b**, is shown in **Scheme 6**. Commercially available 5-amino-4,6-dichloro-2-methylpyrimidine

Scheme 5. Synthesis Route B for synthesis of pyrimidine and side-chain analogues (40a-48).[a]

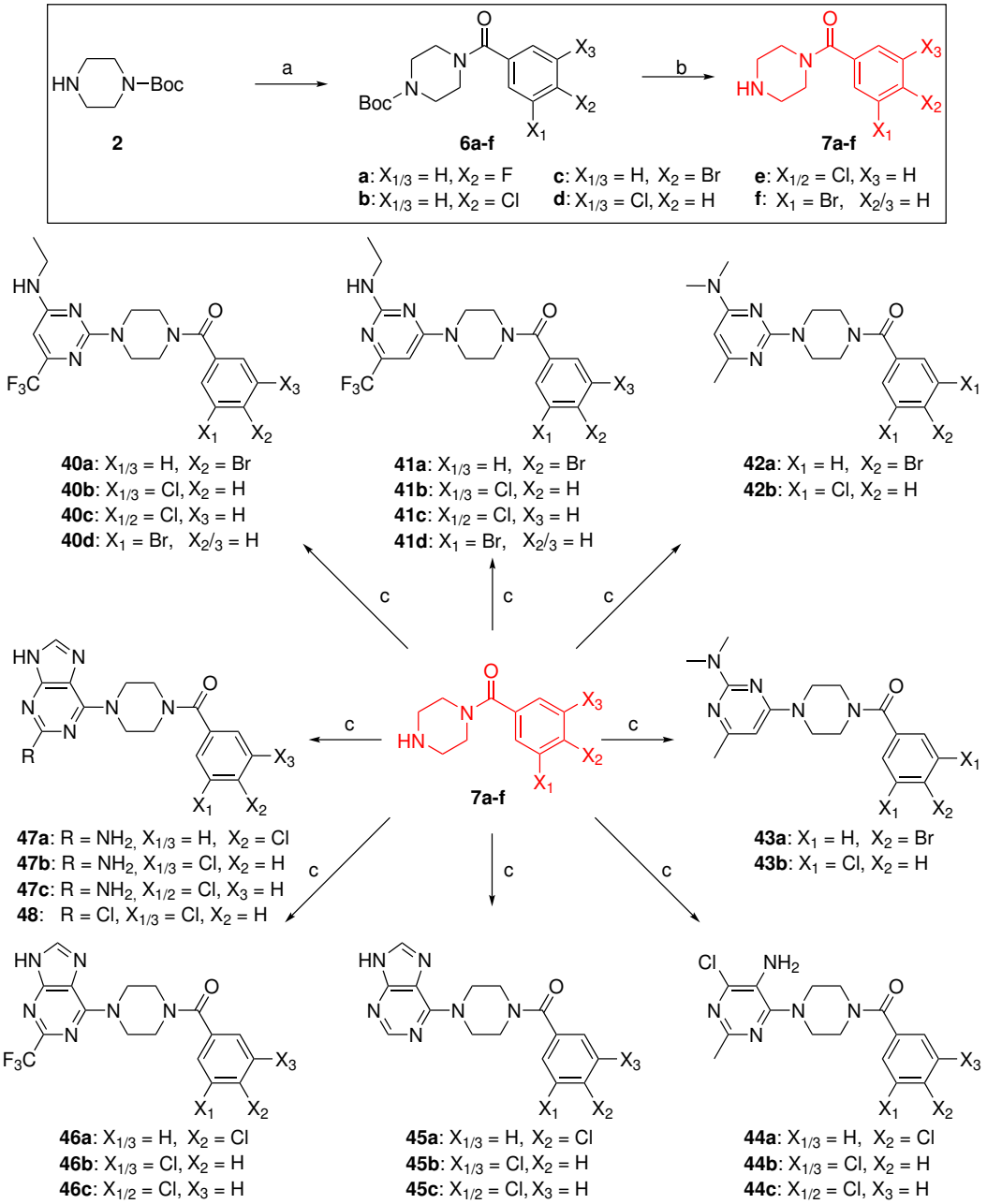

[a]Reagents and conditions: (a) pyridine, DMAP, 0 °C-rt, 15 h, benzoyl chloride; (b) TFA, THF, 1 to 15 h, rt; (c) EtOH, DIPEA, µwave, 30 min, 155 °C, 250 W, 12 bar, aryl halide. Key intermediates **6a-f** are highlighted in red.

Scheme 6. Synthesis of compound (52a-b).[a]

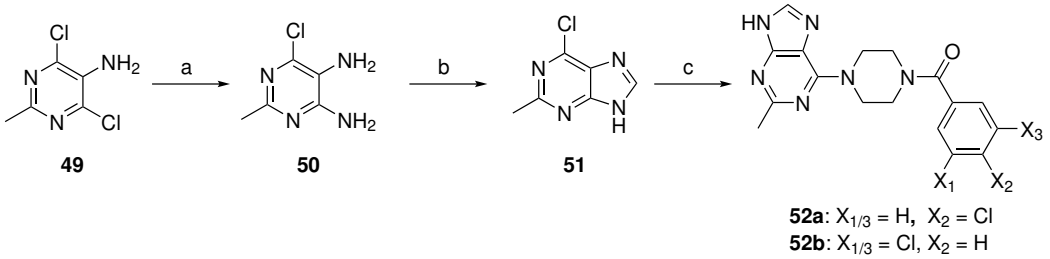

[a]Reagents and conditions: (a) conc. NH_3, 120 °C, 24 h; (b) TEOF, FA, 5.5 h, 120 °C; (c) EtOH, DIPEA, µwave, 30 min, 155 °C, 250 W, 12 bar.

49 was converted to 4,5-diamino-6-chloro-2-methyl-pyrimidine **50** via amination of the aryl halide with concentrated NH_3 at 120 °C.[18] Treatment with formic acid (FA) and triethyl orthoformate (TOFA) afforded the intermediate **51** via Traube purine synthesis.[18]

To investigate the importance of the piperazine and to confirm the previous results published earlier, which indicate that the piperazine functions solely as a linker between the two more critical aromatic parts of the compound series, a set of piperazine-analogues was designed and synthesized applying Synthesis Route B (**Scheme 7**). Similarly, the reaction between the commercially available spiro[chromane-2,4'-piperidin]-4-one **63** and the pyrimidine intermediates **3a** and **9a** afforded **64a** and **64b**, respectively (**Scheme 8**).

Structure-Activity Relationship Study. This structure-activity relationship (SAR) study focused mainly on the combination of scaffold changes. All 100 final compounds were evaluated for their inhibitory activity against the Chikungunya virus via virus cell-based CPE reduction assay in Vero cells, and their results are summarised in **Table 1-5**. As stated by Moesslacher et al., the nitrogen positions on the pyrimidine ring can positively impact the antiviral activity.[15] From all studied nitrogen positions on the pyrimidine ring, the position P3/5 gave the best antiviral result ($EC_{50} = 3.2 \pm 0.2$ µM). Surprisingly, when combined with other alterations, the activity got lost.[15] To further investigate these unexpected results and to find a combination of the promising nitrogen positions, 100 P1/3,

Scheme 7. Synthesis Route B for the synthesis of piperazine analogues (55a-62d).[a]

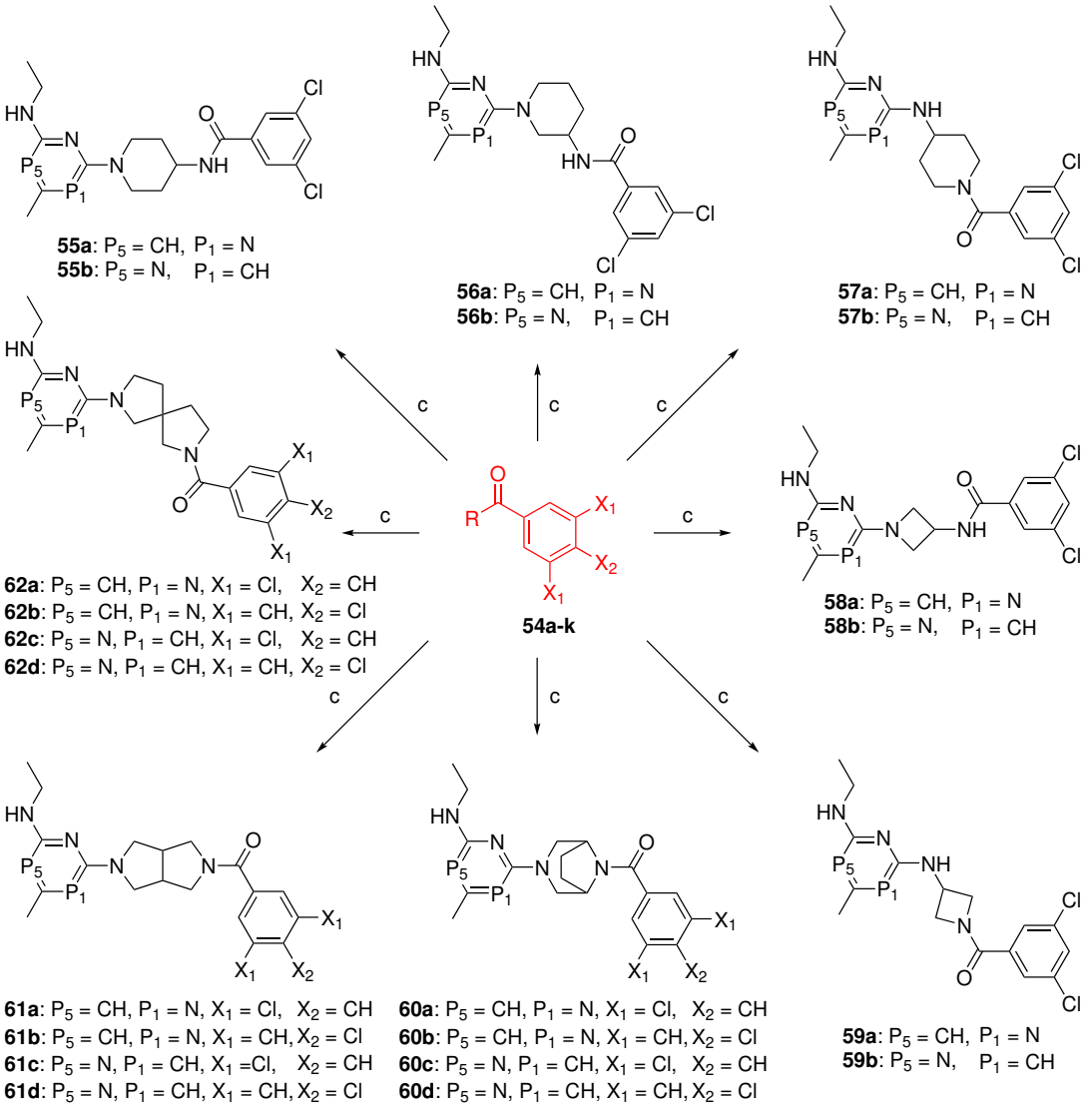

[a]Reagents and conditions: (a) EtOH, DIPEA, µwave, 30 min, 155 °C, 250 W, 12 bar, aryl halide. Key intermediates **54a-k** are highlighted in red and are synthesized according to Synthesis Route B.

P3/5 and P1/ 5 analogues were analyzed – focusing on different alterations alone and in combination (with/without/substituted methyl group; ethylamine/smaller or larger sidechains; sulfonamide/amide/methylene; various phenyl-substitutions on different positions).

Pyrimidine Nitrogen Position 1/3 Scaffold. First, the impact of various functional groups was investigated by replacing them with different classical and non-classical bioisosteres and by testing analogues without them. Therefore, the influence of the phenyl

Scheme 8. Synthesis of compound (64a-b).[a]

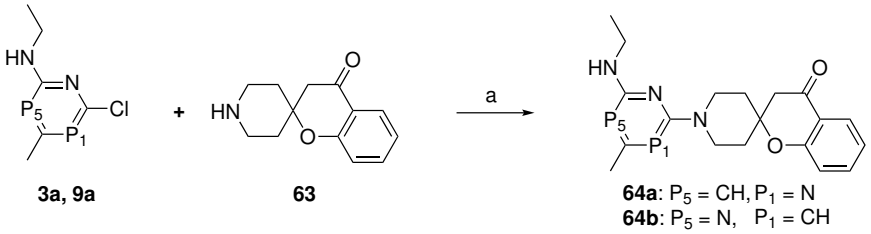

3a, 9a **63**

64a: P_5 = CH, P_1 = N
64b: P_5 = N, P_1 = CH

[a] Reagents and conditions: (a) EtOH, DIPEA, µwave, 30 min, 155 °C, 250 W, 12 bar.

Table 1. Antiviral activity and ADME properties of sulfonamide analogues 12a-16 (P1/3 scaffold) and with 23-28 (P3/5 scaffold).[a]

Compounds[b]	EC_{50} (µM)[f]	CC_{50} (µM)[g]	SI[h]	Half-Life (min)[i]	Aq. Sol. (pH 7.4; µM)[j]	$cLogD_{pH\ 7.4}$[k]
12a[c]	70 ± 18	n.d.	n.d.		>120	2.93
12b[c]	10 ± 0.4	17 ± 3.8	1.7	20 ± 0.6	90 ± 22	3.53
12c[c]	103	180	1.8		68 ± 11.5	3.11
12d[c]	121	97	0.8		115 ± 1.1	2.81
13[c]	310	n.d.	n.d.		64 ± 14	2.40
14[c]	10 ± 1.2	n.d.	n.d.	46 ± 1.2	100 ± 13	3.41
15[c]	10 ± 3.1	28 ± 23	2.7	19 ± 0.78	94 ± 37	3.33
16[c]	9.6 ± 0.23	193 ± 11	20	48 ± 4.5	>120	3.02
23[c,d]	22 ± 24	46 ± 47	2.1	78 ± 5.5	106 ± 15	3.35
24[e]	16 ± 3.7	44 ± 6.6	2.7	62 ± 8.6	95 ± 5	3.33
25[e]	2.8	11 ± 3.1	3.9	49 ± 2.6	104 ± 22	3.44
26[e]	3.8 ± 1.07	19 ± 4.2	4.9	54 ± 3.5	76 ± 15	3.62
27[e]	11 ± 0.94	99 ± 35	9.2	226 ± 13	>120	2.93
28[e]	25 ± 7	47 ± 21	1.9		>120	3.44

(a) Data represent mean values ± SD from at least three independent experiments. ND - not detectable. (b) Compounds synthesized according to Synthesis Route A. (c) Compounds with a P1/3 scaffold. (d) Compound with a methylene scaffold. (e) Compounds with a P3/5 scaffold. (f) The 50 % effective concentration (EC_{50}) is the concentration of compound that is required to inhibit virus-induced cell death by 50 %. (g) The 50 % cytostatic/cytotoxic concentration (CC_{50}) is the concentration of compound that reduces the overall metabolic activity of the uninfected, compound-treated cells by 50 % as compared to the untreated, uninfected cell. (h) The selectivity index (SI) is the ration between CC_{50} and EC_{50}. (i) The half-life (min) in human liver microsomes with 60 min incubation is estimated from the slope of the initial linear range of the logarithmic curve of compound remaining (%) vs time, assuming the first-order kinetics. (j) The aqueous solubility ($pH_{7.4}$) is measured by HPLC and calculated by the AUC (Absorbance Unit under the Curve) values of the buffered samples divided by the AUC values of the control samples. (k) clogD is calculated by the Graph Neural Network D-GIN [19]

was examined with different aliphatic and (hetero)aromatic replacements (**11a-b** and **12a-d**) in combination with an amide or sulfonamide linker. None of the tested analogues showed any antiviral activity (see **Table 1-2**). Similar, **13** - missing the ethylamine and the methyl group on the pyrimidine ring - showed no antiviral activity at all - underlying the importance of the two aliphatic groups on the pyrimidine ring.

To further explore the impact of the methyl group, various analogues with scaffold modifications combined with a missing methyl group were designed and tested for antiviral activity. Neither of these analogues gave any advantage on the viral activity (**15** and **17a-b**). In-

Table 2. Antiviral activity and ADME properties of P1/3 nitrogen and amide scaffold analogues.[a]

Compounds	EC_{50} (µM)[d]	CC_{50} (µM)[e]	SI[f]	Half-Life (min)[g]	Aq. Sol. (pH 7.4 µM)[h]	$cLogD_{pH\ 7.4}$[i]
10a[b]	2.4	89 ± 10	37	148 ± 13	>120	3.30
10b[b]	9.6	>100	10	91 ± 2.2	116 ± 6	3.25
10c[b]	2.9	>100	34	76 ± 3.8	116 ± 2.8	2.91
11a[b]	67	n.d.	n.d.		>120	2.64
11b[b]	70 ± 6	147 ± 61	2.1		119 ± 1	3.30
17a[b]	3.9 ± 1.5	183 ± 42	47	328 ± 6	>120	3.01
17b[b]	15 ± 3.7	47 ± 24	3.1	137 ± 25	>120	3.19
18a[b]	5.1 ± 1.7	>100	20	9.5 ± 0.57	>120	3.28
18b[b]	4.2 ± 1.9	>100	24	57 ± 1.5	119 ± 1.20	2.87
19[b]	67	>100	1.5		11	3.52
40a[c]	>6.3	>25	4	56 ± 3	1.2	3.66
40b[c]	>6.3	>25	4	18 ± 1.2	3.5	3.81
40c[c]	>6.3	>25	4	36 ± 0.7	0	3.80
40d[c]	41 ± 19	n.d.	n.d.	17 ± 1.2	0.80	3.68
42a[c]	13	76	6.02	29 ± 1.5	114 ± 8.6	3.28
42b[c]	>100	>100	1		95 ± 1.4	3.51

(a) Data represent mean values ± SD from at least three independent experiments. ND - not detectable. (b) Compounds synthesized according to Synthesis Route A. (c) Compounds synthesized according to Synthesis Route B. (d) The 50 % effective concentration (EC_{50}) is the concentration of compound that is required to inhibit virus-induced cell death by 50 %. (e) The 50 % cytostatic/cytotoxic concentration (CC_{50}) is the concentration of compound that reduces the overall metabolic activity of the uninfected, compound-treated cells by 50 % as compared to the untreated, uninfected cell. (f) The selectivity index (SI) is the ration between CC_{50} and EC_{50}. (g) The half-life (min) in human liver microsomes with 60 min incubation is estimated from the slope of the initial linear range of the logarithmic curve of compound remaining (%) vs time, assuming the first-order kinetics. (h) The aqueous solubility ($pH_{7.4}$) is measured by HPLC and calculated by the AUC (Absorbance Unit under the Curve) values of the buffered samples divided by the AUC values of the control samples. (i) clogD is calculated by the Graph Neural Network D-GIN [19]

terestingly, combined with the bigger and flexible side chain isopropylamine, the missing methyl group in **14** had no impact on the antiviral activity (EC_{50} = 10.6 µM). Moreover, the shortened methylamine side-chain gave a similar good antiviral activity (**16**, EC_{50} = 9.62 µM, see **Table 1-2**).

In addition, other substitution patterns and different rests on the phenyl were tested for their antiviral impact. Therefore, **10a-c** with different halogen substitutions on the para position were synthesized. The chloride and iodide substitution showed good antiviral activity (EC_{50} of 2.4 and 2.9 µM), whereas the bromide analogue **10b** remained active but with a declined activity (EC_{50} = 9.58 µM). Interestingly, the shift of the bromide from the para to the meta position in **18a** improved the antiviral activity to an EC_{50} value of 5.11 µM. On the other hand, the di-para halogen substituted analogue **19** showed no antiviral activity (see **Table 2**).

Pyrimidine Nitrogen Position 3/5 Scaffold. The biological data of the compounds bearing a P3/5 scaffold is shown in **Table 1**, **3**, and **5**. First, the impact of the methyl

Table 3. Antiviral activity and ADME properties of P3/5 nitrogen and amide scaffold analogues.[a]

Compounds	EC_{50} (µM)[d]	CC_{50} (µM)[e]	SI[f]	Half-Life (min)[g]	Aq. Sol. (pH 7.4 µg)[h]	$cLogD_{pH\ 7.4}$[i]
22[b]	216 ± 7.1	>304	1.4		>120	2.99
29[b]	18 ± 5.4	46 ± 15	2.6	176 ± 30	115 ± 6.5	3.43
30[b]	2.05 ± 1.1	>308	150	329 ± 119	>120	2.43
31a[b]	1.5 ± 0.84	165 ± 28	109	388 ± 5	>120	3.00
31b[b]	0.6 ± 0.08	>96	159	192 ± 28	>120	3.22
31c[b]	0.7 ± 0.28	58 ± 17	82	148 ± 2	112 ± 11	2.84
31d[b]	0.91 ± 0.18	>100	110	3536 ± 528	>120	2.81
31e[b]	2.4 ± 0.45	45	19	92 ± 7	120 ± 0.28	3.81
31f[b]	2.4 ± 0.25	203 ± 79	84	458 ± 195	>120	3.21
31g[b]	1.4 ± 0.07	136 ± 130	97	584 ± 77	>120	2.70
32a[b]	6.6 ± 0.79	248	38	93 ± 5	>120	3.29
32b[b]	0.94 ± 0.03	>100	107	74 ± 2	>120	3.25
32c[b]	1	>100	98	42 ± 3	>120	2.89
32d[b]	0.7 ± 0.05	>100	143	391 ± 140	>120	2.83
32e[b]	1.3 ± 0.18	80	60	91 ± 19	>120	3.51
33a[b]	0.57	46 ± 12	81	94 ± 9.4	111 ± 12.8	3.51
33b[b]	0.95 ± 0.46	65	68	123 ± 35	118 ± 2.6	3.42
33c[b]	0.98 ± 0.06	>20	20	187 ± 24	>120	3.07
33d[b]	1.9 ± 0.41	>20	11	75 ± 17	101 ± 12	3.69
34[b]	0.47 ± 0.06	80	173	90 ± 18	108 ± 17	3.49
35a[b]	>100	47	0.47		>120	3.38
35b[b]	>100	>100	>1		n.d.	2.92
35c[b]	>100	>100	>1		n.d.	2.93
35d[b]	>0.78	>100	128	204 ± 4	111 ± 13	3.09
41a[c]	>100	>100	1		33 ± 1.6	3.66
41b[c]	>12.5	>50	4	29 ± 1.6	2 ± 1.7	3.83
41c[c]	>100	>100	1		0	3.83
41d[c]	100	>100	1		n.d.	3.78
43a[c]	6.6	>100	15	108 ± 14	>120	3.28
43b[c]	4.4	67	15	108 ± 1.1	109 ± 2.1	3.51

(a) Data represent mean values ± SD from at least three independent experiments. ND - not detectable. (b) Compounds synthesized according to Synthesis Route A. (c) Compounds synthesized according to Synthesis Route B. (d) The 50 % effective concentration (EC_{50}) is the concentration of compound that is required to inhibit virus-induced cell death by 50 %. (e) The 50 % cytostatic/cytotoxic concentration (CC_{50}) is the concentration of compound that reduces the overall metabolic activity of the uninfected, compound-treated cells by 50 % as compared to the untreated, uninfected cell. (f) The selectivity index (SI) is the ration between CC_{50} and EC_{50}. (g) The half-life (min) in human liver microsomes with 60 min incubation is estimated from the slope of the initial linear range of the logarithmic curve of compound remaining (%) vs time, assuming the first-order kinetics. (h) The aqueous solubility ($pH_{7.4}$) is measured by HPLC and calculated by the AUC (Absorbance Unit under the Curve) values of the buffered samples divided by the AUC values of the control samples. (i) clogD is calculated by the Graph Neural Network D-GIN [19]

group regarding the anti-CHIKV-activity was investigated. Therefore, compounds without the methyl group and the P3/5 variation were designed and subsequently compared with the corresponding methylated analogues for their biological activity. In line with the results discussed above, all the un-methylated compounds showed a much higher EC_{50} value (**24** with EC_{50} = 15.9 µM vs. **25** with EC_{50} = 2.76 µM) or even a loss of activity (**22** with EC_{50} = 216 µM vs. **31a** with EC_{50} = 1.52 µM). Interestingly, compared to the corresponding

Table 4. Antiviral activity and ADME properties of P1/5 nitrogen and/or purine scaffold analogues.[a]

Compounds[b]	EC_{50} (µM)[c]	CC_{50} (µM)[d]	SI[e]	Half-Life (min)[f]	Aq. Sol. (pH 7.4 µg)[g]	$cLogD_{pH\ 7.4}$[h]
39	>274	n.d.	n.d.		94 ± 12	3.20
44a	>88	>88	>1		n.d.	2.41
44b	32 ± 0.7	n.d.	n.d.		94 ± 8	3.16
44c	9.8 ± 0.35	n.d.	n.d.	128 ± 3.3	118 ± 3	3.15
45a	94 ± 2	n.d.	n.d.		114 ± 5	2.60
45b	32 ± 3.7	n.d.	n.d.		112 ± 0.4	3.17
45c	66 ± 6.5	n.d.	n.d.		104 ± 13	3.00
46a	26 ± 0.06	n.d.	n.d.		36 ± 2.1	3.39
46b	77	n.d.	n.d.		73 ± 16	3.55
46c	9.5 ± 0.39	n.d.	n.d.	120 ± 16	71 ± 13	3.44
47a	>100	n.d.	n.d.		116 ± 3.7	2.56
47b	>100	n.d.	n.d.		47 ± 12	2.81
47c	>100	n.d.	n.d.		106 ± 17	2.71
48	18 ± 2.8	n.d.	n.d.	142 ± 1.8	66 ± 6.5	3.30
52a	97 ± 0.47	n.d.	n.d.		84 ± 51	2.56
52b	>100	n.d.	n.d.		92 ± 22	3.21

(a) Data represent mean values ± SD from at least three independent experiments. ND - not detectable. (b) Compounds synthesized according to Synthesis Route B. (c) The 50 % effective concentration (EC_{50}) is the concentration of compound that is required to inhibit virus-induced cell death by 50 %. (d) The 50 % cytostatic/cytotoxic concentration (CC_{50}) is the concentration of compound that reduces the overall metabolic activity of the uninfected, compound-treated cells by 50 % as compared to the untreated, uninfected cell. (e) The selectivity index (SI) is the ration between CC_{50} and EC_{50}. (f) The half-life (min) in human liver microsomes with 60 min incubation is estimated from the slope of the initial linear range of the logarithmic curve of compound remaining (%) vs time, assuming the first-order kinetics. (g) The aqueous solubility ($pH_{7.4}$) is measured by HPLC and calculated by the AUC (Absorbance Unit under the Curve) values of the buffered samples divided by the AUC values of the control samples. (h) clogD is calculated by the Graph Neural Network D-GIN [19]

analogue **17a** with the pyrimidine nitrogen pattern P1/3 and an EC_{50} value of 3.89 µM, the missing methyl group had a much greater impact on the inactive **22** – indicating that the P3/5 nitrogen position is much more sensitive to the presence of the methyl group. Further, also the nitrogen position P1/5 seems to be affected by the missing methyl group as **39** demonstrated no antiviral activity.

Notably, analogues bearing a CF_3 with a similar size but higher lipophilicity than the replaced methylgroup exhibit low activity (**41a-d**) - whereas in the case of P1/3 pyrimidine analogues, no activity was observed (**40a-c**; except of **40d** with weak antiviral activity of $EC_{50} = 40.95 \pm 19.33$ µM).

Subsequently, different ethylamine replacements were tested to investigate the requirements (i.e., lipophilic, H-bonding, or steric requirements/limitations) for antiviral activity combined with the P3/5 nitrogen shift. Two analogues with various lengths and steric requirements were prepared and evaluated to examine the influence of different steric sizes (**Table 1** and **3**). The bulkier and more rigid pyrrolidine replacement **28** showed almost

Table 5. Antiviral activity and ADME properties of piperazine bioisostere scaffold analogues.[a]

Compounds[b]	EC_{50} (µM)[e]	CC_{50} (µM)[f]	SI[g]	Half-Life (min)[h]	Aq. Sol. (pH 7.4 µg)[i]	$cLogD_{pH\ 7.4}$[j]
55a[c]	>100	48	0.48		52 ± 29	3.56
55b[d]	>25	>100	4		100 ± 28	3.53
56a[c]	>25	49	1.95		31 ± 26	3.59
56b[d]	>100	12	0.12	44 ± 0.28	22 ± 1.6	3.57
57a[c]	12	25	2.02	30 ± 0.71	94 ± 3	3.15
57b[d]	14	47	3.4	78 ± 10	101 ± 2.6	3.17
58a[c]	>88	n.d.	n.d.		47 ± 7.6	3.28
58b[d]	>100	n.d.	n.d.		81 ± 0.92	3.27
59a[c]	>100	n.d.	n.d.		93 ± 1.6	3.30
59b[d]	8.5 ± 0.52	n.d.	n.d.	37 ± 1.8	104 ± 5	3.30
60a[c]	>100	n.d.	n.d.		97 ± 19	3.45
60b[c]	79 ± 14	>88	1.11		n.d.	3.21
60c[d]	14 ± 1.9	n.d.	n.d.	85 ± 0.57	111 ± 13	3.42
60d[d]	17 ± 3.4	84 ± 9.9	5		n.d.	3.19
61a[c]	23 ± 1.9	n.d.	n.d.		108 ± 15	3.34
61b[c]	12 ± 1.3	>88	7.5		n.d.	3.09
61c[d]	19 ± 1.7	n.d.	n.d.	64 ± 6.2	109 ± 5.1	3.35
61d[d]	3.2 ± 0.28	72 ± 6	23		n.d.	3.09
62a[c]	28 ± 1.5	n.d.	n.d.		108 ± 18	3.42
62b[c]	32 ± 3.8	74	2.3		n.d.	3.17
62c[d]	11 ± 0.33	n.d.	n.d.	74 ± 12	98 ± 3	3.40
62d[d]	18 ± 2.1	45 ± 1.7	2.5		n.d.	3.17
64a[c]	23 ± 4	n.d.	n.d.		100 ± 3	2.61
64b[d]	4.2 ± 0.15	n.d.	n.d.	91 ± 5	98 ± 8	2.49

(a) Data represent mean values ± SD from at least three independent experiments. ND - not detectable. (b) Compounds synthesized according to Synthesis Route B. (c) Compounds with a P1/3 scaffold. (d) Compounds with a P3/5 scaffold. (e) The 50 % effective concentration (EC_{50}) is the concentration of compound that is required to inhibit virus-induced cell death by 50 %. (f) The 50 % cytostatic/cytotoxic concentration (CC_{50}) is the concentration of compound that reduces the overall metabolic activity of the uninfected, compound-treated cells by 50 % as compared to the untreated, uninfected cell. (g) The selectivity index (SI) is the ration between CC_{50} and EC_{50}. (h) The half-life (min) in human liver microsomes with 60 min incubation is estimated from the slope of the initial linear range of the logarithmic curve of compound remaining (%) vs time, assuming the first-order kinetics. (i) The aqueous solubility ($pH_{7.4}$) is measured by HPLC and calculated by the AUC (Absorbance Unit under the Curve) values of the buffered samples divided by the AUC values of the control samples. (j) clogD is calculated by the Graph Neural Network D-GIN [19]

no antiviral activity against the CHIKV, whereas the shortened methylamine counterpart **27** was still active. Based on these findings, further analogues with shorter side chains but without H-bonding capability were investigated. Compared to their ethylamine counterparts **31b** and **34** a 10-fold loss of activity was observed within the nitrogen P3/5 dimethylamine-analogues **43a-b**, respectively. Moreover, combined with the original nitrogen positions (P1/3), the dimethylamine variation led to a loss of activity in **42b** (**Table 2**). Further, a small set of analogues without the hydrogen bond capability of the ethylamine (replaced by chloride) and a primary amine on position 3 showed no gain of activity (**44a-c** with the lowest EC_{50} value of 9.84 ± 0.35 µM of **44c**; **Table 4**), thus supporting our former results that the hydrogen bond donor (HBD) is not essential, but its pure absence seems to decrease

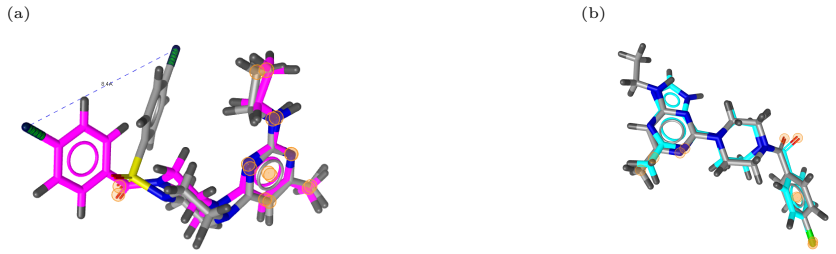

Figure 2. Minimum energy conformations after MMFF94 energy minimisation until the local minimum was reached and following alignment. (a) An example illustrating the conformational effects of amide replacement and the torsional angle difference of sulfonamide and amide scaffold.; the sulfonamide **25** (grey) shows a significant difference in structural conformation compared to the corresponding amide analogue (violet). (b) Alignment of purine-modified analogue to CHVB-compound series showing the conformational similarity of the purine-modified compound (blue) and the corresponding CHVB scaffold (grey) - resulting in similar relative positions of critical functional groups.

---

the activity.[15] Nevertheless, the possibility to replace the ethylamine with the bifurcated isopropylamine also holds true for the P3/5 nitrogen scaffold as analogue **26** gave similar antiviral results as its comparable ethylamine compound **25** (EC_{50} = 3.84 and 2.76 µM). On the other hand, the additional conversion of the sulfonamide to the amide linker in **29** resulted in an almost 6-fold decrease in activity.

Moesslacher et al. reported that the sulfonamide replacement by an amide linker enhances the activity twofold, while the methylene variation results in even more active albeit cytotoxic analogues.[15] This also holds true for most of the new designed analogues except the ones with altered or omitted pyrimidine side chains i.e. the methyl and ethylamine (e.g., **26** vs. **29**, or **15** vs. **17b**). This considerable difference in potency between the sulfonamide and its replacements (amide and methylene) may not only be the result of a possible hydrogen bond or its absence but also the consequence of a drastically different three-dimensional conformational change of the sp^3 hybridised sulfonamide and the sp^2 hybridised carboxamide. As the replacement of the linker takes place in the middle of the molecule, that torsional angle difference forces the substituted phenyl and the pyrimidine ring to change their relative distances. This may influence the desired antiviral activity since the aromatic ring with the appropriately placed substituent and the pyrimidine ring with the carefully positioned nitrogens, ethylamine chain, and methyl are most likely interacting with the target protein (nsP1) and are directly responsible for the activity (see **Figure 2a** and Molecular Docking

in Supporting Information). This hypothesis may lead further to the conclusion that the established SAR for the pyrimidine and phenyl regions of sulfonyl-analogues is *not transferable* to the amide-bearing compounds - giving an explanation why the combined optimizations with the introduction of an amide linker made by Moesslacher et al. did not give the desired gain of activity.[15]

Therefore, we shifted our focus to the phenyl substitutions in combination with the P3/5 nitrogen variation and the amide linker. To rationalise the SAR, we first evaluated **30** without any substitutions and then analyzed the effect of different electron-donating and withdrawing groups on various phenyl positions. Surprisingly, **30** was slightly more active against the CHIKV in Vero cells than our lead compound **1b** - indicating that the nitrogen shift on the pyrimidine ring has the suspected favourable impact on the activity (see **Table 2** vs. **3**). Moreover, all para-substituted analogues demonstrated a similar (**31e-f**) or even higher antiviral activity (**31a-d** and **31g**) than the un-substituted compound **30**. Especially the electron-withdrawing NO_2 and the weak deactivating halides I and Br led to a significant increase of potency with EC_{50} values of $0.91 \pm 0.18\,\mu M$, $0.70 \pm 0.28\,\mu M$, and $0.60 \pm 0.08\,\mu M$. Shifting this three promising substituents to meta position resulted only with the NO_2 modification (**32d**) in an even higher activity than the correspondent para analogues (e.g., **31d**). Nevertheless, all tested meta-substituted analogues (**32a-e**) showed strong activity.

In addition, the combined para and meta substitutions in **33a-d** achieved all similar impressive EC_{50} values around $1\,\mu M$ - with surprisingly the 3,4-dichloro substituted analogue **33a** as the most potent variation ($EC_{50} = 0.57\,\mu M$). Consequently, further di-substituted analogues with meta-meta (**34**) or ortho-para (**35a-d**) modifications were designed with two halogens, two methyl groups, and/or the Cl/NO_2 substitution. The 3,5-dichloro analogue **34** gave the most impressive antiviral activity with EC_{50} values of $0.47 \pm 0.06\,\mu M$ - an even more remarkably outcome considering that the correspondent P1/3 analogue with the same phenyl-substitutions **19** and the 2,4-dichloro analogue **35a** were completely inactive

with EC_{50} values of 66.5 and >100 µM, respectively. Further, all the ortho-para substituted compounds (**35a-d**) showed no antiviral activity. Interestingly, also the additional chloride in NO_2-substituted compounds seems not to have the desired beneficial impact on the anti-CHIKV activity as the single-substituted **32d** remains the most active of the tested NO_2 analogues (see **18b**, **32d**, **33c**, and **35b**).

Keeping these results in mind, we designed the next series of analogues with the most encouraging substitutions: i) 3,5-dichloro and 3,4-dichloro substitutions as they achieved the lowest EC_{50} values - with focus on the 3,5-dichloro variation considering the higher cytotoxicity of the 3,4-dichloro analogue **33a**, and ii) a para halide substitution as they have been demonstrating strong influence on the activity of the compound.

Purine Scaffold. The following pyrimidine modification was inspired by a major and potent class of antiviral chemotherapeutics - the nucleoside/tide analogues with the commonly used pyrimidine and purine ring system.[20,21] Moreover, the non-structural protein (nsP1) of the Chikungunya virus was determined as the main site of action of the CHVB-compound series, and almost all of the few published small molecules targeting the same viral protein contain a purine or a purine-like ring system (e.g. the MADPT-series, 6-fluoro-homoaristeromycin (FAH), 6-fluoro-homoneplanocin A (FHNA), and 5-Iodotubercidine (5-IT)).[13,16,22–24] In addition, *in silico* designed analogues in which the ethylamine side chain merges into the additional ring of the purine system showed a high structural analogy to the parent compound with all three (essential for the activity) nitrogens of the pyrimidine and ethylamine structure (see **Figure 2b**). Therefore, different analogues bearing the purine variation with various replacements for the former pyrimidine-methyl group were designed and tested. Almost none of these purine compounds showed any antiviral improvement of the anti-CHIKV activity in Vero cells. Only **45b, 46a, 46c, and 48** gave some antiviral activity - whereby **46c** gave the most interesting results with an EC_{50} value of 9.48 ± 0.39 µM and could be an interesting starting point for a new lead optimization process.

Piperazine-Bioisostere Scaffold. The final part of the SAR assessment focused on the

core region of the compound structures - the piperazine ring. Previous results with mostly sulfonamide analogues concluded that this region functions solely as a linker that keeps the needed distance between the phenyl and the pyrimidine ring - groups considered to interact most probable directly with the target protein.[15] A set of compounds with different heterocycle replacements of the piperazine ring were designed to investigate whether this conclusion still holds for analogues with an amide linker (see **Table 5**, **55a-62d**).

Analogues with an enlarged core system and a secondary amide instead of the usual tertiary amide bearing a *tert*-butyl 4-aminopiperidine-1-carboxylate (**55a-b**) or *tert*-butyl 3-aminopiperidine-1-carboxylate (**56a-b**) replacement, showed no antiviral activity. Surprisingly, moving the additional hydrogen bond donor (HBD) from the sec. amide next to the pyrimidine ring as a sec. amine, resulted in active albeit toxic and less stable **57a-b** compounds (see section *In Vitro Absorption, Distribution, Metabolism, and Excretion (ADME) Profiling*). Although the two nitrogens were retained in all three heterocycles, their relative distance increased - enlarging the area between the two main target-interacting features. To confirm whether this phenomenon was the consequence of the sec. amine and not the increased core system, analogues with the same additional HBD with the original distance between the core nitrogens as piperazine were assessed. Corresponding to the enlarged analogues, the sec. amide containing **58a-b** exhibited no antiviral activity, whereas **59b** with a sec. amine next to the pyrimidine ring was active but also unstable. From these facts, one may conclude that an additional HBD next to the pyrimidine ring is a possible variation of the lead structure, but it also leads to a decline in metabolic stability. Further, keeping a similar relative distance between the two main interacting groups as a piperazine ring also seems beneficial in combination with the amide linker. Therefore, the following compounds were designed using bridged, fused, and spiro piperazine bioisosteres with a conserved diameter and partial configuration but more rigid characteristics. From all of these compounds **61d** was the most active one with an EC_{50} value of $3.20 \pm 0.28\,\mu M$ - revealing octahydropyrrolo[3,4-c]pyrrole as a viable and interesting modification for future studies.

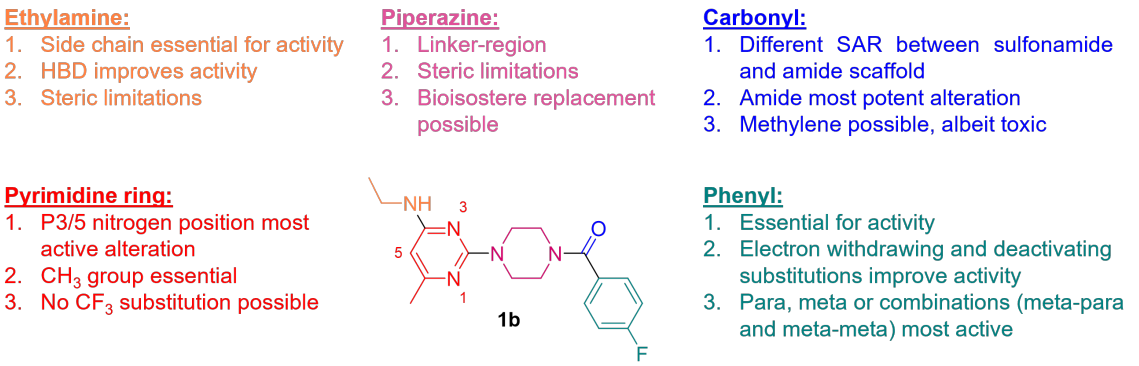

Figure 3. Summary of the structural requirements for antiviral activity described in chapter *Structure-Activity Relationship Study*.

Figure 3 summarises the structural requirements for antiviral activity described in the SAR study.

Scaffold Hopping. Taken together all the discovered requirements for a potent CHIKV-nsp1 interacting small molecule, we performed a scaffold hop for a future hit to lead drug development studies. As described above, an ethylamine sidechain- and CH_3-modifications on the pyrimidine ring are most favourable in terms of activity in combination with a P3/5 nitrogen scaffold. Considering analogues' overall much higher bioactivity with pyrimidine nitrogen P3/5 scaffold, we decided to preserve this part of the compound structure. Moreover, to keep the required relative distance and angle between the pyrimidine and the substituted phenyl regions, a quaternary carbon in the form of a spiro atom was positioned at the center of the new scaffold. This modification leads to a higher conformational rigidity and enhances the three-dimensionality of the chemical structure and hence an increased number of possible interactions with the target binding site.[25,26] Moreover, compounds with a higher fraction of sp^3 (Fsp^3) as the newly introduced spiro atom would induce, are estimated to succeed more likely in clinical trials.[27,28]

Further, by adding the carbonyl group to the chromane heterocycle, we retained the two hydrogen bond acceptors (from the carbonyl and dihydropyran) from the CHVB scaffold, which may have a positive impact on the bioactivity. The chromane was further selected for

the scaffold hop as the benzol part mirrors the former phenyl ring. The two synthesized compounds with the new scaffold **64a-b** demonstrated interesting anti-CHIKV potential (**Table 5**). According to our expectations, **64b** with the pyrimidine nitrogen pattern P3/5 was much more potent than the P1/3 variation (**64a**). With a EC_{50} value of $4.16 \pm 0.15\,\mu M$ **64b** could be a excellent starting point for a lead optimization through an additional structure-activity study.

Antiviral Profiling. The CHVB-series has been identified as a selective Chikungunya virus inhibitor with EC_{50} values against various CHIKV isolates (899 (laboratory), OPY1 (La Reunion), Venturini [Italy 2008], St Martin 20235 P2, St Martin 20236 P3, EFS-1 P3 Martinique, and Congo 95 [2011]) in the low micromolar range and no shown bioactivity against other alphaviruses.[16] Accordingly, the assessed second-generation CHVB compounds (**11a**, **12a**, **13**, and **31a**) demonstrated no activity against other alphaviruses (Semiliki Forest virus (Vietnam strain) and Sindbis virus (HRsp strain)) in virus-cell-based CPE-reduction assays on Vero cells. Additionally, screening for bioactivity against Human Enterovirus 71 and Zika virus in Vero cells gave negative results for the second-generation CHVB compounds (data not shown).

The anti-CHIKV activity was further confirmed in a virus yield assay in which treatment with selected CHVB compounds (**31b**, **31d**, **32d**, **34**, and **35d**) resulted in a pronounced dose-dependent reduction of viral RNA replication (**Figure 4c**). Compound **31b** had the most potent activity resulting in a >5 $\log_{10}$ reduction in intracellular CHIKV levels at the highest concentration tested ($60\,\mu M$). At the concentration of $2.22\,\mu M$, compounds **31b** and **32d** still reduced CHIKV replication with $\sim$4.5 $\log_{10}$.

A mechanism of action study identified the CHIKV capping machinery as the target of the CHVB series. A CHVB-resistant variant ($CHVB^{res}$) carrying two mutations in the gene encoding nsP1 (responsible for the viral capping, S454G and W456R), one mutation in nsP2 (M703T), and one mutation in nsP3 (L494P) showed a high barrier to resistance to the first

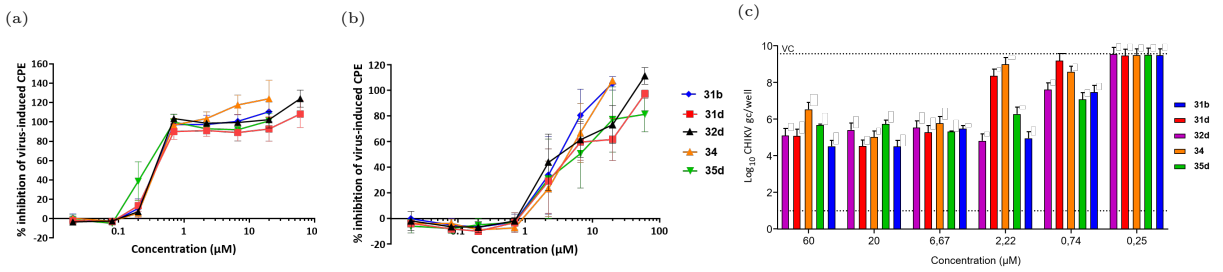

Figure 4. (a), (b): Cross-resistance of all tested CHVB compounds with the CHVB-resistant virus (CHVB^{res}). Vero cells infected with wild-type CHIKV899 (a) and CHVB^{res} (b) were assessed in a CPE reduction assay with increasing doses of selected CHVB compound. Vero cells were treated with 0 to 100 µM CHVB-compound and infected with wt or the CHIKV mutant at an MOI of 0.01. The MTS/PMS method determined the cell viability three days postinfection. Data are mean values ± SD from three independent experiments. (c): The effect of different concentrations of selected CHVB-compounds on the intracellular CHIKV RNA levels in CHIKV899-infected Vero cells (MOI, 0.01) was quantified by real-time qRT-PCR at 48 h p.i. Data shown are mean values ± SD from two independent experiments. CPE, cytopathic effect; wt, wild type; VC, virus control (untreated).

generation CHVB-compounds.[16] To investigate whether this second-generation CHVB compounds also exerted less antiviral activity against the CHVB^{res} virus, a selection of CHVB-compounds was additionally assessed for cross-resistance with CHVB^{res} (**Figure 4a** and **4b**). A similar level of resistance was measured with a fold resistance (EC_{50} CHVB^{res}/EC_{50} CHKVwt) ranging from 9.7 (**34**) up to 15 (**35d**) - suggesting that the viral capping machinery remains the main target for the optimized compounds of the CHVB series. Therefore, a molecular docking study was performed to identify possible molecular interactions and important chemical features of the CHVB compounds with their main viral target protein (nsP1, see Supporting Information).[29]

***In Vitro* Absorption, Distribution, Metabolism, and Excretion (ADME) Profiling.** The objective of discovering new analogues with improved antiviral potency over **1b** was realised for a remarkable number of compounds described above. However, high antiviral activity is one of many essential parameters in successful drug development. Therefore, to better understand the druggability of the compounds, the analogues were evaluated for their physiochemical properties and their metabolic stability in human liver microsomes (HLMs).

Physiochemical parameters, such as the aqueous solubility and $LogD_{pH\ 7.4}$, are crucial criteria in early drug design as they highly influence the absorption and distribution of the

drug.[30] Therefore, we assessed these parameters for all 100 compounds. The $LogD_{pH\ 7.4}$ value ranged from 2.40 to 3.83 (pH = 7.4). Further, the aqueous solubility at pH 7.4 differed from poor solubility (13 compounds with <50 µM) to a vast number of highly soluble compounds (56 compounds with >100 µM) including all the most potent compounds with EC_{50} values under 3 µM.

With a view to *in vivo* pharmacological experiments, we further characterised the *in vitro* microsomal half-life ($t_{1/2}$) after 60 min incubation of the compounds in human liver microsomes (HLMs). Therefore, 55 analogues were selected according to their antiviral profile and/or structural scaffold to investigate the influence of various structural changes on their pharmacokinetic profile. The results of the *in vitro* HLM metabolism study are summarised in **Table 1-5**.

The compounds showed an overall high stability with a mean half-life time of >60 min for 37 analogues. These results confirmed the previously conducted *in silico* investigation, in which all 100 compounds were screened according to their metabolic stability - revealing possible sites of metabolism (SoMs) such as the methyl and ethylamine side-chain on the pyrimidine ring.[31,32]

Scaffold-dependent metabolic stability was observed through the investigated CHVB series. All analogues with the preferable nitrogen P3/5 scaffold showed a significantly higher metabolic stability than their P1/3 counterparts (e.g., **32d** vs **18b**, and **24** vs **15**), which may indicate that the difference in local electron density (introduced by the electronegative nitrogen atoms) could influence the metabolic property. Further, almost all tested sulfonamide-analogues were not stable in human liver microsome - suggesting that the liver would rapidly metabolise them. Only in combination with the stabilising P3/5 nitrogen position in the pyrimidine ring enhanced metabolic stability could be observed within the sulfonamide analogues **24** and **27**.

A similar effect was seen within analogues without the CH_3 group at the pyrimidine ring. Both, **14** and **15** with a P1/3 scaffold were less stable than the P3/5 **23** and **24**

compounds. Interestingly, even higher stability was reached when the lacking CH_3 scaffold was combined with an amide as it is in **17a-b**. In addition, the conversion of the methyl to a trifluoromethyl showed no gain in stability (see **40a-d** and **41b**). As the introduction of a fluorine atom at the SoM is a commonly used strategy to enforce higher stability, the destabilising effect of the CF_3 group may be caused by the rupture of the C-F bond (despite its strength) during metabolism.[33–36] The two assessed purine analogues **46c** and **48** with CF_3 or Cl at the methyl position resulted, on the other hand, in a good half-life time.

Compounds with a piperazine-bioisostere scaffold showed heterogeneous results. While the primary amide compound **56b** and the sec. amine analogues **57a** and **59b** demonstrated low half-life time, all the other assessed piperazine-variations gave similar metabolic stability as the piperazine compound **34**. It is worthy to note that also the P3/5 variation of the sec. amine **57b** exhibited a $t_{1/2}$ of >60 min.

The most potent compounds (bearing a P3/5 and amide scaffold) gave a high half-life time over 60 min with the high active **31d** as the overall most stable compound (100 % compound remaining after 60 min incubation).

Toxicological Profiling. The ten most promising compounds (**31a-d**, **31g**, **32b**, **32d**, **33a**, **34**, and **35d**) were evaluated for their cytotoxic activity *in vitro* against the CaCo-2 cell line. No significant cytotoxic effects were detected (see Supporting Information). Additionaly, to analyze whether the CHVB compound series increases the expression of the apoptosis proteins caspase-3 and PARP, western blot experiments were performed with the same ten analogues. Since the caspase and PARP are apoptosis-indicating proteins, they can be used for the detection of cytotoxicity and to assess programmed cell death, respectively.[37] All compounds showed compared to the control (DMSO) neither for caspase-3 nor for PARP increased expression in all assessed concentrations. A representative blot is given in **Figure 5**.

Moreover, the Inte:Ligand Tox Pharmacophore DB was used for toxicity profiling of all

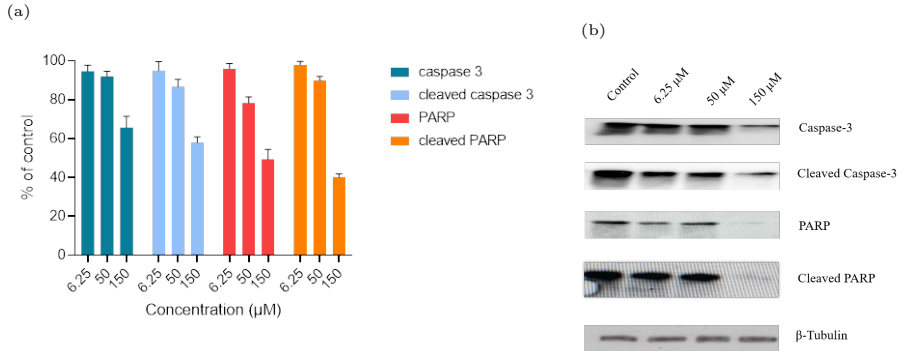

Figure 5. The assessed CHVB analogues have no increasing effect on the expression of the apoptosis proteins (cleaved caspase-3, caspase-3, cleaved PARP, and PARP). (a) Mean data of western blots of CaCo-2 cells lysate after 72 h treatment of different concentration of **32d** and control (n = 3). (b) Representative western blot from **32d**. The densitometry values were normalized to β-tubulin and set in relation to the control (DMSO).

100 synthesized compounds, but no significant effect was discovered on the hERG channel.[38] The predicted biological safety regarding possible hERG interactions was further investigated in a patch-clamp assay in Xenopus oocytes with thioridazine hydrochloride as a positive control.[39,40] A 30 % reduction of peak tail current was defined as the border for positive hERG blockade. **13** (core structure of the molecule series) was tested up to a concentration of 30 µM, showing an inhibition of 9.63 ± 5.13 % (n = 5) and thus no significant interaction above the critical defined borderlines.

Overall, neither the *in silico* nor the *in vitro* assay showed any relevant interactions of our CHVB-series with the hERG potassium channel and no significant cytotoxicity was determined - making the CHVB compound series overall a safe candidate for antiviral drug development.

Conclusion

In this study, we present the lead optimization of the CHVB-compound **1b** in light of the *in vitro* anti-CHIKV activity and ADMET profile. Further, we report an optimized synthesis route (Synthesis Route B), which improved the accessibility of the designed analogues, and the overall yield in remarkable shorter synthesis and work-up time. Altogether, 100

CHVB analogues were synthesized, tested for their antiviral activity against CHIKV by CPE-reduction assays in Vero cells, and assessed for their *in vitro* physicochemical and toxicological profile. The compounds showed overall an excellent safety profile and favourable physicochemical characteristics. The antiviral activity was confirmed in a virus yield assay. Out of this 100 novel CHVB compounds, 68 were active ($EC_{50} \leq 40\,\mu M$), 43 in a low micromolar range ($EC_{50} \leq 10\,\mu M$) and 24 more active than the initial lead compound **1b** (EC_{50} value of $3.95 \pm 0.01\,\mu M$). Moreover, 10 compounds demonstrated a remarkable high antiviral activity with EC_{50} values under $1\,\mu M$.

A thorough SAR study focusing mainly on the combination of scaffold changes revealed the structural requirement for a high antiviral activity against the CHIKV (see **Figure 3**). Of these requirements, the positions of the nitrogens in the pyrimidine ring in combination with a sulfonamide or an amide bridge significantly impacted the biological activity. Interestingly, a structure-metabolism relationship study (SMR) identified the same functional groups as the SAR study to be highly influential in metabolic stability - making the most active compounds the most stable. Hence, the discussed analogues can be categorized according to their positioning of the nitrogens in the pyrimidine ring (P1/3, P3/5, and P1/5) and whether their scaffold has a sulfonamide or an amide.

Furthermore, a cross-resistance study confirmed the viral capping machinery to be the viral target of these second-generation CHVB compounds. An additional molecular docking study showed possible interactions between the compound series and their biological target protein (nsP1, Supporting Information). Neither hERG channel interactions nor *in vitro* cytotoxicity in CaCo-2 cells was detected for this compound series - making this compound series an overall safe candidate for further *in vivo* studies.

Together, these data identify five compounds, namely **31b**, **31d**, **32d**, **34**, and **35d**, as highly potent, safe, and stable lead compounds for further development as antiviral inhibitors

of the CHIKV. Of all promising new lead compounds, **32d** demonstrates the most druggable characteristics throughout all assessed assays. Finally, the collected insight and knowledge led to a successful scaffold hop (**64b**) for future antiviral research studies.

Experimental

Chemistry Materials and General Analytical Methods. All reagents and solvents (of analytical and HPLC grades) were purchased from Sigma-Aldrich or other commercial suppliers like Fluka and Alfa Aesar and were used without further purification. Moisture-sensitive reactions were performed using anhydrous solvents and under an argon atmosphere. EtOH, THF and DCM were dried before use. Disposable needles and syringes (B— Braun Inject and B— Braun Sterican®) were applied to transfer the solvents into the reaction flask. The solvents were removed under reduced pressure using the Heildolph Laborota 4000 efficient evaporator. Analytical thin-layer chromatography (TLC) was carried out on Polygram® SIL G/UV254 plates, layer 0.2 mm silica gel with fluorescent indicator. The spots were visualised by UV light (254 and 366 nm) with CAMAG UV Lamp 4. A part of the syntheses was performed in Cem Discover to obtain microwave conditions. Compounds were purified, performing a flash chromatography on a glass column using Merck silica gel ($40-60$ mesh) or on the Biotage® Isolera™ One System. The solvent mixtures for chromatography are always referred to as a vol/vol ratio, and the melting points were determined on Cambridge Instruments.

NMR spectra were recorded on a Bruker Avance 500 NMR spectrometer (UltraShield) using a 5 mm switchable probe (TCI Prodigy Kryo-probe head, 5 mm, triple resonance-inverse-detection probe head) with z-axis gradients and automatic tuning and matching accessory (Bruker BioSpin). The resonance frequency for ^{1}H NMR was 500.13 MHz and for ^{13}C NMR 125.75 MHz. All measurements were performed for a solution in fully deuterated dimethylsulfoxide at 298 K. Standard 1D and gradient-enhanced 2D experiments, like double

quantum filtered (DQF) COSY, HSQC, and HMBC, were used as supplied by the manufacturer. Chemical shifts are referenced internally to the residual, non-deuterated solvent signal ^{1}H (δ 2.50 ppm) and the carbon signal ^{13}C (δ 39.50 ppm) of dimethylsulfoxide. ^{19}F NMR spectra were recorded on a Bruker Avance III 400 NMR spectrometer (UltraShield) using a 5 mm switchable probe (BBFOPLUS, BB/19F – 1H/D) with z-axis gradients and automatic tuning and matching accessory (Bruker BioSpin). The resonance frequency for ^{1}H NMR was 400.23 MHz and for ^{19}F NMR 376.55 MHz. All measurements were performed for a solution in fully deuterated dimethylsulfoxide at 298 K. ^{19}F NMR spectra (broadband decoupled for 1H) were measured as supplied by the manufacturer using absolute referencing via Ξ ratio. Chemical shifts are given in ppm and are reported relative to TMS and referenced to the residual proton signal of d6-DMSO (2.50 ppm). d6-DMSO with 0.03 % TMS (V/V), purchased at Euriso-top®, was used as a solvent for the samples. The specified abbreviations were used to characterize the signals: s = singlet, d = doublet, t = triplet, q = quartet, quint = quintet, sext = sextet, m = multiplet, and br = broad signal. The spectra were analysed by a computer using the software MestReNova 6 (Mestrelab research, 1994).

HRESIMS spectra were obtained on a maXis HD ESI-Qq-TOF mass spectrometer (Bruker Daltonics, Bremen, Germany). Samples were dissolved to 20 µg/mL in MeOH and directly infused into the ESI source at a flow rate of 3 µL/min with a syringe pump. The ESI ion source was operated as follows: capillary voltage: 0.9 to 4.0 kV (individually optimized), nebulizer: 0.4 bar (N_2), dry gas flow: 4 L/min (N_2), and dry temperature: 200 °C. Mass spectra were recorded in the range of m/z 50 to 1550 in the positive-ion mode. The sum formulas were determined using Bruker Compass DataAnalysis 4.2 based on the mass accuracy ($\Delta m/z \leq 2$ ppm) and isotopic pattern matching (SmartFormula algorithm).

The purity of the compounds was determined by HPLC on LC-2010A HT Liquid Chromatograph device (Shimadzu Corporation, Tokyo, Japan). The separation was carried out on an Acclaim 120 C18, 2.1×150 mm, 3 µm HPLC column (Thermo Fisher Scientific) using LCMS-grade water with 0.1 % FA and acetonitrile with 0.1 % FA as mobile phase A and

B, respectively. The sample components were separated and eluted with a linear gradient from 5 to 95 % B in 30 min, followed by an isocratic column cleaning and re-equilibration step. The flow rate was 0.1 mL/min, and the column oven temperature was set to 25 °C. The purity was determined from the UV chromatogram (254 nm) as the ratio of the peak area of the compound to the total peak area (i.e., the sum of the areas of all peaks that were not present in the solvent blank). Based on the HPLC data, all final compounds are ≥95 % pure.

General Synthetic Procedures.

Arylamine alkylation reaction for the synthesis of pyrimidine amines 3a-h and 9a-h can be performed according to General Synthetic Procedure A1 or General Synthetic Procedure A2.

General Synthetic Procedure A1. A stirred solution of pyrimidine (1 equiv) in anhydrous ethanol under an inert atmosphere was cooled to 0 °C before amine (2 equiv) was added dropwise. The reaction mixture was brought to room temperature and stirred for 48 hours. After evaporating the solvent, the residue was dissolved in dichloromethane and washed twice with water and brine. The organic layer was dried over sodium sulphate and then evaporated to dryness. To afford the desired pyrimidine amines, the crude product was purified by column chromatography (SiO_2, eluent: hexane/EtOAc or DCM/MeOH).

General Synthetic Procedure A2. A stirred solution of pyrimidine (1 equiv) in anhydrous THF under an inert atmosphere was cooled to 0 °C before amine (2 equiv) was added dropwise. The reaction mixture was brought to room temperature and stirred for 14 hours. After evaporation of the solvent, the residue was dissolved in dichloromethane and washed twice with H_2O and brine. The organic layer was dried over sodium sulphate and then evaporated to dryness. To afford the desired pyrimidine amines, the crude product was purified by column chromatography (SiO_2, eluent: DCM/MeOH).

Synthesis Route A

General Synthetic Procedure B: Synthesis of compounds 4a-d, 20a-20e, and 37. The pyrimidine amine **3a-h**/**9a-h** (1 equiv) and the Boc-protected pyridine **2** (2 equiv) were dissolved/suspended in 1.5 mL dry ethanol. The mixture was heated to 155 °C for 30 minutes under microwave irradiation (250 Watt, 12 bars). After the solvent was evaporated, the resulting crude product was dissolved in dichloromethane and washed twice with K_2CO_3 solution (10 % in water) and with water. The organic layer was dried over sodium sulphate, filtered, and then evaporated to dryness. To obtain the pure product, the crude was purified by column chromatography (SiO_2, eluent: 80% dichloromethane/20% methanol).

General Synthetic Procedure C: Acid-catalysed deprotection of tert-butoxycarbonyl-protected amines 5a-d, 21a-e, and 38. Carboxylate (1 equiv) was dissolved in dry tetrahydrofuran and stirred at room temperature, and then the hydrochloric acid solution (4.0 M in dioxane, 10 equiv) was added dropwise. The mixture was stirred for 24 hours and evaporated to dryness. The residuum was dissolved in dichloromethane, washed twice with an aqueous solution of potassium carbonate (10 %) and with water. The organic phase was dried over sodium sulphate and filtered to obtain the desired product.

General Synthetic Procedure D: Acylation reaction of nitrogen heterocycles. The pyrimidine (1 equiv) was dissolved in DCM. Sulfonyl chloride/benzoyl chloride (1 equiv) and triethylamine (1 equiv) as a base was added and stirred overnight at room temperature. The mixture was diluted in DCM and washed twice with H_2O and brine. The organic layer was dried over Na_2SO_4, filtered and concentrated in vacuum. The crude product was purified by recrystallization (DIPE/EtOAc; DIPE/EtOH or Hexane/EtOAc) or by column chromatography (SiO_2, eluent: DCM/MeOH).

Synthesis Route B

General Synthetic Procedure E: Nucleophilic acyl substitution for the synthesis of 6a-f and 53a-k. To a stirring solution of N-BOC-protected aminopiperazine/piperidines

(1 equiv) in pyridine, 0.006 equiv of DMAP was added. The solution was cooled down to 0 °C, and the benzoyl chloride (1.5 equiv) was added dropwise over 5 minutes. The reaction mixture was brought to room temperature and stirred for 15 hours. The crude was poured on ice, and the precipitated solid was collected by vacuum filtration and dried.

General Synthetic Procedure F: Acid-catalysed deprotection of tert-butoxycarbonyl-protected amines 7a-f and 54a-k. The boc-deprotection was performed similarly as in Synthesis Route A (General Synthetic Procedure C). After cooling down the dissolved intermediate to 0 °C TFA (50 equiv) was added. The reaction mixture was brought to room temperature and stirred for 15 hours. The solvent was evaporated, and the residue was re-dissolved in DCM. The organic layer was washed with saturated $NaHCO_3$ and H_2O, dried over sodium sulphate, and filtered to obtain the desired product.

General Synthetic Procedure G: Amination of aryl halides. The pyrimidine amine (**3a-h**/**9a-h**, 1 equiv) and the piperazine/pyridine (1-2 equiv) were dissolved/suspended with TEA (15-30 equiv) in 1.5 mL dry EtOH under inert atmosphere. The mixture was heated to 155 °C for 30 minutes under microwave irradiation (250 Watt, 12 bars). After the solvent was evaporated, the resulting crude was dissolved in dichloromethane and washed twice with K_2CO_3 solution (10 % in water) and H_2O. The organic layer was dried over sodium sulphate, filtered, and evaporated to dryness. The crude was purified by flash column chromatography (SiO_2, eluent: gradient from 0 to 15 % MeOH in DCM) to obtain the pure product.

Characterization and Spectral Data.

(4-chlorophenyl)(4-(4-(ethylamino)-6-methylpyrimidin-2-yl)piperazin-1-yl)methanone (10a). Compound **10a** was prepared following General Synthetic Procedure D using **5a** (150 mg, 0.68 mmol), 4-chlorobenzoyl chloride (118 mg, 0.67 mmol) and TEA (69 mg, 0.68 mmol) in DCM. The crude product was purified by recrystallization (DIPE/EtOAc), resulting in 123 mg of pure product (yield 50 %) as white solid.

Mp 142.4 to 144.1 °C. Ret. Time 13.41 min, purity 99.0 %. HRESIMS *m/z* 360.1588 $[M+H]^+$ (calcd for $C_{18}H_{23}ClN_5O_2^+$, 360.1586, Δ = -0.7 ppm). ^{1}H NMR (500 MHz, d_6DMSO) δ = 1.08 (t, 3H, CH_3), 2.04 (s, 3H, pyr-CH_3), 3.22 (br, 2H, NCH_2), 3.34-3.73 (br, 4H, pip-H2,6), 3.64 (br, 4H, pip-H3,5), 5.63 (s, 1H, pyr-H), 6.84 (br, 1H, NH), 7.46 (m, 2H, Ph-H2,6), 7.52 (m, 2H, Ph-H3,5). ^{13}C NMR (125 MHz, d_6DMSO) δ = 14.73 (CH_3), 23.83 (pyr-CH_3), 34.90 (NCH_2), 41.76/43.61 (pip- C3,5), 43.09/47.17 (pip-C2,6), 94.61 (pyr-C5), 128.61 (Ph-C3,5), 129.15 (Ph-C2,6), 134.29 (Ph-C4), 134.74 (Ph-C1), 161.13 (pyr-C2), 163.03 (pyr-C6), 168.21 (amide-C), n.d. (pyr-C4).

(4-bromophenyl)(4-(4-(ethylamino)-6-methylpyrimidin-2-yl)piperazin-1-yl)methanone (10b). Compound **10b** was prepared following General Synthetic Procedure D using **5a** (57 mg, 0.3 mmol), 4-bromobenzoyl chloride (84.9 mg, 0.39 mmol, 1.5 equiv) and TEA (31 mg, 0.3 mmol) in DCM. The crude product was by column chromatography (SiO_2, eluent: DCM/MeOH), resulting in 24 mg of pure product (yield 23 %) as white solid.

Mp 74 to 77 °C. Ret. time. 14.17 min, purity 95.6 %. HRESIMS *m/z* 404.1084 $[M+H]^+$ (calcd for $C_{18}H_{23}BrN_5O^+$, 404.1080, Δ = -0.8 ppm). ^{1}H NMR (500 MHz, d_6DMSO) δ = 1.08 (t, 3H, CH_3), 2.05 (s, 3H, pyr-CH_3), 3.23 (br, 2H, NCH_2), 3.65 (d, 4H, pip-H3,5), 3.73 (d, 4H, pip-H2,6), 5.63 (s, 1H, pyr-H5), 6.84 (br, 1H, NH), 7.39 (d, 2H, Ph-H2,6), 7.66 (d, 2H, Ph-H3,5). ^{13}C NMR (125 MHz, d_6DMSO) δ = 14.65 (CH_3), 23.79 (pyr-CH_3), 34.63 (NCH_2), 43.33 (pip-C2,6), 43.33 (pip-C3,5), 122.93 (Ph-C4), 129.29 (Ph-C2,6), 131.44 (Ph-C3,5), 135.07 (Ph-C1), 168.14 (amide-C), n.d. (pyr-C2), n.d. (pyr-C4), n.d. (pyr-C5), n.d. (pyr-C6).

(4-(4-(ethylamino)-6-methylpyrimidin-2-yl)piperazin-1-yl)(4-iodophenyl)methanone (10c). Compound **10c** was prepared following General Synthetic Procedure D using **5a** (200 mg, 0.9 mmol), 4-iodoobenzoyl chloride (240 mg,

0.9 mmol) and TEA (100 mg, 0.9 mmol) in DCM. The crude product was purified by column chromatography (SiO_2, eluent: DCM/MeOH) resulting in 152 mg of pure product (yield 37 %) as white/yellow solid.

MP 86 to 88 °C. Ret. time. 13.42 min, purity 96.7 %. HRESIMS m/z 452.0955 $[M+H]^+$ (calcd for $C_{18}H_{23}IN_5O^+$, 452.0942, Δ = -2.9 ppm). ^{1}H NMR (500 MHz, d_6DMSO) δ = 1.08 (t, 3H, CH_3), 2.05 (s, 3H, pyr-CH_3), 3.22 (br, 2H, NCH_2), 3.63 (d, 4H, pip-H3,5), 3.73 (d, 4H, pip-H2,6), 5.62 (s, 1H, pyr-H5), 6.84 (br, 1H, NH), 7.23 (d, 2H, Ph-H2,6), 7.83 (d, 2H, Ph-H3,5). ^{13}C NMR (125 MHz, d_6DMSO) δ = 14.68 (CH_3), 23.80 (pyr-CH_3), 34.68 (NCH_2), 43.11 (pip-C2,6), 43.49 (pip-C3,5), 96.46 (Ph-C4), 129.18 (Ph-C2,6), 135.35 (Ph-C1), 137.25 (Ph-C3,5), 161.06 (pyr-C4), 163.17 (pyr-C6), 168.36 (amide-C), n.d. (pyr-C2), n.d. (pyr-C5).

1-(4-(4-(ethylamino)-6-methylpyrimidin-2-yl)piperazin-1-yl)butan-1-one (11a). Compound **11a** was prepared following General Synthetic Procedure D using **5a** (100 mg, 0.45 mmol), butyryl chloride (49 mg, 0.45 mmol) and TEA (46 mg, 0.45 mmol) in DCM. The crude product was purified by column chromatography (SiO_2, eluent: DCM/MeOH, 8:2), resulting in 50 mg of pure product (yield 38 %) as white/yellow solid.

Mp 77 %. Ret. Time 10.66 min, purity 96.6 %. HRESIMS m/z 292.2139 $[M+H]^+$ (calcd for $C_{15}H_{26}N_5O_2^+$, 292.2132, Δ = -2.4 ppm). ^{1}H NMR (500 MHz, d_6DMSO) δ = 0.89 (t, 3H, CH_3), 1.09 (t, 3H, CH_3), 1.52 (m, 2H, CH_2), 2.05 (s, 3H, pyr-CH_3), 2.31 (t, 2H, CH2), 3.24 (br, 2H, NCH_2), 3.45-3.46 (m, 4H, pip-H2,6), 3.60-3.66 (m, 4H, pip-H3,5), 5.62 (s, 1H, pyr-H), 6.82 (br, 1H, NH). ^{13}C NMR (125 MHz, d_6DMSO) δ = 13.91 (C4), 14.74 (CH_3), 18.29 (C3), 23.84 (pyr-CH_3), 34.35 (C2), 34.79 (NCH_2), 40.98/44.91 (pip- C2,6), 43.24/43.68 (pip-C3,5), 94.08 (pyr-C5), 161.15 (pyr-C2), 163.03 (pyr-C6), 170.79 (amide-C), n.d. (pyr-C4).

cyclohexyl(4-(4-(ethylamino)-6-methylpyrimidin-2-yl)piperazin-1-yl)methanone (11b). Compound **11b** was prepared following General Synthetic Procedure D using **5a** (100 mg, 0.45 mmol), cyclohexanecarbonyl chloride (82 mg,

0.55 mmol) and TEA (46 mg, 0.45 mmol) in DCM. The crude product was purified by column chromatography (SiO_2, eluent: DCM/MeOH, 8:2), resulting in 67 mg of pure product (yield 45 %) as white/yellow solid.

Mp resinous substance. Ret. Time 14.06 min, purity 95.8 %. HRESIMS m/z 332.2406 $[M+H]^+$ (calcd for $C_{18}H_{29}N_5O^+$, 332.2411, Δ = -1.4 ppm). ^{1}H NMR (500 MHz, d_6DMSO) δ = 1.08 (t, 3H, CH_3), 1.12/1.60 (m, 2H, cyc-H4), 1.26/1.76 (m, 4H, cyc-3,5), 1.35/1.98 (m, 4H, cyc-H2,6), 2.05 (s, 3H, pyr-CH_3), 3.12 (m, 1H, cyc-H1), 3.23 (t, 2H, NCH_2), 3.24 (t, 4H, pip-H3,5), 3.69 (t, 4H, pip-H2,6), 5.63 (s, 1H, pyr-H), 6.86 (br, 1H, NH); ^{13}C NMR (125 MHz, d_6DMSO) δ = 14.71 (CH_3), 23.81 (pyr-CH_3), 24.55 (cyc-C3,5), 24.86 (cyc-C4), 26.28 (cyc-C2,6), 34.68 (NCH_2), 43.73 (pip-C2,6), 45.58 (pip- C3,5), 59.33 (cyc-C1), 94.22 (pyr-C5), 163.03 (pyr-C6), 160.98 (amide-C), n.d. (pyr-C2), n.d. (pyr-C4).

N-ethyl-6-methyl-2-(4-(propylsulfonyl)piperazin-1-yl)pyrimidin-4-amine (12a). Compound **12a** was prepared following General Synthetic Procedure D using **5a** (100 mg, 0.45 mmol), propane-1-sulfonyl chloride (64 mg, 0.45 mmol) and TEA (46 mg, 0.45 mmol) in DCM. The crude product was purified by column chromatography (SiO_2, eluent: DCM/MeOH, 8:2), resulting in 55 mg of pure product (yield 37 %) as white solid.

Mp 114 °C. Ret. time 11.90 min, purity 99.3 %. HRESIMS m/z 328.1809 $[M+H]^+$ (calcd for $C_{14}H_{26}N_5O_2S^+$, 328.1802, Δ = -2.3 ppm). ^{1}H NMR (500 MHz, d_6DMSO) δ = 0.97 (t, 3H, propyl-CH_3), 1.09 (t, 3H, CH_3), 1.69 (s, 2H, propyl-CH22), 2.05 (m, 3H, pyr-CH_3), 3.00 (m, 2H, propyl-CH2), 3.15 (m, 4H, pip-H3,5), 3.23 (br, 2H, NCH_2), 3.73 (m, 4H, pip-H2,6), 5.63 (s, 1H, pyr-H), 6.85 (br, 1H, NH). ^{13}C NMR (125 MHz, d_6DMSO) δ = 14.71 (CH_3), 12.93 (propyl-C3), 16.37 (propyl-C2), 23.82 (pyr-CH_3), 34.67 (NCH_2), 43.18 (pip-C2,6), 45.23 (pip-C3,5), 48.88 (propyl-C1), 94.29 (pyr-C5), 160.97 (pyr-C2), 163.06 (pyr-C6), n.d. (pyr-C4).

N-ethyl-6-methyl-2-(4-(naphtalen-2-ylsulfonyl)piperazin-1-yl)pyrimidin-4-amine (12b). Compound **12b** was prepared following General Synthetic Procedure D

using **5a** (100 mg, 0.45 mmol), naphtalene-2-sulfonyl chloride (105 mg, 0.46 mmol) and TEA (46 mg, 0.45 mmol) in DCM. The crude product was purified by recrystallization (DIPE/EtOAc), resulting in 60 mg of pure product (yield 32 %) as white solid.

Mp 180.7 °C. Ret. time 15.91 min, purity 99.3 %. HRESIMS m/z 412.1810 $[M+H]^+$ (calcd for $C_{21}H_{26}N_5O_2S^+$, 412.1802, Δ = -2.1 ppm). ^{1}H NMR (500 MHz, d_6DMSO) δ = 1.03 (t, 3H, CH_3), 1.97 (s, 3H, pyr-CH_3), 2.96 (m, 4H, pip-3,5), 3.16 (br, 2H, NCH_2), 3.74 (m, 4H, pip-H2,6), 5.55 (s, 1H, pyr-H), 6.80 (br, 1H, NH), 7.69 (ddd, 1H, J = 8.1 Hz, 4.9 Hz, 1.3 Hz, nap-H7), 7.73 (ddd, 1H, J = 8.1 Hz, 6.9 Hz, 1.4 Hz, nap-H6), 7.77 (dd, 1H, J = 8.7 Hz, 1.9 Hz, nap-H3), 8.07 (d, 1H, J = 8.1 Hz, nap-H5), 8.15 (d, 1H, J = 8.7 Hz, nap-H4), 8.21 (d, 1H, J = 8.1 Hz, nap-H8), 8.44 (d, 1H, J = 1.9 Hz, nap-H1). ^{13}C NMR (125 MHz, d_6DMSO) δ = 14.58 (CH_3), 23.67 (pyr-CH_3), 34.54 (NCH_2), 42.50 (pip-C2,6), 45.87 (pip-C3,5), 94.08 (pyr-C5), 122.89 (nap-C3), 127.70 (nap-C7), 127.90 (nap-C5), 128.84 (nap-C1), 129.08 (nap-C6), 129.38 (nap-C4), 129.38 (nap-C8), 132.12 (nap-C2), 131.79 (nap-C8a), 134.46 (nap-C4a), 160.61 (pyr-C2), 162.88 (pyr-C6), n.d. (pyr-C4).

N-ethyl-6-methyl-2-(4-(thiophen-2-ylsulfonyl)piperazin-1-yl)pyrimidin-4-amine (12c). Compound **12c** was prepared following General Synthetic Procedure D using **5a** (100 mg, 0.45 mmol), thiophene-2-sulfonyl chloride (83 mg, 0.46 mmol) and TEA (46 mg, 0.45 mmol) in DCM. The crude product was purified by recrystallization (DIPE/EtOAc), resulting in 25 mg of pure product (yield 15 %) as white/yellow solid.

Mp 160.4 to 171.1 °C. Ret. time 13.55 min, purity 98.3 %. HRESIMS m/z 368.1218 $[M+H]^+$ (calcd for $C_{15}H_{22}N_5O_2S^+$, 368.1209, Δ = -2.4 ppm). ^{1}H NMR (500 MHz, d_6DMSO) δ = 1.06 (t, 3H, CH_3), 2.02 (s, 3H, pyr-CH_3), 2.92 (m, 4H, pip-H3,5), 3.20 (br, 2H, NCH_2), 3.77 (m, 4H, pip-H2,6), 5.60 (s, 1H, pyr-H), 6.86 (br, 1H, NH), 7.28 (dd, 1H, J = 8.8 Hz, th-H4), 7.65 (dd, 1H, J = 5.1 Hz, th-H3), 8.05 (dd, 1H, J = 6.3 Hz, th-H5). ^{13}C NMR (125 MHz, d_6DMSO) δ = 14.61 (CH_3), 23.69 (pyr-CH_3), 34.56 (NCH_2), 42.38 (pip-C2,6), 45.79 (pip-C3,5), 94.55 (pyr-C5), 128.42 (th-C4), 133.25 (th-C3), 134.03 (th-C5), 134.45 (th-C2), 160.71 (pyr-C2), 162.94 (pyr-C6), 174.77 (pyr-C4).

2-(4-((6-chloropyridin-3-yl)sulfonyl)piperazin-1-yl)-N-ethyl-6-methylpyrimidin-4-amine (12d). Compound **12d** was prepared following General Synthetic Procedure D using **5a** (100 mg, 0.45 mmol), 6-chloropyridine-3-sulfonyl chloride (109 mg, 0.52 mmol) and TEA (46 mg, 0.45 mmol) in DCM. The crude product was purified by recrystallization (DIPE/EtOAc), resulting in 106 mg of pure product (yield 59 %) as white/yellow solid.

Mp 179.8 to 180.6 °C; Ret. time 13.61 min, purity 97.5 %. HRESIMS m/z 397.1220 $[M+H]^+$ (calcd for $C_{16}H_{22}ClN_6O_2S^+$, 397.1208, Δ = -3.1 ppm). ^{1}H NMR (500 MHz, d_6DMSO) δ = 1.06 (t, 3H, CH_3), 2.01 (s, 3H, pyr-CH_3), 2.99 (m, 4H, pip-H3,5), 3.19 (br, 2H, NCH_2), 3.76 (m, 4H, pip-H2,6), 5.59 (s, 1H, pyr-H), 6.84 (br, 1H, NH), 7.78 (dd, 1H, J = 8.8 Hz, pyridine-H5), 8.18 (dd, 1H, J = 11.0 Hz, pyridine-H4), 8.75 (dd, 1H, J = 3.0 Hz, pyridine-H2). ^{13}C NMR (125 MHz, d_6DMSO) δ = 14.62 (CH_3), 23.70 (pyr-CH_3), 34.48 (NCH_2), 42.39 (pip-C2,6), 45.58 (pip-C3,5), 94.41 (pyr-C5), 125.40 (pyridine-C5), 131.26 (pyridine-C3), 138.95 (pyridine-C4), 148.55 (pyridine-C2), 154.57 (pyridine-C6), 160.59 (pyr-C2), 162.94 (pyr-C6), 174.29 (pyr-C4).

2-(4-((4-fluorophenyl)sulfonyl)piperazin-1-yl)pyrimidine (13). Compound **13** was prepared following General Synthetic Procedure D using 2-(piperazin-1-yl)pyrimidine (127 mg, 0.77 mmol), 4-fluorobenzenesulfonyl chloride (150 mg, 0.77 mmol) and TEA (78 mg, 0.78 mmol) in DCM. The crude product was purified by column chromatography (SiO_2, eluent: DCM/MeOH, 9:1), resulting in 215 mg of pure product (yield 86 %) as white solid.

Mp 198.4 to 200.0 °C. Ret. Time 23.46 min, purity 97.2 %. HRESIMS m/z 323.0972 $[M+H]^+$ (calcd for $C_{14}H_{16}FN_4O_2S^+$, 323.0973, Δ = -0.1 ppm). ^{1}H NMR (500 MHz, d_6DMSO) δ = 2.95 (t, 4H, pip-H3,5), 3.82 (t, 4H, pip-H2,6), 6.64 (t, 1H, pyr-H5), 7.47 (m, 2H, Ph-3,5), 7.82 (m, 2H, Ph-H2,6), 8.33 (d, 2H, pyr-H4,6). ^{13}C NMR (125 MHz, d_6DMSO) δ = 42.58 (pip-C2,6), 45.68 (pip- C3,5), 110.81 (pyr-C5), 116.79 (^{3}J(^{13}C,^{19}F) = 22.3 Hz, Ph-C3,5),

130.75 (^{3}J(^{13}C,^{19}F) = 9.4 Hz, Ph-C2,6), 131.20 (^{3}J(^{13}C,^{19}F) = 3.1 Hz, Ph-C1), 158.09 (pyr-C4,6), 160.84 (pyr-C2), 164.79 (^{3}J(^{13}C,^{19}F) = 250.49 Hz, Ph-C4). ^{19}F NMR (376.55 MHz, d_6DMSO) δ = -105.56 (Ph-F).

2-(4-((4-fluorophenyl)sulfonyl)piperazin-1-yl)-N-isopropylpyrimidin-4-amine (14). Compound **14** was prepared following General Synthetic Procedure D using **5b** (86 mg, 0.39 mmol), 4-fluorobenzenesulfonyl chloride (75 mg, 0.38 mmol) and TEA (40 mg, 0.39 mmol) in DCM. The crude product was purified by column chromatography (SiO_2, eluent: DCM/MeOH, 8:2), resulting in 98 mg of pure product (yield 67 %) as white solid.

Mp 147 °C. Ret. Time 13.25 min, purity 98.5 %. HRESIMS m/z 380.1558 $[M+H]^+$ (calcd for $C_{17}H_{23}FN_5O_2S^+$, 380.1551, Δ = -1.9 ppm. ^{1}H NMR (500 MHz, d_6DMSO) δ = 1.09 (d, 3H, ipr-CH_3), 2.91 (t, 4H, pip-H3,5), 3.74 (t, 4H, pip-H2,6), 4.00 (br, 1H, ipr-H), 5.75 (d, 1H, pyr-H5), 7.13 (br, 1H, NH), 7.47 (t, 2H, Ph-3,5), 7.63 (s, 1H, pyr-H6), 7.82 (q, 2H, Ph-H2,6). ^{13}C NMR (125 MHz, d_6DMSO) δ = 22.30 (ipr-CH_3), 41.37 (ipr-CH), 42.64 (pip-C2,6), 45.68 (pip- C3,5), 96.74 (pyr-C5), 116.77 (^{3}J(^{13}C,^{19}F) = 22.7 Hz, Ph-C3,5), 130.77 (^{3}J(^{13}C,^{19}F) = 9.7 Hz, Ph-C2,6), 131.15 (^{3}J(^{13}C,^{19}F) = 2.4 Hz, Ph-C1), 161.58 (pyr-C4), 164.78 (^{3}J(^{13}C,^{19}F) = 250.6 Hz, Ph-C4), n.d. (pyr-C2), n.d. (pyr-C6). ^{19}F NMR (376.55 MHz, d_6DMSO) δ = -105.55 (Ph-F).

2-(4-((4-chlorophenyl)sulfonyl)piperazin-1-yl)-N-ethylpyrimidin-4-amine (15). Compound **15** was prepared following General Synthetic Procedure D using **5c** (88 mg, 0.42 mmol), 4-chlorobenzenesulfonyl chloride (90 mg, 0.42 mmol) and TEA (43 mg, 0.42 mmol) in DCM. The crude product was purified by column chromatography (SiO_2, eluent: DCM/MeOH, 8:2), resulting in 75 mg of pure product (yield 46 %) as white solid.

Mp 66.6 °C. Ret. Time 14.57 min, purity 98.9 %. HRESIMS m/z 382.1110 $[M+H]^+$ (calcd for $C_{16}H_{21}ClN_5O_2S^+$, 382.1099, Δ = -2.9 ppm). ^{1}H NMR (500 MHz, d_6DMSO) δ = 1.06 (t, 3H, CH_3), 2.90 (m, 4H, pip-H3,5), 3.20 (m, 2H, NCH_2), 3.74 (m, 4H, pip-H2,6), 5.72 (d, 1H, pyr-H5), 7.02 (br, 1H, NH), 7.64 (br, 1H, pyr-H6), 7.70 (m, 2H, Ph-H2,6), 7.75

(m, 2H, Ph-3,5). ^{13}C NMR (125 MHz, d_6DMSO) δ = 14.54 (CH_3), 34.45 (NCH_2), 42.52 (pip-C2,6), 45.76 (pip- C3,5), 96.46 (pyr-C5), 129.57 (Ph-C3,5), 129.70 (Ph-C2,6), 133.71 (Ph-C4), 138.40 (Ph-C1), 154.44 (pyr-C6), 160.77 (pyr-C2), 162.32 (pyr-C4).

2-(4-((4-fluorophenyl)sulfonyl)piperazin-1-yl)-N,6-dimethylpyrimidin-4-amine (16). Compound **16** was prepared following General Synthetic Procedure D using **5d** (83 mg, 0.4 mmol), 4-fluorobenzenesulfonyl chloride (78 mg, 0.4 mmol) and TEA (46 mg, 0.45 mmol) in DCM. The crude product was purified by recrystallization (DIPE/EtOAc), resulting in 15 mg of pure product (yield 10 %) as white solid.

Mp 126.9 to 128.4 °C. Ret. time 13.24 min, purity 99.0 %. HRESIMS m/z 366.1405 $[M+H]^+$ (calcd for $C_{16}H_{21}FN_5O_2S^+$, 3666.1395, Δ = -3.0 ppm). ^{1}H NMR (500 MHz, d_6DMSO) δ = 2.01 (s, 3H, pyr-CH_3), 2.69 (d, 3H, NCH_2), 2.88 (t, 4H, pip-H3,5), 3.75 (t, 4H, pip-H2,6), 5.59 (s, 1H, pyr-H5), 6.80 (br, 1H, NH), 7.47 (t, 2H, Ph-H3,5), 7.81 (q, 2H, Ph-H2,6). ^{13}C NMR (125 MHz, d_6DMSO) δ = 23.74 (pyr-CH_3), 26.79 (NCH_2), 42.50 (pip-C2,6), 45.87 (pip-C3,5), 94.48 (pyr-C5), 116.75 (d, $^3J(^{13}C,^{19}F)$ = 22.3 Hz, Ph-C3,5), 130.76 (d, $^3J(^{13}C,^{19}F)$ = 9.8 Hz, PH-C2,6), 131.13 (d, $^3J(^{13}C,^{19}F)$ = 2.5 Hz, Ph-C1), 160.64 (pyr-C2), 163.70 (pyr-C4), 163.77 (pyr-C6), 164.77 (d, $^3J(^{13}C,^{19}F)$ = 250.5 Hz, Ph-C4). ^{19}F NMR (376.55 MHz, d_6DMSO) δ = -105.56 (Ph-F).

(4-(4-(ethylamino)pyrimidin-2-yl)piperazin-1-yl)(4-fluorophenyl)methanone (17a). Compound **17a** was prepared following General Synthetic Procedure D using **5c** (97 mg, 0.47 mmol), 4-fluorobenzoyl chloride (74 mg, 0.47 mmol) and TEA (46 mg, 0.45 mmol) in DCM. The crude product was purified by recrystallization (DIPE/EtOAc), resulting in 50 mg of pure product (yield 32 %) as white solid.

Mp 164.8 °C. Ret. Time 12.74 min, purity 95.1 %. HRESIMS m/z 330.1733 $[M+H]^+$ (calcd for $C_{17}H_{21}FN_5O^+$, 330.1725, Δ = -2.7 ppm). ^{1}H NMR (500 MHz, d_6DMSO) δ = 1.09 (t, 3H, CH_3), 3.24 (br, 2H, NCH_2), 3.68 (br, 4H, pip-H3,5), 3.68 (br, 4H, pip-H2,6), 5.76 (d, 1H, pyr-H5), 7.02 (br, 1H, NH), 7.29 (m, 2H, Ph-3,5), 7.50 (m, 2H, Ph-H2,6), 7.70 (br, 1H, pyr-H6). ^{13}C NMR (125 MHz, d_6DMSO) δ = 14.54 (CH_3), 34.39 (NCH_2), 43.30 (pip-

C2,6), 43.30 (pip- C3,5), 96.19 (pyr-C5), 115.41 ($^3J(^{13}C,^{19}F)$ = 21.3 Hz, Ph-C3,5), 129.65 ($^3J(^{13}C,^{19}F)$ = 8.2 Hz, Ph-C2,6), 132.33 ($^3J(^{13}C,^{19}F)$ = 3.3 Hz, Ph-C1), 154.47 (pyr-C6), 161.12 (pyr-C2), 162.29 (pyr-C4), 162.55 ($^3J(^{13}C,^{19}F)$ = 245.0 Hz, Ph-C4), 168.28 (amide-C). ^{19}F (376.55 MHz, d_6DMSO) δ = -111.18 (Ph-F).

(4-chlorophenyl)(4-(4-(ethylamino)pyrimidin-2-yl)piperazin-1-yl)methanone (17b). Compound **17b** was prepared following General Synthetic Procedure D using **5c** (62 mg, 0.3 mmol), 4-chlorobenzoyl chloride (52 mg, 0.3 mmol) and TEA (31 mg, 0.3 mmol) in DCM. The crude product was purified by column chromatography (SiO_2, eluent: DCM/MeOH, 8:2), resulting in 90 mg of pure product (yield 87 %) as white solid.

Mp 185 °C. Ret. Time 13.29 min, purity 95.1 %. HRESIMS m/z 346.1436 $[M+H]^+$ (calcd for $C_{17}H_{21}ClN_5O^+$, 346.1429, Δ = -2.1 ppm). ^1H NMR (500 MHz, d_6DMSO) δ = 1.09 (t, 3H, NCH_3), 3.24 (br, 2H, NCH_2), 3.34/3.74 (m, 4H, pip-H2,6), 3.64 (br, 4H, pip-H3,5), 5.76 (d, 1H, pyr-H5), 7.03 (br, 1H, NH), 7.46 (m, 2H, Ph-2,6), 7.52 (m, 2H, Ph-H3,5), 7.70 (br, 1H, pyr-H6). ^{13}C NMR (125 MHz, d_6DMSO) δ = 14.60 (NCH_3), 34.49 (NCH_2), 41.70/43.59 (pip- C3,5), 43.04/47.11 (pip-C2,6), 96.32 (pyr-C5), 128.62 (Ph-C3,5), 129.14 (Ph-C2,6), 134.30 (Ph-C4), 134.74 (Ph-C1), 154.42 (pyr-C6), 161.12 (pyr-C2), 162.37 (pyr-C4), 168.24 (amide-C).

(3-bromophenyl)(4-(4-(ethylamino)-6-methylpyrimidin-2-yl)piperazin-1-yl)methanone (18a). Compound **18a** was prepared following General Synthetic Procedure D using **5a** (60 mg, 0.27 mmol), 3-bromobenzoyl chloride (87 mg, 0.4 mmol, 1.5 equiv) and TEA (27 mg, 0.27 mmol) in DCM. The crude product was purified by column chromatography (SiO_2, eluent: DCM/MeOH, 8:2), resulting in 36 mg of pure product (yield 33 %) as white solid.

Mp 152 to 153 °C. Ret. time. 14.17 min, purity 95.2 %. HRESIMS m/z 404.1092 $[M+H]^+$ (calcd for $C_{18}H_{23}BrN_5O^+$, 404.1080, Δ = -2.7 ppm). ^1H NMR (500 MHz, d_6DMSO) δ = 1.08 (t, 3H, CH_3), 2.05 (s, 3H, pyr-CH_3), 3.23 (br, 2H, NCH_2), 3.33-3.63 (d, 4H, pip-H2,6), 3.65-3.75 (br, 4H, pip-H3,5), 5.63 (s, 1H, pyr-H5), 6.84 (br, 1H, NH), 7.42 (d, 1H, Ph-H5), 7.43

(m, 1H, Ph-H6), 7.62 (t, 1H, Ph-H2), 7.67 (m, 1H, Ph-H4). ^{13}C NMR (125 MHz, d_6DMSO) δ = 14.67 (CH_3), 23.77 (pyr-CH_3), 34.50 (NCH_2), 41.61-43.49 (pip-C3,5), 42.97-47.04 (pip-C2,6), 121.73 (Ph-C3), 125.94 (Ph-C6), 129.64 (Ph-C2), 130.70 (Ph-C5), 132.36 (Ph-C4), 138.29 (Ph-C1), 161.06 (pyr-C2), 162.96 (pyr-C6), 167.42 (amide-C), n.d. (pyr-C4), n.d. (pyr-C5).

(4-(4-(ethylamino)-6-methylpyrimidin-2-yl)piperazin-1-yl)(3-nitrophenyl)methanone (18b). Compound **18b** was prepared following General Synthetic Procedure D using **5a** (60 mg, 0.27 mmol), 3-nitrobenzoyl chloride (49 mg, 0.27 mmol) and TEA (27 mg, 0.27 mmol) in DCM. The crude product was purified by column chromatography (SiO_2, eluent: DCM/MeOH, 8:2), resulting in 60 mg of pure product (yield 61 %) as white solid.

Mp 127 to 129 °C. Ret. time. 12.75 min, purity 95.5 %. HRESIMS m/z 371.1831 $[M+H]^+$ (calcd for $C_{18}H_{23}N_6O_3^+$, 371.1826, Δ = -1.4 ppm). ^{1}H NMR (500 MHz, d_6DMSO) δ = 1.08 (t, 3H, CH_3), 2.05 (s, 3H, pyr-CH_3), 3.23 (br, 2H, NCH_2), 3.35-3.67 (d, 4H, pip-H2,6), 3.67-3.78 (d, 4H, pip-H3,5), 5.63 (s, 1H, pyr-H5), 6.85 (br, 1H, NH), 7.76 (dd, J = 15.8 Hz, 1H, Ph-H5), 7.89 (ddd, J = 10.1 Hz, 1H, Ph-H6), 8.24 (dd, J = 3.6 Hz, 1H, Ph-H2). ^{13}C NMR (125 MHz, d_6DMSO) δ = 14.66 (CH_3), 23.76 (pyr-CH_3), 34.59 (NCH_2), 41.71-47.04 (pip-C2,6), 42.98-43.50 (pip-C3,5), 122.00 (Ph-C2), 124.28 (Ph-C4), 130.27 (Ph-C5), 133.47 (Ph-C6), 137.45 (Ph-C1), 147.70 (Ph-C3), 162.96 (pyr-C6), 166.90 (amide-C), n.d. (pyr-C2), n.d. (pyr-C4), n.d. (pyr-C5).

(3,5-dichlorophenyl)(4-(4-(ethylamino)-6-methylpyrimidin-2-yl)piperazin-1-yl)methanone (19). Compound **19** was prepared following General Synthetic Procedure D using **5a** (50 mg, 0.2 mmol), 3,5-dichlorobenzoyl chloride (63 mg, 0.34 mmol, 1.5 equiv) and TEA (27 mg, 0.27 mmol) in DCM. The crude product was purified by column chromatography (SiO_2, eluent: DCM/MeOH, 8:2), resulting in 51 mg of pure product (yield 65 %) as brown solid.

Mp 197 °C. Ret. time. 24.70 min, purity 97.6 %. HRESIMS m/z 394.1201 $[M+H]^+$ (calcd

for $C_{18}H_{22}Cl_2N_5O^+$, 394.1196, Δ = -1.4 ppm). ^{1}H NMR (500 MHz, d_6DMSO) δ = 1.08 (t, 3H, CH_3), 2.06 (s, 3H, pyr-CH_3), 3.24 (br, 2H, NCH_2), 3.32-3.63 (d, 4H, pip-H2,6), 3.66-3.75 (d, 4H, pip-H3,5), 5.64 (s, 1H, pyr-H5), 6.86 (br, 1H, NH), 7.51 (d, 2H, Ph-H2,6), 7.73 (t, 1H, Ph-H4). ^{13}C NMR (125 MHz, d_6DMSO) δ = 14.65 (CH_3), 23.73 (pyr-CH_3), 34.59 (NCH_2), 41.62-46.91 (pip-C2,6), 42.93-43.42 (pip-C3,5), 125.65 (Ph-C2,6), 129.06 (Ph-C4), 134.32 (Ph-C3,5), 139.49 (Ph-C1), 166.10 (amide-C), n.d. (pyr-C2), n.d. (pyr-C4), n.d. (pyr-C5), n.d. (pyr-6).

The characterization and spectral data of final compounds and intermediates 20a-64b are reported in Supporting Information.

Cell Lines and Virus Strains. Chikungunya virus, Indian Ocean strain 899, isolated in 2006 (Genbank FJ959103.1), was kindly provided by Prof. C. Drosten (Institute of Virology, University of Bonn, Germany). CHVB-resistant CHIKV was generated previously by passaging.[16] CHIKV was cultured on African green monkey kidney (Vero) cells (ATCC CCL-81) in minimum essential medium MEM Rega3 (Invitrogen, Belgium) supplemented with 10 % Foetal Bovine Serum (FBS; Integro, The Netherlands), 1 % L-glutamine and 1 % sodium bicarbonate (Invitrogen). Antiviral assays were performed in MEM Rega-3 medium supplemented with 2 % FBS.

Chikungunya virus-cell-based Antiviral Assay. Serial dilutions of compound were prepared in assay medium [MEM Rega3 (Cat. N°19993013; Invitrogen), 2 % FCS (Integro), 5 mL 200 mM L-glutamine (25030024), and 5 mL 7.5 % sodium bicarbonate (25080060)] that was added to empty wells of a 96-well microtiter plate (Falcon, BD). Subsequently, 50 µL of CHIKV (wt or CHVB-resistant) in assay medium was added (resulting in a MOI of 0.01), followed by 50 µL of Vero cell suspension (25 000 cells/50 µL). The assay plates were returned to the incubator (37 °C, 5 % CO_2, 95 to 99 % relative humidity) for 5 days (for the high-throughput screening) or 3 days (for the cross-resistance study), a time at which maximal virus-induced cell death or cytopathic effect (CPE) was observed in untreated, infected

controls. Subsequently, the assay medium was aspirated, replaced with 75 µL of a 5 % MTS (Promega) solution in phenol red-free medium and incubated for 1.5 hours. Absorbance was measured at a wavelength of 498 nm (Safire2, Tecan; optical densities (OD values) reached 0.6-0.8 for the untreated, uninfected controls). The EC_{50} (50 % effective concentration or concentration which is calculated to inhibit virus-induced cell death by 50 %) and CC_{50} (50 % antimetabolic concentration or concentration which is calculated to inhibit the overall cell metabolism by 50 %) values were derived from the dose-response curves. The 50 % effective concentration (EC_{50}) and the 90 % effective concentration (EC_{90}) are the concentrations of compound that inhibit virus replication by 50 % and 90 %, respectively. The overall antimetabolic effect of the compounds is shown as Cytostatic/Cytotoxic Concentration (CC_{50}). The CC_{50} is the calculated concentration of compound that causes a 50 % adverse effect on non-infected host cells (incorporates cytotoxic, cytostatic, and antimetabolic effect). All assay conditions producing an antiviral effect exceeding 50 % were checked microscopically for minor signs of CPE or adverse effects on the host cell (i.e. altered cell morphology). A compound was only considered to elicit a selective antiviral effect on virus replication when, following microscopic quality control, at least at one concentration of the compound, no CPE nor any adverse effect is observed (image resembling untreated, uninfected cells). Multiple independent experiments were performed.

Virus Yield Assay. Vero cells were seeded in 96-well plates at a density of 5×10^4 cells/well. The next day, cells were treated with serial dilutions of the compound and then infected with CHIKV-899 (MOI of 0.01). Two hours postinfection, the cells were washed to remove the nonadsorbed virus, followed by incubation with the same serial dilutions of compounds. After 48 h of incubation, viral RNA was quantified by real-time quantitative RT-PCR (qRT-PCR) as described previously.[16]

Aqueous Solubility. Samples were diluted in DMSO (control), phosphate buffer pH = 7.4 and pH = 2.0, from 5 mM stock solutions (dissolved in DMSO), to 120 µM final concentration. The samples were incubated for 24 hours at room temperature, followed by 30 minutes of centrifugation at 3700 rpm. Two individual sample solutions were made and measured.

40 µL of the supernatants were injected into HPLC (gradient elution, eluent A 0.1 % formic acid in water, eluent B acetonitrile, waters 2795 separation module and 996 PDA detector controlled by MassLynx 4.1 Column: X-Bridge C18 3.5 µm 4.6 × 50 mm) and the AUC (Absorbance Unit under the Curve) values (measured on sample-specific wavelength) of the buffered samples were divided by the AUC values (same wavelength as buffered samples) of the DMSO control samples.

***In Silico* cLogD.** The Graph Neural Network (GNN) was used for clogD calculation.[19]

***In Silico* Metabolic Stability.** The machine learning program FAst MEtabolizer 3 (FAME 3) was used for metabolic stability profiling and to assess critical sites of metabolism (SoMS).[31,32]

Metabolic Stability in Human Liver Microsomes. The stability of a test compound was determined in human liver microsomes (mixed gender and pool of 50) in 96-well plate format. The test compound is quantified at five time points by HPLC-MS/MS analysis with final microsomal protein concentration: 0.1 mg/mL and test concentration 0.1 µM with 0.01 % DMSO, 0.25 % acetonitrile and 0.25 % methanol.

The test compound is pre-incubated with pooled liver microsomes in phosphate buffer (pH 7.4) for 5 min in a 37 °C shaking water bath. The reaction is initiated by adding an NADPH-generating system and incubated for 0, 15, 30, 45 and 60 min. The reaction is stopped by transferring the incubation mixture to acetonitrile/methanol. Samples are then

mixed and centrifuged. Supernatants are used for HPLC-MS/MS analysis. Four reference compounds were used: propranolol and imipramine as relatively stable, whereas verapamil and terfenadine as readily metabolized reference compounds.

Samples are analyzed by HPLC-MS/MS using selected reaction monitoring. The HPLC system consists of a binary LC pump with an autosampler, a C-18 column, and a gradient. Peak areas corresponding to the test compound are recorded for data analysis. The compound remaining is calculated by comparing the peak area at each time point to time zero. The half-life is calculated from the slope of the initial linear range of the logarithmic curve of the compound remaining (%) vs time, assuming first-order kinetics. In addition, the intrinsic clearance (Clint) is calculated from the half-life using the following equation.

$$CLint_{(\mu L/min/mg\ protein)} = \frac{0.693}{T_{1/2} \times Protein\ Conc.}$$

***In Silico* hERG Channel Activity Profiling.** The Inte:Ligand Tox Pharmacophore DB was used for toxicity profiling of compounds within a KNIME workflow.[38,41]

***In Vitro* hERG Channel Activity Profiling.** Initial hERG Block Screening in Oocytes. Preparation of stage V–VI oocytes from Xenopus laevis (NASCO, Fort Atkinson, WI, USA), synthesis of capped runoff complementary ribonucleic acid (cRNA) transcripts from linearised complementary deoxyribonucleic acid (cDNA) templates, and injection of cRNA were performed as described previously.[40,42]

Currents through hERG channels were studied 1-3 days after cRNA injection using a two microelectrode voltage-clamp technique with a Turbo TEC-03X amplifier (npi electronic GmbH, Tamm, Germany). The extracellular recording solution contained: 96 mM NaCl, 2 mM KCl, 1 mM $MgCl_2$, 5 mM HEPES and 1.8 mM $CaCl_2$ (pH 7.5). Voltage-recording and current-injecting microelectrodes were filled with 3 M KCl and had resistances between 0.5 to 2 MΩ. Endogenous currents did not exceed 0.2 µA. Currents >3 µA were discarded to minimize voltage clamp errors. A precondition for all measurements was the achievement of

stable peak current amplitudes over periods of 10 min after an initial run-up period. Stocks were diluted in extracellular solution on the day of each experiment, and the maximal DMSO concentration (1 %) did not affect hERG currents. All compounds (30 µM) were applied by means of a fast perfusion system (ScreeningTool, npi electronic GmbH, Tamm, Germany).[39] Thioridazine hydrochloride (Sigma-Aldrich GmbH, Vienna, Austria) was used as positive control. The pClamp software package version 10.1 (Molecular Devices, Sunnyvale, CA, USA) was used for data acquisition.

Cytotoxicity Assay. Human colorectal adenocarcinoma cells CaCo-2 cells were seeded in 96 well plates at density 2000 cells/well in 100 µL/well medium and incubated for 24 hours. After that, cells were incubated with 100 µL of CHVB compound at different concentrations. The proportion of viable cells was determined after 24, 48 and 72 hours after exposure to CHVB compound by 3-(4,5-dimethylthiazol-2-yl)-2,-5 diphenyltetrazolium bromide (MTT)-based viability assay (EZ4U, Biomedica, Vienna, Austria). Briefly, 20 µL of EZ4U solution was added to each well. After incubation for 2 hours at 37 °C the absorbance was measured by a microplate reader at 450 nm with 620 nm as reference to reduce the unspecific background values. All experiments were carried out three times in triplicates.

Western Blot. Experiments were done as previously described.[43–46] Briefly, cells were grown in 100 µL cell culture dishes in 5% CO_2 incubator in DMEM medium supplemented with 5% fetal bovine serum. Medium was then aspirated, cells washed twice with PBS. Cells scrapped in lysis buffer (200 mM sodium acetate, 150 mM NaCL, pH 5.5 supplemented with 40 µM E-64 and transferred to 1.5 mL centrifuge tube. The cells were then homogenized on ice by ultrasonication then 0.1%triton X-100 were added. The homogenized cells were then extracted on ice for 30 minutes. Samples were then cleared by centrifugation 15000 x g for 10 minutes. The proteins were separated under reducing conditions by SDS-PAGE using 12.5% polyacrylamide gel along with prestained marker (cell signalling). Proteins were then transferred to nitrocellulose membrane (Santa Cruz Biotechnology) by semi-dry blot-

ting at 25 V for 30 minutes. Unspecific sites were then blocked for 3 hours by blocking solution (3% BSA in PBS). Membrane were then incubated for 90 minutes with the primary antibodies, caspase-3, cleaved caspase-3, PARP, and cleaved PARP (Thermo Fisher Scientific Inc.), washed five times with PBST and incubated another 90 minutes with the corresponding secondary antibodies and washed three times with PBST and once PBS. Enhanced chemiluminescence (Amersham ECL plus western blotting detection reagent, GE Healthcare, Vienna, Austria) was used for visualization. Membranes were exposed to X-ray films (Ammersham Hyper film ECL, GE Healthcare). Exposed films were scanned and quantified using ImageJ (NIH, Maryland, USA).

Authors Contributions

V.B. wrote the manuscript, coordinated the project, collected physiochemical, metabolic stability, and *in silico* data, and analysed the data from all reported assays; V.B. and J.M designed research project, designed synthesis routes and synthesized compounds; V.B. and E.U. analyzed identity of compounds; R.A., P.L., A.L.R.R., L.L., J.N, and L.D. performed antiviral assays; M.A, C.S, J.K, and J.R performed toxicological assays; L.D., E.U. and T.L. contributed with feedback and corrections. T.L., E.U., and G.P. supervised the project. All authors have given approval to the final version of the manuscript.

Funding Sources

This work was funded in parts (University of Innsbruck, KU Leuven, and University of Vienna) by European Union Seventh Framework Program (FP7/2007–2013) under SILVER grant (No. HEALTH-F3-2010-260644).

Notes

The authors declare no competing financial interest.

Abbreviations

CHIKV, Chikungunya virus; CHIKF, Chikungunya Fever, ADMET, absorption, distribution, metabolism, excretion, toxicity; HLM, human liver microsome; SAR, structure-activity relationship; SMR, structure-metabolism relationship; nsP1, non-structural protein 1, DMAP, 4-dimethylaminopyridine; Boc, tert-butyloxycarbonyl; TFA, trifluoroacetic acid; HCl, hydrochloric acid; DIPEA, N,N-diisopropylethylamine; THF, tetrahydrofuran; FA, formic acid; TOFA, triethyl orthoformate; DCM, dichloromethane; EtOAc, ethyl acetate; CPE, cytopathic effect; CHVBres, CHVB-resistant virus; wt, wild type.

Acknowledgement

We thank Caroline Collard for her excellent technical assistance in the acquisition of the antiviral data. Furthermore, we a grateful to J. Wackerlig and D. Dobusch for the assistance with the chemical analysis of the compounds. We further thank M. Sanguinetti (University of Utah, UT, USA) for kindly providing the cDNA used for the hERG Assay. We are also thankful for the excellent support by E. V. Dalietou, C. Dworschak, M. Guèrin, and A. Hodzic.

Supporting Information Available

Molecular Docking study, cytotoxic results, synthesis route for synthesis of **39** (Scheme S1), experimental procedures, and characterisation data for final compounds and intermediates **20a-64b** are reported in the Supporting Information.

References

(1) Robinson, M. C. An epidemic of virus disease in Southern Province, Tanganyika Territory, in 1952-53. I. Clinical features. *Transactions of The Royal Society of Tropical Medicine and Hygiene* **1955**, *49*, 28–32.

(2) Chretien, J. P.; Anyamba, A.; Bedno, S. A.; Breiman, R. F.; Sang, R.; Sergon, K.; Powers, A. M.; Onyango, C. O.; Small, J.; Tucker, C. J.; Linthicum, K. J. Drought-associated chikungunya emergence along coastal East Africa. *American Journal of Tropical Medicine and Hygiene* **2007**, *76*, 405–407.

(3) Vazeille, M.; Moutailler, S.; Coudrier, D.; Rousseaux, C.; Khun, H.; Huerre, M.; Thiria, J.; Bastien Dehecq, J.-S.; Fontenille, D.; Schuffenecker, I.; Despres, P.; Failloux, A.-B. Two Chikungunya isolates from the outbreak of La Reunion (Indian Ocean) exhibit different patterns of infection in the mosquito, Aedes albopictus. *PloS ONE* **2007**, *2*, e1168.

(4) Zeller, H.; Van Bortel, W.; Sudre, B. Chikungunya: Its History in Africa and Asia and Its Spread to New Regions in 2013-2014. *The Journal of Infectious Diseases* **2015**, *214*, 436–440.

(5) Venturi, G. et al. Detection of a chikungunya outbreak in central Italy, August to September 2017. *Eurosurveillance* **2017**, *22*, 11–14.

(6) Calba, C. et al. Preliminary report of an autochthonous chikungunya outbreak in France, July to September 2017. *Eurosurveillance* **2017**, *22*, 5–10.

(7) WHO Media Centre, Chikungunya - key facts. 2020; `https://www.who.int/news-room/fact-sheets/detail/chikungunya`, Accessed: 31.05.2022.

(8) Campbell, L. P.; Luther, C.; Moo-Llanes, D.; Ramsey, J. M.; Danis-Lozano, R.; Peterson, A. T. Climate change influences on global distributions of dengue and chikungunya virus vectors. *Philos Trans R Soc Lond B Biol Sci* **2015**, *370*, 1–9.

(9) Thiberville, S.-D.; Moyen, N.; Dupuis-Maguiraga, L.; Nougairede, A.; Gould, E. A.; Roques, P.; De Lamballerie, X. Chikungunya fever: epidemiology, clinical syndrome, pathogenesis and therapy. *Antiviral Research* **2013**, *99*, 345–370.

(10) Ross, R. W. The Newala epidemic. III. The virus: isolation, pathogenic properties and relationship to the epidemic. *Journal of Hygiene* **1956**, *54*, 177–191.

(11) Borgherini, G.; Poubeau, P.; Jossaume, A.; Gouix, A.; Cotte, L.; Michault, A.; Arvin-Berod, C.; Paganin, F. Persistent arthralgia associated with chikungunya virus: a study of 88 adult patients on reunion island. *Clinical Infectious Diseases* **2008**, *47*, 469–475.

(12) Lebrun, G.; Chadda, K.; Reboux, A. H.; Martinet, O.; Gaüzère, B. A. Guillain-Barré Syndrome after Chikungunya Infection. *Emerging Infectious Diseases* **2009**, *15*, 495–496.

(13) Battisti, V.; Urban, E.; Langer, T. Antivirals against the Chikungunya Virus. *Viruses* **2021**, *13*, 1307.

(14) Kennedy Amaral Pereira, J.; Schoen, R. T. Management of chikungunya arthritis. *Clinical Rheumatology* **2017**, *36*, 2179–2186.

(15) Moesslacher, J.; Battisti, V.; Delang, L.; Neyts, J.; Abdelnabi, R.; Pürstinger, G.; Urban, E.; Langer, T. Identification of 2-(4-(Phenylsulfonyl)piperazine-1-yl)pyrimidine Analogues as Novel Inhibitors of Chikungunya Virus. *ACS Medicinal Chemistry Letters* **2020**, *11*, 906–912.

(16) Abdelnabi, R. et al. Novel Class of Chikungunya Virus Small Molecule Inhibitors That Targets the Viral Capping Machinery. *Antimicrobial Agents and Chemotherapy* **2020**, *64*, e00649–20.

(17) Moussa, I. A.; Banister, S. D.; Beinat, C.; Giboureau, N.; Reynolds, A. J.; Kassiou, M. Design, Synthesis, and Structure-Affinity Relationships of Regioisomeric N-Benzyl Alkyl Ether Piperazine Derivatives as σ-1 Receptor Ligands. *Journal of Medicinal Chemistry* **2010**, *53*, 6228–6239.

(18) Leonczak, P.; Srivastava, P.; Bande, O.; Schepers, G.; Lescrinier, E.; Herdewijn, P. N8-Glycosylated 8-Azapurine and Methylated Purine Nucleobases: Synthesis and Study of Base Pairing Properties. *Journal of Organic Chemistry* **2019**, *84*, 13394–13409.

(19) Wieder, O.; Kuenemann, M.; Wieder, M.; Seidel, T.; Meyer, C.; Bryant, S. D.; Langer, T. Improved Lipophilicity and Aqueous Solubility Prediction with Composite Graph Neural Networks. *Molecules* **2021**, *26*.

(20) Seley-Radtke, K. L.; Yates, M. K. The evolution of nucleoside analogue antivirals: A review for chemists and non-chemists. Part 1: Early structural modifications to the nucleoside scaffold. *Antiviral Research* **2018**, *154*, 66–86.

(21) Eyer, L.; Nencka, R.; de Clercq, E.; Seley-Radtke, K.; Růžek, D. Nucleoside analogs as a rich source of antiviral agents active against arthropod-borne flaviviruses. *Antiviral Chemistry and Chemotherapy* **2018**, *26*, 1–28.

(22) Delang, L. et al. The viral capping enzyme nsP1: a novel target for the inhibition of chikungunya virus infection. *Scientific Reports* **2016**, *6*, 31819.

(23) Kovacikova, K.; Morren, B. M.; Tas, A.; Albulescu, I. C.; Van Rijswijk, R.; Jarhad, D. B.; Shin, Y. S.; Jang, M. H.; Kim, G.; Lee, H. W.; Jeong, L. S.; Snijder, E. J.; Van Hemert, M. J. 6'-β-Fluoro-Homoaristeromycin and 6'-Fluoro-Homoneplanocin A

Are Potent Inhibitors of Chikungunya Virus Replication through Their Direct Effect on Viral Nonstructural Protein 1. *Antimicrobial Agents and Chemotherapy* **2020**, *64*, 02532–19.

(24) Mudgal, R.; Mahajan, S.; Tomar, S. Inhibition of Chikungunya virus by an adenosine analog targeting the SAM-dependent nsP1 methyltransferase. *FEBS Letters* **2020**, *594*, 678–694.

(25) Hiesinger, K.; Dar'In, D.; Proschak, E.; Krasavin, M. Spirocyclic Scaffolds in Medicinal Chemistry. *Journal of Medicinal Chemistry* **2021**, *64*, 150–183.

(26) Talele, T. T. Opportunities for Tapping into Three-Dimensional Chemical Space through a Quaternary Carbon. *Journal of Medicinal Chemistry* **2020**, *63*, 13291–13315.

(27) Wei, W.; Cherukupalli, S.; Jing, L.; Liu, X.; Zhan, P. Fsp^3: A new parameter for drug-likeness. *Drug Discovery Today* **2020**, *25*, 1839–1845.

(28) Lovering, F.; Bikker, J.; Humblet, C. Escape from flatland: Increasing saturation as an approach to improving clinical success. *Journal of Medicinal Chemistry* **2009**, *52*, 6752–6756.

(29) Bassetto, M.; Massarotti, A.; Coluccia, A.; Brancale, A. Structural biology in antiviral drug discovery. *Current Opinion in Pharmacology* **2016**, *30*, 116–130.

(30) Hughes, J.; Rees, S.; Kalindjian, S.; Philpott, K. Principles of early drug discovery. *British Journal of Pharmacology* **2011**, *162*, 1239–1249.

(31) Stork, C.; Embruch, G.; Šícho, M.; De Bruyn Kops, C.; Chen, Y.; Svozil, D.; Kirchmair, J. NERDD: a web portal providing access to in silico tools for drug discovery. *Bioinformatics* **2020**, *36*, 1291–1292.

(32) Šícho, M.; Stork, C.; Mazzolari, A.; De Bruyn Kops, C.; Pedretti, A.; Testa, B.; Vistoli, G.; Svozil, D.; Kirchmair, J. FAME 3: Predicting the Sites of Metabolism in Synthetic Compounds and Natural Products for Phase 1 and Phase 2 Metabolic Enzymes. *Journal of Chemical Information and Modeling* **2019**, *59*, 3400–3412.

(33) Penning, T. D. et al. Synthesis and biological evaluation of the 1,5-diarylpyrazole class of cyclooxygenase-2 inhibitors: identification of 4-[5-(4-methylphenyl)-3-(trifluoromethyl)-1H-pyrazol-1-yl]benze nesulfonamide (SC-58635, celecoxib). *Journal of Medicinal Chemistry* **1997**, *40*, 1347–1365.

(34) Clader, J. W. The Discovery of Ezetimibe: A View from Outside the Receptor. *Journal of Medicinal Chemistry* **2004**, *47*, 1–9.

(35) Johnson, B. M.; Shu, Y.-Z.; Zhuo, X.; Meanwell, N. A. Metabolic and Pharmaceutical Aspects of Fluorinated Compounds. *Journal of Medicinal Chemistry* **2020**, *63*, 6315–6386.

(36) Purser, S.; Moore, P. R.; Swallow, S.; Gouverneur, V. Fluorine in medicinal chemistry. *Chemical Society Reviews* **2008**, *37*, 320–330.

(37) Chaitanya, G. V.; Alexander, J. S.; Babu, P. P. PARP-1 cleavage fragments: Signatures of cell-death proteases in neurodegeneration. *Cell Communication and Signaling* **2010**, *8*, 31.

(38) Wolber, G.; Langer, T. LigandScout: 3-D pharmacophores derived from protein-bound ligands and their use as virtual screening filters. *Journal of Chemical Information and Modeling* **2005**, *45*, 160–169.

(39) Baburin, I.; Beyl, S.; Hering, S. Automated fast perfusion of Xenopus oocytes for drug screening. *Pflugers Archiv European Journal of Physiology* **2006**, *453*, 117–123.

(40) Kratz, J. M.; Schuster, D.; Edtbauer, M.; Saxena, P.; Mair, C. E.; Kirchebner, J.; Matuszczak, B.; Baburin, I.; Hering, S.; Rollinger, J. M. Experimentally validated hERG pharmacophore models as cardiotoxicity prediction tools. *Journal of Chemical Information and Modeling* **2014**, *54*, 2887–2901.

(41) Berthold, M. R.; Cebron, N.; Dill, F.; Gabriel, T. R.; Kötter, T.; Meinl, T.; Ohl, P.; Sieb, C.; Thiel, K.; Wiswedel, B. In *Data Analysis, Machine Learning and Applications*; Preisach, C., Burkhardt, H., Schmidt-Thieme, L., Decke, R., Eds.; Springer: New York, 2008.

(42) Stork, D.; Timin, E. N.; Berjukow, S.; Huber, C.; Hohaus, A.; Auer, M.; Hering, S. State dependent dissociation of HERG channel inhibitors. *British Journal of Pharmacology* **2007**, *151*, 1368–1376.

(43) Shabbir, W.; Topcagic, N.; Aufy, M. Activation of autosomal recessive Pseudohypoaldosteronism1 ENaC with aldosterone. *European Journal of Pharmacology* **2021**, *901*, 174090.

(44) Willam, A.; Aufy, M.; Tzotzos, S.; Evanzin, H.; Chytracek, S.; Geppert, S.; Fischer, B.; Fischer, H.; Pietschmann, H.; Czikora, I.; Lucas, R.; Lemmens-Gruber, R.; Shabbir, W. Restoration of epithelial sodium channel function by synthetic peptides in pseudohypoaldosteronism type 1B mutants. *Frontiers in Pharmacology* **2017**, *8*, 85.

(45) Shabbir, W.; Topcagic, N.; Aufy, M.; Oz, M. CRISPR/CAS9 mediated knock down of δ-ENaC blunted the TNF-induced activation of ENaC in A549 cells. *International Journal of Molecular Sciences* **2021**, *22*, 1–10.

(46) Willam, A. et al. TNF lectin-like domain restores epithelial sodium channel function in frameshift mutants associated with pseudohypoaldosteronism type 1B. *Frontiers in Immunology* **2017**, *8*, 601.

TOC Graphic

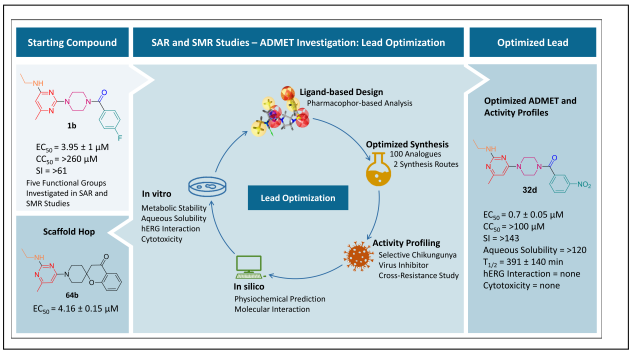
Starting Compound
SAR and SMR Studies – ADMET Investigation: Lead Optimization
Optimized Lead
1b
EC50 = 3.95 ± 1 µM
CC50 = >260 µM
SI = >61
Five Functional Groups Investigated in SAR and SMR Studies
Scaffold Hop
64b
EC50 = 4.16 ± 0.15 µM
Ligand-based Design
Pharmacophor-based Analysis
Optimized Synthesis
100 Analogues
2 Synthesis Routes
Activity Profiling
Selective Chikungunya Virus Inhibitor
Cross-Resistance Study
In silico
Physiochemical Prediction
Molecular Interaction
In vitro
Metabolic Stability
Aqueous Solubility
hERG Interaction
Cytotoxicity
Lead Optimization
Optimized ADMET and Activity Profiles
32d
EC50 = 0.7 ± 0.05 µM
CC50 = >100 µM
SI = >143
Aqueous Solubility = >120
T1/2 = 391 ± 140 min
hERG Interaction = none
Cytotoxicity = none

4.3 Molecular Interactions and Docking

Molecular Docking

Molecular docking was considered valuable to get a better understanding of the possible interactions between our CHVB series and the proposed biological target. However, no structural data is available for any co-crystal of CHVB analogues and the non-structural protein 1 (nsP1). Nevertheless, to gain insight into possible binding modes, we started our experiment by detecting and investigating potential binding sites. Five possible binding sites were identified by deploying the Protein Preparation Wizard and SiteMap pocket prediction tools.[1,2] Due to the circular shape formed by 12 subunits, three of the predicted pocket sites were omitted as they were located at the same position of the protein - just in another subunit. The docking was performed with our lead compound **1b** in the two identified binding pockets located in the crown/waist area of the dodecameric ring protein (see Figure S1).[3]

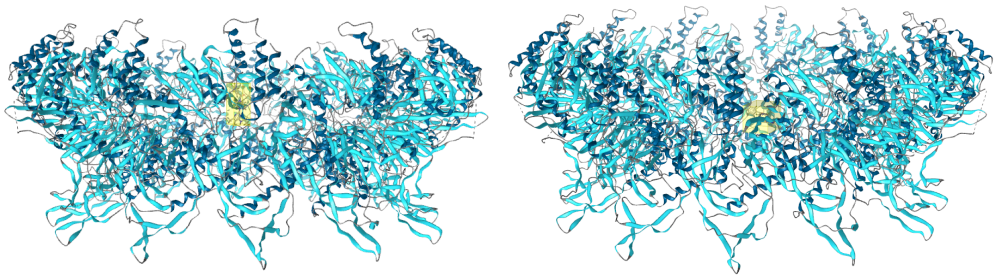

(a) NsP1 with pocket A. (b) NsP1 with pocket B.

Figure S1: Lateral view of the CHIKV nsP1 CHIKV with the investigated binding sites (yellow boxes) in the crown/waist area.

Interestingly, both investigated binding sites showed similar interactions with **1b** (see Figure S2). Further, all the unveiled essential functional groups and structural aspects of the CHVB series in the structure-activity relationship studies were also observed interaction sites of the compound **1b** in both binding pockets.[4] Both the phenyl and the pyrimidine regions had the most substantial influence on the biological activity and also showed in this docking study interaction with the target protein (lipophilic and $\pi - \pi$ interactions). Moreover, the crucial ethylamine sidechain on the pyrimidine ring demonstrated a lipophilic interaction (ALA69/THR378) and additional hydrogen bond donor activity with GLU283

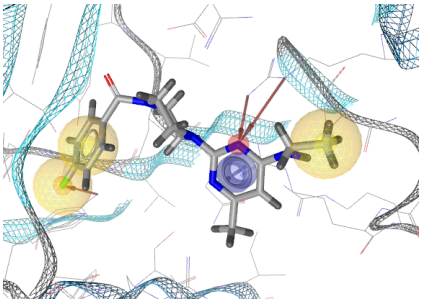

(a) **1b** binding pose in pocket A.

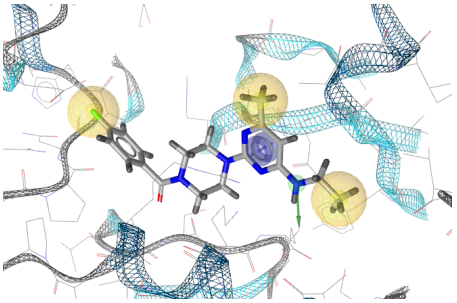

(b) **1b** binding pose in pocket B.

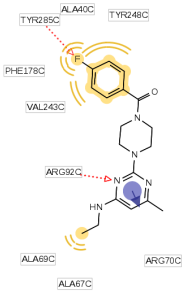

(c) Protein-ligand interactions of pocket A.

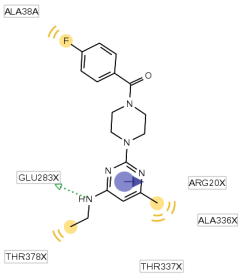

(d) Protein-ligand interactions of pocket B.

Figure S2: **1b** in possible binding pockets of the CHIKV nsp1. Ligand-protein interactions are color coded: green = hydrogen bond interaction (donor), red = hydrogen bond interaction (acceptor), violet = aromatic interaction, yellow = hydrophobic interactions. (a)/(c) Binding pose and interactions of **1b** and nsP1 in pocket A. (b)/(d) Binding pose and interactions of **1b** and nsP1 in pocket A.

---

in the case of pocket B. As discussed in the SAR chapter, the position of the nitrogens on the pyrimidine ring is connected with the antiviral outcome and, therefore, a possible interaction site of our compound series. Consistent with our observations in the SAR study, the lone electron pair of the pyrimidine nitrogen interacts with the target protein ARG92 as a hydrogen bond acceptor (pocket A, Figure S2c) and may be therefore essential or beneficial for a good biological activity. Additionally, the core region formed by the piperazine and carbonyl groups exhibits no interactions with the protein in both binding sites, which agrees with the SAR observation that this area functions solely as a linker that keeps the needed distance between the phenyl and pyrimidine regions.

However, the results of this docking study should be interpreted with caution, as the *in silico* investigations (although accurately and thoroughly performed) remain an approximation tool to predict possible binding sites and interactions but still need experimental confirmations.

Molecular Docking - Experimental Procedure

The CryoEM structure of the Chikungunya virus non-structural protein 1 (nsP1; PDB code: 6Z0V) was retrieved from the protein data bank (RSCB-PDB, www.rscb.org) for docking analysis.[3] The protein was prepared for the docking study (e.g., the addition of missing hydrogen atoms, removing of co-crystallized water) utilizing the Protein Preparation Wizard tool and the ligand **1b** with LigPrep by Schrödinger.[1] The pocket prediction tool SiteMap was applied to investigate possible binding sites for the protein-ligand interactions, and the docking was performed with AutoDock Vina.[2,5] A maximum of 10 conformers of the ligand **1b** for each binding site was investigated. Interactions between the ligand and the protein were explored using the LigandScouts 3D interaction pharmacophores.[6]

References

(1) Madhavi Sastry, G.; Adzhigirey, M.; Day, T.; Annabhimoju, R.; Sherman, W. Protein and ligand preparation: parameters, protocols, and influence on virtual screening enrichments. *Journal of Computer-Aided Molecular Design* **2013**, *27*, 221–234.

(2) Halgren, T. New Method for Fast and Accurate Binding-site Identification and Analysis. *Chemical Biology & Drug Design* **2007**, *69*, 146–148.

(3) Jones, R.; Bragagnolo, G.; Arranz, R.; Reguera, J. Capping pores of alphavirus nsP1 gate membranous viral replication factories. *Nature* **2021**, *589*, 615–619.

(4) Moesslacher, J.; Battisti, V.; Delang, L.; Neyts, J.; Abdelnabi, R.; Pürstinger, G.; Urban, E.; Langer, T. Identification of 2-(4-(Phenylsulfonyl)piperazine-1-yl)pyrimidine Analogues as Novel Inhibitors of Chikungunya Virus. *ACS Medicinal Chemistry Letters* **2020**, *11*, 906–912.

(5) Trott, O.; Olson, A. J. AutoDock Vina: Improving the speed and accuracy of docking with a new scoring function, efficient optimization, and multithreading. *Journal of Computational Chemistry* **2010**, *31*, 455–461.

(6) Wolber, G.; Langer, T. LigandScout: 3-D pharmacophores derived from protein-bound ligands and their use as virtual screening filters. *Journal of Chemical Information and Modeling* **2005**, *45*, 160–169.

4.4 Conclusion

In this publication, a thorough lead optimisation of the lead **1b** (former **6a**, elaborated in [64]) is presented, and additional assays to expand the knowledge about the antiviral profile of the CHVB series were conducted.

An optimised synthesis route (Synthesis Route B) improved the accessibility of the designed analogues by starting with a nucleophilic acyl substitution between Boc-protected piperazine and benzoyl chloride, followed by acidic catalysed Boc-deprotection and substitution reaction of the previously prepared arylamine intermediate under microwave irradiation. Shortened reaction times, a more manageable or sometimes unrequired purification, and a higher-yielding outcome lead to remarkable time- and yield-wise advantage to the previous established Synthesis Route A (described in [64]) and facilitates the synthesis of CHVB analogues.

Overall, 100 CHVB analogues (second-generation CHVB analogues) were synthesised and assessed for their antiviral activity against the CHIKV by CPE-reduction assays in Vero cells, which was further validated in a virus yield assay. With all 100 compounds, an extensive SAR investigation was performed - focusing mainly on the combination of scaffold changes and the structural requirements for a high anti-CHIKV inhibition. Mainly, the positions of the nitrogens in the pyrimidine ring in combination with a sulfonamide or an amide bridge influenced the biological activity of the CHVB series.

A thorough absorption, distribution, metabolism, excretion, and toxicity (ADMET) analysis was realised to examine the compounds for their physicochemical properties, metabolic stability, possible hERG channel interactions, and toxicological profile. As physiochemical parameters, such as the aqueous solubility and $\mathrm{LogD_{pH\ 7.4}}$, highly influence the absorption and distribution of a potential drug, all 100 analogues were assessed for their physiochemical profile [8]. Overall this second-generation of CHVB compounds showed druggable physiochemical characteristics.

Further, neither *in silico* nor *in vitro* hERG channel interactions were observed. The *in vitro* cytotoxicity investigation in a cancer cell line (CaCo-2) determined no significant toxicity for this compound series. Additionally, no increased expression of the apoptosis proteins caspase-3 and poly ADP ribose polymerase (PARP) in western blot analysis was observed - making this compound series an overall safe candidate for further *in vivo* studies.

The *in silico* metabolic stability investigation, followed by the *in vitro* determination of the microsomal half-life ($t_{1/2}$) in human liver microsomes (HLMs) of 55 CHVB analogues unveiled through a structure-metabolism relationship (SMR) study the structural

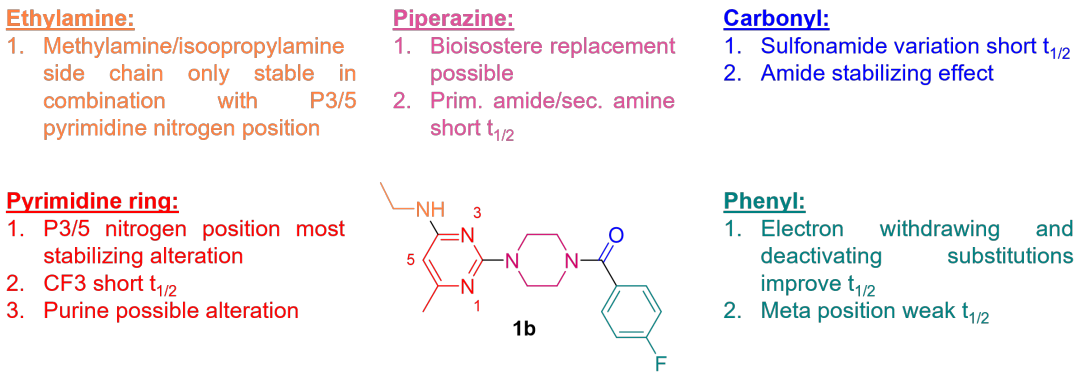

FIGURE 4.4.1: Summary of the structural requirements for metabolic stability

requirements for good metabolic stability. Figure 4.4.1 summarises the outcome of the conducted SMR study. The compounds showed overall high stability with a mean half-life time of >60 min for 37 analogues. Interestingly, similar to the biological activity, the positions of the nitrogens in the pyrimidine ring in combination with a sulfonamide or an amide bridge had a significant impact on the metabolic stability - making the most active compounds also the most stable.

As described in chapter 3 the viral capping machinery was identified as the viral target of the CHVB series. Further, CPE reduction assays with various other alphaviruses unveiled the CHVB series as selective CHIKV inhibitors [69]. Additional assays with the second-generation CHVB compounds with different (alpha)viruses showed similar selective biological activity. Moreover, a cross-resistance study confirmed the viral capping machinery to be the viral target of these novel CHVB compounds. Therefore, a molecular docking study was performed to get an insight into possible interactions between the compound series and their antiviral target protein (nsP1, published in the Supporting Material of [65] and incorporated in this thesis in section 4.3). Further, a successful scaffold hop for future antiviral research studies was carried out (described further in section 5.2.2).

Overall, out of the 100 novel CHVB compounds:

- 68 were active ($EC_{50} \leq 40\,\mu M$),
- 43 were in a low micromolar range ($EC_{50} \leq 10\,\mu M$),
- 34 were more active than the initial hit compound **1a** (EC_{50}: $8.7 \pm 0.1\,\mu M$),
- 24 were more active than the lead compound **1b** (EC_{50}: $3.95 \pm 0.01\,\mu M$),
- and 10 compounds demonstrated a remarkable high antiviral activity ($EC_{50} \leq 1\,\mu M$).

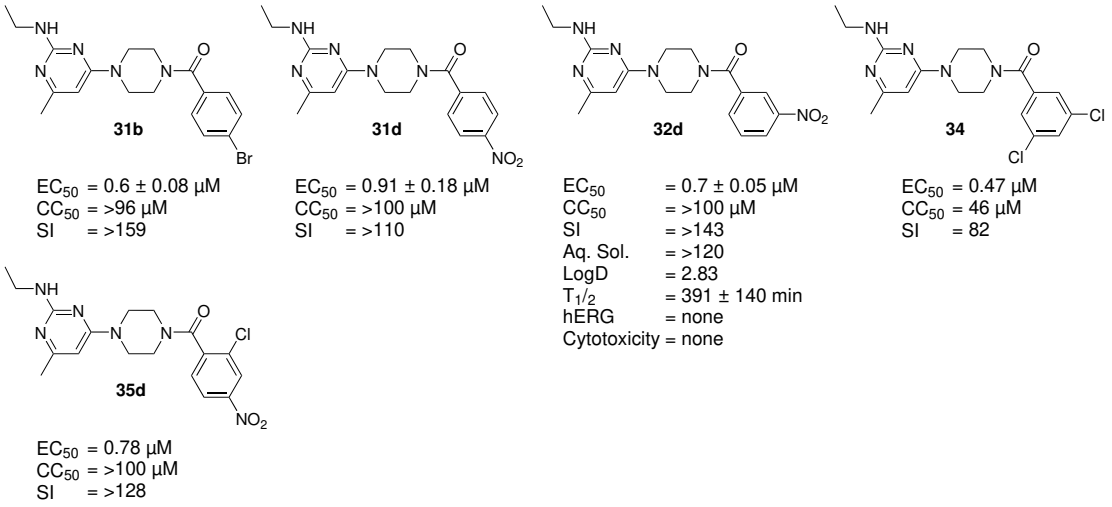

FIGURE 4.4.2: The most promising lead compounds for further drug development. **32d** demonstrates overall the most druggable characteristics.

Figure 4.4.2 depicts the identified most promising compounds, namely **31b**, **31d**, **32d**, **34**, and **35d**. They can be considered as highly potent, safe, and stable lead compounds for further development as antiviral inhibitors of CHIKV. Of all these new lead compounds, **32d** demonstrates the most druggable characteristics throughout all assessed assays.

Additional *in vitro* assays for evaluating the cytotoxicity of the second-generation CHVB compounds were performed with human embryonic kidney 293 (HEK 293) and adenocarcinomic human alveolar basal epithelial 549 (A549) cells (unpublished). No cytotoxic effects were detected in these cell lines (shown in Appendix 5).

Chapter 5

Virtual Screening and Scaffold Hopping

5.1 Introduction

As the target molecule of the CHVB series (nsP1) had not yet been crystallized and published at this research project stage, two different ligand-based strategies were conducted: i) a pharmacophore-based virtual screening and ii) a SAR-based scaffold hop.

The pharmacophore-based virtual screening was performed to identify compounds with similar chemical features as the CHVB series but with different functional groups. Therefore, the retrieved hits should give ideas for a possible scaffold hop, help to get a deeper insight into the structure-activity relationship of the CHVB series and reveal structural boundaries of the known CHVB scaffold. Moreover, the SAR-based scaffold hop was carried out to identify a possible new hit compound with antiviral activity.

A more detailed discussion about the hit discovery process, ligand-based drug design, the theory behind a SAR study, pharmacophore models, bioisosteric replacement, and the aim of a successful scaffold hop is given in chapter 1.

5.2 Results and Discussion

5.2.1 Pharmacophore-based Virtual Screening

Virtual screening of three databases (Prestwick, DrugBank, and Aldrich Market Select (AMS)) was performed with pharmacophore models based on the most active and safest

CHVB compounds (high EC_{50} and SI values). The screening of the two smaller libraries (Prestwick and DrugBank) yielded zero hits, showing that the created pharmacophore models were selective enough for the following screening of the 8 million AMS library.

Three thousand fifty compounds were retrieved from the AMS screening from which duplicates (481), already synthesized (28), predicted cytotoxic (28), and not drug-like compounds (449) were removed. The remaining hits (2064) were clustered according to their chemical scaffold. Visual inspection revealed that a majority of the retrieved hits showed similar chemical features as the starting scaffold. Therefore, compounds with an interesting deviation of the known CHVB scaffold were prioritized as they could give ideas for a new hit compound and give some more insight into the structure-activity relationship of the CHVB compounds, improving the CHVB lead optimisation simultaneously.

The 56 hits retrieved from the pharmacophore model generated from the two most potent and safest compounds (**33b** and **34**) were compared with the remaining hit list, and twelve compounds with six different scaffolds were selected for biological testing against the CHIKV. The chemical structures and the biological activity are shown in figure 5.2.1. To facilitate the compound referencing and to improve the readability, the compound numbering was carried on from the [65] publication, and hence the first hit was numbered **65a**. Their chemical data and NMR spectra are given in Appendix .0.1.

The biological outcome of the hits corresponds with the conclusion made from the two SAR studies in [64] and [65]. All compounds with a flexible core and an ethylamine-urea (**65a-d**) or an ethylamine-sulfonamide (**66**) show either very weak or no activity at all. Previous results concluded that this region functions as a linker that keeps the relative distance between the two target-interacting groups. Moreover, structural changes with more rigid characteristics were identified as possible modifications for future studies [64]. The loss of activity when the piperazine core structure gets altered into a flexible chain further confirms the need for a rigid linker.

Interestingly, the secondary amine next to the pyrimidine ring had not the beneficial effect on the biological activity as observed in the analogues **57a-b** and **59b** in publication [65]. Therefore, the effect of the additional HBD may also depend on the stability of the compound's core structure. Moreover, compounds with the additional HBD as a sec. amide (**55a-56b**, and **58a-b** in publication [65] of chapter 4) showed no anti-CHIKV activity. This still holds for **67a-b** bearing an urea substructure.

Three compounds with a much bulkier p-toluidine side chain as the CHVB's ethylamine were chosen for biological testing to investigate whether a possible scaffold change was, until now, overlooked at this part of the chemical structure. As discussed in [65], chapter 4

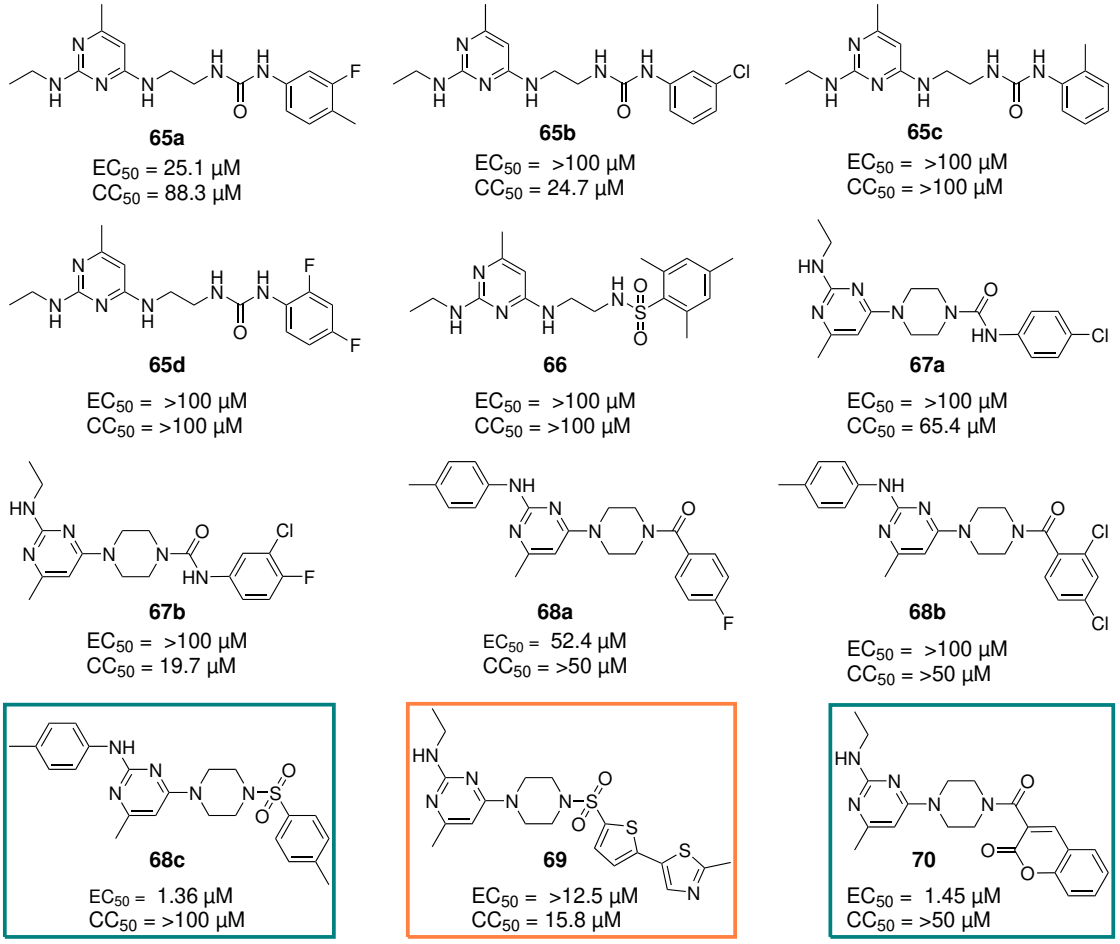

FIGURE 5.2.1: Compounds retrieved from virtual screening and their biological activity against the CHIKV. The compounds with antiviral activity are colour-coded (green: good activity, orange: medium activity).

and [64], chapter 2, a bifurcated isopropylamine or even tert. butylamine side chain is tolerated in the sulfonamide but not in the amide scaffold. Following the SAR studies, the two amide compounds **68a-b** did not show any activity against the CHIKV. Interestingly, the p-toluidine with the sulfonamide scaffold in **68c** gave an impressive EC_{50} value of 1.34 µM - indicating a new site for a potential scaffold change. Further, this outcome reinforces the theory that the sulfonamide influences the activity not only as a potential interacting partner but probably also as a linker for keeping the desired active groups (pyrimidine and phenyl) at the proper distance and angle (see [64] and [65]).

Surprisingly, the two compounds with a heterocycle replacement **69** and **70** showed biological activities. **69** with a 2-methyl-5-(thiophen-2-yl)thiazole group gave some antiviral activity but also toxic characteristics, whereas the coumarin bearing **70** was highly active and safe in the performed *in vitro* assays. Other investigated (hetero)aromatic replacements of the phenyl group showed neither cytotoxicity nor antiviral activity (see **11a-12d**

published in [65]) - except the naphthalen-2-yl analogue **12b**. Therefore, naphthalene/-coumarin bioisostere replacement of the phenyl group was considered an interesting approach for a possible scaffold hop (see [65] and section 5.2.2).

5.2.2 SAR-based Scaffold Hopping

Based on the two SAR studies discussed in chapter 2 and 4, the result of the virtual screening and the theory of bioisosteric replacement, a scaffold hop was realised, and a new hit compound incorporating important chemical features was found (published as compound **64b** in [65]). Keeping the high active pyrimidine nitrogen position P3/5 and ethylamine structure, a new spiro[chromane-2,4'-piperidin]-4-one group was introduced based on the outcome discussed in section 5.2.1 and most of the essential structural features were preserved (e.g., the required relative distance and angle of the piperazine group, two hydrogen bond acceptors, and an aromatic ring).

The chemical structure is shown in figure 5.2.2 and a more detailed discussion of the SAR-based scaffold hop is given [65].

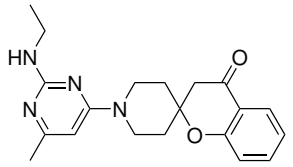

64b
EC_{50} : 4.16 ± 0.15 µM

FIGURE 5.2.2: Structures of the new hit compound **64b** identified based on the two SAR studies performed with the CHVB compounds and the outcome of the pharmacophore-based virtual screening [65].

5.3 Conclusion

Due to the lack of the target protein, two ligand-based approaches were conducted to broaden the knowledge about the CHVB series and to discover a possible new starting point for future research projects.

The pharmacophore-based virtual screening retrieved twelve compounds with interesting variations of the known CHVB scaffold. Their anti-CHIKV activity was assessed via CPE assay in Vero cells, and the identified structural influence on the biological activity was in line with the two conducted SAR studies. **68c** and **70** showed strong CHIKV inhibition with EC_{50} values of 1.36 µM and 1.45 µM, respectively.

Further, a SAR-based scaffold hop was performed, which resulted in **64b** with a spiro[chromane-2,4'-piperidin]-4-one group. The assessed EC_{50} value of $4.16 \pm 0.15\,\mu M$ demonstrates that **64b** could be a excellent starting point for a lead optimisation study.

5.4 Experimental Procedure

5.4.1 Pharmacophore-based Virtual Screening

The ligand-based strategy was applied on at that point synthesized and tested 76 CHVB compounds (all 38 published compounds in [64] discussed in chapter 2, and additional 38 compounds (**10a**, **11-17b**, **22-31b**, **31d-43**, and **39**) published in [65] discussed in chapter 4.

The 3D pharmacophoric features of these compounds were generated considering their conformational flexibility and rigidity utilizing the LigandScout pharmacophore generator [75, 76]. Compounds with the highest SI and lowest EC_{50} were selected for the training set, whereas the remaining compounds formed the test set - including the compounds with higher CC_{50} values than their biological activity ($EC_{50} < CC_{50}$, toxic test set) and compounds with none or very weak activity (decoy test set). Further, a toxic pharmacophore model (toxicophore) based on the toxic test set was made for additional filtering of the screening results.

The identified necessary scaffold features guided a refinement process of the pharmacophore models retrieved from the training set from the conducted SAR study discussed in chapter 2. The validation of the refined pharmacophore models was assessed by screening the test sets. A satisfactory outcome was reached by retrieving none of the decoy or toxic test set but all of the active and safe compounds in the test set. On the other hand, the toxicophore model was modified to retrieve only the compounds in the toxic test set and non of the safe compounds.

Three different chemical libraries were used for screening: the two smaller libraries, DrugBank and Prestwick Chemical Library, followed by the large library AMS [77–79]. A hit rate <0.01% was aimed to prove the model's selectivity. Duplicates and already synthesized compounds, as well as the retrieved hits from the toxicophore model, were removed from the hit lists. Based on the Lipinski Rule of Five, the remaining compounds were evaluated according to their physicochemical properties and drug-likeness [80]. Subsequently, the compounds fulfilling these criteria were clustered via the radial distribution function (RDF) code similarity algorithm of LigandScout to reveal structural similarities between the remaining hits. Twelve compounds with interesting scaffold variations of

the CHVB series were selected, and their anti-CHIKV activity was assessed via CPE reduction assay in Vero Cells.

5.4.2 SAR-based Scaffold Hopping

Two thorough SAR studies were performed throughout this research project (see capter 2 and 4). The gathered structural information and their relevance for a good antiviral activity led to designing a new antiviral compound based on the CHVB scaffold. This SAR-based scaffold hop is further discussed in [65] (chapter 4).

Chapter 6

Conclusion

In this thesis, a thorough lead optimisation study discovered new potent small-molecule inhibitors against CHIKV. This second-generation CHVB compounds show favourable ADMET and biological characteristics to reach the next step in drug development (*in vivo* studies and clinical phase).

After the identification of a new hit compound (**1a**) by an HTS, the first SAR study under the lead of Dr Moesslacher was performed. Thirty-seven 2-(4-(phenylsulfonyl)piperazine-1-yl)pyrimidine analogues were synthesised in a four-step synthesis route and analysed for their biological activity. These compounds are the first-generation of the CHVB series [64]. The generated new lead compound **1b** forms with additional twenty-eight compounds, which were incorporated in [65], the basis for this thesis.

1b showed interesting *in vitro* biological activity and an excellent toxicological profile. Nevertheless, these properties could still be improved, and crucial assays of critical parameters in early drug development were missing. Further, the viral target of this compound series was still unknown. Therefore, a thorough lead optimisation based on the 2-(4-(phenylsulfonyl)piperazine-1-yl)pyrimidine scaffold (CHVB-scaffold) was made to identify analogues with enhanced antiviral activity, and favourable ADMET properties and a mode of action study was conducted to identify the viral target.

A delay-of-treatment assay pointed to the postentry step in the CHIKV replication cycle as the target of the CHVB series. Additionally, $CHVB^{res}$ was determined through resistance identification and showed a high resistance level in the first and second-generation CHVB compounds. A cross-resistant study with a known CHIKV-nsP1 inhibitor (MADTP series) and enzymatic assays, where CHVB compounds inhibited the MTase and GTase activities of alphavirus nsP1 proteins, suggests that the CHVB compounds directly inhibit the enzymatic activities of nsP1 [69]. Interestingly, both

compound series (MADTP and CHVB) are selective CHIKV inhibitors with biological activities in all tested CHIKV isolates but with no or modest antiviral activity against other (alpha)viruses [69]. Further, the second-generation CHVB compounds showed the same selectivity toward the CHIKV [65]. Identifying the viral target allowed the investigation of possible interactions between the compound series and their antiviral target protein via a molecular docking study [65].

The second-generation CHVB compounds were developed to enhance the anti-CHIKV activity and the ADMET properties of this compound series. The 100 novel analogues were assessed for their biological activities, physicochemical characteristics, possible hERG channel interactions and cytotoxic profile. An optimised synthesis route (Synthesis Route B) improved the accessibility of the designed analogues and showed remarkable time- and yield-wise advantages to the previously established Synthesis Route A. Thus, making the exploration of the CHVB series more versatile and straightforward.

An additional SAR study confirmed some structural requirements found in the first-generation's SAR study and further broadened the knowledge about the structural influence of all five molecular subgroups on biological activity. Fifty-five compounds were additionally evaluated for their metabolic stability in HLMs, and an SMR study gave insight into the structural requirements for high metabolic stability [65].

Out of this 100 second-generation CHVB compounds, 68 were active ($EC_{50} \leq 40\,\mu M$), 43 in a low micromolar range ($EC_{50} \leq 10\,\mu M$), 34 more active than the initial hit compound **1a** (EC_{50} value of $8.7 \pm 0.1\,\mu M$), and 24 with an even higher activity than the generated lead compound **1b** (EC_{50} value of $3.95 \pm 0.01\,\mu M$). Moreover, 10 compounds demonstrated a remarkable high antiviral activity with EC_{50} values under $1\,\mu M$. Throughout all assessed assays, five compounds (**31b**, **31d**, **32d**, **34**, and **35d**) showed the highest activity in combination with favorable ADMET properties [65].

Two ligand-based approaches were conducted to broaden the knowledge about the CHVB series and identify possible scaffold changes that would allow reaching new territories of chemical space and free intellectual properties: i) a pharmacophore-based virtual screening and ii) a SAR-based scaffold hop.

Twelve compounds with interesting CHVB-scaffold variations were retrieved from the pharmacophore-based virtual screening, and their anti-CHIKV activity was assessed via CPE reduction assay. Two hits (**68c** and **70**) showed strong CHIKV inhibition with EC_{50} values of $1.36\,\mu M$ and $1.45\,\mu M$, respectively. Further, a SAR-based scaffold hop resulted in **64b** with a spiro[chromane-2,4'-piperidin]-4-one group. The good EC_{50} value of $4.16 \pm 0.15\,\mu M$ demonstrates that **64b** could be a excellent starting point for a lead optimisation study.

References

[1] Food & Drug Administration. Fda at a glance. https://www.fda.gov/media/154548/download, 2021. Accessed: 03.05.2022.

[2] Michael Dickson and Jean Paul Gagnon. Key factors in the rising cost of new drug discovery and development. *Nature Reviews Drug Discovery*, 3(5):417–429, 5 2004.

[3] Steven M Paul, Daniel S Mytelka, Christopher T Dunwiddie, Charles C Persinger, Bernard H Munos, Stacy R Lindborg, and Aaron L Schacht. How to improve r&d productivity: the pharmaceutical industry's grand challenge. *Nature Reviews Drug Discovery*, 9(3):203–214, 3 2010.

[4] Joseph A DiMasi, Henry G Grabowski, and Ronald W Hansen. Innovation in the pharmaceutical industry: New estimates of r&d costs. *Journal of Health Economics*, 47:20–33, 5 2016.

[5] Catherine S Adamson, Kelly Chibale, Rebecca J. M Goss, Marcel Jaspars, David J Newman, and Rosemary A Dorrington. Antiviral drug discovery: preparing for the next pandemic. *Chemical Society Reviews*, 50(6):3647–3655, 2 2021.

[6] Helen Onyeaka, Christian K Anumudu, Zainab T Al-Sharify, Esther Egele-Godswill, and Paul Mbaegbu. Covid-19 pandemic: A review of the global lockdown and its far-reaching effects. *Science Progress*, 104(2):368504211019854, 4-6 2021.

[7] Verena Battisti, Oliver Wieder, Arthur Garon, Thomas Seidel, Ernst Urban, and Thierry Langer. A computational approach to identify potential novel inhibitors against the coronavirus sars-cov-2. *Molecular Informatics*, 39(10):e2000090, 10 2020.

[8] JP Hughes, S Rees, SB Kalindjian, and KL Philpott. Principles of early drug discovery. *British Journal of Pharmacology*, 162(6):1239–1249, 3 2011.

[9] Sandeep Sinha and Divya Vohora. Chapter 2 - drug discovery and development: An overview. In Divya Vohora and Gursharan Singh, editors, *Pharmaceutical Medicine and Translational Clinical Research*, pages 19–32. Academic Press, Boston, 2018.

[10] György M Keserű and Gergely M Makara. Hit discovery and hit-to-lead approaches. *Drug Discovery Today*, 11(15-16):741–748, 8 2006.

[11] Lorenz M Mayr and Dejan Bojanic. Novel trends in high-throughput screening. *Current Opinion in Pharmacology*, 9(5):580–588, 10 2009.

[12] Regine S. Bohacek, Colin McMartin, and Wayne C. Guida. The art and practice of structure-based drug design: A molecular modeling perspective. *Medicinal Research Reviews*, 16(1):3–50, 1 1996.

[13] Mike M Hann and Tudor I Oprea. Pursuing the leadlikeness concept in pharmaceutical research. *Current Opinion in Chemical Biology*, 8(3):255–263, 6 2004.

[14] Zi-Yi Yang, Jun-Hong He, Ai-Ping Lu, Ting-Jun Hou, and Dong-Sheng Cao. Frequent hitters: nuisance artifacts in high-throughput screening. *Drug Discovery Today*, 25(4):657–667, 4 2020.

[15] Ioana G Popa-Burke, Olga Issakova, James D Arroway, Paul Bernasconi, Min Chen, Louis Coudurier, Scott Galasinski, Ajit P Jadhav, William P Janzen, Dennis Lagasca, Darren Liu, Roderic S Lewis, Robert P Mohney, Nikolai Sepetov, Darren A Sparkman, and C. Nicholas Hodge. Streamlined system for purifying and quantifying a diverse library of compounds and the effect of compound concentration measurements on the accurate interpretation of biological assay results. *Analytical Chemistry*, 76(24):7278–7287, 12 2004.

[16] Hans-Joachim Boehm, Markus Boehringer, Daniel Bur, Hans Gmuender, Walter Huber, Werner Klaus, Dirk Kostrewa, Holger Kuehne, Thomas Luebbers, Nathalie Meunier-Keller, and Francis Mueller. Novel inhibitors of dna gyrase: 3d structure based biased needle screening, hit validation by biophysical methods, and 3d guided optimization. a promising alternative to random screening. *Journal of Medicinal Chemistry*, 43(14):2664–2674, 6 2000.

[17] Roderick E. Hubbard. The role of fragment-based discovery in lead finding. In Daniel A. Erlanson and Wolfgang Jahnke, editors, *Fragment-based Drug Discovery Lessons and Outlook*, chapter 1, pages 1–36. John Wiley & Sons, Ltd, 2016.

[18] Miles Congreve, Robin Carr, Chris Murray, and Harren Jhoti. A 'rule of three' for fragment-based lead discovery? *Drug Discovery Today*, 8(19):876–877, 10 2003.

[19] Mike Cherry and Tim Mitchell. Introduction to fragment-based drug discovery. In Edward R. Zartler and Michael J. Shapiro, editors, *Fragment-Based Drug Discovery*, chapter 1, pages 1–13. John Wiley & Sons, Ltd, 2008.

[20] Andreas Mayr, Günter Klambauer, Thomas Unterthiner, Marvin Steijaert, Jörg K. Wegner, Hugo Ceulemans, Djork-Arné Clevert, and Sepp Hochreiter. Large-scale comparison of machine learning methods for drug target prediction on chembl. *Chemical Science*, 9(24):5441–5451, 6 2018.

[21] Gisbert Schneider. Automating drug discovery. *Nature Reviews Drug Discovery*, 17(2):97–113, 2 2018.

[22] Wenbo Yu and Alexander D Jr MacKerell. Computer-aided drug design methods. *Methods in Molecular Biology*, 1520:85–106, 2017.

[23] Simone Brogi, Teodorico Castro Ramalho, Kamil Kuca, José L. Medina-Franco, and Marian Valko. Editorial: In silico methods for drug design and discovery. *Frontiers in Chemistry*, 8:612, 8 2020.

[24] Zhe Wang, Huiyong Sun, Chao Shen, Xueping Hu, Junbo Gao, Dan Li, Dongsheng Cao, and Tingjun Hou. Combined strategies in structure-based virtual screening. *Physical Chemistry Chemical Physics*, 22(6):3149–3159, 1 2020.

[25] Thomas Seidel, Gökhan Ibis, Fabian Bendix, and Gerhard Wolber. Strategies for 3d pharmacophore-based virtual screening. *Drug Discovery Today: Technologies*, 7(4):e221–e228, 2010.

[26] Thomas Seidel, Oliver Wieder, Arthur Garon, and Thierry Langer. Applications of the pharmacophore concept in natural product inspired drug design. *Molecular Informatics*, 39(11):e2000059, 11 2020.

[27] M.P.A Sanders, R McGuire, L Roumen, I.J de Esch, J. de Vlieg, J.P.G Klomp, and C de Graaf. From the proteins perspective: the benefits and challenges of protein structure-based pharmacophore modeling. *MedChemComm*, 3(1):28–38, 1 2012.

[28] C. G Wermuth, C. R Ganellin, P Lindberg, and L. A Mitscher. Glossary of terms used in medicinal chemistry (iupac recommendations 1998). *Pure and Applied Chemistry*, 70(5):1129–1143, 1998.

[29] Camille G Wermuth. Pharmacophores: Historical perspective and viewpoint from a medicinal chemist. In Thierry Langer and Rémy D. Hoffmann, editors, *Pharmacophores and Pharmacophore Searches*, pages 1–13. Wiley-VCH Verlag GmbH & Co. KGaA, Weinheim, FRG, 2006.

[30] Sarah R. Langdon, Julian Blagg, and Nathan Brown. Scaffold diversity in medicinal chemistry space. In Nathan Brown, editor, *Scaffold Hopping in Medicinal Chemistry*, chapter 3, pages 39–60. John Wiley & Sons, Ltd, 2013.

[31] Ye Hu, Dagmar Stumpfe, and Jürgen Bajorath. Recent advances in scaffold hopping. *Journal of Medicinal Chemistry*, 60(4):1238–1246, 2 2017.

[32] Hans-Joachim Böhm, Alexander Flohr, and Martin Stahl. Scaffold hopping. *Drug Discovery Today: Technologies*, 1(3):217–224, 12 2004.

[33] Sarah R Langdon, Peter Ertl, and Nathan Brown. Bioisosteric replacement and scaffold hopping in lead generation and optimization. *Molecular Informatics*, 29(5):366–385, 5 2010.

[34] H.L. Friedman. Influence of isosteric replacements upon biological activity. In National Research Council, editor, *First Symposium on Chemical-Biological Correlation, May 26-27, 1950*, pages 295–395. National Academies Press, Washington, DC, May 1951.

[35] Irving Langmuir. Isomorphism, isosterism and covalence. *Journal of the American Chemical Society*, 41(10):1543–1559, 10 1919.

[36] George A Patani and Edmond J LaVoie. Bioisosterism: a rational approach in drug design. *Chemical Reviews*, 96(8):3147–3176, 12 1996.

[37] Alfred Burger. Isosterism and bioisosterism in drug design. In Ernst Jucker, editor, *Progress in Drug Research / Fortschritte der Arzneimittelforschung / Progrès des recherches pharmaceutiques*, pages 287–371. Birkhäuser Basel, Basel, 1991.

[38] Caterina Barillari and Nathan Brown. Classical bioisosteres. In Nathan Brown, editor, *Bioisosteres in Medicinal Chemistry*, chapter 2, pages 15–29. John Wiley & Sons, Ltd, 2012.

[39] Nathan Brown. Bioisosterism in medicinal chemistry. In Nathan Brown, editor, *Bioisosteres in Medicinal Chemistry*, chapter 1, pages 1–14. John Wiley & Sons, Ltd, 2012.

[40] Jörg Holenz and Dean G. Brown. Modern lead generation strategies. In Jörg Holenz, editor, *Lead Generation*, chapter 2, pages 13–34. John Wiley & Sons, Ltd, 2016.

[41] Mitchell N. Cayen. Drug discovery and early drug development. In Mitchell N. Cayen, editor, *Early Drug Development*, chapter 1, pages 1–24. John Wiley & Sons, Ltd, 2010.

[42] Li Di, Paul V Fish, and Takashi Mano. Bridging solubility between drug discovery and development. *Drug Discovery Today*, 17(9-10):486–495, 5 2012.

[43] Xiangli Liu, Bernard Testa, and Alfred Fahr. Lipophilicity and its relationship with passive drug permeation. *Pharmaceutical Research*, 28(5):962–977, 5 2011.

[44] Collen M. Masimirembwa, UIf Bredberg, and Tommy B. Andersson. Metabolic stability for drug discovery and development: Pharmacokinetic and biochemical challenges. *Clinical Pharmacokinetics*, 42(6):515–528, 2003.

[45] S. Sonu Singh. Preclinical pharmacokinetics: An approach towards safer and efficacious drugs. *Current Drug Metabolism*, 7(2):165–182, 2 2006.

[46] Richard B van Breemen and Yongmei Li. Caco-2 cell permeability assays to measure drug absorption. *Expert Opinion on Drug Metabolism & Toxicology*, 1(2):175–185, 8 2005.

[47] María José Gómez-Lechón, José Vicente Castell, and María Teresa Donato. Hepatocytes—the choice to investigate drug metabolism and toxicity in man: In vitro variability as a reflection of in vivo. *Chemico-Biological Interactions*, 168(1):30–50, 5 2007.

[48] C E Pollard, J-P Valentin, and T G Hammond. Strategies to reduce the risk of drug-induced qt interval prolongation: a pharmaceutical company perspective. *British Journal of Pharmacology*, 154(7):1538–1543, 8 2008.

[49] James D. McKinney, Ann Richard, Chris Waller, Michael C. Newman, and Frank Gerberick. The practice of structure activity relationships (sar) in toxicology. *Toxicological Sciences*, 56(1):8–17, 7 2000.

[50] Marion C Robinson. An epidemic of virus disease in southern province, tanganyika territory, in 1952-53. i. clinical features. *Transactions of The Royal Society of Tropical Medicine and Hygiene*, 49(1):28–32, 1 1955.

[51] Scott C. Weaver and Naomi L. Forrester. Chikungunya: Evolutionary history and recent epidemic spread. *Antiviral Research*, 120:32–39, 8 2015.

[52] Jean Paul Chretien, Assaf Anyamba, Sheryl A. Bedno, Robert F. Breiman, Rosemary Sang, Kibet Sergon, Ann M. Powers, Clayton O. Onyango, Jennifer Small, Compton J. Tucker, and Kenneth J. Linthicum. Drought-associated chikungunya emergence along coastal east africa. *American Journal of Tropical Medicine and Hygiene*, 76(3):405–407, 3 2007.

[53] Herve Zeller, Wim Van Bortel, and Bertrand Sudre. Chikungunya: Its history in africa and asia and its spread to new regions in 2013-2014. *The Journal of Infectious Diseases*, 214(S5):S436–440, 12 2016.

[54] Giulietta Venturi, Marco Di Luca, Claudia Fortuna, Maria Elena Remoli, Flavia Riccardo, Francesco Severini, Luciano Toma, Martina Del Manso, Eleonora Benedetti,

Maria Grazia Caporali, Antonello Amendola, Cristiano Fiorentini, Claudio De Liberato, Roberto Giammattei, Roberto Romi, Patrizio Pezzotti, Giovanni Rezza, and Caterina Rizzo. Detection of a chikungunya outbreak in central italy, august to september 2017. *Eurosurveillance*, 22(39):17–00646, 9 2017.

[55] Clémentine Calba, Mathilde Guerbois-Galla, Florian Franke, Charles Jeannin, Michelle Auzet-Caillaud, Gilda Grard, Lucette Pigaglio, Anne Decoppet, Joel Weicherding, Marie Christine Savaill, Manuel Munoz-Riviero, Pascal Chaud, Bernard Cadiou, Lauriane Ramalli, Pierre Fournier, Harold Noël, Xavier De Lamballerie, Marie Claire Paty, and Isabelle Leparc-Goffart. Preliminary report of an autochthonous chikungunya outbreak in france, july to september 2017. *Eurosurveillance*, 22(39):17–00647, 9 2017.

[56] World health organisation - chikungunya. https://www.who.int/news-room/fact-sheets/detail/chikungunya. Accessed: 13.05.2022.

[57] Lindsay P. Campbell, Caylor Luther, David Moo-Llanes, Janine M. Ramsey, Rogelio Danis-Lozano, and A. Townsend Peterson. Climate change influences on global distributions of dengue and chikungunya virus vectors. *Philosophical Transactions of the Royal Society B*, 370(1665):20140135, 4 2015.

[58] Simon-Djamel Thiberville, Nanikaly Moyen, Laurence Dupuis-Maguiraga, Antoine Nougairede, Ernest A Gould, Pierre Roques, and Xavier De Lamballerie. Chikungunya fever: epidemiology, clinical syndrome, pathogenesis and therapy. *Antiviral Research*, 99(3):345–370, 9 2013.

[59] Philippe Gasque, Therese Couderc, Marc Lecuit, Pierre Roques, and Lisa F.P. Ng. Chikungunya virus pathogenesis and immunity. *Vector-Borne and Zoonotic Diseases*, 15(4):241–249, 4 2015.

[60] Gaëtan Lebrun, Karim Chadda, Anne Hélène Reboux, Olivier Martinet, and Bernard Alex Gaüzère. Guillain-barré syndrome after chikungunya infection. *Emerging Infectious Diseases*, 15(3):495–496, 3 2009.

[61] Gianandrea Borgherini, Patrice Poubeau, Annie Jossaume, Arnaud Gouix, Liliane Cotte, Alain Michault, Claude Arvin-Berod, and Fabrice Paganin. Persistent arthralgia associated with chikungunya virus: a study of 88 adult patients on reunion island. 47(4):469–475, 8 2008.

[62] J. Kennedy Amaral Pereira and Robert T. Schoen. Management of chikungunya arthritis. *Clinical Rheumatology*, 36(10):2179–2186, 10 2017.

[63] Verena Battisti, Ernst Urban, and Thierry Langer. Antivirals against the chikungunya virus. *Viruses*, 13(7):1307, 7 2021.

[64] Julia Moesslacher, Verena Battisti, Leen Delang, Johan Neyts, Rana Abdelnabi, Gerhard Pürstinger, Ernst Urban, and Thierry Langer. Identification of 2-(4-(phenylsulfonyl)piperazine-1-yl)pyrimidine analogues as novel inhibitors of chikungunya virus. *ACS Medicinal Chemistry Letters*, 11(5):906–912, 3 2020.

[65] Verena Battisti, Julia Moesslacher, Rana Abdelnabi, Pieter Leyssen, Ana Lucia Rosales Rosas, Lana Langendries, Mohammed Aufy, Christian Studenik, Jadel Kratz, Judith M. Rollinger, Gerhard Pürstinger, Johan Neyts, Leen Delang, Ernst Urban, and Thierry Langer. Design, synthesis, and lead optimisation of chvb series analogues as potent small molecule inhibitors of chikungunya virus. *ChemRxiv*, 7 2022. doi: 10.26434/chemrxiv-2022-z50q7, this content is a preprint and is submitted for publishing in a peer-reviewed journal.

[66] Julia Kirchebner. *Novel Small Molecule Inhibitors of Chikungunya Virus*. PhD thesis, University of Innsbruck, Innrain 80/82, A-6020 Innsbruck, Austria, 5 2014.

[67] John G Topliss. Utilization of operational schemes for analog synthesis in drug design. *Journal of Medicinal Chemistry*, 15(10):1006–1011, 10 1972.

[68] John G Topliss. A manual method for applying the hansch approach to drug design. *Journal of Medicinal Chemistry*, 20(4):463–469, 4 1977.

[69] Rana Abdelnabi, Kristina Kovacikova, Julia Moesslacher, Kim Donckers, Verena Battisti, Pieter Leyssen, Thierry Langer, Gerhard Puerstinger, Gilles Quérat, Changqing Li, Etienne Decroly, Ali Tas, Arnaud Marchand, Patrick Chaltin, Bruno Coutard, Martijn Van Hemert, Johan Neyts, and Leen Delang. Novel class of chikungunya virus small molecule inhibitors that targets the viral capping machinery. *Antimicrobial Agents and Chemotherapy*, 64(7):e00649–20, 6 2020.

[70] L Delang, C Li, A Tas, G Quérat, I.C Albulescu, T De Burghgraeve, N.A Segura Guerrero, A Gigante, G Piorkowski, E Decroly, D Jochmans, B Canard, E.J Snijder, M.J Pérez-Pérez, M.J Van Hemert, B Coutard, P Leyssen, and J Neyts. The viral capping enzyme nsp1: A novel target for the inhibition of chikungunya virus infection. *Scientific Reports*, 6(1):31819, 2016.

[71] Changqing Li, Jaime Guillén, Nadia Rabah, Alexandre Blanjoie, Françoise Debart, Jean-Jacques Vasseur, Bruno Canard, Etienne Decroly, and Bruno Coutard. mrna capping by venezuelan equine encephalitis virus nsp1: Functional characterization and implications for antiviral research. *Journal of Virology*, 89(16):8292–8303, 8 2015.

[72] Kristina Kovacikova, Bas M Morren, Ali Tas, Irina C Albulescu, Robin Van Rijswijk, Dnyandev B Jarhad, Young Sup Shin, Min Hwan Jang, Gyudong Kim,

Hyuk Woo Lee, Lak Shin Jeong, Eric J Snijder, and Martijn J Van Hemert. 6--fluoro-homoaristeromycin and 6-fluoro-homoneplanocin a are potent inhibitors of chikungunya virus replication through their direct effect on viral nonstructural protein 1. *Antimicrobial agents and chemotherapy*, 64(4)::e02532–19, 3 2020.

[73] Alba Gigante, Maria-Dolores Canela, Leen Delang, Eva-Maria Priego, Maria-Jose Camarasa, Gilles Querat, Johan Neyts, Pieter Leyssen, and Maria-Jesus Perez-Perez. Identification of [1,2,3]triazolo[4,5-d]pyrimidin-7(6h)-ones as novel inhibitors of chikungunya virus replication. *Journal of Medicinal Chemistry*, 57(10):4000–4008, 5 2014.

[74] Alba Gigante, Asier Gómez-SanJuan, Leen Delang, Changqing Li, Oskía Bueno, Ana-María Gamo, Eva-María Priego, María-José Camarasa, Dirk Jochmans, Pieter Leyssen, Etienne Decroly, Bruno Coutard, Gilles Querat, Johan Neyts, and María-Jesús Pérez-Pérez. Antiviral activity of [1,2,3]triazolo[4,5-d]pyrimidin-7(6h)-ones against chikungunya virus targeting the viral capping nsp1. *Antiviral research*, 144:216–222, 8 2017.

[75] Gerhard Wolber and Thierry Langer. Ligandscout: 3-d pharmacophores derived from protein-bound ligands and their use as virtual screening filters. *Journal of Chemical Information and Modeling*, 45(1):160–169, 1-2 2005.

[76] Thomas Seidel, Sharon D Bryant, Gökhan Ibis, Giulio Poli, and Thierry Langer. 3d pharmacophore modeling techniques in computer-aided molecular design using ligandscout. In Alexandre Varnek, editor, *Tutorials in Chemoinformatics*, pages 279–309. John Wiley & Sons, Ltd, Chichester, UK, 2017.

[77] David S Wishart, Yannick D Feunang, An C Guo, Elvis J Lo, Ana Marcu, Jason R Grant, Tanvir Sajed, Daniel Johnson, Carin Li, Zinat Sayeeda, Nazanin Assempour, Ithayavani Iynkkaran, Yifeng Liu, Adam Maciejewski, Nicola Gale, Alex Wilson, Lucy Chin, Ryan Cummings, Diana Le, Allison Pon, Craig Knox, and Michael Wilson. Drugbank 5.0: a major update to the drugbank database for 2018. *Nucleic Acids Research*, 46(D1):D1074–D1082, 1 2018.

[78] Prestwick chemical library. https://www.prestwickchemical.com/screening-libraries/prestwick-chemical-library/. Accessed: 13.05.2022.

[79] Aldrich market select. https://www.aldrichmarketselect.com/. Accessed: 13.05.2022.

[80] Christopher A Lipinski, Franco Lombardo, Beryl W Dominy, and Paul J Feeney. Experimental and computational approaches to estimate solubility and permeability

in drug discovery and development settings. *Advanced Drug Delivery Reviews*, 46(1-3):3–26, 3 2001.

Cytotoxic Activity

.0.1 Cytotoxic Activity in HEK 293 and A459 cell lines

Experimental Procedure

Experiments were done as previously described [65]. HEK 291 and A559 cells were seeded in 96 well plates at density 2000 cells/well in 100 µL/well medium and incubated for 24 hours. After that, cells were incubated with 100 µL of CHVB compound at different concentrations. The proportion of viable cells was determined after 48 and 72 hours after exposure to CHVB compound by 3-(4,5-dimethylthiazol-2-yl)-2,-5 diphenyltetrazolium bromide (MTT)-based viability assay (EZ4U, Biomedica, Vienna, Austria). Briefly, 20 µL of EZ4U solution was added to each well. After incubation for 2 hours at 37 °C the absorbance was measured by a microplate reader at 450 nm with 620 nm as reference to reduce the unspecific background values. All experiments were carried out three times in triplicates.

TABLE 1: Cytotoxic activity of **31a** in HEK 293 cells.

31a HEK 293						
	48 h			72 h		
Conc. (µM)	Control (DMSO)	31a	Living Cells	Control (DMSO)	31a	Living Cells
200	0.426	0.361		0.340	0.391	
	0.203	0.240		0.331	0.274	
	0.392	0.380		0.356	0.325	
	0.340	**0.327**	**96.08%**	**0.342**	**0.330**	**96.40%**
100	0.409	0.431		0.386	0.441	
	0.207	0.238		0.334	0.402	
	0.377	0.395		0.336	0.410	
	0.331	**0.355**	**107.15%**	**0.352**	**0.418**	**118.66%**
50	0.469	0.567		0.465	0.478	
	0.197	0.240		0.391	0.474	
	0.313	0.352		0.293	0.344	
	0.326	**0.386**	**118.39%**	**0.383**	**0.432**	**112.79%**
25	0.406	0.498		0.412	0.432	
	0.188	0.231		0.318	0.413	
	0.296	0.347		0.352	0.441	
	0.297	**0.359**	**120.90%**	**0.361**	**0.429**	**118.85%**
12.5	0.558	0.463		0.388	0.422	
	0.226	0.213		0.427	0.422	
	0.410	0.489		0.433	0.436	
	0.398	**0.388**	**97.57%**	**0.416**	**0.427**	**102.56%**
6.25	0.465	0.435		0.404	0.465	
	0.221	0.191		0.393	0.366	
	0.387	0.390		0.389	0.385	
	0.358	**0.339**	**94.69%**	**0.395**	**0.405**	**102.53%**
3.125	1.432	1.169		0.426	0.382	
	0.212	0.167		0.388	0.308	
	0.377	0.369		0.378	0.339	
	0.674	**0.568**	**84.36%**	**0.397**	**0.343**	**86.33%**
1.56	0.441	0.369		0.439	0.452	
	0.197	0.231		0.350	0.394	
	0.349	0.380		0.332	0.378	
	0.329	**0.327**	**99.29%**	**0.374**	**0.408**	**109.19%**

TABLE 2: Cytotoxic activity of **31a** in A549 cells.

31a A549						
	48 h			72 h		
Conc. (µM)	Control (DMSO)	31a	Living Cells	Control (DMSO)	31a	Living Cells
200	0.234	0.239		0.202	0.229	
	0.234	0.235		0.227	0.250	
	0.274	0.244		0.220	0.247	
	0.247	**0.239**	**96.77%**	**0.216**	**0.242**	**111.86%**
100	0.240	0.253		0.229	0.235	
	0.241	0.253		0.219	0.222	
	0.240	0.233		0.229	0.249	
	0.240	**0.246**	**102.50%**	**0.226**	**0.235**	**104.28%**
50	0.218	0.224		0.211	0.206	
	0.226	0.236		0.210	0.230	
	0.250	0.250		0.251	0.268	
	0.231	**0.237**	**102.31%**	**0.224**	**0.235**	**104.76%**
25	0.238	0.236		0.220	0.234	
	0.252	0.234		0.220	0.224	
	0.245	0.242		0.230	0.224	
	0.245	**0.237**	**96.87%**	**0.223**	**0.227**	**101.79%**
12.5	0.229	0.227		0.228	0.250	
	0.240	0.235		0.210	0.224	
	0.265	0.233		0.244	0.245	
	0.245	**0.232**	**94.69%**	**0.227**	**0.240**	**105.43%**
6.25	0.233	0.227		0.227	0.234	
	0.247	0.246		0.222	0.218	
	0.242	0.257		0.247	0.273	
	0.241	**0.243**	**101.11%**	**0.232**	**0.242**	**104.17%**
3.125	0.243	0.248		0.230	0.239	
	0.247	0.245		0.219	0.233	
	0.266	0.246		0.262	0.249	
	0.252	**0.246**	**97.75%**	**0.237**	**0.240**	**101.41%**
1.56	0.226	0.228		0.247	0.246	
	0.245	0.255		0.218	0.212	
	0.234	0.241		0.252	0.232	
	0.235	**0.241**	**102.70%**	**0.239**	**0.230**	**96.23%**

TABLE 3: Cytotoxic activity of **31g** in HEK 293 cells.

31g HEK293						
	48 h			72 h		
Conc. (µM)	Control (DMSO)	31g	Living Cells	Control (DMSO)	31g	Living Cells
200	2.346	2.890		0.989	1.554	
	2.879	2.346		0.986	1.092	
	2.654	2.880		1.234	1.450	
	2.626	**2.705**	**103.01%**	**1.070**	**1.365**	**127.65%**
100	2.390	2.650		0.806	1.372	
	2.459	2.571		1.199	1.222	
	2.098	2.514		1.167	1.170	
	2.316	**2.578**	**111.34%**	**1.057**	**1.254**	**118.63%**
50	2.713	2.648		1.176	1.180	
	2.354	2.598		1.465	1.222	
	2.985	2.660		1.332	1.182	
	2.684	**2.635**	**98.19%**	**1.324**	**1.194**	**90.20%**
25	2.656	2.556		0.924	1.550	
	2.894	2.587		1.983	1.486	
	2.690	2.399		1.306	0.815	
	2.747	**2.514**	**91.53%**	**1.404**	**1.284**	**91.43%**
12.5	2.598	2.988		1.569	1.206	
	2.896	2.658		1.450	1.526	
	2.919	2.988		1.448	1.408	
	2.804	**2.878**	**102.63%**	**1.489**	**1.380**	**92.67%**
6.25	2.880	2.298		0.912	1.441	
	2.749	2.677		1.369	1.388	
	2.666	2.989		0.938	1.533	
	2.765	**2.655**	**96.01%**	**1.073**	**1.454**	**135.53%**
3.125	2.514	2.589		1.478	1.200	
	2.013	2.999		1.567	1.392	
	2.950	2.140		1.296	1.299	
	2.492	**2.576**	**103.36%**	**1.447**	**1.297**	**89.63%**
1.56	2.112	2.879		1.508	1.566	
	2.234	1.989		1.429	1.444	
	2.146	1.878		1.504	1.226	
	2.164	**2.249**	**103.92%**	**1.480**	**1.412**	**95.38%**

Characterisation and Spectral Data

.0.2 Characterisation and Spectral Data of Hit Molecules from Virtual Screening.

(1-(2-((2-(ethylamino)-6-methylpyrimidin-4-yl)amino)ethyl)-3-(3-fluoro-4-methylphenyl)urea (65a).

HRESIMS *m/z* 347.2001 $[M+H]^+$ (calcd for $C_{17}H_{24}FN_6O^+$, 347.199, Δ = -3.0 ppm). ^{1}H NMR (500 MHz, d_6DMSO) δ = 1.05 (t, 3H, CH_3), 2.00 (s, 3H, pyr-CH_3), 2,12 (s, 3H, Ph-CH_3), 3.20 (m, 2H, NCH_2), 3.23 (m, 2H, CH_2), 3.23 (m, 2H, CH_2), 5.56 (s, 1H, pyr-H), 6.22 (s, 1H, NH), 6.22 (s, 1H, NH), 6.74 (br, 1H, NH), 6.91 (dd, 1H, Ph-H6), 7.08 (t, 1H, Ph-H5), 7.39 (dd, 1H, Ph-H2), 8.63 (s, 1H, Ph-H1). ^{13}C NMR (125 MHz, d_6DMSO) δ = 13.52 ((^{3}J(^{13}C,^{19}F) = 3.1 Hz, Ph-CH_3), 15.12 (CH_3), 23.56 (pyr-CH_3), 35.17 (NCH_2), 38.87 (CH_2), 38.87 (CH_2), 104.26 (^{3}J(^{13}C,^{19}F) = 27.4 Hz, Ph-C2), 113.11 (Ph-C6), 115.77 (^{3}J(^{13}C,^{19}F) = 17.4 Hz, Ph-C4), 131.21 (^{3}J(^{13}C,^{19}F) = 6.5 Hz, Ph-C5), 140.00 (^{3}J(^{13}C,^{19}F) = 10.8 Hz, Ph-C1), 155.17 (urea-C), 160.49 (^{3}J(^{13}C,^{19}F) = 238.39 Hz, Ph-C3), 161.96 (pyr-C2,4), 163.36 (pyr-C6), n.d. (pyr-C5). ^{19}F NMR (376.55 MHz, d_6DMSO) δ = -116.65 (t, 10.6 Hz, Ph-F3)

1-(3-chlorophenyl)-3-(2-((2-(ethylamino)-6-methylpyrimidin-4-yl)amino)ethyl)urea (65b).

HRESIMS *m/z* 349.1549 $[M+H]^+$ (calcd for $C_{16}H_{22}ClN_6O^+$, 349.1538, Δ = -3.2 ppm). ^{1}H NMR (500 MHz, d_6DMSO) δ = 1.05 (t, 3H, CH_3), 2.00 (s, 3H, pyr-CH_3), 3.21 (m, 2H, NCH_2), 3.24 (m, 2H, CH_2), 3.24 (m, 2H, CH_2), 5.57 (s, 1H, pyr-H5), 6.24 (m, 1H, NH), 6.29 (m, 1H, NH), 6.74 (br, 1H, NH), 6.92 (dd, 1H, Ph-H4), 7.16 (dd, 1H, Ph-H6), 7.23 (t, 1H, Ph-H5), 7.66 (s, 1H, Ph-H2), 8.75 (s, 1H, NH). ^{13}C NMR (125 MHz, d_6DMSO) δ = 15.12 (CH_3), 23.58 (pyr-CH_3), 35.17 (NCH_2), 38.98 (CH_2), 38.98 (CH_2), 115.95 (Ph-C6), 116.92 (Ph-C2), 120.58 (Ph-C4), 130.25 (Ph-C5), 133.08 (Ph-C3), 142.07 (Ph-C1), 155.07 (urea-C), 161.95 (pyr-C2,4), 163.36 (pyr-C6), n.d. (pyr-C5).

1-(2-((2-(ethylamino)-6-methylpyrimidin-4-yl)amino)ethyl)-3-(o-tolyl)urea (65c).

HRESIMS *m/z* 329.2096 $[M+H]^+$ (calcd for $C_{17}H_{25}N_6O^+$, 329.2084, Δ = -3.5 ppm). ^{1}H NMR (500 MHz, d_6DMSO) δ = 1.06 (t, 3H, CH_3), 2.00 (s, 3H, pyr-CH_3), 2.16 (s, 3H, Ph-CH_3), 3.21 (m, 2H, NCH_2), 3.25 (m, 2H, CH_2), 3.25 (m, 2H, CH_2), 5.58 (s, 1H, pyr-H5), 6.25 (br, 1H, NH), 6.63 (t, 1H, NH), 6.75 (br, 1H, NH), 6.86 (t, 1H, Ph-H4), 7.08 (d, 1H, Ph-H5), 7.10 (t, 1H, Ph-H3), 7.67 (s, 1H, NH), 7.80 (dd, 1H, Ph-H6). ^{13}C NMR (125 MHz, d_6DMSO) δ = 15.13 (CH_3), 17.92 (Ph-CH_3), 23.56 (pyr-CH_3), 38.89 (NCH_2), 38.98 (CH_2), 38.98 (CH_2), 120.49 (Ph-C6), 121.85 (Ph-C4), 126.04 (Ph-C5), 126.72 (Ph-C2), 130.04 (Ph-C3), 138.17 (Ph-C1), 155.53 (urea-C), 161.97 (pyr-C2,4), 163.38 (pyr-C6), n.d. (pyr-C5).

1-(2,4-difluorophenyl)-3-(2-((2-(ethylamino)-6-methylpyrimidin-4-yl)amino)ethyl)urea (65d).

HRESIMS *m/z* 351.1755 $[M+H]^+$ (calcd for $C_{16}H_{21}F_2N_6O^+$, 351.1738, Δ = -4.5 ppm). ^{1}H NMR (500 MHz, d_6DMSO) δ = 1.05 (t, 3H, CH_3), 2.00 (s, 3H, pyr-CH_3), 3.20 (m, 2H, NCH_2), 3.24 (m, 2H, CH_2), 3.24 (m, 2H, CH_2), 5.57 (s, 1H, pyr-H5), 6.25 (br, 1H, NH), 6.64 (t, 1H, NH), 6.75 (br, 1H, NH), 6.98 (m, 1H, Ph-H5), 7.23 (m, 1H, Ph-H3), 8.06 (m, 1H, Ph-H6), 8.31 (s, 1H, NH). ^{13}C NMR (125 MHz, d_6DMSO) δ = 15.12 (CH_3), 23.57 (pyr-CH_3), 35.17 (NCH_2), 38.87 (CH_2), 38.87 (CH_2), 103.56 (t, $^3J(^{13}C,^{19}F)$ = 25.2 Hz, Ph-C3), 110.83 (d, $^3J(^{13}C,^{19}F)$ = 17.9 Hz, Ph-C5), 121.28 (m, Ph-C6), 124.87 (dd, $^3J(^{13}C,^{19}F)$ = 10.5 and 3.5 Hz, Ph-C1), 151.6 (d, $^3J(^{13}C,^{19}F)$ = 236.9 Hz, Ph-C2), 155.07 (urea-C), 156.15 (d, $^3J(^{13}C,^{19}F)$ = 228.8 Hz, Ph-C4), 161.96 (pyr-C2,4), 163.36 (pyr-C6), n.d. (pyr-C5). ^{19}F NMR (376.55 MHz, d_6DMSO) δ = -119.44 (m, Ph-F4), -125.58 (m, Ph-F2).

N-(2-((2-(ethylamino)-6-methylpyrimidin-4-yl)amino)ethyl)-2,4,6-trimethylbenzenesulfonamide (66).

HRESIMS *m/z* 378.1972 $[M+H]^+$ (calcd for $C_{18}H_{28}N_5O_2S^+$, 378.1958, Δ = -3.7 ppm). ^{1}H NMR (500 MHz, d_6DMSO) δ = 1.03 (t, 3H, CH_3), 1.97 (s, 3H, pyr-CH_3), 2.24 (s, 3H, CH_3), 2.53 (s, 6H, Ph-2,6CH_3), 2.83 (t, 2H, CH_2), 3.16 (m, 2H, NCH_2), 3.17 (m, 2H, CH_2), 5.43 (s, 1H, pyr-H5), 6.20 (br, 1H, NH), 6.59 (br, 1H, NH), 6.98 (s, 2H, Ph-H3,5), 7.47 (br, 1H, NH). ^{13}C NMR (125 MHz, d_6DMSO) δ = 15.09 (CH_3), 20.39 (Ph-C4-CH_3), 22.54 (Ph-C2,6-CH_3), 23.57 (pyr-CH_3), 35.11 (NCH_2), 41.48 (CH_2), 131.54 (Ph-C3,5), 134.73 (Ph-C1), 138.16 (Ph-C2,6), 141.10 (Ph-C4), 161.86 (pyr-C2), 163.03 (pyr-C4), 163.78 (pyr-C6), n.d. (pyr-C5), n.d. (CH_2).

N-(4-chlorophenyl)-4-(2-(ethylamino)-6-methylpyrimidin-4-yl)piperazine-1-carboxamide (67a).

HRESIMS *m/z* 375.1707 $[M+H]^+$ (calcd for $C_{18}H_{24}ClN_6O^+$, 375.1695, Δ = -3.4 ppm). ^{1}H NMR (500 MHz, d_6DMSO) δ = 1.07 (t, 3H, CH_3), 2.09 (s, 3H, pyr-CH_3), 3.23 (m,

2H, NCH_2), 3.50 (m, 4H, pip-H2,6), 3.57 (m, 4H, pip-H3,5), 5.94 (s, 1H, pyr-H5), 6.44 (br, 1H, NH), 7.28 (d, 2H, Ph-H3,5), 7.51 (d, 2H, Ph-H2,6), 8.71 (s, 1H, NH). ^{13}C NMR (125 MHz, d_6DMSO) δ = 15.01 (CH_3), 23.94 (pyr-CH_3), 35.24 (NCH_2), 43.14 (pip-C3,5), 43.31 (pip-C2,6), 91.25 (pyr-C5), 120.98 (Ph-C2,6), 125.31 (Ph-C4), 128.19 (Ph-C3,5), 139.51 (Ph-C1), 154.76 (urea-C), 161.69 (pyr-C2), 162.80 (pyr-C4), 165.67 (pyr-C6).

1-(2-((2-(ethylamino)-6-methylpyrimidin-4-yl)amino)ethyl)-3-(3-fluoro-4-methylphenyl)urea (67b).

HRESIMS *m/z* 393.1616 $[M+H]^+$ (calcd for $C_{18}H_{23}ClFN_6O^+$, 393.1600, Δ = -3.9 ppm). ^{1}H NMR (500 MHz, d_6DMSO) δ = 1.07 (t, 3H, CH_3), 2.09 (s, 3H, pyr-CH_3), 3.23 (m, 2H, NCH_2), 3.50 (m, 4H, pip-H2,6), 3.57 (m, 4H, pip-H3,5), 5.94 (s, 1H, pyr-H5), 6.44 (br, 1H, NH), 7.30 (t, 1H, Ph-H5), 7.42 (ddd, 1H, Ph-H6), 7.76 (dd, 1H, Ph-H2), 8.77 (s, 1H, NH). ^{13}C NMR (125 MHz, d_6DMSO) δ = 15.01 (CH_3), 23.96 (pyr-CH_3), 35.24 (NCH_2), 43.09 (pip-C3,5), 43.27 (pip-C2,7), 91.15 (pyr-C5), 116.45 (^{3}J(^{13}C,^{19}F) = 21.6 Hz, Ph-C5), 118.67 (^{3}J(^{13}C,^{19}F) = 17.4 Hz, Ph-C3), 119.53 (^{13}C,^{19}F) = 6.1 Hz, Ph-C6), 120.70 (Ph-C2), 137.81 (Ph-C1), 152.32 (^{3}J(^{13}C,^{19}F) = 239.2 Hz, Ph-C4), 154.69 (urea-C), 161.71 (pyr-C2), 162.82 (pyr-C4), 165.70 (pyr-C6). ^{19}F NMR (376.55 MHz, d_6DMSO) δ = -125.415 (m, Ph-F4).

(4-fluorophenyl)(4-(6-methyl-2-(p-tolylamino)pyrimidin-4-yl)piperazin-1-yl)methanone (68a).

HRESIMS *m/z* 406.2052 $[M+H]^+$ (calcd for $C_{23}H_{25}FN_5O^+$, 406.2038, Δ = -3.5 ppm). ^{1}H NMR (500 MHz, d_6DMSO) δ = 2.18 (s, 3H, pyr-CH_3), 2.21 (s, 3H, Ph-CH_3), 3.65 (br, 8H, pip-H2,3,5,6), 6.14 (s, 1H, pyr-H5), 7.03 (d, 2H, Ph-H3',5'), 7.30 (t, 2H, Ph-H3,5), 7.53 (d, 2H, Ph-H2,6), 7.57 (d, 2H, Ph-H2',6'), 8.96 (s, 1H, NH). ^{13}C NMR (125 MHz, d_6DMSO) δ = 20.34 (Ph-CH_3), 23.85 (pyr-CH_3), 43.71 (pip-C2,3,5,6), 93.28 (pyr-C5), 115.46 (^{3}J(^{13}C,^{19}F) = 8.3 Hz, Ph-C2,6), 118.59 (Ph-C2',6'), 128.78 (Ph-C3',6'), 129.15 (Ph-C4'), 129.72 (^{3}J(^{13}C,^{19}F) = 21.7 Hz, Ph-C3,5), 132.15 (^{3}J(^{13}C,^{19}F) = 1.6 Hz, Ph-C1), 138.66 (Ph-C1'), 159.34 (pyr-C2), 162.63 (^{3}J(^{13}C,^{19}F) = 245.0 Hz, Ph-C4), 162.66 (pyr-C4), 165.88 (pyr-C6), 168.34 (amide-C). ^{19}F NMR (376.55 MHz, d_6DMSO) δ = -110.95 (m, Ph-F4).

(2,4-dichlorophenyl)(4-(6-methyl-2-(p-tolylamino)pyrimidin-4-yl)piperazin-1-yl)methanone (68b).

HRESIMS *m/z* 456.1373 $[M+H]^+$ (calcd for $C_{23}H_{24}Cl_2N_5O^+$, 456.1352, Δ = -4.5 ppm). ^{1}H NMR (500 MHz, d_6DMSO) δ = 2.18 (s, 3H, pyr-CH_3), 2.21 (s, 3H, Ph-CH_3), 3.24/3.72 (br, 4H, pip-H2,6), 3.58/3.70 (br, 4H, pip-3,5), 6.14 (s, 1H, pyr-H5), 7.02 (d, 2H, Ph-H3',5'), 7.49 (d, 1H, Ph-H6), 7.55 (m, 1H, Ph-H5), 7.56 (m, 2H, Ph-H2',6'), 7.77 (s, 1H, Ph-H3), 8.96 (s, 1H, NH). ^{13}C NMR (125 MHz, d_6DMSO) δ = 20.33 (Ph-CH_3),

23.84 (pyr-CH_3), 40.92/45.76 (pip-C2,6), 43.27/43.73 (pip-C3,5), 93.30 (pyr-C5), 118.59 (Ph-C2',6'), 127.98 (Ph-C5), 128.79 (Ph-C3',5'), 129.15 (Ph-C3), 129.17 (Ph-C4'), 129.48 (Ph-C6), 130.42 (Ph-C1), 134.36 (Ph-C4), 134.54 (Ph-C2), 138.62 (Ph-C1'), 159.33 (pyr-C2), 162.65 (pyr-C4), 164.92 (amide-C), 165.96 (pyr-C6).

4-methyl-N-(p-tolyl)-6-(4-((4-(trifluoromethyl)phenyl)sulfonyl)piperazin-1-yl)pyrimidin-2-amine (68c).

HRESIMS *m/z* 492.1698 $[M+H]^+$ (calcd for $C_{23}H_{25}F_3N_5O_2S^+$, 492.1676, Δ = -4.6 ppm). ^{1}H NMR (500 MHz, d_6DMSO) δ = 2.14 (s, 3H, pyr-CH_3), 2.21 (s, 3H, Ph-CH_3), 3.03 (m, 4H, pip-H3,5), 3.69 (m, 4H, pip-H2,6), 6.09 (s, 1H, pyr-H5), 7.02 (d, 2H, Ph-H3',5'), 7.53 (d, 2H, Ph-H2',6'), 7.98 (d, 2H, Ph-H2,6), 8.02 (d, 2H, Ph-H3,5), 8.93 (s, 1H, NH). ^{13}C NMR (125 MHz, d_6DMSO) δ = 20.35 (Ph-CH_3), 23.80 (pyr-CH_3), 42.91 (pip-C2,6), 45.44 (pip-C3,5), 93.27 (pyr-C5), 118.63 (Ph-C2',6'), 123.43 ($^3J(^{13}C,^{19}F)$ = 260.0 Hz, CF_3), 126.72 ($^3J(^{13}C,^{19}F)$ = 3.8 Hz, Ph-C3,5), 128.57 (Ph-C2,6), 129.21 (Ph-C3',4',5'), 132.91 ($^3J(^{13}C,^{19}F)$ = 32.3 Hz, Ph-C4), 138.56 (Ph-C1'), 138.94 (Ph-C1), 159.26 (pyr-C2), 162.32 (pyr-C4), 164.92 (amide-C), 166.00 (pyr-C6). ^{19}F NMR (376.55 MHz, d_6DMSO) δ = -61.65 (s, CF_3).

4-(4-((2,4-difluorophenyl)sulfonyl)piperazin-1-yl)-N-ethyl-6-methylpyrimidin-2-amine (69).

HRESIMS *m/z* 465.1213 $[M+H]^+$ (calcd for $C_{19}H_{25}N_6O_2S_3^+$, 465.1196, Δ = -3.8 ppm). ^{1}H NMR (500 MHz, d_6DMSO) δ = 1.03 (t, 3H, CH_3), 2.04 (s, 3H, pyr-CH_3), 2.69 (s, 3H, thia-CH_3), 2.99 (m, 4H, pip-H3,5), 3.18 (m, 2H, NCH_2), 3.66 (m, 4H, pip-2,6), 5.87 (s, 1H, pyr-H5), 6.44 (br, 1H, NH), 7.63 (d, 1H, thi-H3), 7.69 (d, 1H, thi-H4), 8.10 (s, 1H, thia-H4). ^{13}C NMR (125 MHz, d_6DMSO) δ = 14.94 (CH_3), 18.64 (thia-CH_3), 23.91 (pyr-CH_3), 35.19 (NCH_2), 42.51 (pip-C2,6), 45.60 (pip-C3,5), 91.15 (pyr-C5), 115.87 (thia-C4), 124.31 (thi-C4), 132.49 (thi-C2), 134.23 (thi-C3), 144.85 (thi-C5), 146.42 (thia-C5), 161.64 (pyr-C2), 162.44 (pyr-C4), 165.94 (pyr-C6), 168.89 (thia-C2).

3-(4-(2-(ethylamino)-6-methylpyrimidin-4-yl)piperazine-1-carbonyl)-2H-chromen-2-one (70).

HRESIMS *m/z* 394.1887 $[M+H]^+$ (calcd for $C_{21}H_{24}N_5O_3^+$, 394.1874, Δ = -3.5 ppm). ^{1}H NMR (500 MHz, d_6DMSO) δ = 1.06 (t, 3H, CH_3), 2.09 (s, 3H, pyr-CH_3), 3.21 (m, 2H, NCH_2), 3.45/3.65 (m, 4H, pip-H2,6), 3.53/3.61 (m, 4H, pip-H3,5), 5.92 (s, 1H, pyr-H5), 6.47 (br, 1H, NH), 7.41 (t, 1H, chr-H6), 7.47 (d, 1H, chr-H8), 7.69 (t, 1H, chr-H7), 7.78 (d, 1H, chr-H5), 8.24 (s, 1H, chr-H4). ^{13}C NMR (125 MHz, d_6DMSO) δ = 15.00 (CH_3), 23.94 (pyr-CH_3), 35.22 (NCH_2), 41.18/45.89 (pip-C2,6), 43.02/43.61 (pip-C3,5), 91.22 (pyr-C5), 116.32 (chr-C8), 118.40 (chr-C4a), 124.60 (chr-C3), 124.86 (chr-C6), 129.05

(chr-C5), 132.76 (chr-C7), 142.47 (chr-C4), 153.54 (chr-C8a), 157.73 (chr-C2), 161.69 (pyr-C2), 162.75 (pyr-C4), 163.04 (amide-C), 165.82 (pyr-C6).

1H- and 13C-NMR Spectra in DMSO-d6 of compound 65a

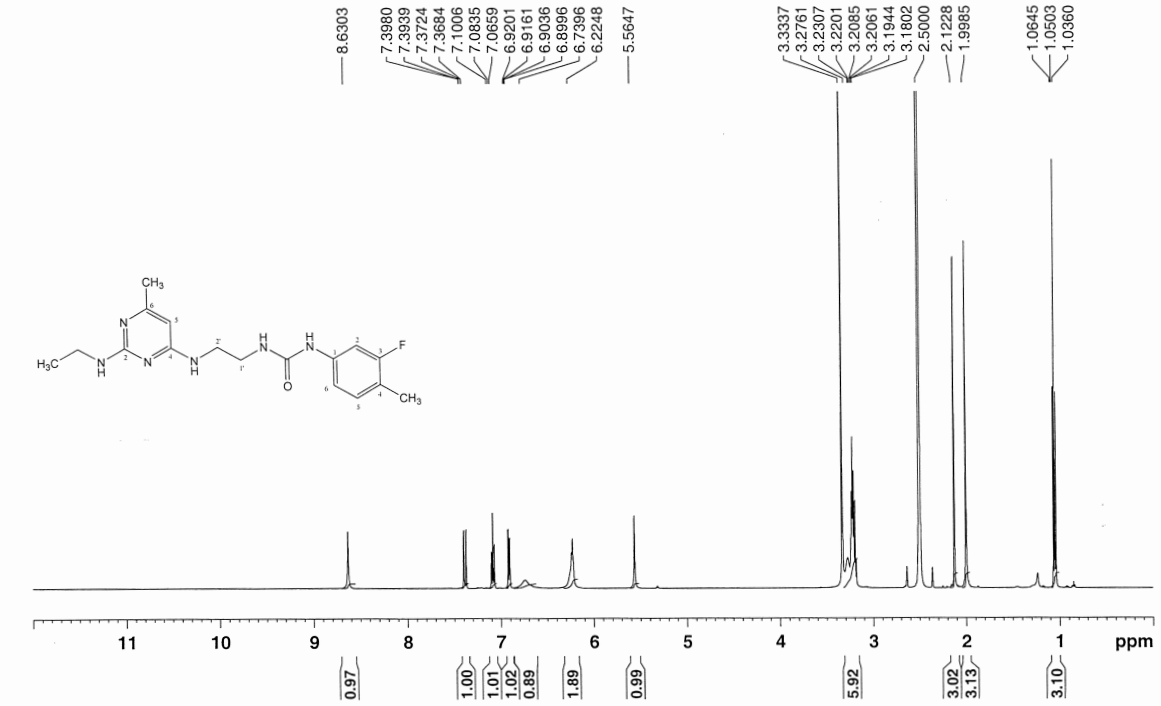

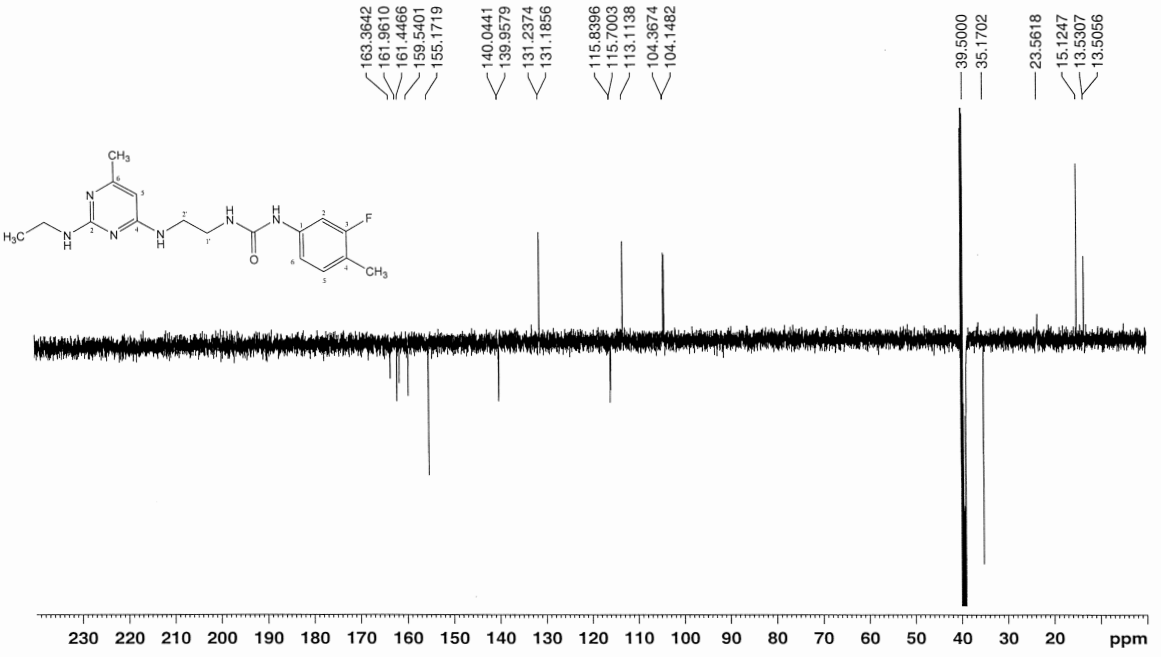

1H- and 13C-NMR Spectra in DMSO-d6 of compound 65b

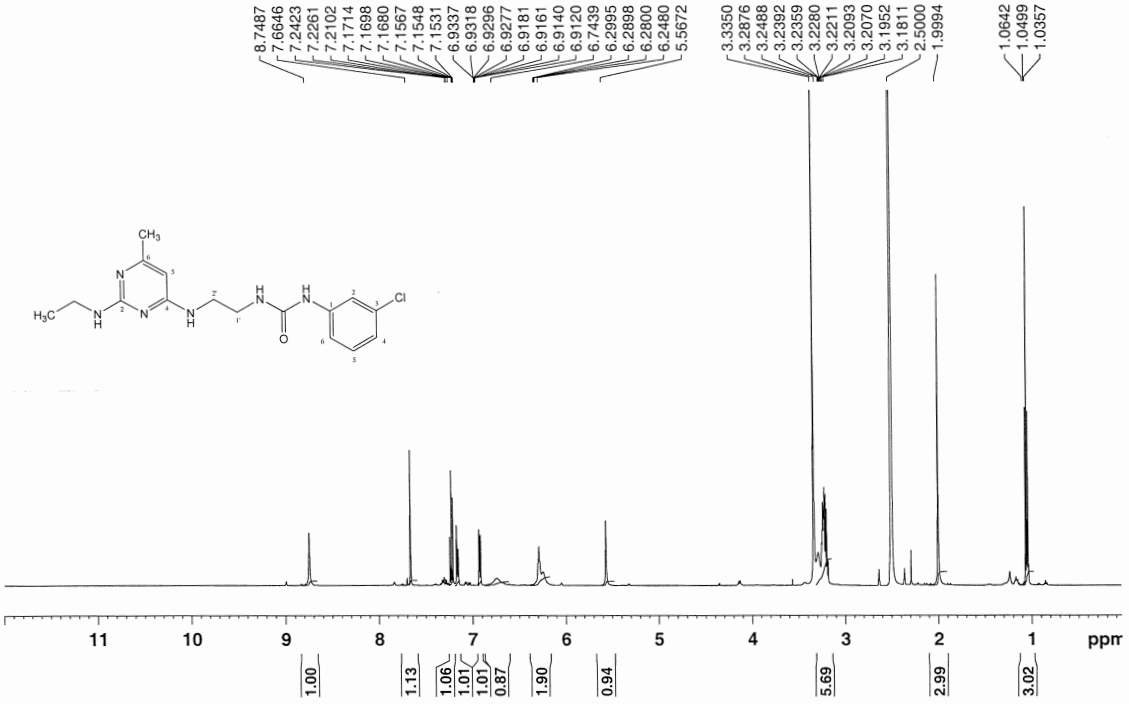

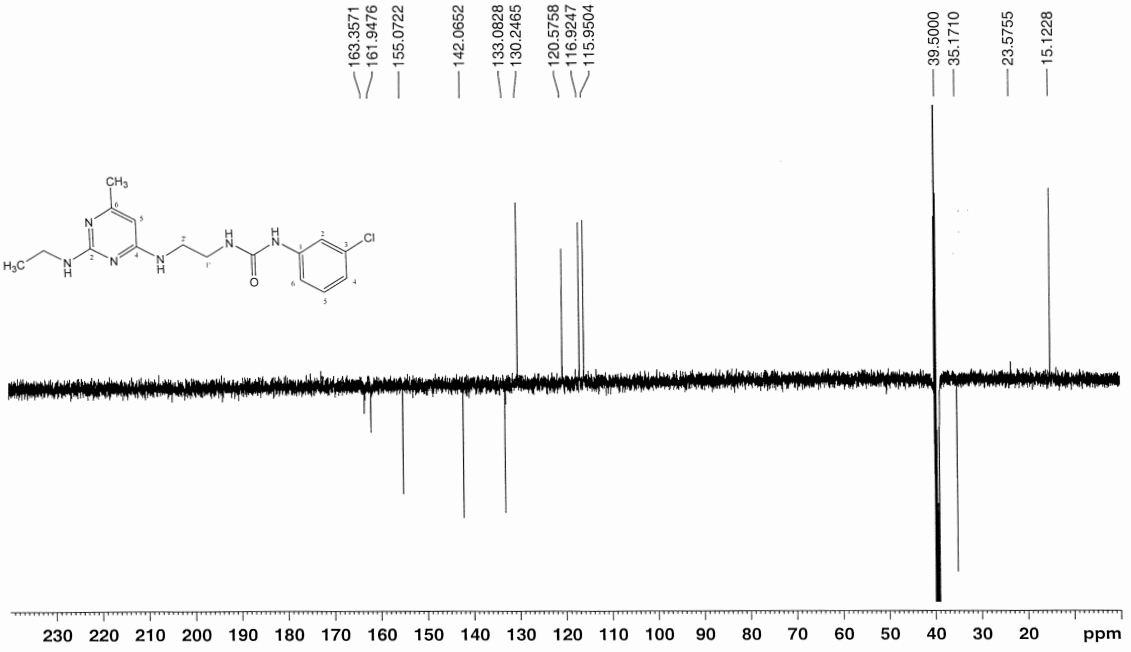

1H- and 13C-NMR Spectra in DMSO-d6 of compound 65c

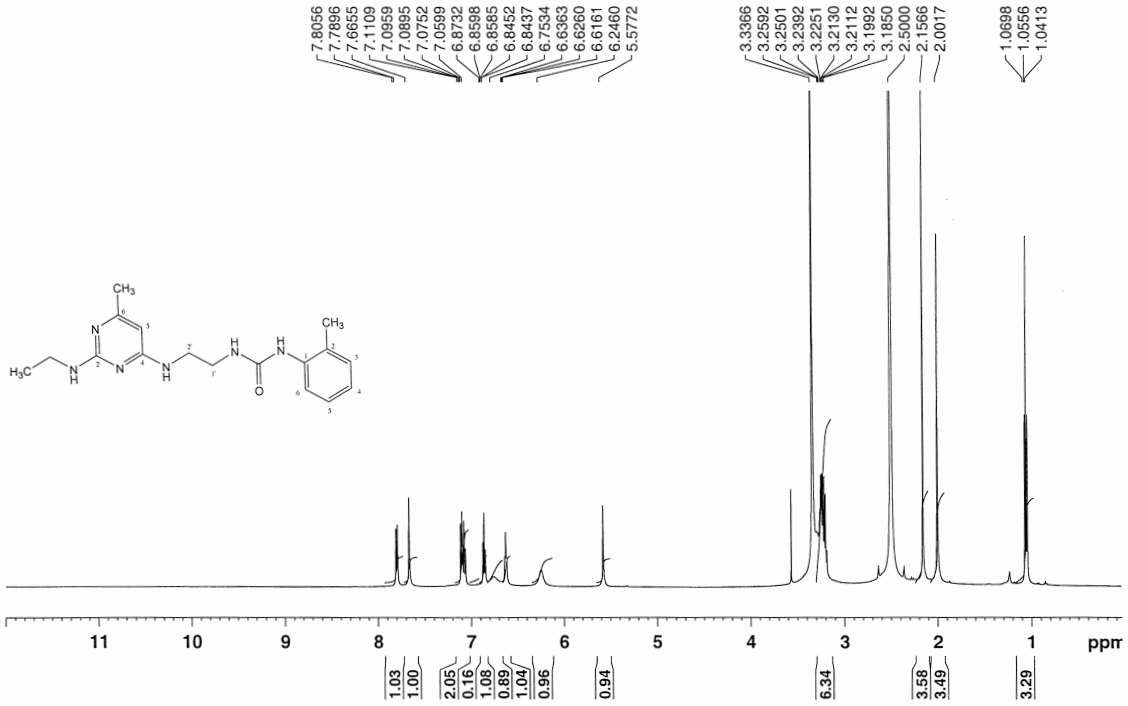

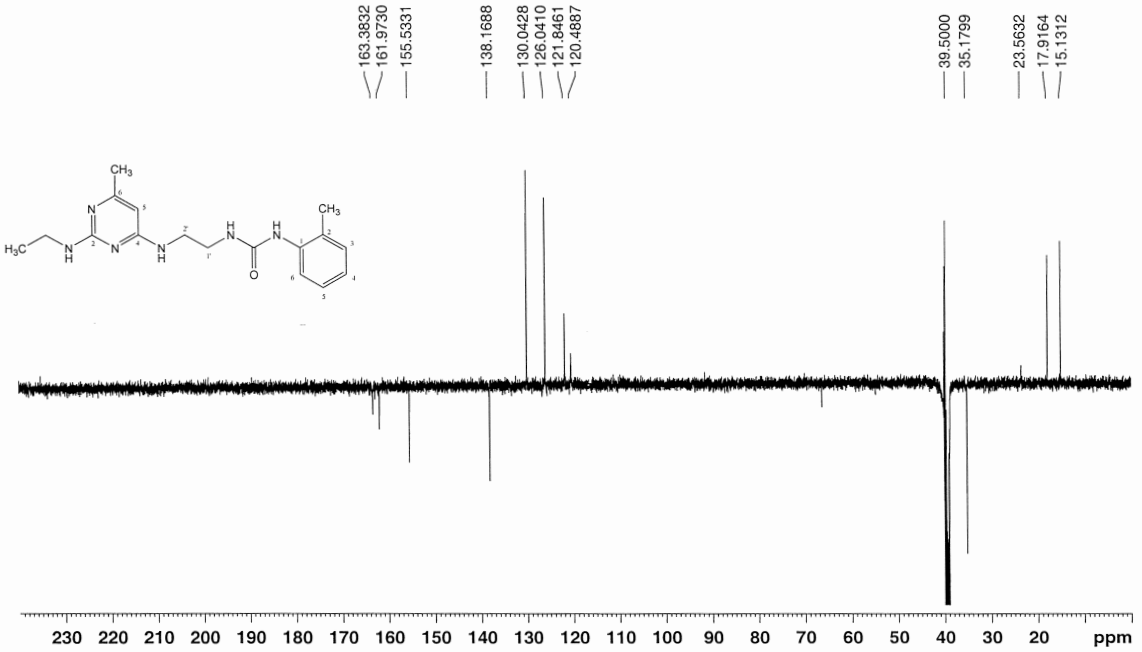

1H- and 13C-NMR Spectra in DMSO-d6 of compound 65d

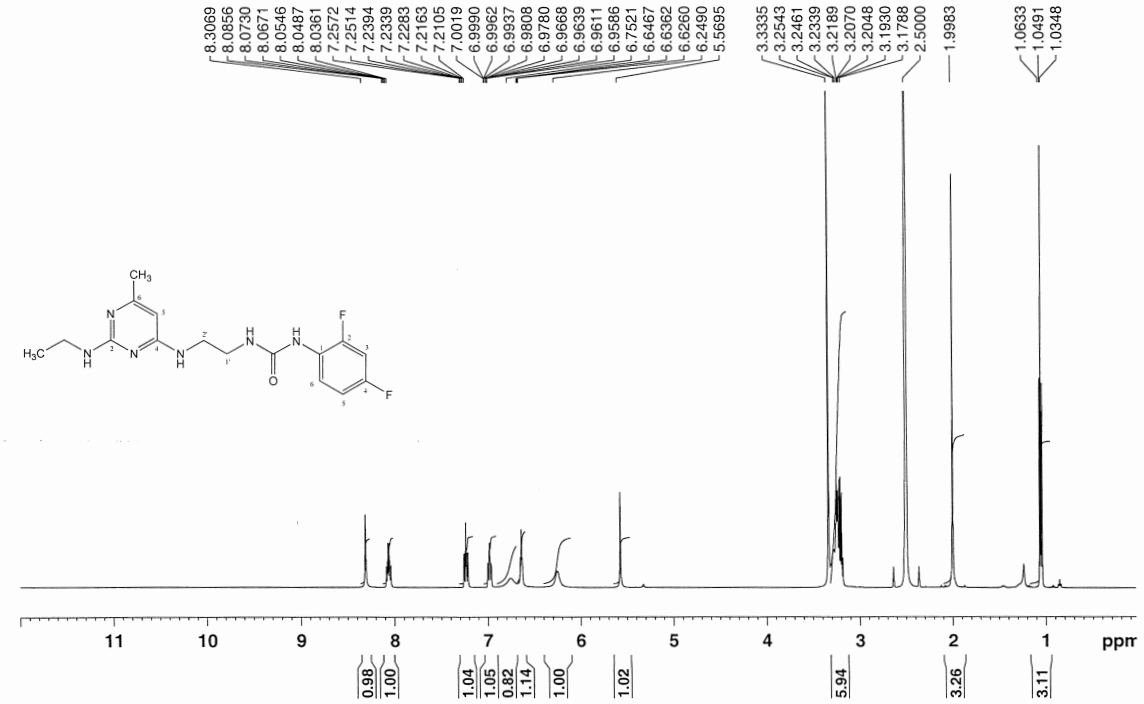

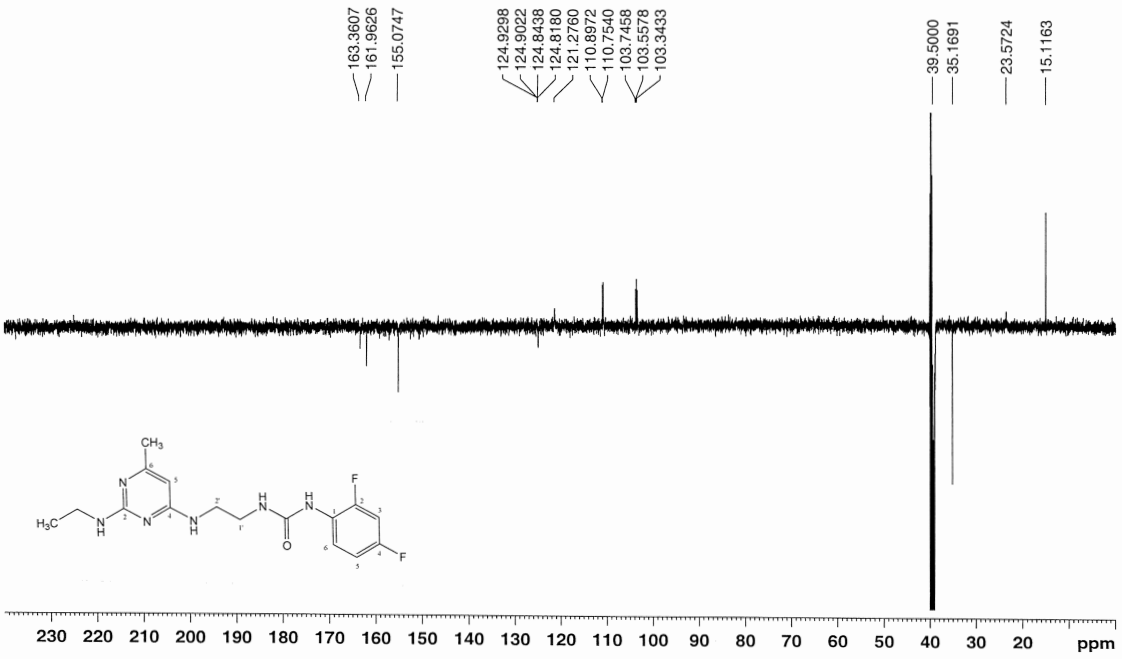

1H- and 13C-NMR Spectra in DMSO-d6 of compound 66

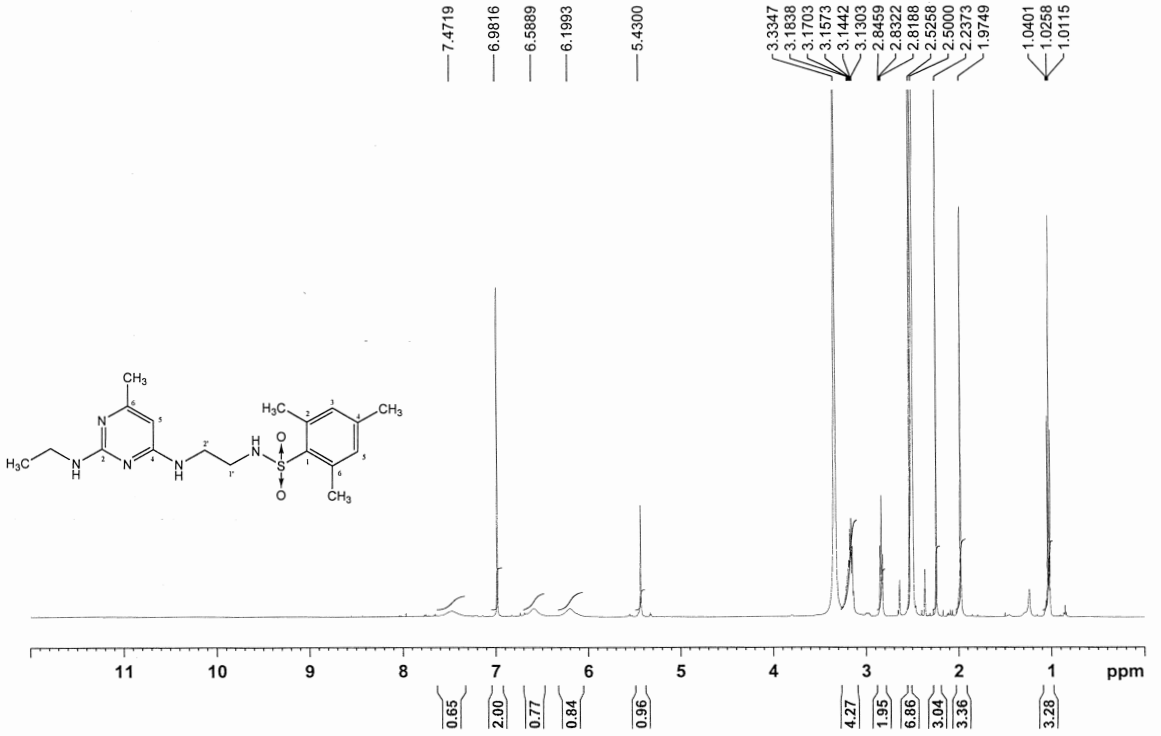

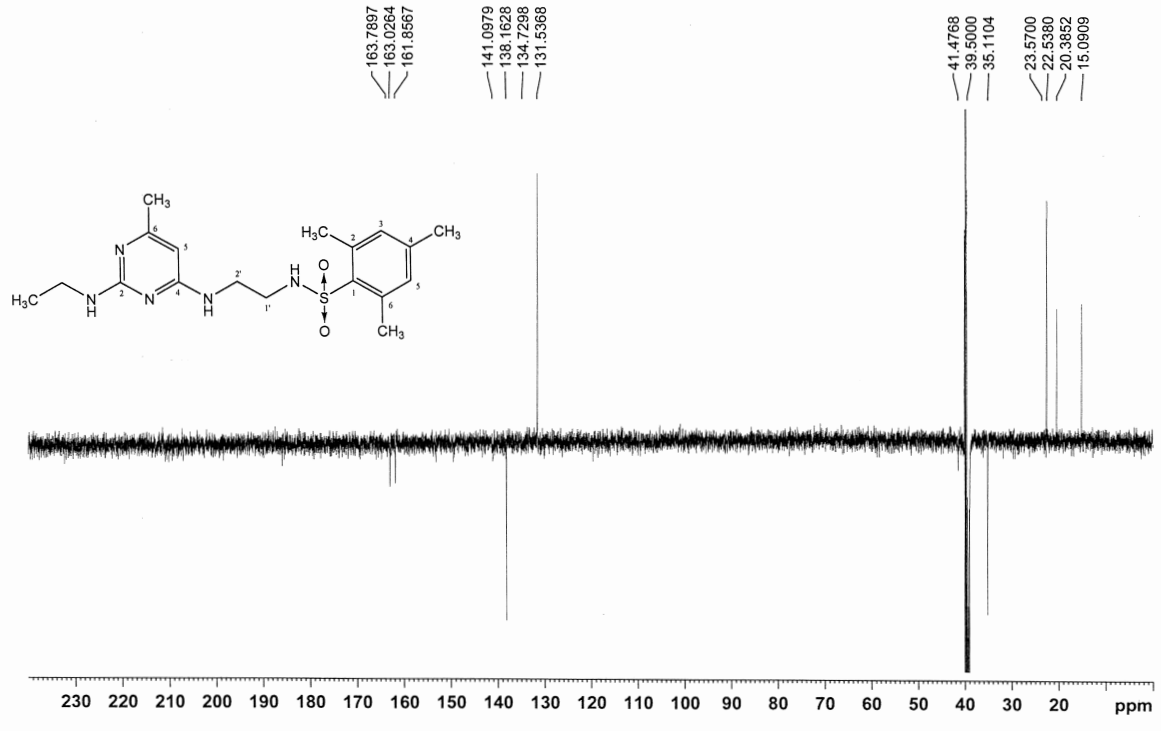

1H- and 13C-NMR Spectra in DMSO-d6 of compound 67a

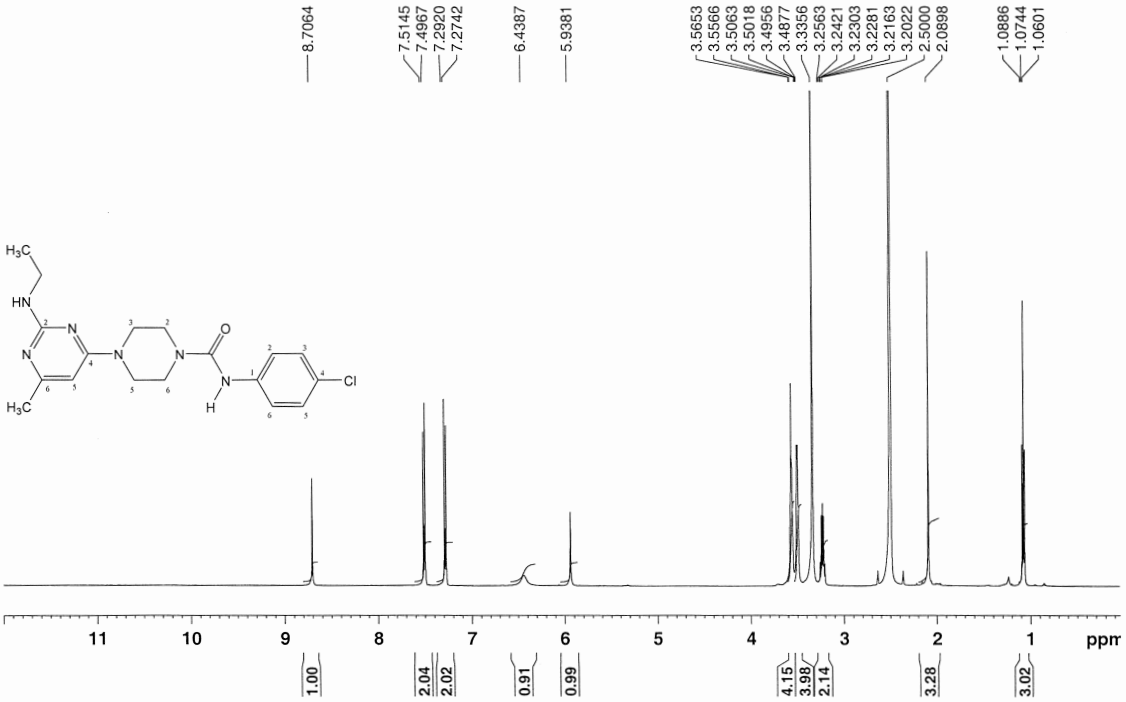

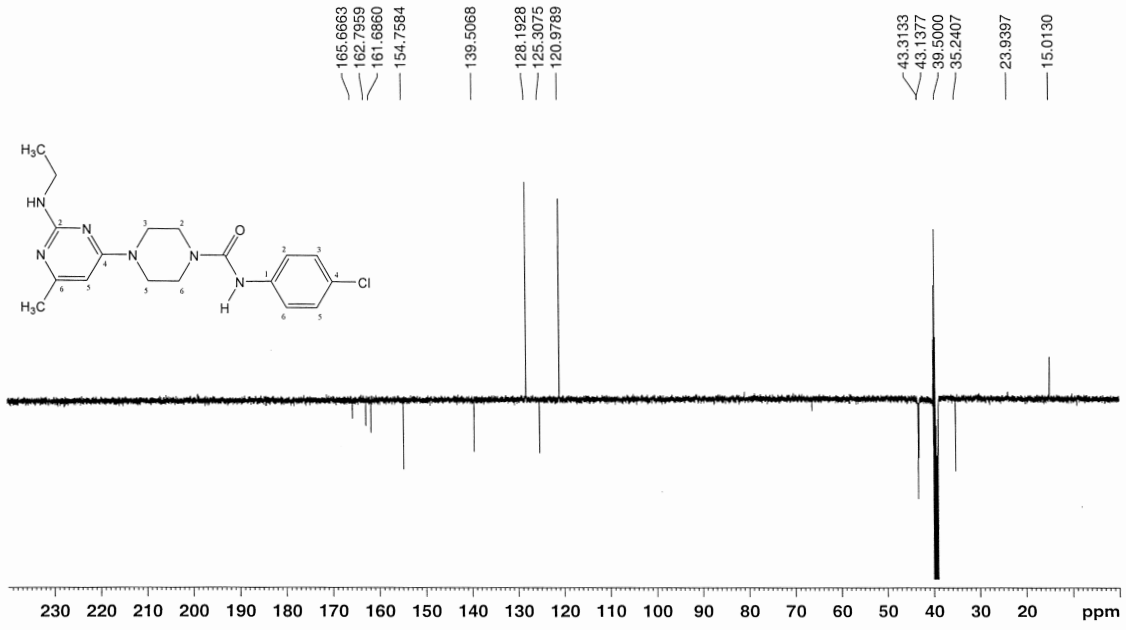

1H- and 13C-NMR Spectra in DMSO-d6 of compound 67b

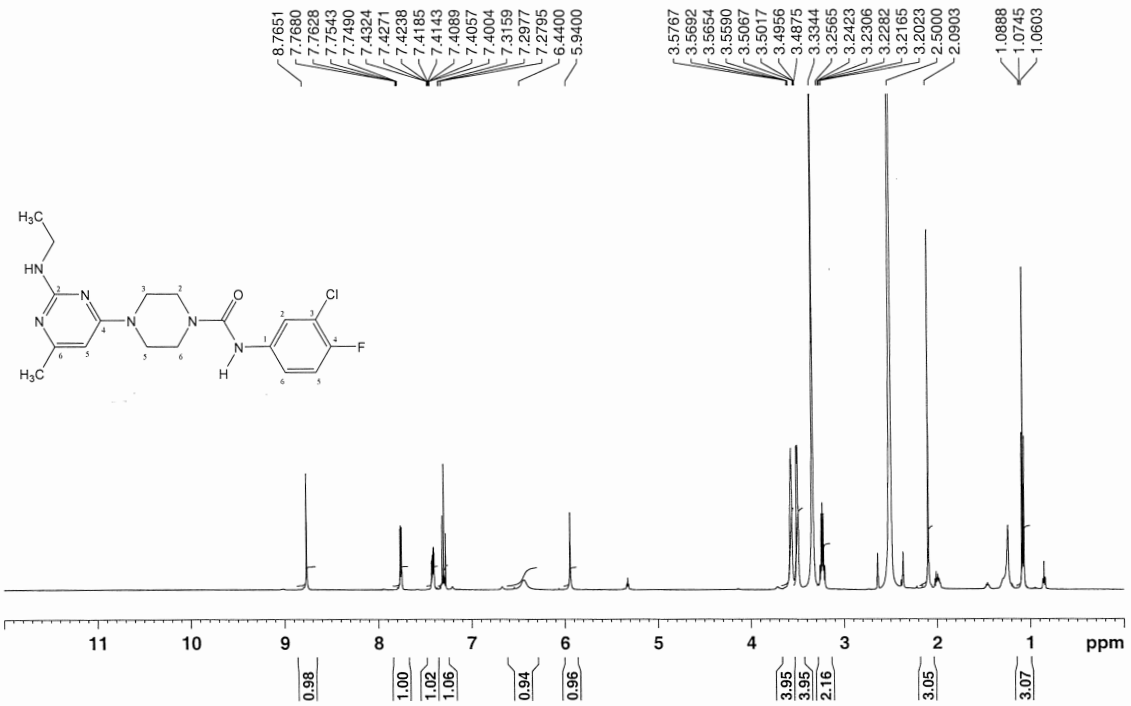

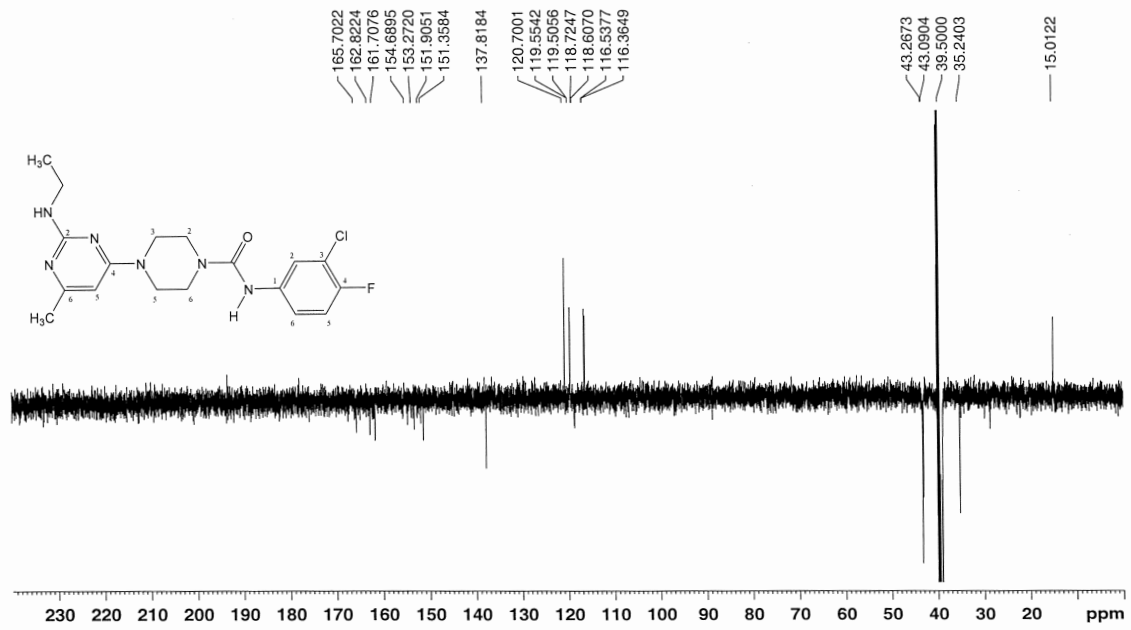

1H- and 13C-NMR Spectra in DMSO-d6 of compound 68a

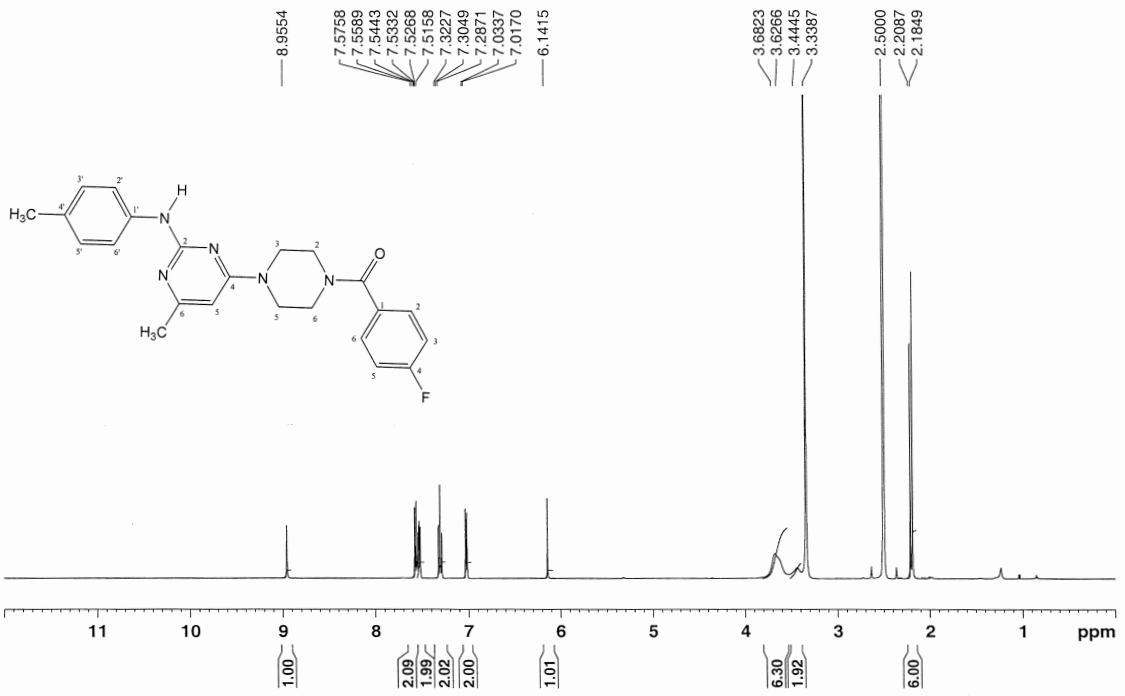

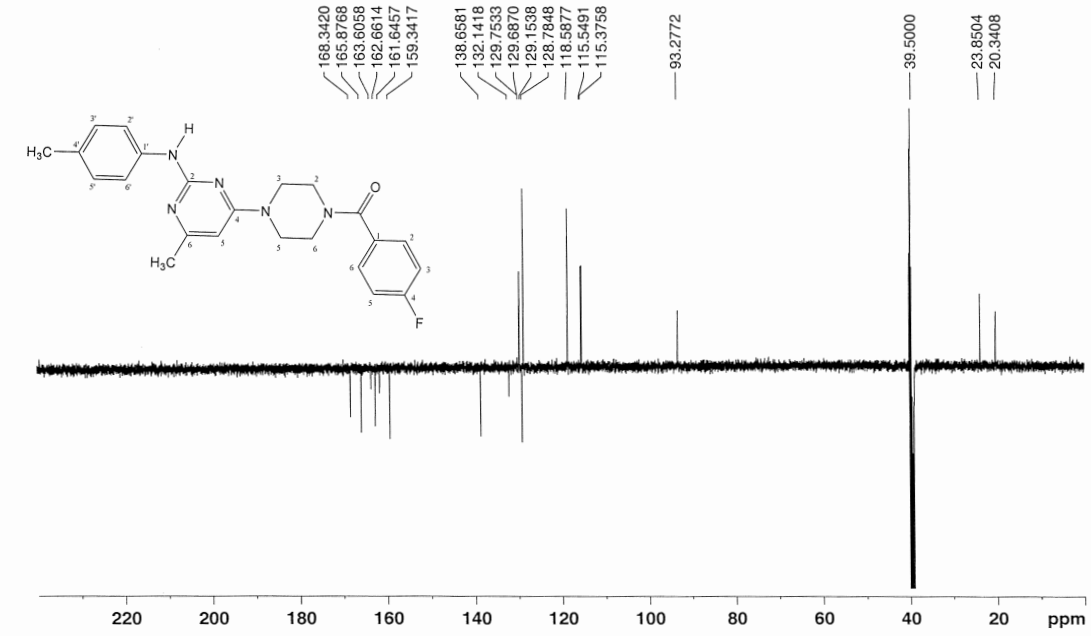

1H- and 13C-NMR Spectra in DMSO-d6 of compound 68b

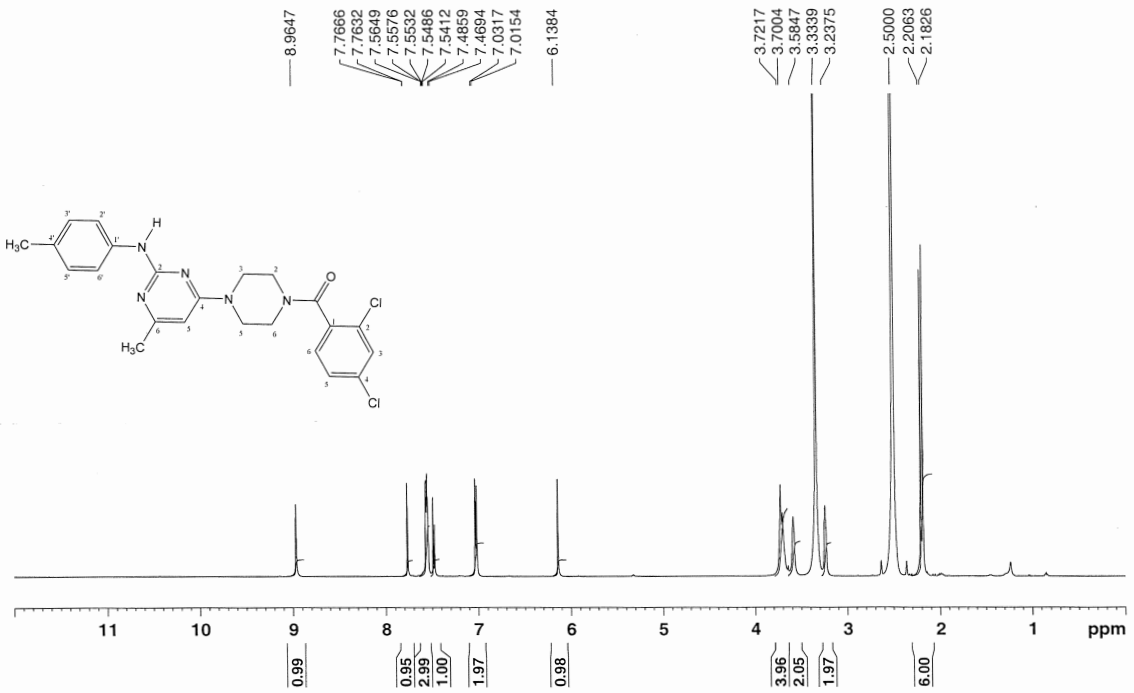

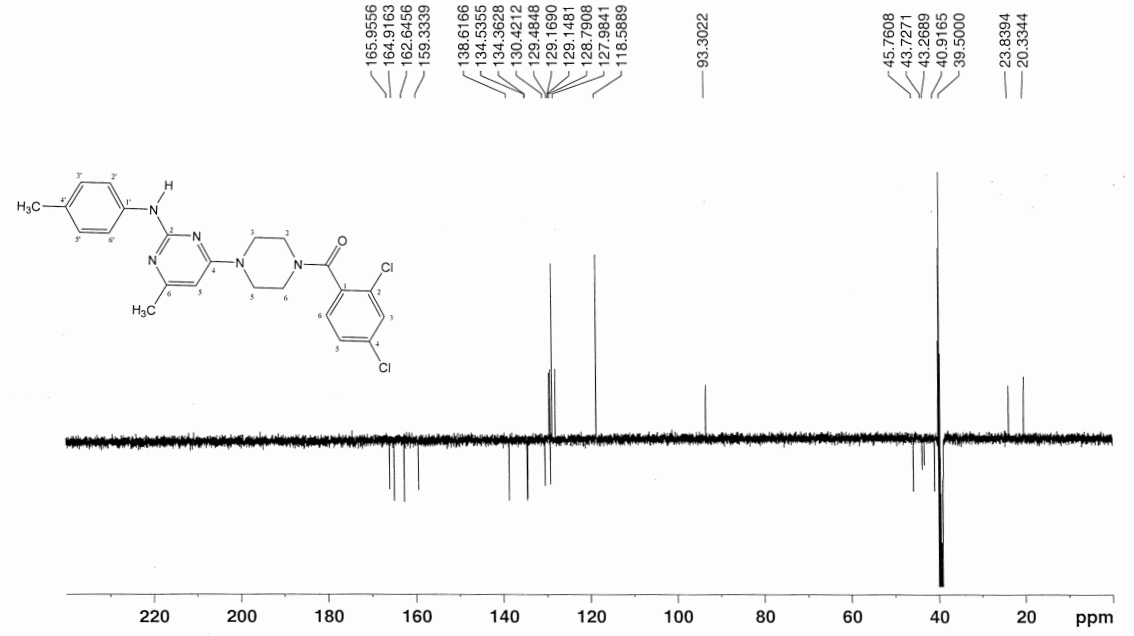

1H- and 13C-NMR Spectra in DMSO-d6 of compound 68c

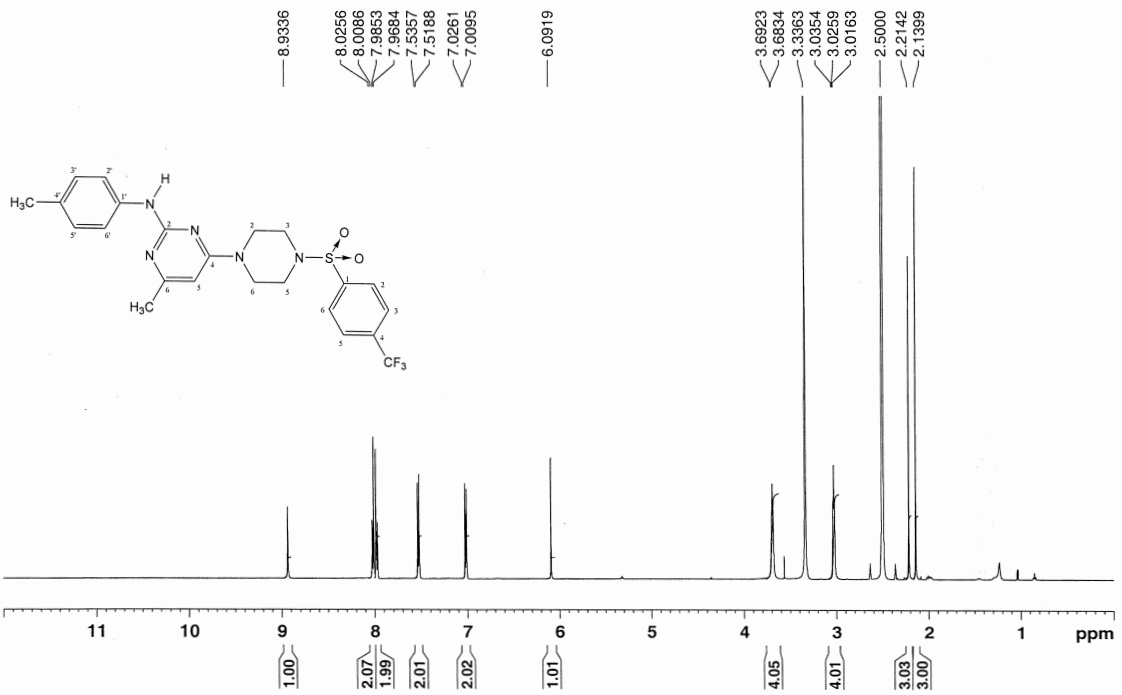

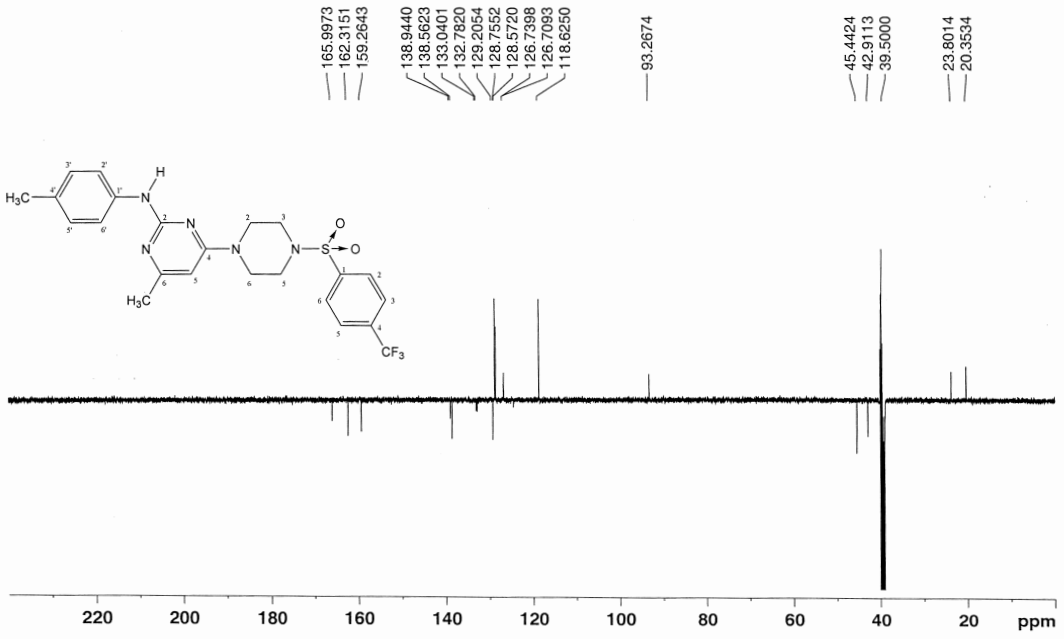

1H- and 13C-NMR Spectra in DMSO-d6 of compound 69

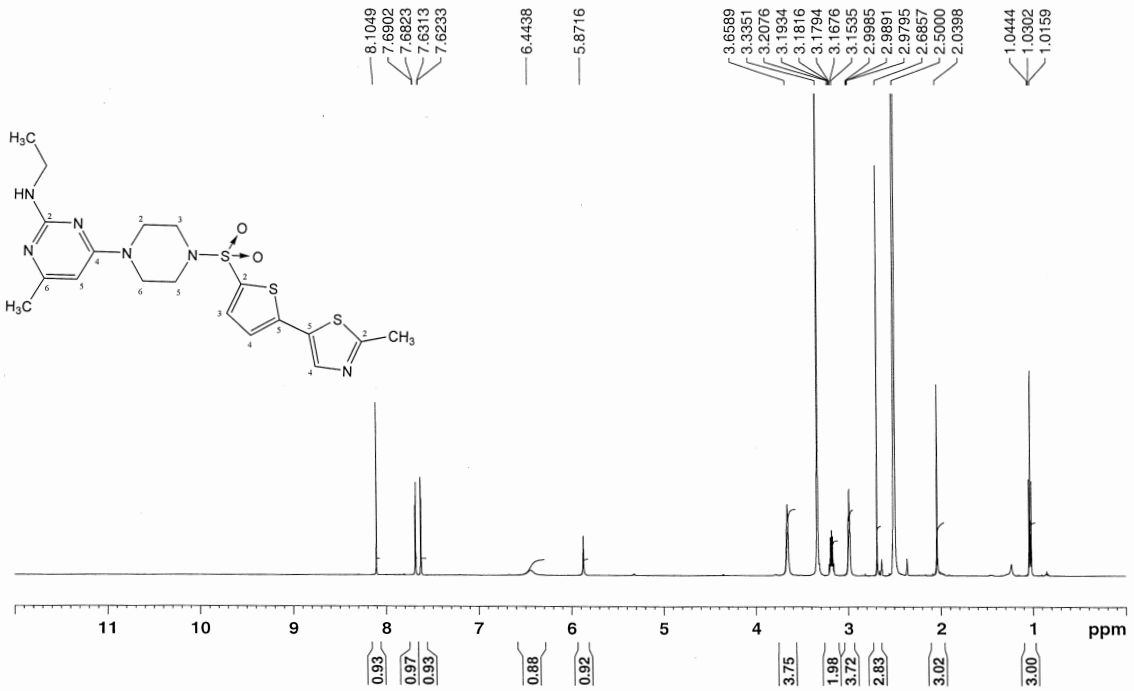

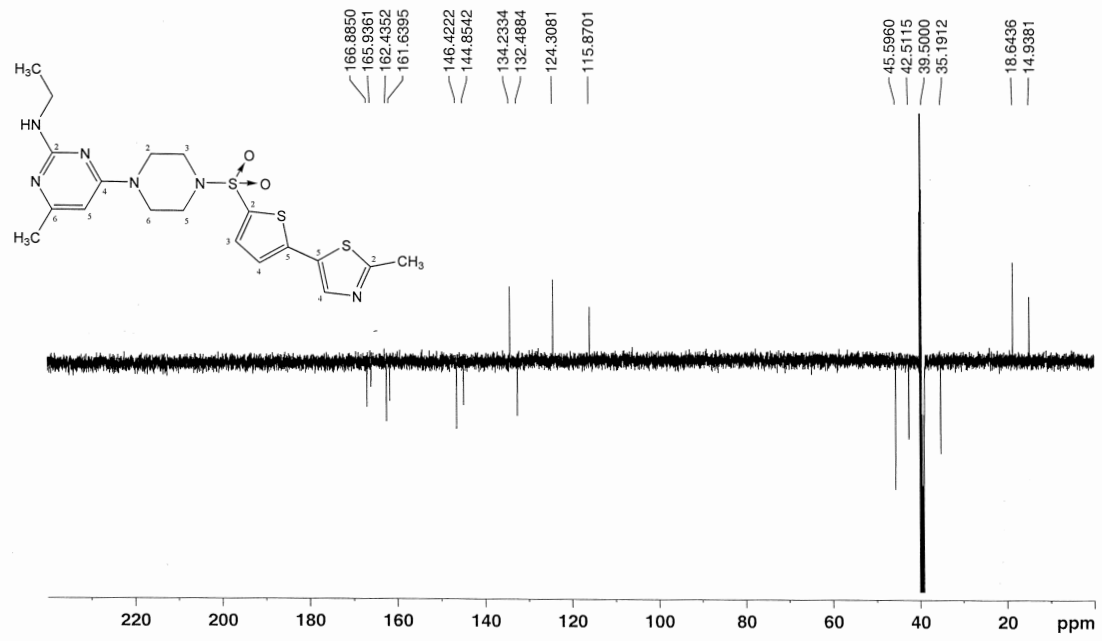

1H- and 13C-NMR Spectra in DMSO-d6 of compound 70

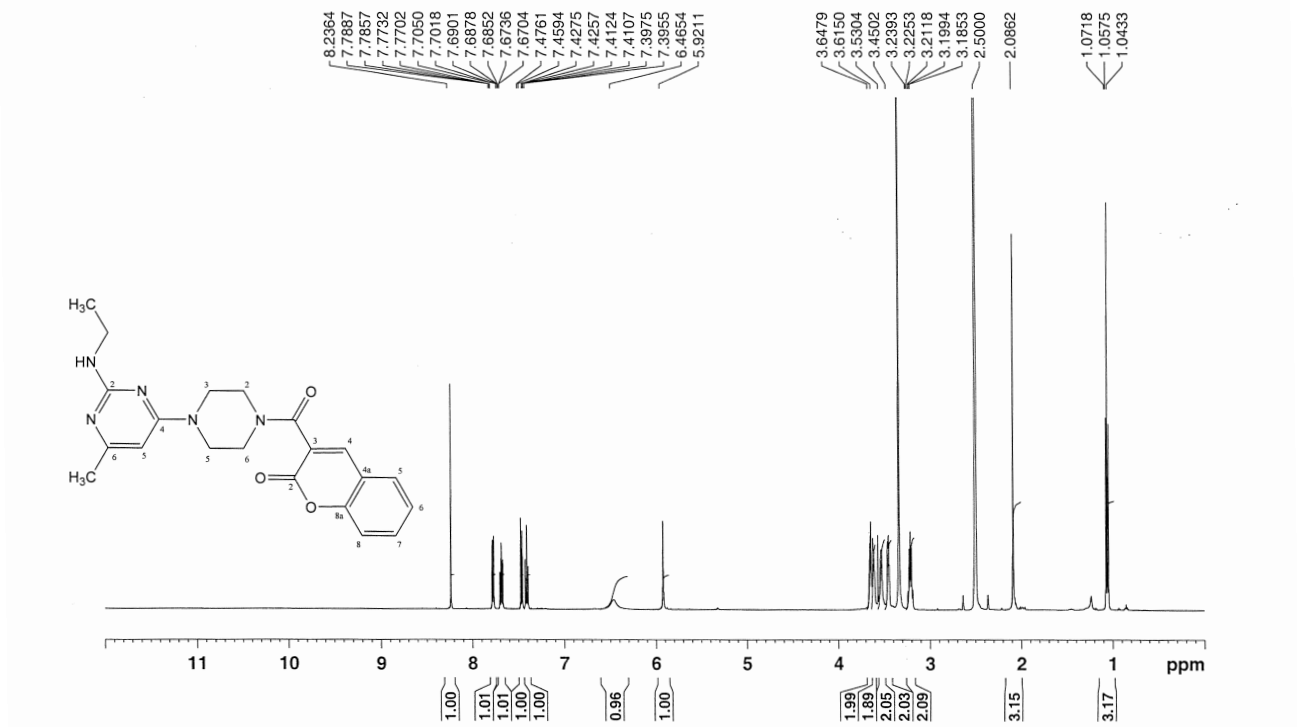

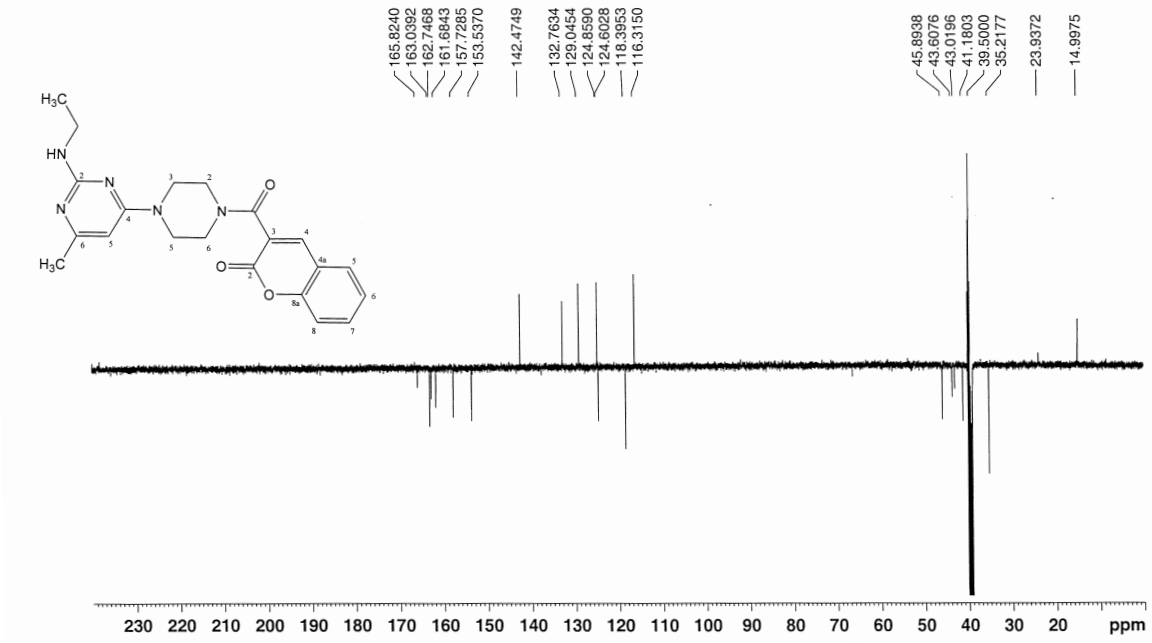

Abstract

Despite the worldwide re-emerge of the Chikungunya virus (CHIKV) and its high morbidity, no antiviral treatment or vaccine is available - making the development of a potent CHIKV-inhibitor highly desirable.

The hit compound **1a** was identified by an extensive high-throughput screening (HTS), which marks the starting point of a promising and novel CHIKV-inhibitor: the CHVB series. A structure-activity relationship study (SAR) with thirty-seven first-generation 2-(4-(phenylsulfonyl)piperazine-1-yl)pyrimidine analogues led to the discovery of the new lead compound **1b**. Further, a thorough lead optimisation of **1b** was performed to improve the already good antiviral activity (EC_{50}: 3.95 ± 1 µM) and to optimise crucial ADMET properties.

Therefore, one hundred analogues were designed, synthesized, and tested for their antiviral activity and physiochemical characteristics. These second-generation CHVB compounds were screened for possible hERG channel interactions, their cytotoxic characteristics in three cell lines (CaCo-2, HEK-293, and A459), and their viral profile. The compounds showed excellent safety and physiochemical profile and high selectivity towards CHIKV. In addition, the viral mRNA capping machinery (nsP1) was identified as the viral target of the CHVB series.

Furthermore, fifty-five compounds were assessed for their metabolic stability in human liver microsomes (HLMs), leading to a structure-metabolism relationship study (SMR). An extensive SAR study with the second-generation CHVB compounds confirmed some structural requirements identified earlier in the first-generation's SAR study and revealed the critical chemical features for a high CHIKV inhibition. In addition, two different synthesis routes (Synthesis Route A and B) were established to synthesize the CHVB analogues, whereby Synthesis Route B demonstrated a remarkable time- and yield-wise advantage.

In addition, a pharmacophore-based virtual screening retrieved two hits with strong CHIKV inhibition (**68c** and **70**) and a SAR-driven scaffold hop (**64b**) led to the identification of a new hit molecule with anti-CHIKV activity.

This research study identified five compounds (**31b**, **31d**, **32d**, **34**, and **35d**) as potent, safe, and stable lead compounds for further development as selective CHIKV inhibitors - with **32d** as the overall most promising candidate (EC_{50}: 0.7 ± 0.05 µM).

Abstrakt

Trotz der immer stärkeren Verbreitung des Chikungunya-Virus (CHIKV) und der damit verbundenen hohen Morbidität, gibt es weder spezifische antivirale Arzneistoffe noch einen geeigneten Impfstoff. Aus diesem Grund rückt die Entwicklung eines wirksamen CHIKV Inhibitors immer mehr in den Fokus der Arzneimittelforschung.

Der Ausgangspunkt der vielversprechenden CHVB-Molekülklasse bildet die Entdeckung des Hitmoleküls **1a** durch ein High-Throughput Screening (HTS). Eine erste Struktur-Wirkungsbeziehung (SAR) wurde mit 37 2-(4-(Phenylsulfonyl)piperazin-1-yl)pyrimidin-Analoga (erste Generation von CHVB-Analoga) durchgeführt und führte zur Identifizierung der Leitverbindung **1b**. Darüber hinaus wurde eine gründliche Leitstrukturoptimierung von **1b** durchgeführt, um die bereits gute antivirale Aktivität (EC_{50}: 3,95 ± 1 µM) zu verbessern und um zusätzlich zentrale ADMET-Eigenschaften zu optimieren.

Hundert Analoga wurden deshalb synthetisiert und auf ihre antivirale Aktivität und physikalisch-chemischen Eigenschaften getestet. Diese zweite Generation von CHVB-Analoga wurde zusätzlich auf mögliche Interaktionen mit dem hERG-Kanal, hinsichtlich ihrer zytotoxischen Eigenschaften in drei relevanten Zelllinien (CaCo-2, HEK-293 und A459) und ihrer biologischen Charakteristika untersucht, wobei ein ausgezeichnetes Sicherheitsprofil, gute physiochemische Eigenschaften und eine hohe Selektivität gegenüber des CHIKV festgestellt wurde. Zusätzlich wurde die virale mRNA-abbauende Maschinerie (nsP1) als Zielprotein der CHVB-Molekülklasse identifiziert. 55 Verbindungen wurden auf ihre metabolische Stabilität in humanen Lebermikrosomen (HLMs) untersucht und eine Struktur-Stabilitätsbeziehung (SMR) sowie eine zweite umfassende SAR-Studie mit der zweiten Generation CHVB-Analoga durchgeführt. Darüber hinaus wurden zwei verschiedene Syntheserouten (Syntheseroute A und B) für die Synthese der CHVB-Analoga entwickelt, wobei die Syntheseroute B erhebliche Vorteile in Bezug auf Reaktionszeit und Ausbeute aufweist.

Anhand eines virtuellen Screenings konnten zwei Hitmoleküle mit starker antiviraler Aktivität (**68c** und **70**) ermittelt werden. Zusätzlich führte ein Scaffold Hopping zur Entdeckung einer neuen Ausgangsverbindung mit guter antiviraler Aktivität (**64b**). In Zuge dieses Forschungsprojektes konnten fünf Verbindungen (**31b**, **31d**, **32d**, **34** und **35d**) als hochwirksame, sichere und stabile Leitverbindungen identifiziert werden, wobei **32d** der vielversprechendste Wirkstoffkandidat ist (EC_{50}: 0,7 ± 0,05 µM).